DISSERTATION

EFFICACY OF LOCALLY DELIVERED PARATHYROID HORMONE FOR TREATMENT OF CRITICAL SIZE BONE DEFECTS

Submitted by

Samantha J. Wojda

Department of Mechanical Engineering

In partial fulfillment of the requirements

For the Degree of Doctor of Philosophy

Colorado State University

Fort Collins, Colorado

Spring 2018

Doctoral Committee:

Advisor: Seth Donahue

Ketul Popat
Melissa Reynolds
Michael Yaszemski

ABSTRACT

EFFICACY OF LOCALLY DELIVERED PARATHYROID HORMONE FOR TREATMENT OF CRITICAL SIZE BONE DEFECTS

Large segmental defects in bone (e.g., due to trauma or tumor resection) commonly have complications or fail to heal properly, resulting in delayed or non-union. Around 2.2 million orthopaedic procedures utilize autografts or allografts each year to repair large defects; however, neither is without disadvantages. Disability due to orthopaedic injury has a significant impact on both the patient and the healthcare system. Quality of life for these patients can be severely impacted as healing time may exceed 9 months and multiple treatment attempts may be required if the first is unsuccessful. Research into bone graft substitutes, like Infuse® and OP-1® (Bone Morphogenetic Protein and a collagen sponge), has become prominent. PTH is another bioactive molecule that may promote bone regeneration and provide an alternative to autograft and BMP use for treatment of large segmental defects and non-unions. Daily injections of PTH are well known to have an anabolic effect on bone and are presently FDA approved for use as an osteoporosis treatment that results in increases in both bone mineral density and bone volume. Off label PTH 1-84 treatment also resulted in the healing of a non-union fracture that was unresponsive to BMP. Current FDA approval is for daily injections of PTH (intermittent administration), as continuously elevated PTH often has a catabolic effect on bone. However, post-menopausal women with mild primary hyperparathyroidism (PTH levels are not as severely elevated) demonstrate trabecular bone preservation. Low levels of continuous PTH have also

been shown to increase bone formation rate and marrow vascularity in mice. Thus, there is some evidence to suggest that low dose continuous PTH could be beneficial as an anabolic therapy in bone and may enhance bone regeneration. Continuously released, locally delivered PTH has been shown to improve healing/formation around dental implants in dogs and drill defects in sheep. However, dose response to local continuously delivered PTH is still unknown. Whether or not the benefits of PTH treatment observed in these models translate to critical size defect models is also unknown. The contribution of the research described in this dissertation increases understanding of the effects of locally delivered PTH on osteoblasts as well as its potential to enhance bone regeneration in a critical size long bone defect. This contribution is significant because presently the effects of low dose continuous PTH are not well understood. Continued development of the approaches described herein could lead to improved therapies for treatment of non-union and critical size defects in bone. Bone regeneration through locally delivered parathyroid hormone has the potential to improve functional restoration, even beyond that of allografts and without the drawbacks of current treatments, which would improve the quality of life for patients.

ACKNOWLEDGEMENTS

Dr. Seth Donahue
Dr. Matt Barron
Dr. Meghan McGee-Lawrence
Sarah Gookin
Claire Tucker
Megan Sanders

Dr. Michael Yaszemski
Mahrokh Dadsetan
Brett Runge
Jim Herrik
Lee Alan Miller

Dr. Kristi Anseth
Daniel Algae
Ian Marozas

Dr. Nicole Ehrhart
Dr. Ruth Rose
Laura Chubb
Morgan Woodard

Keith Condon

Dr. Ryan Gilbert
Chris Rivet
Shreel Joshi

TABLE OF CONTENTS

LIST OF FIGURES

Chapter 1: Literature Review and Aims

1.1 Bone Healing

Normal fracture healing in bone occurs in a series of stages. The disruption of tissue integrity that occurs with a bone break first leads to a state of inflammation and formation of a hematoma. As inflammatory cells infiltrate the hematoma a temporary soft healing tissue (granulation tissue) is formed. Following hematoma/granulation tissue formation a cartilage callus is formed which lays the groundwork for hard callus formation. The cartilaginous template is infiltrated by blood vessels and replaced by woven bone which is eventually remodeled into lamellar bone and then eventually a more chronic stage of bone remodeling persists (as does in normal bone maintenance) (Frost 1989, Frost 1989, Einhorn 1998, Schindeler, McDonald et al. 2008). It is generally accepted that normal fracture healing is complete after 3 months of healing and healing is considered delayed if the healing process exceeds 3 months. If healing is not achieved by 6 - 9 months and there is no new evidence of healing the fracture is considered a non-union (Paridis and Karachalios 2011).

Non-unions can be classified as hypertrophic, avascular/avital, atrophic, or pseudoarthrosis (Rüedi and Murphy 2000). Hypertrophic non-union (hypervascular, viable, vital) is linked with inadequate immobilization and appears to have an adequate blood supply and healing response. Avascular/avital non-unions (with or without bone loss) originate in the devascularization of the bone fragments due to the injury and or surgery. Atrophic non-unions (avascular, nonviable, avital) are poorly vascularized and have a very poor potential for bone forming cells/healing response. Pseudoarthrosis is non-union characterized by formation of a false joint as a result of persistent motion at the fracture site (Rüedi and Murphy 2000, Megas

2005). Thus, delayed or non-union at a fracture site can occur due to a multitude of reasons and incidence varies (reported incidence ranges from 1.9% - 30%) based on fracture location, configuration and associated soft tissue damage as well as other treatment and lifestyle factors (Tzioupis and Giannoudis 2007, Mills, Aitken et al. 2017). An estimated five to ten percent of the 7.9 million fractures that occur annually result in delayed or non-union (Marsell and Einhorn 2010). Non-union may occur as a result of healing being complicated by segmental bone loss, infection or previous surgery. Other factors that may disrupt healing and put patients at higher risk for non-union include, but are not limited to, inadequate immobilization, excessive soft tissue damage, obesity, smoking, age (over 50), and multiple injury (Buckwalter and Cruess 1991, Green, Lubahn et al. 2005, Perumal and Roberts 2007). Malnutrition may also negatively affect fracture healing (Dodds, Catterall et al. 1986, Guarniero, de Barros Filho et al. 1992). Large bone defects caused by trauma, cancer and metabolic disease can result in a similar non-union situation (Karladani, Granhed et al. 2001, Livingston, Gordon et al. 2003, Harris, Althausen et al. 2009)). Open fractures, like those potentially caused by high energy trauma have a higher relative risk for developing to non-union (Karladani, Granhed et al. 2001, Harris, Althausen et al. 2009)).

Treatment options are dependent on location and type of non-union. Open fractures, non-unions complicated by segmental defects , or when removal of tissue at a site of non-union is necessary for treatment (Ring, Barrick et al. 1997), can be addressed in two ways; shortening the bone or filling the defect (Mahendra and Maclean 2007). Shortening the bone changes the non-union from complex to simple but has a limitation of 3 cm in the upper limb and 1 cm in the lower before inducing a functional deficit for that limb. Filling the gap is traditionally achieved via bone graft or bone transport (Mahendra and Maclean 2007). However, present treatment

options are not without their downfalls. As such, orthopaedic injuries that require grafting may result in long term disability (Hinsley, Phillips et al. 2006, Owens, Wenke et al. 2006, Cross, Ficke et al. 2011).

1.2 Current methods for treating non-unions or critical size defects

Autografts and Allografts

Around 2.2 million autografts or allografts are used in orthopaedic procedures each year (Jahangir, Nunley et al. 2008). Both autografts and allografts can be performed with either cortical or trabecular bone. However, the two bone types differ in how graft incorporation occurs. Revascularization of a cortical graft takes about two months compared to the two weeks it takes for a trabecular bone graft. The response to a trabecular graft is osteoblastic, meaning woven bone can form before all necrotic trabeculae are resorbed, thus trabecular grafts are resorbed in the remodeling process. In a cortical graft, necrotic tissue needs to be removed prior to woven bone formation and the grafts can remain a mixture of necrotic tissue and new bone and may never completely heal (Yaszemski, Payne et al. 1996).

Autograft is the gold standard, as it provides a scaffold for bone growth as well as the growth factors and osteoprogenitor cells naturally present in the bone (Livingston, Gordon et al. 2003, Mahendra and Maclean 2007). Autografts are also histocompatible and nonimmunogenic and are usually well incorporated. Time to union is similar for vascularized and non-vascularized autografts. Non-vascularized (conventional) grafts become more porous and have more new-bone formation than vascularized grafts, but vascularized grafts retain more of their original cross-sectional area. Vascularized cortical grafts heal rapidly at host-graft interface whereas non-vascularized grafts do not undergo resorption and revascularization, rather they undergo

creeping substitution and therefore provide superior structural strength during the first six weeks (Dell, Burchardt et al. 1985). Though autografts have the benefits of growth factors and osteoprogenitor cells and potentially even vascularization, they have the major downfalls of limited availability as well as donor site pain and morbidity (Coventry and Tapper 1972, Damien and Parsons 1991, Banwart, Asher et al. 1995). In regard to treatment of critical size bone defects, it is impractical to harvest a sufficient amount of bone for repairing the defect.

As a result of the limited availability of autografts, allografts are commonly used to fill large bone defects. Allografts have a higher rate of failure (delayed or non-union, infection, or fracture) compared to autografts as they lack many of cells and growth factors that may have been present in the bone, as they are lost during preparation (washing, freeze drying, or irradiation) of the graft for implantation (Mahendra and Maclean 2007, Meijer, de Bruijn et al. 2007). Allografts also have the potential for immunogenicity problems, which may affect incorporation of the graft (Friedlaender 1983, Stevenson and Horowitz 1992, Tiyapatanaputi, Rubery et al. 2004). To reduce the potential immunogenic response, and further reduce potential for transmissible infection cadaveric bone may be even further processed, decalcified and additionally treated to make demineralized bone matrix (DBM). Demineralized bone matrix retains the structure of original tissue but loses structural strength (Tuli and Singh 1978, Vaccaro 2002). Similar to allografts, due to processing, demineralized bone matrix loses many of the growth factors and osteoprogenitor cells autografts benefit from. However, DBM with or without autologous bone marrow have been successfully used as an alternative to autograft (Connolly 1995, Tiedeman, Garvin et al. 1995, Nandi, Roy et al. 2010).

Beyond (and possibly a result of) the lack of biologic factors, another problem plaguing allografts is they are not entirely incorporated into the bone. Bone remodeling at the graft host junction only penetrates up to about 20% of the graft, even after 5 years (Enneking and Mindell 1991, Enneking and Campanacci 2001, Tiyapatanaputi, Rubery et al. 2004). As a result, the allografts cannot remodel and microcracks accumulate over time causing allograft strength to decrease 50% and mineral density to decrease 10% over 10 years in vivo (Wheeler and Enneking 2005). Primary union has not been observed between host and graft cortices in retrieved human allografts. Cortical-cortical junction healing takes place by bridging external callus originating from periosteum of host bone and extending up to 3 cm along the surface of the allograft. Once bone in the gap of the osteotomy is filled in, haversian systems perpendicular to long axis of bone (not stress oriented) formed and persisted for up to 11 years. Little or no fibrovascular repair tissue is observed in these allografts even up to 5 years after implantation. Specimens that were mechanically tested failed at the cement line denoting the histological line of union between host bone and allograft (Enneking and Campanacci 2001). Cancellous-cancellous healing occurs with no external callus, fibrovascular repair tissue from host bone invades marrow spaces of allograft to unite host and graft bone. Union occurs uniformly and is present as early as 4 months. Bone ingrowth penetrates 2-4 mm into the graft, beyond which a dense hypovascular fibrous tissue appears to block additional penetration by repair tissue, and the original architecture of graft below the repair area is well preserved even after many years (Enneking and Campanacci 2001).

The limitations of autografts and allografts have spurred a number of efforts at finding a suitable alternative to bone grafts for treating non-union or segmental bone defects. Materials like collagen, calcium phosphate, and numerous other natural and synthetic materials have been

explored as a means for providing a scaffold for bone ingrowth as an alternative to grafting (Hak 2007). As not all non-union scenarios are the same, and some are difficult to simulate in a research setting, a segmental (critical size) bone defect model is common in laboratory exploration of bone graft substitutes for these applications. A critical size defect is one in in which the defect is of sufficient size that it will not heal within the lifetime of the animal (Schmitz and Hollinger 1986). However, this lack of healing is evident at time points much more reasonable than the lifetime of an animal. For example, in a cranial defect in a rat model, critical size (8.8 mm) vs not critical size (3.8 mm) showed new bone formation ceased within 24 weeks, at which point small defect was filled and large was not. In week 24, bone lining cells on the surface of the new bone and osteocytes in bone matrix expressed/produced little type I collagen and osteocalcin (Honma, Itagaki et al. 2008). Segmental defects in the femur of rats of at least 5 mm are likewise considered critical size defects (ASTM 2014). In a clinical setting, normal healing is expected to occur within 3 months (Paridis and Karachalios 2011), thus, this is a time point of interest for bone healing and regeneration in pre-clinical studies as well. Critical size defects, whether in the femur, ulna, calvaria, or another site, have become a common way to test potential bone graft substitute materials.

Biomaterial scaffolds for bone regeneration

Bone regeneration is a complex process that is dependent on cytokines, proteins, and progenitor cells, as well as spatial and temporal cues. Thus, if a graft or bone graft substitute is used to aid the healing process, the physical and chemical properties of the given scaffold play a role in how bone cells adhere to the scaffold and lay down matrix. Various tissue regeneration approaches have been taken to promote bone healing using biomaterial scaffolds. Biomaterials

used for bone tissue regeneration include both natural, like collagen, and synthetic materials, like ceramics, metals and polymers.

Ceramics, for example, are popular in bone regeneration research due to the structural similarity to bone, and are commonly used as bone graft substitute materials or bone cements, not only in a research setting, but also clinically (Bohner 2000, Le Guehennec, Goyenvalle et al. 2005). Calcium phosphates, are popular due to their osteoconductivity, potentially high compressive strength and the potential to be injectable (Hak 2007). βeta-tricalcium phosphate (β-TCP) and hydroxyapatite (HA) have been commonly explored as bone graft substitutes. Zimmer, for example, has both an IngeniOs β-TCP™ bioactive scaffold and IngeniOs HA™ synthetic bone particles on the market. Both β-TCP and HA provide osteoconductivity and biocompatibility; but they have different resorption rates, which may make one more useful than the other depending on the application (Yaszemski, Payne et al. 1996, Vaccaro 2002). Actifuse ™ (Baxter) and Norian SRS Cement™ (Synthes) are calcium phosphate based bone graft substitute materials implicated for filling bone voids or gaps. Coralline hydroxyapatite, produced from marine coral exoskeletons and calcium sulfate (plaster of paris) were approved by FDA in 1992 and 1996 respectively as effective bone graft substitute materials (Hak 2007). Hydroxyapatite can also be combined with a collagen-based matrix, or as a coating for a polymer scaffold as well as other applications for use in bone defects (Hak 2007). ProOsteon 500R™ (Interpore Cross, Irvine, CA) is a calcium carbonate core coated in HA. Though there are a number of commercially available ceramic based options as bone graft substitute materials a variety of other materials have also been explored as bone graft substitutes.

Polymers can also be useful as bone graft substitutes. Polymers are very versatile in that various processing techniques can be used to create different of types of scaffolds, whether the goal is mechanical support, cell attachment, or even drug or biomolecule delivery. Polymers may be cross-linked in a mold, created using stereolithography, electrospun into a mesh, as well as a variety of other processing techniques to attain the desired form. Polymers may even be designed to have an end form of a putty-like consistency instead of a rigid form, for situations requiring filling of an irregularly shaped defect. Electrospun poly (lactic acid) scaffolds, poly(ε-caprolactone) nanofiber meshes, polylactide membranes, and many other polymers, have all shown promise as potential materials for enhancing bone regeneration (Yaszemski, Payne et al. 1996, Kim, Jeong et al. 2005, Kim, Lee et al. 2006, Kolambkar, Peister et al. 2010). Beyond customizable structural parameters, polymer scaffolds may also be tailored to allow and promote cell attachment and proliferation through selection of type of polymer or by addition of factors like arginylglycylaspartic acid (RGD peptide) or other bioactive molecules to the polymer chain (Burdick and Anseth 2002, Liu and Ma 2004, Tang and Wu 2006).

A number of materials are commercially available or are promising options for bone graft substitute materials in the development phase; however, a strong demand for bone graft substitute options resulting in healing comparable to, or better than, autograft (the gold standard) persists. Efforts at creating a novel bone graft substitute material are one method by which new products may come to market. However, creating a novel material is not the only way to create a more effective bone graft substitute. For example, a material that has already been FDA approved for use or is already well researched in a pre-clinical setting may also be built upon by modifying structural parameters or by combining it with cell therapies or bioactive molecules.

For example, a variety of HA scaffolds have been FDA approved for use. If porous HA scaffolds are seeded with cells and cultured in vitro, such that in vitro bone formed on the scaffold before implantation, upon implantation improved healing is observed (Mendes, Sleijster et al. 2002). Likewise, ex vivo expanded endothelial progenitor cells seeded on Gel-foam™ scaffolds and placed in 5 mm femoral defects in rats resulted in significantly higher bone formation and higher torsional strength than defects treated with only Gel-foam™ (Atesok, Li et al. 2010, Li, Atesok et al. 2011). Taking different approaches at using cells to enhance bone regeneration potential has been explored with a variety of natural and synthetic materials, including, but not limited to, polycaprolactone (PCL) scaffolds, bovine collagen, collagen-glycosaminoglycan scaffolds, and collagen-calcium phosphate scaffolds (Hunt, Schwappach et al. 1996, Lyons, Al-Munajjed et al. 2010, Wojtowicz, Templeman et al. 2010). However, incorporation of cells is not the only way biomaterial scaffolds can be made more efficacious. Biomaterial scaffolds may also be used to deliver growth factors or bioactive molecules to a bone defect site. Due to their customizable nature polymers are an effective way to deliver drugs, growth factors or other bioactive molecules in a controllable fashion. Hydrogels as well as rigid scaffolds are popular for delivery of bioactive molecules. Chitosan hydrogels, hyaluronic acid based hydrogels, Poly(ethylene glycol) (PEG) based hydrogels, Poly(L-lactide-co-ε-caprolactone) and heparin based hydrogels, RGD-modified alginate and electrospun Poly(ε-caprolactone) nanofiber meshes, and a number of other polymer scaffolds have been utilized as carriers for bioactive molecules for varying applications (Kim, Hefferan et al. 2009, Kolambkar, Dupont et al. 2011, Lee, Choi et al. 2011, Luca, Rougemont et al. 2011, Martinez-Sanz, Ossipov et al. 2011).

Incorporation of bioactive molecules into biomaterial scaffolds for bone tissue regeneration

Bioactive molecules and the biomaterial carrier may be chosen for a variety of reasons, as numerous molecules play a variety of integral roles in fracture healing and bone regeneration. For example, bone morphogenic proteins (BMPs) play a role in bone regeneration and are known to promote osteogenic differentiation. BMPs have, therefore, been combined with materials like hydroxyapatite, Di-calcium phosphate dehydrate (DCPD), collagen, PLGA, and many others in an attempt to create a more efficacious bone graft substitute (Tuominen, Jamsa et al. 2001, Cowan, Soo et al. 2005, Chu, Sargent et al. 2006, Kempen, Lu et al. 2008). In 2001 use of OP-1™, a BMP-7 implant, was approved by the FDA as a potential alternative to autograft in recalcitrant long bone non-union situations. A short time later, Infuse™, bovine collagen with BMP-2, was also approved. BMP-2 has become a prominent treatment option for spinal fusion applications, tibial fractures and sinus repair. BMP-2 and BMP-7 have been shown to perform as well as (but not better than) iliac crest bone grafts (ICBG) for spinal fusion and long bone non-union applications. BMP has also been shown to effectively enhance chances of union after failed grafting in both tibial and femur non-unions (Kanakaris, Lasanianos et al. 2009, Zimmermann, Wagner et al. 2009), and in upper limb non-unions (used in conjunction with autologous bone graft) (Singh, Bleibleh et al. 2016). Though FDA approval for BMP use in humans is presently delivery via collagen sponge. Research into whether a different biomaterial carrier may improve healing further has been abundant. The customizability of polymers makes them ideal candidates for biomolecule delivery. For example, poly(propylene fumarate) (PPF) is an osteoconductive and biodegradable polymer that has been studied both as a scaffold for bone ingrowth as well as a method by which to deliver bioactive molecules (Kempen, Lu et al. 2006, Lee, Wang et al. 2007).

As a scaffold for bone regeneration applications, PPF has been utilized in the form of an injectable foaming cement (Lewandrowski, Cattaneo et al. 1999) as well as a preformed scaffold (Lee, Wang et al. 2007). As a mode of bioactive molecule delivery preformed PPF scaffolds may be coated with the desired bioactive molecule (Vehof, Fisher et al. 2002), or it may be incorporated into the structure of the scaffold. For example, controlled release of BMP-2 from injectable PPF was achieved by incorporating PLGA and PPF microspheres that contained BMP-2 in the scaffold itself. By adjusting the ratio of PLGA and PPF making up the microspheres, release of BMP-2 could be modified (Kempen, Lu et al. 2006). Hydrogels also allow for customizable control of biomolecules. For example, thiol-ene hydrogels can be utilized to entrap biomolecules within their matrix to allow release by diffusion. Biomolecules may also be cross-linked to the hydrogel matrix to control release by breaking the chemical bonds (Grim, Marozas et al. 2015). BMP-2 entrapped within the matrix of a thiol-ene hydrogel enhanced healing in a cranial defect model to a greater extent than when delivered via the commercially available collagen sponge (Mariner, Wudel et al. 2013).

Bioactive molecule delivery capabilities of materials like PPF and thiol-ene hydrogels are not necessarily specific to delivery of BMP, and BMPs may not be the ultimate bone graft substitute supplement. Serious adverse events may lead to a need for additional surgeries when BMP is used in non-spinal orthopaedic procedures (Woo 2013) and BMP use comes with the possibility of an increased risk of cancer at 24 months (Fu, Selph et al. 2013), and is similarly, if not more, financially burdensome than ICBG (Dahabreh, Calori et al. 2009, Giorgio Calori, Capanna et al. 2013). Other bioactive molecules could similarly be incorporated into these hydrogels or encapsulated in microspheres for local delivery to a bone defect. Some growth

factors or bioactive molecules (like BMP or transforming growth factor beta (TGF-β)) are of interest because they have a known effect on bone formation (Oest, Dupont et al. 2007). However, direct effect on osteogenic differentiation may not be the only reason a bioactive molecule is selected for bone regeneration applications. For example, vascular endothelial growth factor (VEGF) is a cytokine involved in angiogenesis and improving blood vessel ingrowth. There are a variety of reasons that angiogenesis in healing may be inhibited after a grafting procedure, whether it is an autograft, allograft, or bone graft substitute. In the case of allografts, freezing of the graft, histocompatibility antigen differences between donor and recipient, local and systemic interference with biologic activity of graft and surrounding tissue (e.g. irradiation) all have potential to delay or inhibit angiogenesis (Stevenson, Emery et al. 1996). Because blood vessel ingrowth is vital to fracture healing , incorporation of VEGF and/or other factors known to up-regulate VEGF with a graft or graft have been explored as a possible approach to improving fracture healing (Street, Wang et al. 2001, Murphy, Simmons et al. 2004). Another option explored for enhancing bone regeneration via improving blood vessel growth is erythropoietin, a growth factor that controls red blood cell development in bone marrow. When delivered intraperitoneally, 500 IE/kg/d resulted in increased rate of bridging as well as increased bone volume in segmental defects (Holstein, Orth et al. 2011). Likewise, platelet rich plasma (PRP) delivered via a polycaprolactone-20% tricalcium phosphate scaffold resulted in a greater proportion broken femurs achieving bone union in comparison to empty controls (Rai, Oest et al. 2007).

Anti-resorptive agents, like those used to treat osteoporosis, have also been explored as a means by which to promote bone healing. Alendronate treatment has been shown to improve

the fixation of porous-HA coated implants (Jakobsen, Baas et al. 2009). Strontium ranelate (an antiosteoporotic agent) has been shown to improve fracture healing in an osteoporotic rat model (Ozturan, Demir et al. 2011). Estrogen and raloxifene have been shown to improve metaphyseal fracture healing in the early phase of osteoporosis (Stuermer, Sehmisch et al. 2010). Though anti-resorptive agents have shown promise in enhancing implant fixation or bone regeneration, parathyroid hormone (PTH), which has an anabolic effect on bone, may promote bone regeneration to an even greater extent. In osteoporotic women, bone mineral density of the lumbar spine increases 6.3% with PTH treatment compared to an increase of 4.6% with alendronate (an anti-resorptive) treatment (Black, Greenspan et al. 2003). Similarly, a 14% increase in bone volume was observed in women with osteoporosis that received daily injections of PTH 1-34 compared the 24% loss in bone volume in women with osteoporosis who were not treated with PTH (Jiang, Zhao et al. 2003). The unique ability of PTH to increase bone formation as opposed to decreasing resorption makes it a molecule of interest for bone regeneration applications.

1.3 Parathyroid Hormone

Parathyroid hormone, an 84 amino acid protein, is a key regulator of calcium homeostasis in the body. Normal secretion (from the parathyroid gland) is an ultradian rhythm with tonic and pulsatile components (70% tonic, 30% pulsatile), and is dependent on serum calcium and phosphorous. The half-life of PTH in humans is approximately 2-5 minutes and the pulsatile component is in low amplitude high frequency bursts every 10-20 minutes superimposed on the tonic secretion (Chiavistelli, Giustina et al. 2015). The pulsatile component is highly sensitive to changes in ionized calcium and calcitrol levels. When extracellular calcium concentrations are

outside of the normal range the parathyroid glands change secretion of PTH to return serum calcium levels to normal (using the skeleton as a calcium reservoir). The classic actions of PTH, including stimulating bone resorption and increasing calcium reabsorption, reside in the N-terminal 1-34 region of the protein (Potts, Kronenberg et al. 1982). PTH acts through a g-protein coupled receptor, type 1 PTH receptor (PTHR1). When PTH binds to the receptor, adenylate cyclase or phospholipase C is activated starting a cascade resulting in stimulation of protein kinase A (PKA) or protein kinase C (PKC), respectively (Karaplis and Goltzman 2000). Activation of the PKA pathway is mediated by the $G\alpha_s$ part of the receptor, this cascade stimulates cAMP production, and subsequently PKA. Activation of the PKC pathway is a $G\alpha_q$ mediated response. PKC is activated through phospholipase C dependent and independent pathways, which leads to activation of osteoblastic bone formation (Jilka 2007). Through these pathways PTH can mediate both bone formation and bone resorption. The overall response of osteoblasts to PTH stimulation, however, is dependent on concentration and timing among other factors.

In vitro effects

Though they lack the complexity of in vivo models, studies in osteoblastic cells have allowed at least a preliminary understanding of the mechanisms by which PTH impacts the skeletal system. Studies in cultured osteoblastic cells show PTH rapidly activates the cAMP-mediated activation of PKA which subsequently inactivates pro-apoptotic proteins and increases survival genes (Bellido, Ali et al. 2003). Marrow cells from C57BL/6 mice cultured for 6 days then treated for 96 hours with continuous PTH exposure (10 nM) demonstrated an increase in promoters of osteoclast formation (and bone resorption activation and decrease in factors that inhibit osteoclast formation and activation) (Nakagawa, Kinosaki et al. 1998, Yasuda, Shima et al.

1998, Huang, Sakata et al. 2004). The effect of continuous PTH 1-34 on osteoclastogenesis can be reproduced using PTH 1-31, which activates the PKA pathway, but not PTH 3-34, which activates the PKC pathway. This combined with a lack of osteoclasts in culture supports the idea that stimulation of osteoclastogenesis in these studies may be mediated though the cAMP/PKA pathway but not the calcium/PKC pathway. Neither PTH 1-31 nor PTH 3-34 induced as large an increase as PTH 1-34, but both increased expression of bone formation markers. Thus, in vitro work indicates the effects of intermittent PTH 1-34 on induction of osteoblast markers appear to involve both the PKA and PKC pathways (Locklin, Khosla et al. 2003). This is supported by the ALP response of cells isolated from newborn rat calvaria when treated with PTH 1-34 (50 ng/mL) continuously or intermittently. With continuous exposure of PTH, ALP decreased on day 5 (first day sampled) and remained that way for the remainder of the period. Calcium content and number of mineralized bone nodules were suppressed as well. However, intermittent exposure to PTH (the first 6 hours of each 48 hour cycle) stimulated osteoblast differentiation. This was demonstrated by an increase in ALP, calcium content, and number of mineralized bone nodules for all time points (Ishizuya, Yokose et al. 1997).

Cell culture experiments have not only contributed to the understanding of the pathways that may lead to the functional outcomes of PTH but also to understanding what the functional outcomes of various treatment regimens are. This is particularly important considering the differing effects of intermittent and continuous treatment. Bone marrow cells isolated from femora and tibiae of PTH or vehicle treated rats (30 μg/kg s.c.) and cultured at a high density, demonstrated a significant increase in ALP expression (a phenotypic marker of osteoblast differentiation). When cultured at a low density to generate colonies (colony forming unit-

fibroblastic (CFU-F)) PTH induced apparent increases in CFU-F and the number of ALP-positive CFU-F. These findings suggest PTH may stimulate proliferation and differentiation of osteoprogenitor cells in bone marrow (Nishida, Yamaguchi et al. 1994). Similarly, experiments in MC3T3-E1 cells have shown upregulation of ALP, Runx2, osteocalcin, bone sialoprotein and β-catenin (markers of bone formation) with intermittent PTH 1-34 treatment (Tian, Xu et al. 2011). Whether PTH is intermittently or continuously administered may not be the only key variable in outcome of studies. Timing of treatment may also affect how osteoblasts respond to PTH treatment. In MC3T3-E1 cells cultured for 30 days, continuous PTH treatment initiated before day 20 resulted in a decrease in mineralization compared to controls. However, if it began on or after day 20 mineralization was unaffected. If continuous exposure to PTH began on day 20 and stopped on day 25, mineralization on day 30 was increased 5 fold (Schiller, D'Ippolito et al. 1999). PTH also affects osteoblasts differently depending on if they're pre-confluent or post-confluent, suggesting responsiveness to PTH differs depending on differentiation stage of osteoblast development. In vitro studies indicate PTH may preferentially stimulate osteoblast differentiation in immature osteoblasts but inhibit in in more mature cells (Isogai, Akatsu et al. 1996, Kondo, Ohyama et al. 1997). These studies may have implications in understanding whether or not delaying PTH treatment in bone regeneration could be beneficial. Or similarly, if treatment is only necessary during a specific stage of healing (for example, the beginning).

In vitro studies only demonstrate part of what occurs in vivo, as the complexities of the in vivo remodeling and healing mechanisms have yet to be duplicated in vitro. However, in vitro studies have demonstrated the effect of PTH on osteoblasts seems to be dependent on whether the exposure to PTH is continuous or intermittent. Though there is a good knowledge base for in

vitro studies, there is little literature on the effects of low concentrations of continuously administered PTH on osteoblasts and whether or not there are concentration effects seen with lower concentrations that aren't observed with higher concentrations. Limitations of the in vitro work are that it lacks the complexity of an in vivo situation. For example, in vitro studies are typically done in osteoblasts. Though osteoblasts are target cells for PTH, looking only at osteoblasts excludes the effect of other cells and signaling molecules found in vivo and how that may affect the signaling cascade. Though there are limitations to in vitro work, it does provide an excellent basis for exploring the in vivo response and mechanism of how PTH affects bone.

In vivo, systemic effects

As PTH is a regulator of calcium homeostasis, it has been studied extensively as an osteoporosis treatment. Parathyroid hormone 1-34 is FDA approved and currently on the market (FORTEO®, generic name teriparatide) as a treatment for osteoporosis. Presently, recombinant PTH 1-34 is FDA approved as FORTEO® (Eli Lilly) in the United States for use as an osteoporosis treatment (administered as daily injections). Recombinant PTH 1-84 (Preotact®) was approved in Europe in 2006 for the treatment of osteoporosis (but was withdrawn in 2014). Recombinant PTH 1-84 (Natpara®) is also approved in the United States for treatment of hypocalcemia in persons with hyperparathyroidism. When intermittently administered, both PTH 1-34 and 1-84 have an anabolic effect on bone (Mosekilde, Sogaard et al. 1991, Hock and Gera 1992, Ejersted, Andreassen et al. 1993, Jerome, Burr et al. 2001, Neer, Arnaud et al. 2001, Fox, Miller et al. 2007, Jodar-Gimeno 2007). When PTH 1-34 and 1-84 are given at an equivalent molar dose as once daily injections no difference in the anabolic effect on bone is observed in Wistar rats (Mosekilde, Sogaard et al. 1991). PTH decreases the risk of fragility fractures, increases cortical thickness and

improves trabecular bone architecture in the ilium of postmenopausal women (Neer, Arnaud et al. 2001, Jiang, Zhao et al. 2003). Daily injections of PTH 1-34 results in a 14% increase in bone volume in women with osteoporosis (Jiang, Zhao et al. 2003) and a 6.3% increase bone mineral density of the lumbar spine (Dempster, Cosman et al. 2001, Black, Greenspan et al. 2003). These changes occur due to an imbalance in remodeling, favoring formation, caused by intermittent PTH (daily subcutaneous injection) therapy (Jilka 2007, Dempster, Zhou et al. 2017). In postmenopausal women with osteoporosis PTH treatment increases serum markers of bone formation and resorption increases within one month of treatment; whereas the increase in bone resorption makers did not occur until between 3 and 12 months (McClung, San Martin et al. 2005). Similar changes are observed in mice, intermittent PTH increases osteoblast number by stimulating differentiation, attenuating apoptosis or both (Jilka, O'Brien et al. 2009).

Generally, continuously elevated serum PTH levels are considered to have catabolic effects in bone. This effect is observed in both animal and human models. Treatment of rats with continuous infusion of PTH 1-84 resulted in an increase in both formation and resorption. However, the increases in formation and resorption favored resorption resulting in a net decrease in trabecular bone (Tam, Heersche et al. 1982). Similarly, continuously administered PTH 1-34 caused a dose dependent decrease in dry weight of the femur and a hyperparathyroidism-like condition in the highest dose (214 ng/kg/h) group in rats (Uzawa, Hori et al. 1995). This is also consistent with the findings (on a cellular level) of Bellido et al. in female Swiss Webster mice. Continuous PTH 1-84 treatment for 7 days resulted in an increase in osteoclast number at day 2 followed by an increase in osteoblast number at day 4. Whereas, daily injections of PTH 1-84 did not affect osteoclast number and the increase in osteoblast number

was significantly larger than that of continuous treatment (Bellido, Ali et al. 2003). However, in male Sprague Dawley rats infused continuously with PTH 1-34 for 12 days (4 μg/100g/day) the effect of PTH was inconsistent. Upon repeating the experiment 3 times, one of the three experiments showed bone formation was increased with continuous PTH treatment (n =7 per group) over that of vehicle treated animals. However, the other two experiments showed no difference between animals receiving vehicle treatment versus continuous PTH 1-34 treatment (Hock and Gera 1992).

This variable response to continuous exposure to PTH on the cellular level and in rats is somewhat similar to variation between the effects on cortical and trabecular bone in humans with primary hyperparathyroidism (PHPT). Cortical bone loss is characteristic of primary hyperparathyroidism, however trabecular bone may be preserved or even enhanced (Silverberg, Shane et al. 1989, Parisien, Silverberg et al. 1990). In the classic presentation of PHPT, transiliac biopsies exhibit increased cortical porosity as well as reduced cortical width, but preservation or enhancement of trabecular bone architecture (Parisien, Silverberg et al. 1990). Patients with asymptomatic PHPT demonstrated reduced bone mineral density at cortical sites, but at more cancellous sites (like the lumbar spine) it was preserved (Silverberg, Walker et al. 2013). Furthermore, postmenopausal women with mild PHPT, resulting in increased PTH levels (normal: 10-65 pg/mL, elevated: 116 +/- 19 pg/mL), have demonstrated a preservation of cancellous bone (Dempster, Parisien et al. 1999, Dempster, Muller et al. 2007). The benefits of this preservation may, however, be limited. Older studies show no correlation between mild asymptomatic PHPT and risk factor for vertebral fractures (Wilson, Rao et al. 1988). However, more recent studies indicate even if bone mineral density is preserved, the risk of vertebral fracture is higher in

postmenopausal patients with mild PHPT. The risk of vertebral fracture appears independent of severity of PHPT. It has been suggested that bone quality may play a role (De Geronimo, Romagnoli et al. 2006). Microarchitectural abnormalities in trabecular bone at the radius and tibia, resulted in decreased whole bone stiffness and trabecular stiffness (Stein, Silva et al. 2013). Ultimately, there is inconsistency in skeletal response to continuously elevated PTH. The factors responsible for this variability are not entirely clear. Studies have examined the correlation of demographic factors as well as co-existing deficiencies (i.e. serum 25-hydroxyvitamin D (25OHD)) with severity of PHPT as well as the impact on BMD and bone turnover (Grey, Lucas et al. 2005, Moosgaard, Christensen et al. 2008, Stein, Dempster et al. 2011, Walker, Nishiyama et al. 2016, Makras and Anastasilakis 2017). However, no clear explanation stands out. Perhaps there is a threshold above which continuously elevated PTH is catabolic and below which it is anabolic.

Based on the success seen with the anabolic capabilities of PTH as an osteoporosis treatment, it follows that there may also be implications for use in bone regeneration studies. Though it may seem the benefits of utilizing PTH for bone regeneration are limited to intermittent administration, some of the aforementioned findings suggest continuously elevated PTH can be anabolic in certain circumstances. The catabolic effects of continuous administration/elevation of PTH are somewhat inconsistent dependent on concentration, skeletal site, and bone type (cortical or trabecular). The observation of the protective effect PHPT has on trabecular bone volume and mineral density as well as the inconsistencies seen in animal studies raise the possibility of beneficial potential for continuously administered PTH at sites of relatively high remodeling as well. The unique ability of PTH to increase bone formation, as opposed to decreasing resorption, makes it a molecule of interest for bone regeneration applications.

Effect of systemically delivered PTH on fracture healing/bone regeneration

The ability of PTH to increase remodeling in bone gives it great potential in the realm of fracture healing. In general, the biggest impacts of PTH are seen at high remodeling sites (like in trabecular bone or the spine). This appears to be the case for both the anabolic effect of intermittently administered PTH as well as any positive effects observed with continuously elevated PTH. Though many bone regeneration models are at cortical bone sites (relatively lower remodeling than trabecular bone), a noticeable effect may still be observed as a fracture site is an area of high bone turn over (Skripitz, Andreassen et al. 2000). Incorporation of PTH into the treatment process for segmental defects could enhance the healing process and greatly improve quality of life for the people affected by segmental bone defects or non-union fractures. A study comparing the effects of PTH 1-34 on new bone formation and normal baseline remodeling in rats showed PTH 1-34 (60 μg/kg) having a strong regenerative effect on bone (Skripitz, Andreassen et al. 2000). Similarly, treatment with PTH 35 μg/kg or 105 μg/kg 3 times per week resulted in a dose dependent increase in bone formation in bone chambers in calvaria of rats (Tsunori, Sato et al. 2015). Intermittent injections of PTH 1-34 have also been shown to enhance guided bone healing in rat calvarial defects (Andreassen and Cacciafesta 2004). More recently, treatment with 100 μg/kg 3 times per week for 8 weeks increased union rate and accelerated healing in a refractory fracture model in rats (Kumabe, Lee et al. 2017). PTH delivered at 10, 40 and 200 μg/kg/day similarly results in dose dependent increases in bone formation in the fracture callus in mice (Milstrey, Wieskoetter et al. 2017). In male rats, 75 μg/kg/d PTH 1-84 for 12 weeks resulted in a significantly higher percentage of the defect filled (Hamann, Picke et al. 2014). Daily injections of PTH 1-34 (15 nmol/kg/day) and PTH 1-31 (15 nmol/kg/day) have been shown to

increase the external volume and strength of closed fracture calluses (Andreassen, Willick et al. 2004). Similarly, closed fractures in rats treated with daily injections of PTH showed an increase in bone mineral content, bone mineral density, and cartilage volume (Alkhiary, Gerstenfeld et al. 2005); and accelerated healing was observed with PTH treatment in a closed fracture model in female cynomolgus monkeys (Manabe, Mori et al. 2007).

An increase in union rate has not been observed in research models as a result of PTH treatment for open fractures. However, like with closed fractures, treatment has been shown to increase callus volume, bone mineral content, and bone volume fraction (Tagil, McDonald et al.). Subcutaneous injections of 40 μg/kg PTH in mice resulted in enhanced healing (increased bone volume and BMC) in an open defect reconstructed with a PLA/βTCP scaffold (Jacobson, Yanoso-Scholl et al. 2011). Likewise, rats subject to injections of PTH 1-34 every other day during distraction osteogenesis showed an increased callus volume, mechanical strength and an increase in the amount of mineralized bone (Seebach, Skripitz et al. 2004). Daily systemic injections of PTH 1-34 (40 μg/kg) have also been shown to enhance osseointegration of devitalized femoral allografts in a critical size femoral defect model in mice (Reynolds, Takahata et al. 2011). Subcutaneous injections of PTH 1-34 for 8 weeks have also been shown to increase titanium implant anchorage in low-density trabecular bone in rats (Gabet, Muller et al. 2006). Data for use of PTH for bone regeneration in humans is less prevalent than animal data, however, it is noteworthy. An “off label” clinical dose of PTH 1-84 given to a 48 year old male with a femoral non-union that would not heal despite an autograft in combination with BMP-7, enhanced healing sufficiently that the patient regained use of the limb by the one year follow up (Paridis and Karachalios 2011).

The cellular mechanism involved in how PTH affects bone regeneration as well as the ideal treatment regime are not entirely clear. In mice, when duration of treatment was investigated, it was found that immediate treatment for only 2 weeks was sufficient to increase the ultimate torque of the grafted femur. Four weeks of treatment showed no increased benefit in terms of bone strength. In regard to timing of the start of treatment, delaying PTH treatment until 4 weeks after surgery was completely ineffective, whereas delaying only 1 or 2 weeks resulted in equivalent biomechanical properties as initiation of treatment at day 1 (Takahata, Schwarz et al. 2012). When used in conjunction with devitalized allografts, PTH 1-34 (40 μg/kg/d) increased callus volume and mineral content, but did not affect allograft bone volume or osteoclasts or resorption surfaces suggesting no increase in graft resorption (Reynolds, Takahata et al. 2011). Similarly, bone chambers in rats treated with PTH bone ingrowth filled the cavity, whereas the chambers in untreated rats formed marrow cavities and the corresponding decrease in bone volume, implying PTH treatment had a net anti-resorptive effect (Skripitz, Andreassen et al. 2000). However, a closed fracture model in female cynomolgus monkeys indicated PTH accelerated natural fracture healing process by shrinking callus size and increasing degree of mineralization of the fracture callus (accelerating callus remodeling) (Manabe, Mori et al. 2007). Low dose intermittent PTH (10 μg/kg) has also been shown to induce a larger cartilaginous callus during fracture healing, though it does not delay chondrocyte differentiation (Nakazawa, Nakajima et al. 2005). Intermittent PTH (10 μg/kg/day) appeared to enhance (closed) fracture healing in rats by early stimulation of proliferation and differentiation of osteoprogenitor cells, increased production of bone matrix proteins, and enhanced osteoclastogenesis during callus remodeling (Nakajima, Shimoji et al. 2002). Similarly, PTH mediated enhancement of (closed)

fracture repair has also been associated with amplified chondrocyte recruitment and maturation in early fracture callus. There was also an increase in canonical Wnt signaling (expression of Wnts 4,5a,5b,10b) indicating that PTH effects are in part mediated through Wnt-signaling pathways (Kakar, Einhorn et al. 2007); a signaling pathway that plays a pivotal role in regulation of bone mass and has potential to improve healing (Chen and Alman 2009).

The potential positive impacts of PTH use for bone regeneration applications may extend beyond bone cells. Systemic PTH has been shown to not only modulate bone parameters (higher bone volume, mineralization) but also vascular parameters in rats (decrease in blood vessel volume, increase in vessel thickness) which could also aid in fracture healing (Langer, Prisby et al. 2011). Bone endothelial cells are capable of responding to bone modulators including PTH (Brandi and Collin-Osdoby 2006). PTH also enhances migration of CD45+/CD34+ (angiogenic progenitor cells) stem cells (Zaruba, Huber et al. 2008). Similarly, patients with primary hyperparathyroidism show an increased number of circulating CD45+/CD34+ stem cells in the peripheral blood (Brunner, Theiss et al. 2007), as well as elevated circulating levels of bone marrow-derived progenitor cells that are positively correlated to PTH levels (Brunner, Theiss et al. 2007). The ability of PTH to facilitate stem cell mobilization is corroborated by phase 1 clinical trial where PTH enhanced CD34+ cells in patients with inadequate CD34+ cell counts (Ballen, Shpall et al. 2007). PTH also has been shown to increase proliferation of bone marrow stem cells and facilitated homing to lethally irradiated recipients (Calvi, Adams et al. 2003). PTH increases number of hematopoietic stem cells in the bone marrow that can be mobilized into the peripheral circulation without G-CSF. With granulocyte-colony stimulating factor (G-CSF), PTH does not affect progenitor cells, rather increases the number of hematopoietic cells that can be mobilized

(Adams, Martin et al. 2007). Thus, the impact PTH has on vascular regeneration as well as proliferation may aid in its anabolic capabilities.

In pursuit of mechanisms behind bone maintenance a variety of models have been explored. An interesting model that provides some unique insight is hibernating animals. Hibernating bears have been explored as a model for disuse osteoporosis (McGee-Lawrence, Carey et al. 2008). Mechanical unloading (disuse) typically results in an imbalance in bone formation and resorption which leads to bone loss. Bears are of interest because though they hibernate approximately 6 months of the year, they do not experience bone loss associated with this disuse period (McGee-Lawrence, Wojda et al. 2009). Based on serum measurements of bone remodeling markers it has been proposed that PTH may have a dominant role in preserving bone formation in hibernating bears (Donahue, Galley et al. 2006). These studies have stimulated exploration of bear PTH as a treatment for osteoporosis. Black bear PTH (bbPTH) is similar to human PTH, differing by only 9 amino acids (only 2 of which are in the functional 1-34 region of the protein). Studies in mice showed bbPTH 1-84 (28 nmol/kg/d) to have an anabolic effect on both wild type mice and dystrophin knockout mice (which exhibit the osteoporotic state associated with duchenne muscular dystrophy). However, the anabolic response was much more robust in mdx mice (7-fold increase) than wild type (2-fold increase) in regard to bone volume fraction (Gray, McGee-Lawrence et al. 2012). Black bear PTH has also been shown to be more anabolic than human PTH in mouse studies as well. Thus, black bear PTH may also provide a greater anabolic response in bone regeneration applications as well as osteoporosis applications. Regardless of type of PTH (species: human or bear, and fragment: 1-34 and 1-84), the positive implications on healing of systemically administered PTH seem evident. Local delivery of PTH may

provide a better method for PTH administration for bone regeneration applications by providing a similar (or possibly better) anabolic effect while also mitigating overall systemic impacts of treatment.

Effect of locally delivered PTH on fracture healing/bone regeneration

The effect of locally delivered PTH on fracture healing and bone regeneration has not been extensively investigated. However, the existing literature yields a generally positive result. Parathyroid hormone delivered via polyethylene glycol (PEG) matrix resulted in a 1.9 fold increase in mineralized bone and 2.3 fold increase in area of regeneration in bone chambers in rabbit calvaria (Jung, Hammerle et al. 2007). Polyethylene glycol (PEG) matrices infused with PTH 1-34 (20 μg/mL) were used to fill a cylindrical defect around a titanium implant in the mandible between the first premolar and second molar. After 12 weeks, matrices infused with PTH had a significantly greater area fraction of newly formed bone within the defect compared to empty defects or defects filled with the PEG matrix alone. The PEG matrix with PTH was as effective as an autogeneous bone graft when comparing newly formed bone volume between groups (Jung, Cochran et al. 2007). Similarly, PTH 1-34 linked to a fibrin gel with a plasmin sensitive link has also been investigated as a method for accelerated bone healing. Cylindrical drill defects in the femur of sheep (8 mm diameter, 13 mm depth) were filled with the gel containing 50, 100, 400, or 1000 μg/mL. After 8 weeks the defects containing the gel with 100 μg/ml PTH exhibited an increased bone volume fraction as compared to the gel control (Arrighi, Mark et al. 2009). Similarly implantation of a gene-activated matrix containing a plasmid coding for PTH fragment 1-34 resulted in new bone filling a segmental defect in a rat (Fang, Zhu et al. 1996). These studies indicate that combinations of PTH and other matrix materials may prove to be a viable option as

a substitute for certain procedures that require bone grafts or the treatment of open fractures or critical size bone defects. PTH 1-34 covalently linked to a fibrin hydrogel (1 mg PTH/mL hydrogel) has also been shown to improve postoperative prognosis of subchondral bone cysts in the distal aspect of the proximal phalanx in horses. Four months after treatment no lameness was observed in the trot, and compared to previous radiographs the subchondral cyst defect and drill hole were narrower and less radiolucent. At 8 months the cyst and drill hole were difficult to discern on radiographs (Fuerst, Derungs et al. 2007). Data for improved healing as a result of locally delivered PTH are presently limited to biomaterial scaffolds continuously delivering PTH to a bone defect. Though pulsatile release of PTH from biomaterial scaffolds has been explored, pulsatile release scaffolds have not been tested in vivo for bone regeneration applications (Liu, Pettway et al. 2007, Jeon and Puleo 2008). The successes seen in the few studies that have explored local PTH delivery have been with biomaterials that continuously release PTH to the local environment. Though these studies indicate locally delivered PTH is a promising method for enhancing bone regeneration it is still unclear what doses are most effective as well as whether or not the successes seen in these applications translate to a critical size defect.

Summary

Large segmental defects in bone (e.g., due to trauma or tumor resection) commonly have complications or fail to heal properly, resulting in delayed or non-union (Livingston, Gordon et al. 2003, Marsell and Einhorn 2010). Factors that may disrupt the healing and put patients at higher risk for non-union include, but are not limited to, inadequate immobilization, high energy trauma/excessive soft tissue damage, ischemia at the fracture site, repeat operations, obesity, smoking, age (over 50), and multiple injury (Buckwalter and Cruess 1991, Karladani, Granhed et

al. 2001, Meyer, Tsahakis et al. 2001, Reed, Joyner et al. 2003, Green, Lubahn et al. 2005, Hinsley, Phillips et al. 2006, Owens, Wenke et al. 2006, Lu, Miclau et al. 2007, Cross, Ficke et al. 2011). Around 2.2 million orthopaedic procedures utilize autografts or allografts each year (Jahangir, Nunley et al. 2008). Autograft is the gold standard, but has the downfalls of limited availability as well as donor site pain and morbidity (Livingston, Gordon et al. 2003, Mahendra and Maclean 2007). Allografts have a higher rate of failure (delayed or non-union) compared to autografts and may present complications due to immunogenicity (Mahendra and Maclean 2007, Meijer, de Bruijn et al. 2007). Disability due to orthopaedic injury has a significant impact on both the patient and the healthcare system. Quality of life for these patients can be severely impacted as healing time may exceed 9 months and multiple treatment attempts may be required if the first is unsuccessful (Paridis and Karachalios 2011). For example, in a case study, treatment attempts with internal fixation, external fixation, and autograft in combination with BMP-7, non-union persisted until off label use of PTH 1-84 was utilized (Paridis and Karachalios 2011). Intermittent PTH is well known to have an anabolic effect on bone (Fox, Miller et al. 2007). Although continuously elevated PTH is often catabolic, postmenopausal women with mild primary hyperparathyroidism (PHPT) demonstrate trabecular bone preservation (Dempster, Muller et al. 2007). Low levels of continuous PTH have also been shown to increase bone formation rate and marrow vascularity in mice (Jilka, O'Brien et al. 2010). PTH 1-34 and PTH 1-84 have similar anabolic effects on bone when delivered intermittently. However, PTH 1-84 may be advantageous because it has a protective effect in postmenopausal women with primary hyperparathyroidism (Dempster, Parisien et al. 1999), PTH 1-84 treatment resulted in the healing of a non-union fracture that was unresponsive to BMP treatment (Paridis and Karachalios 2011)

and PTH 1-84 has an osteosarcoma incidence curve shifted to the right of PTH 1-34 (indicating, given the same exposure of PTH 1-84 as PTH 1-34 there is a lower incidence of osteosarcoma in rats given PTH 1-84) (Jolette, Wilker et al. 2006). Furthermore, the 1-34 fragment of PTH does not naturally occur in vivo (MacGregor, Jilka et al. 1986, Bringhurst, Stern et al. 1988) and may lack biological function that would result from the presence of the c-terminal portion of PTH 1-84 (Divieti, John et al. 2002). There is some evidence to suggest that low dose continuous PTH could be beneficial as an anabolic therapy in bone and may enhance bone regeneration. Continuously released, locally delivered PTH has been shown to improve healing/formation around dental implants in dogs and drill defects in sheep (Jung, Cochran et al. 2007, Arrighi, Mark et al. 2009). However, dose response to local continuously delivered PTH is still unknown. Whether or not the benefits of PTH treatment observed in these models translate to critical size defect models is also unknown. The contribution of the research presented in this dissertation is an increased understanding of the effects of locally delivered PTH on osteoblasts as well as its potential to enhance bone regeneration in a critical size long bone defect. This contribution is significant because presently the skeletal effects of low dose continuous PTH are not well understood. With this increased understanding of the effects of locally delivered continuous administration of PTH on bone regeneration, improved methods for treating segmental defects could be pursued. Bone regeneration through locally delivered parathyroid hormone has the potential to improve functional restoration, even beyond that of allografts and without the drawbacks of current treatments, which would improve the quality of life for patients.

Hypotheses and Aims

Specific Aim 1.

Examine concentration dependent osteogenic responses to PTH in osteoblastic cells in culture. It was hypothesized that low concentrations of continuous PTH stimulation would result in osteoblastic cell activity favorable to bone formation. *Approach 1:* Effects of culturing osteoblastic cells stimulated continuously with 0, 0.00001, 0.0001, 0.001, 0.01, 0.1, 1, 10 or 100 nM PTH or 100 nM PTH intermittently were examined. Osteoblast differentiation (alkaline phosphatase activity) and mineralization (alizarin red staining) were quantified. MC3T3-E1 cells were seeded at 15,000 cells/cm^2 in basal medium (alpha-MEM, supplemented with 10% fetal bovine serum, 1% penicillin/streptomycin solution). Cells were incubated at 37 °C with 5% CO_2 for 24 hours. Basal medium was then changed to osteogenic medium (basal + 50 µg/mL ascorbic acid + 10mM β-Glycerophosphate) (Day 0). Osteogenic medium changes occurred every 72 hours. Cells exposed to continuous concentrations of PTH had PTH combined with media at each change. Cells exposed to intermittent PTH, were exposed to media with 100 nM PTH for 2.5 hours daily 5 days/week. Cell lysate was collected at days 3, 7, 14, 21 and 28 and used to measure ALP. Staining for mineralization was done with Alizarin Red at the same timepoints.

Analyses. Two way analysis of variance (ANOVA) was used to determine differences between treatment groups and timepoints, a p-value of less than 0.05 was considered significant. When significant differences were detected by ANOVA, a Tukey post hoc test was used to compare individual groups to one another.

Specific Aim 2.

Characterize in vitro release of PTH from thiol-ene hydrogels and in vivo thiol-ene hydrogel degradation. It was hypothesized that PTH can be delivered from a scaffold system in a consistent and controllable fashion and in vivo gel degradation can be tracked over time through fluorescent imaging. *Approach 2: PTH release:* Thiol-ene hydrogels were placed in PBS and stored at 37 °C for up to 28 days. Supernatant was collected at 3, 7, 14, 21 and 28 days. Samples were stored at -80 °C until the last sample was collected, at which time the amount of PTH in the supernatant was measured to determine amounts of PTH released from the scaffold.

Verification of PTH bioactivity after release from hydrogel: Thiol-ene hydrogels containing PTH or vehicle solutions were placed in PBS at 37 °C until the desired timepoint. PTH released from hydrogels was collected at days 7, 14, and 21 MC3T3 osteoblastic cells were seeded at 10^4 cells/cm^2 in 6 well plates in basal medium. After 24 hours basal medium was changed to osteogenic medium (basal + 50 μg/mL ascorbic acid+ 10 mM β-Glycerophosphate) (Day 0). On day 3 medium was replaced. On day 5 cells were stimulated with PTH released from the hydrogel, PTH (reconstituted that day) or vehicle for 10 minutes. A cyclic AMP assay was used to verify bioactivity of the PTH released from the scaffold.

In vivo hydrogel degradation: Alexa Fluor 680 was crosslinked to the thiol-ene hydrogel matrix, with or without PPF scaffolds. The labeled hydrogels were placed in subcutaneous pockets in Sprague Dawley rats. Rats were imaged daily until the fluorophore could no longer be detected, or up to 8 weeks in an IVIS Spectrum imaging system.

Analyses. PTH release data was plotted as a function of time to attain a representation of the amount of hydrogel released over the course of 28 days. Similarly, degradation data was plotted

over time to attain a representation of over what time course the hydrogels degrade in vivo.

Specific Aim 3.

Quantify dose dependent effects of locally delivered PTH on bone regeneration in a rat critical size bone defect model. It was hypothesized that locally delivered PTH would enhance bone healing in a critical size defect model. *Approach 3:* Critical size (> 5mm) femoral defects, stabilized by an internal fixation plate, were created in Sprague Dawley rats (250-300g). Local treatment with PTH was delivered via thiol-ene hydrogel and defects were allowed to heal for 12 weeks. Healing was monitored at weeks 4, 8, and 12. At week 12 femurs were collected for micro-computed tomography analysis.

Analyses. One way analysis of variance (ANOVA) was used to determine differences between treatment groups, a p-value of less than 0.05 was considered significant. When significant differences were detected by ANOVA, a Tukey post hoc test was used to compare individual groups to one another.

References.

Adams, G. B., R. P. Martin, I. R. Alley, K. T. Chabner, K. S. Cohen, L. M. Calvi, H. M. Kronenberg and D. T. Scadden (2007). "Therapeutic targeting of a stem cell niche." Nat Biotechnol **25**(2): 238-243.

Alkhiary, Y. M., L. C. Gerstenfeld, E. Krall, M. Westmore, M. Sato, B. H. Mitlak and T. A. Einhorn (2005). "Enhancement of experimental fracture-healing by systemic administration of recombinant human parathyroid hormone (PTH 1-34)." J Bone Joint Surg Am **87**(4): 731-741.

Andreassen, T. T. and V. Cacciafesta (2004). "Intermittent parathyroid hormone treatment enhances guided bone regeneration in rat calvarial bone defects." J Craniofac Surg **15**(3): 424-427; discussion 428-429.

Andreassen, T. T., G. E. Willick, P. Morley and J. F. Whitfield (2004). "Treatment with parathyroid hormone hPTH(1-34), hPTH(1-31), and monocyclic hPTH(1-31) enhances fracture strength and callus amount after withdrawal fracture strength and callus mechanical quality continue to increase." Calcif Tissue Int **74**(4): 351-356.

Arrighi, I., S. Mark, M. Alvisi, B. von Rechenberg, J. A. Hubbell and J. C. Schense (2009). "Bone healing induced by local delivery of an engineered parathyroid hormone prodrug." Biomaterials **30**(9): 1763-1771.

ASTM (2014). Standard for preclinical in vivo evaluation in critical size segmental bone defects.

Atesok, K., R. Li, D. J. Stewart and E. H. Schemitsch (2010). "Endothelial progenitor cells promote fracture healing in a segmental bone defect model." J Orthop Res **28**(8): 1007-1014.

Ballen, K. K., E. J. Shpall, D. Avigan, B. Y. Yeap, D. C. Fisher, K. McDermott, B. R. Dey, E. Attar, S. McAfee, M. Konopleva, J. H. Antin and T. R. Spitzer (2007). "Phase I trial of parathyroid hormone to facilitate stem cell mobilization." Biology of Blood and Marrow Transplantation **13**(7): 838-843.

Banwart, J. C., M. A. Asher and R. S. Hassanein (1995). "Iliac crest bone graft harvest donor site morbidity. A statistical evaluation." Spine (Phila Pa 1976) **20**(9): 1055-1060.

Bellido, T., A. A. Ali, L. I. Plotkin, Q. Fu, I. Gubrij, P. K. Roberson, R. S. Weinstein, C. A. O'Brien, S. C. Manolagas and R. L. Jilka (2003). "Proteasomal degradation of Runx2 shortens parathyroid

hormone-induced anti-apoptotic signaling in osteoblasts. A putative explanation for why intermittent administration is needed for bone anabolism." J Biol Chem **278**(50): 50259-50272.

Black, D. M., S. L. Greenspan, K. E. Ensrud, L. Palermo, J. A. McGowan, T. F. Lang, P. Garnero, M. L. Bouxsein, J. P. Bilezikian and C. J. Rosen (2003). "The effects of parathyroid hormone and alendronate alone or in combination in postmenopausal osteoporosis." N Engl J Med **349**(13): 1207-1215.

Bohner, M. (2000). "Calcium orthophosphates in medicine: from ceramics to calcium phosphate cements." Injury **31 Suppl 4**: 37-47.

Brandi, M. L. and P. Collin-Osdoby (2006). "Vascular biology and the skeleton." J Bone Miner Res **21**(2): 183-192.

Bringhurst, F. R., A. M. Stern, M. Yotts, N. Mizrahi, G. V. Segre and J. T. Potts, Jr. (1988). "Peripheral metabolism of PTH: fate of biologically active amino terminus in vivo." Am J Physiol **255**(6 Pt 1): E886-893.

Brunner, S., H. D. Theiss, A. Murr, T. Negele and W. M. Franz (2007). "Primary hyperparathyroidism is associated with increased circulating bone marrow-derived progenitor cells." Am J Physiol Endocrinol Metab **293**(6): E1670-1675.

Buckwalter, J. and R. Cruess (1991). Fractures in Adults. Philadelphia, J.B. Lippincott Company.

Burdick, J. A. and K. S. Anseth (2002). "Photoencapsulation of osteoblasts in injectable RGD-modified PEG hydrogels for bone tissue engineering." Biomaterials **23**(22): 4315-4323.

Calvi, L. M., G. B. Adams, K. W. Weibrecht, J. M. Weber, D. P. Olson, M. C. Knight, R. P. Martin, E. Schipani, P. Divieti, F. R. Bringhurst, L. A. Milner, H. M. Kronenberg and D. T. Scadden (2003). "Osteoblastic cells regulate the haematopoietic stem cell niche." Nature **425**(6960): 841-846.

Chen, Y. and B. A. Alman (2009). "Wnt Pathway, an Essential Role in Bone Regeneration." Journal of Cellular Biochemistry **106**(3): 353-362.

Chiavistelli, S., A. Giustina and G. Mazziotti (2015). "Parathyroid hormone pulsatility: physiological and clinical aspects." Bone Res **3**: 14049.

Chu, T. M., P. Sargent, S. J. Warden, C. H. Turner and R. L. Stewart (2006). "Preliminary evaluation of a load-bearing BMP-2 carrier for segmental defect regeneration." Biomed Sci Instrum **42**: 42-47.

Connolly, J. F. (1995). "Injectable bone marrow preparations to stimulate osteogenic repair." Clin Orthop Relat Res(313): 8-18.

Coventry, M. B. and E. M. Tapper (1972). "Pelvic instability: a consequence of removing iliac bone for grafting." J Bone Joint Surg Am **54**(1): 83-101.

Cowan, C. M., C. Soo, K. Ting and B. Wu (2005). "Evolving concepts in bone tissue engineering." Curr Top Dev Biol **66**: 239-285.

Cross, J. D., J. R. Ficke, J. R. Hsu, B. D. Masini and J. C. Wenke (2011). "Battlefield orthopaedic injuries cause the majority of long-term disabilities." J Am Acad Orthop Surg **19 Suppl 1**: S1-7.

Dahabreh, Z., G. M. Calori, N. K. Kanakaris, V. S. Nikolaou and P. V. Giannoudis (2009). "A cost analysis of treatment of tibial fracture nonunion by bone grafting or bone morphogenetic protein-7." Int Orthop **33**(5): 1407-1414.

Damien, C. J. and J. R. Parsons (1991). "Bone graft and bone graft substitutes: a review of current technology and applications." J Appl Biomater **2**(3): 187-208.

De Geronimo, S., E. Romagnoli, D. Diacinti, E. D'Erasmo and S. Minisola (2006). "The risk of fractures in postmenopausal women with primary hyperparathyroidism." Eur J Endocrinol **155**(3): 415-420.

Dell, P. C., H. Burchardt and F. P. Glowczewskie, Jr. (1985). "A roentgenographic, biomechanical, and histological evaluation of vascularized and non-vascularized segmental fibular canine autografts." J Bone Joint Surg Am **67**(1): 105-112.

Dempster, D. W., F. Cosman, E. S. Kurland, H. Zhou, J. Nieves, L. Woelfert, E. Shane, K. Plavetic, R. Muller, J. Bilezikian and R. Lindsay (2001). "Effects of daily treatment with parathyroid hormone on bone microarchitecture and turnover in patients with osteoporosis: a paired biopsy study." J Bone Miner Res **16**(10): 1846-1853.

Dempster, D. W., R. Muller, H. Zhou, T. Kohler, E. Shane, M. Parisien, S. J. Silverberg and J. P. Bilezikian (2007). "Preserved three-dimensional cancellous bone structure in mild primary hyperparathyroidism." Bone **41**(1): 19-24.

Dempster, D. W., M. Parisien, S. J. Silverberg, X. G. Liang, M. Schnitzer, V. Shen, E. Shane, D. B. Kimmel, R. Recker, R. Lindsay and J. P. Bilezikian (1999). "On the mechanism of cancellous bone preservation in postmenopausal women with mild primary hyperparathyroidism." J Clin Endocrinol Metab **84**(5): 1562-1566.

Dempster, D. W., H. Zhou, V. A. Ruff, T. E. Melby, J. Alam and K. A. Taylor (2017). "Longitudinal Effects of Teriparatide or Zoledronic Acid on Bone Modeling- and Remodeling-based Formation in the SHOTZ Study." J Bone Miner Res.

Divieti, P., M. R. John, H. Juppner and F. R. Bringhurst (2002). "Human PTH-(7-84) inhibits bone resorption in vitro via actions independent of the type 1 PTH/PTHrP receptor." Endocrinology **143**(1): 171-176.

Dodds, R. A., A. Catterall, L. Bitensky and J. Chayen (1986). "Abnormalities in fracture healing induced by vitamin B6-deficiency in rats." Bone **7**(6): 489-495.

Donahue, S. W., S. A. Galley, M. R. Vaughan, P. Patterson-Buckendahl, L. M. Demers, J. L. Vance and M. E. McGee (2006). "Parathyroid hormone may maintain bone formation in hibernating black bears (Ursus americanus) to prevent disuse osteoporosis." Journal of Experimental Biology **209**(Pt 9): 1630-1638.

Einhorn, T. A. (1998). "The cell and molecular biology of fracture healing." Clin Orthop Relat Res(355 Suppl): S7-21.

Ejersted, C., T. T. Andreassen, H. Oxlund, P. H. Jorgensen, B. Bak, J. Haggblad, O. Torring and M. H. Nilsson (1993). "Human parathyroid hormone (1-34) and (1-84) increase the mechanical strength and thickness of cortical bone in rats." J Bone Miner Res **8**(9): 1097-1101.

Enneking, W. F. and D. A. Campanacci (2001). "Retrieved human allografts : a clinicopathological study." J Bone Joint Surg Am **83-A**(7): 971-986.

Enneking, W. F. and E. R. Mindell (1991). "Observations on massive retrieved human allografts." J Bone Joint Surg Am **73**(8): 1123-1142.

Fang, J., Y. Y. Zhu, E. Smiley, J. Bonadio, J. P. Rouleau, S. A. Goldstein, L. K. McCauley, B. L. Davidson and B. J. Roessler (1996). "Stimulation of new bone formation by direct transfer of osteogenic plasmid genes." Proc Natl Acad Sci U S A **93**(12): 5753-5758.

Fox, J., M. A. Miller, R. R. Recker, C. H. Turner and S. Y. Smith (2007). "Effects of treatment of ovariectomized adult rhesus monkeys with parathyroid hormone 1-84 for 16 months on trabecular and cortical bone structure and biomechanical properties of the proximal femur." Calcif Tissue Int **81**(1): 53-63.

Friedlaender, G. E. (1983). "Immune responses to osteochondral allografts. Current knowledge and future directions." Clin Orthop Relat Res(174): 58-68.

Frost, H. M. (1989). "The biology of fracture healing. An overview for clinicians. Part I." Clin Orthop Relat Res(248): 283-293.

Frost, H. M. (1989). "The biology of fracture healing. An overview for clinicians. Part II." Clin Orthop Relat Res(248): 294-309.

Fu, R., S. Selph, M. McDonagh and et al. (2013). "Effectiveness and harms of recombinant human bone morphogenetic protein-2 in spine fusion: A systematic review and meta-analysis." Annals of Internal Medicine **158**(12): 890-902.

Fuerst, A., S. Derungs, B. von Rechenberg, J. A. Auer, J. Schense and J. Watson (2007). "Use of a parathyroid hormone peptide (PTH(1-34))-enriched fibrin hydrogel for the treatment of a subchondral cystic lesion in the proximal interphalangeal joint of a warmblood filly." J Vet Med A Physiol Pathol Clin Med **54**(2): 107-112.

Gabet, Y., R. Muller, J. Levy, R. Dimarchi, M. Chorev, I. Bab and D. Kohavi (2006). "Parathyroid hormone 1-34 enhances titanium implant anchorage in low-density trabecular bone: a correlative micro-computed tomographic and biomechanical analysis." Bone **39**(2): 276-282.

Giorgio Calori, M., R. Capanna, M. Colombo, P. De Biase, C. O'Sullivan, V. Cartareggia and C. Conti (2013). "Cost effectiveness of tibial nonunion treatment: A comparison between rhBMP-7 and autologous bone graft in two Italian centres." Injury **44**(12): 1871-1879.

Gray, S. K., M. E. McGee-Lawrence, J. L. Sanders, K. W. Condon, C. J. Tsai and S. W. Donahue (2012). "Black bear parathyroid hormone has greater anabolic effects on trabecular bone in dystrophin-deficient mice than in wild type mice." Bone.

Green, E., J. D. Lubahn and J. Evans (2005). "Risk factors, treatment, and outcomes associated with nonunion of the midshaft humerus fracture." J Surg Orthop Adv **14**(2): 64-72.

Grey, A., J. Lucas, A. Horne, G. Gamble, J. S. Davidson and I. R. Reid (2005). "Vitamin D repletion in patients with primary hyperparathyroidism and coexistent vitamin D insufficiency." J Clin Endocrinol Metab **90**(4): 2122-2126.

Grim, J. C., I. A. Marozas and K. S. Anseth (2015). "Thiol-ene and photo-cleavage chemistry for controlled presentation of biomolecules in hydrogels." J Control Release **219**: 95-106.

Guarniero, R., T. E. de Barros Filho, U. Tannuri, C. J. Rodrigues and J. D. Rossi (1992). "Study of fracture healing in protein malnutrition." Rev Paul Med **110**(2): 63-68.

Hak, D. J. (2007). "The use of osteoconductive bone graft substitutes in orthopaedic trauma." J Am Acad Orthop Surg **15**(9): 525-536.

Hamann, C., A. K. Picke, G. M. Campbell, M. Balyura, M. Rauner, R. Bernhardt, G. Huber, M. M. Morlock, K. P. Gunther, S. R. Bornstein, C. C. Gluer, B. Ludwig and L. C. Hofbauer (2014). "Effects of Parathyroid Hormone on Bone Mass, Bone Strength, and Bone Regeneration in Male Rats With Type 2 Diabetes Mellitus." Endocrinology **155**(4): 1197-1206.

Harris, A. M., P. L. Althausen, J. Kellam, M. J. Bosse and R. Castillo (2009). "Complications following limb-threatening lower extremity trauma." J Orthop Trauma **23**(1): 1-6.

Hinsley, D. E., S. L. Phillips and J. S. Clasper (2006). "Ballistic fractures during the 2003 Gulf conflict--early prognosis and high complication rate." J R Army Med Corps **152**(2): 96-101.

Hock, J. M. and I. Gera (1992). "Effects of continuous and intermittent administration and inhibition of resorption on the anabolic response of bone to parathyroid hormone." J Bone Miner Res **7**(1): 65-72.

Holstein, J. H., M. Orth, C. Scheuer, A. Tami, S. C. Becker, P. Garcia, T. Histing, P. Morsdorf, M. Klein, T. Pohlemann and M. D. Menger (2011). "Erythropoietin stimulates bone formation, cell proliferation, and angiogenesis in a femoral segmental defect model in mice." Bone **49**(5): 1037-1045.

Honma, T., T. Itagaki, M. Nakamura, S. Kamakura, I. Takahashi, S. Echigo and Y. Sasano (2008). "Bone formation in rat calvaria ceases within a limited period regardless of completion of defect repair." Oral Dis **14**(5): 457-464.

Huang, J. C., T. Sakata, L. L. Pfleger, M. Bencsik, B. P. Halloran, D. D. Bikle and R. A. Nissenson (2004). "PTH differentially regulates expression of RANKL and OPG." J Bone Miner Res **19**(2): 235-244.

Hunt, T. R., J. R. Schwappach and H. C. Anderson (1996). "Healing of a segmental defect in the rat femur with use of an extract from a cultured human osteosarcoma cell-line (Saos-2). A preliminary report." J Bone Joint Surg Am **78**(1): 41-48.

Ishizuya, T., S. Yokose, M. Hori, T. Noda, T. Suda, S. Yoshiki and A. Yamaguchi (1997). "Parathyroid hormone exerts disparate effects on osteoblast differentiation depending on exposure time in rat osteoblastic cells." J Clin Invest **99**(12): 2961-2970.

Isogai, Y., T. Akatsu, T. Ishizuya, A. Yamaguchi, M. Hori, N. Takahashi and T. Suda (1996). "Parathyroid hormone regulates osteoblast differentiation positively or negatively depending on the differentiation stages." J Bone Miner Res **11**(10): 1384-1393.

Jacobson, J. A., L. Yanoso-Scholl, D. G. Reynolds, T. Dadali, G. Bradica, S. Bukata, E. J. Puzas, M. J. Zuscik, R. Rosier, R. J. O'Keefe, E. M. Schwarz and H. A. Awad (2011). "Teriparatide therapy and beta-tricalcium phosphate enhance scaffold reconstruction of mouse femoral defects." Tissue Eng Part A **17**(3-4): 389-398.

Jahangir, A. A., R. M. Nunley, S. Mehta and A. Sharan (2008) "Bone-graft substitutes in orthopaedic surgery." AAOS Now.

Jakobsen, T., J. Baas, S. Kold, J. E. Bechtold, B. Elmengaard and K. Soballe (2009). "Local Bisphosphonate Treatment Increases Fixation of Hydroxyapatite-Coated Implants Inserted with Bone Compaction." Journal of Orthopaedic Research **27**(2): 189-194.

Jeon, J. H. and D. A. Puleo (2008). "Formulations for intermittent release of parathyroid hormone (1-34) and local enhancement of osteoblast activities." Pharm Dev Technol **13**(6): 505-512.

Jerome, C. P., D. B. Burr, T. Van Bibber, J. M. Hock and R. Brommage (2001). "Treatment with human parathyroid hormone (1-34) for 18 months increases cancellous bone volume and

improves trabecular architecture in ovariectomized cynomolgus monkeys (Macaca fascicularis)." Bone **28**(2): 150-159.

Jiang, Y., J. J. Zhao, B. H. Mitlak, O. Wang, H. K. Genant and E. F. Eriksen (2003). "Recombinant human parathyroid hormone (1-34) [teriparatide] improves both cortical and cancellous bone structure." J Bone Miner Res **18**(11): 1932-1941.

Jilka, R. L. (2007). "Molecular and cellular mechanisms of the anabolic effect of intermittent PTH." Bone **40**(6): 1434-1446.

Jilka, R. L., C. A. O'Brien, A. A. Ali, P. K. Roberson, R. S. Weinstein and S. C. Manolagas (2009). "Intermittent PTH stimulates periosteal bone formation by actions on post-mitotic preosteoblasts." Bone **44**(2): 275-286.

Jilka, R. L., C. A. O'Brien, S. M. Bartell, R. S. Weinstein and S. C. Manolagas (2010). "Continuous elevation of PTH increases the number of osteoblasts via both osteoclast-dependent and -independent mechanisms." J Bone Miner Res **25**(11): 2427-2437.

Jodar-Gimeno, E. (2007). "Full length parathyroid hormone (1-84) in the treatment of osteoporosis in postmenopausal women." Clin Interv Aging **2**(1): 163-174.

Jolette, J., C. E. Wilker, S. Y. Smith, N. Doyle, J. F. Hardisty, A. J. Metcalfe, T. B. Marriott, J. Fox and D. S. Wells (2006). "Defining a noncarcinogenic dose of recombinant human parathyroid hormone 1-84 in a 2-year study in Fischer 344 rats." Toxicol Pathol **34**(7): 929-940.

Jung, R. E., D. L. Cochran, O. Domken, R. Seibl, A. A. Jones, D. Buser and C. H. Hammerle (2007). "The effect of matrix bound parathyroid hormone on bone regeneration." Clin Oral Implants Res **18**(3): 319-325.

Jung, R. E., C. H. F. Hammerle, V. Kokovic and F. E. Weber (2007). "Bone regeneration using a synthetic matrix containing a parathyroid hormone peptide combined with a grafting material." International Journal of Oral & Maxillofacial Implants **22**(2): 258-266.

Kakar, S., T. A. Einhorn, S. Vora, L. J. Miara, G. Hon, N. A. Wigner, D. Toben, K. A. Jacobsen, M. O. Al-Sebaei, M. Song, P. C. Trackman, E. F. Morgan, L. C. Gerstenfeld and G. L. Barnes (2007). "Enhanced chondrogenesis and Wnt signaling in PTH-treated fractures." J Bone Miner Res **22**(12): 1903-1912.

Kanakaris, N. K., N. Lasanianos, G. M. Calori, R. Verdonk, T. J. Blokhuis, P. Cherubino, P. De Biase and P. V. Giannoudis (2009). "Application of bone morphogenetic proteins to femoral non-unions: a 4-year multicentre experience." Injury **40 Suppl 3**: S54-61.

Karaplis, A. C. and D. Goltzman (2000). "PTH and PTHrP effects on the skeleton." Rev Endocr Metab Disord **1**(4): 331-341.

Karladani, A. H., H. Granhed, J. Karrholm and J. Styf (2001). "The influence of fracture etiology and type on fracture healing: a review of 104 consecutive tibial shaft fractures." Arch Orthop Trauma Surg **121**(6): 325-328.

Kempen, D. H., L. Lu, T. E. Hefferan, L. B. Creemers, A. Maran, K. L. Classic, W. J. Dhert and M. J. Yaszemski (2008). "Retention of in vitro and in vivo BMP-2 bioactivities in sustained delivery vehicles for bone tissue engineering." Biomaterials **29**(22): 3245-3252.

Kempen, D. H., L. Lu, C. Kim, X. Zhu, W. J. Dhert, B. L. Currier and M. J. Yaszemski (2006). "Controlled drug release from a novel injectable biodegradable microsphere/scaffold composite based on poly(propylene fumarate)." J Biomed Mater Res A **77**(1): 103-111.

Kim, H. W., H. H. Lee and J. C. Knowles (2006). "Electrospinning biomedical nanocomposite fibers of hydroxyapatite/poly(lactic acid) for bone regeneration." J Biomed Mater Res A **79**(3): 643-649.

Kim, J., T. E. Hefferan, M. J. Yaszemski and L. Lu (2009). "Potential of hydrogels based on poly(ethylene glycol) and sebacic acid as orthopedic tissue engineering scaffolds." Tissue Eng Part A **15**(8): 2299-2307.

Kim, K. H., L. Jeong, H. N. Park, S. Y. Shin, W. H. Park, S. C. Lee, T. I. Kim, Y. J. Park, Y. J. Seol, Y. M. Lee, Y. Ku, I. C. Rhyu, S. B. Han and C. P. Chung (2005). "Biological efficacy of silk fibroin nanofiber membranes for guided bone regeneration." J Biotechnol **120**(3): 327-339.

Kolambkar, Y. M., K. M. Dupont, J. D. Boerckel, N. Huebsch, D. J. Mooney, D. W. Hutmacher and R. E. Guldberg (2011). "An alginate-based hybrid system for growth factor delivery in the functional repair of large bone defects." Biomaterials **32**(1): 65-74.

Kolambkar, Y. M., A. Peister, A. K. Ekaputra, D. W. Hutmacher and R. E. Guldberg (2010). "Colonization and osteogenic differentiation of different stem cell sources on electrospun nanofiber meshes." Tissue Eng Part A **16**(10): 3219-3230.

Kondo, H., T. Ohyama, K. Ohya and S. Kasugai (1997). "Temporal changes of mRNA expression of matrix proteins and parathyroid hormone and parathyroid hormone-related protein (PTH/PTHrP) receptor in bone development." J Bone Miner Res **12**(12): 2089-2097.

Kumabe, Y., S. Y. Lee, T. Waki, T. Iwakura, S. Takahara, M. Arakura, Y. Kuroiwa, T. Fukui, T. Matsumoto, T. Matsushita, K. Nishida, R. Kuroda and T. Niikura (2017). "Triweekly administration of parathyroid hormone (1-34) accelerates bone healing in a rat refractory fracture model." BMC Musculoskelet Disord **18**(1): 545.

Langer, M., R. Prisby, Z. Peter, A. Guignandon, M. H. Lafage-Proust and F. Peyrin (2011). "Simultaneous 3D Imaging of Bone and Vessel Microstructure in a Rat Model." Ieee Transactions on Nuclear Science **58**(1): 139-145.

Le Guehennec, L., E. Goyenvalle, E. Aguado, P. Pilet, M. Bagot D'Arc, M. Bilban, R. Spaethe and G. Daculsi (2005). "MBCP biphasic calcium phosphate granules and tissucol fibrin sealant in rabbit femoral defects: the effect of fibrin on bone ingrowth." J Mater Sci Mater Med **16**(1): 29-35.

Lee, J., W. I. Choi, G. Tae, Y. H. Kim, S. S. Kang, S. E. Kim, S. H. Kim and Y. Jung (2011). "Enhanced regeneration of the ligament-bone interface using a poly(L-lactide-co-epsilon-caprolactone) scaffold with local delivery of cells/BMP-2 using a heparin-based hydrogel." Acta Biomater **7**(1): 244-257.

Lee, K. W., S. Wang, B. C. Fox, E. L. Ritman, M. J. Yaszemski and L. Lu (2007). "Poly(propylene fumarate) bone tissue engineering scaffold fabrication using stereolithography: effects of resin formulations and laser parameters." Biomacromolecules **8**(4): 1077-1084.

Lewandrowski, K. U., M. V. Cattaneo, J. D. Gresser, D. L. Wise, R. L. White, L. Bonassar and D. J. Trantolo (1999). "Effect of a poly(propylene fumarate) foaming cement on the healing of bone defects." Tissue Eng **5**(4): 305-316.

Li, R., K. Atesok, A. Nauth, D. Wright, E. Qamirani, C. M. Whyne and E. H. Schemitsch (2011). "Endothelial progenitor cells for fracture healing: a microcomputed tomography and biomechanical analysis." J Orthop Trauma **25**(8): 467-471.

Liu, X. and P. X. Ma (2004). "Polymeric scaffolds for bone tissue engineering." Ann Biomed Eng **32**(3): 477-486.

Liu, X., G. J. Pettway, L. K. McCauley and P. X. Ma (2007). "Pulsatile release of parathyroid hormone from an implantable delivery system." Biomaterials **28**(28): 4124-4131.

Livingston, T. L., S. Gordon, M. Archambault, S. Kadiyala, K. McIntosh, A. Smith and S. J. Peter (2003). "Mesenchymal stem cells combined with biphasic calcium phosphate ceramics promote bone regeneration." J Mater Sci Mater Med **14**(3): 211-218.

Locklin, R. M., S. Khosla, R. T. Turner and B. L. Riggs (2003). "Mediators of the biphasic responses of bone to intermittent and continuously administered parathyroid hormone." J Cell Biochem **89**(1): 180-190.

Lu, C., T. Miclau, D. Hu and R. S. Marcucio (2007). "Ischemia leads to delayed union during fracture healing: a mouse model." Journal of Orthopaedic Research **25**(1): 51-61.

Luca, L., A. L. Rougemont, B. H. Walpoth, L. Boure, A. Tami, J. M. Anderson, O. Jordan and R. Gurny (2011). "Injectable rhBMP-2-loaded chitosan hydrogel composite: osteoinduction at ectopic site and in segmental long bone defect." J Biomed Mater Res A **96**(1): 66-74.

Lyons, F. G., A. A. Al-Munajjed, S. M. Kieran, M. E. Toner, C. M. Murphy, G. P. Duffy and F. J. O'Brien (2010). "The healing of bony defects by cell-free collagen-based scaffolds compared to stem cell-seeded tissue engineered constructs." Biomaterials **31**(35): 9232-9243.

MacGregor, R. R., R. L. Jilka and J. W. Hamilton (1986). "Formation and secretion of fragments of parathormone. Identification of cleavage sites." J Biol Chem **261**(4): 1929-1934.

Mahendra, A. and A. D. Maclean (2007). "Available biological treatments for complex non-unions." Injury **38 Suppl 4**: S7-12.

Makras, P. and A. D. Anastasilakis (2017). "Bone Disease in Primary Hyperparathyroidism." Metabolism.

Manabe, T., S. Mori, T. Mashiba, Y. Kaji, K. Iwata, S. Komatsubara, A. Seki, Y. X. Sun and T. Yamamoto (2007). "Human parathyroid hormone (1-34) accelerates natural fracture healing process in the femoral osteotomy model of cynomolgus monkeys." Bone **40**(6): 1475-1482.

Mariner, P. D., J. M. Wudel, D. E. Miller, E. E. Genova, S. O. Streubel and K. S. Anseth (2013). "Synthetic hydrogel scaffold is an effective vehicle for delivery of INFUSE (rhBMP2) to critical-sized calvaria bone defects in rats." J Orthop Res **31**(3): 401-406.

Marsell, R. and T. A. Einhorn (2010). "Emerging bone healing therapies." J Orthop Trauma **24 Suppl 1**: S4-8.

Martinez-Sanz, E., D. A. Ossipov, J. Hilborn, S. Larsson, K. B. Jonsson and O. P. Varghese (2011). "Bone reservoir: Injectable hyaluronic acid hydrogel for minimal invasive bone augmentation." J Control Release **152**(2): 232-240.

McClung, M. R., J. San Martin, P. D. Miller, R. Civitelli, F. Bandeira, M. Omizo, D. W. Donley, G. P. Dalsky and E. F. Eriksen (2005). "Opposite bone remodeling effects of teriparatide and alendronate in increasing bone mass." Arch Intern Med **165**(15): 1762-1768.

McGee-Lawrence, M. E., H. V. Carey and S. W. Donahue (2008). "Mammalian hibernation as a model of disuse osteoporosis: the effects of physical inactivity on bone metabolism, structure, and strength." American Journal of Physiology Regulatory, Integrative and Comparative Physiology **295**(6): R1999-2014.

McGee-Lawrence, M. E., S. J. Wojda, L. N. Barlow, T. D. Drummer, K. Bunnell, J. Auger, H. L. Black and S. W. Donahue (2009). "Six months of disuse during hibernation does not increase intracortical porosity or decrease cortical bone geometry, strength, or mineralization in black bear (Ursus americanus) femurs." Journal of Biomechanics **42**(10): 1378-1383.

Megas, P. (2005). "Classification of non-union." Injury **36 Suppl 4**: S30-37.

Meijer, G. J., J. D. de Bruijn, R. Koole and C. A. van Blitterswijk (2007). "Cell-based bone tissue engineering." PLoS Med **4**(2): e9.

Mendes, S. C., M. Sleijster, A. Van Den Muysenberg, J. D. De Bruijn and C. A. Van Blitterswijk (2002). "A cultured living bone equivalent enhances bone formation when compared to a cell seeding approach." J Mater Sci Mater Med **13**(6): 575-581.

Meyer, R. A., Jr., P. J. Tsahakis, D. F. Martin, D. M. Banks, M. E. Harrow and G. M. Kiebzak (2001). "Age and ovariectomy impair both the normalization of mechanical properties and the accretion of mineral by the fracture callus in rats." J Orthop Res **19**(3): 428-435.

Mills, L. A., S. A. Aitken and A. Simpson (2017). "The risk of non-union per fracture: current myths and revised figures from a population of over 4 million adults." Acta Orthop **88**(4): 434-439.

Milstrey, A., B. Wieskoetter, D. Hinze, N. Grueneweller, R. Stange, T. Pap, M. Raschke and P. Garcia (2017). "Dose-dependent effect of parathyroid hormone on fracture healing and bone formation in mice." J Surg Res **220**: 327-335.

Moosgaard, B., S. E. Christensen, P. Vestergaard, L. Heickendorff, P. Christiansen and L. Mosekilde (2008). "Vitamin D metabolites and skeletal consequences in primary hyperparathyroidism." Clin Endocrinol (Oxf) **68**(5): 707-715.

Mosekilde, L., C. H. Sogaard, C. C. Danielsen and O. Torring (1991). "The anabolic effects of human parathyroid hormone (hPTH) on rat vertebral body mass are also reflected in the quality of bone, assessed by biomechanical testing: a comparison study between hPTH-(1-34) and hPTH-(1-84)." Endocrinology **129**(1): 421-428.

Murphy, W. L., C. A. Simmons, D. Kaigler and D. J. Mooney (2004). "Bone regeneration via a mineral substrate and induced angiogenesis." J Dent Res **83**(3): 204-210.

Nakagawa, N., M. Kinosaki, K. Yamaguchi, N. Shima, H. Yasuda, K. Yano, T. Morinaga and K. Higashio (1998). "RANK is the essential signaling receptor for osteoclast differentiation factor in osteoclastogenesis." Biochem Biophys Res Commun **253**(2): 395-400.

Nakajima, A., N. Shimoji, K. Shiomi, S. Shimizu, H. Moriya, T. A. Einhorn and M. Yamazaki (2002). "Mechanisms for the enhancement of fracture healing in rats treated with intermittent low-dose human parathyroid hormone (1-34)." J Bone Miner Res **17**(11): 2038-2047.

Nakazawa, T., A. Nakajima, K. Shiomi, H. Moriya, T. A. Einhorn and M. Yamazaki (2005). "Effects of low-dose, intermittent treatment with recombinant human parathyroid hormone (1-34) on chondrogenesis in a model of experimental fracture healing." Bone **37**(5): 711-719.

Nandi, S. K., S. Roy, P. Mukherjee, B. Kundu, D. K. De and D. Basu (2010). "Orthopaedic applications of bone graft & graft substitutes: a review." Indian J Med Res **132**: 15-30.

Neer, R. M., C. D. Arnaud, J. R. Zanchetta, R. Prince, G. A. Gaich, J. Y. Reginster, A. B. Hodsman, E. F. Eriksen, S. Ish-Shalom, H. K. Genant, O. Wang and B. H. Mitlak (2001). "Effect of parathyroid hormone (1-34) on fractures and bone mineral density in postmenopausal women with osteoporosis." N Engl J Med **344**(19): 1434-1441.

Nishida, S., A. Yamaguchi, T. Tanizawa, N. Endo, T. Mashiba, Y. Uchiyama, T. Suda, S. Yoshiki and H. E. Takahashi (1994). "Increased bone formation by intermittent parathyroid hormone administration is due to the stimulation of proliferation and differentiation of osteoprogenitor cells in bone marrow." Bone **15**(6): 717-723.

Oest, M. E., K. M. Dupont, H. J. Kong, D. J. Mooney and R. E. Guldberg (2007). "Quantitative assessment of scaffold and growth factor-mediated repair of critically sized bone defects." J Orthop Res **25**(7): 941-950.

Owens, B. D., J. C. Wenke, S. J. Svoboda and D. W. White (2006). "Extremity trauma research in the United States Army." J Am Acad Orthop Surg **14**(10 Spec No.): S37-40.

Ozturan, K. E., B. Demir, I. Yucel, H. Cakici, F. Yilmaz and A. Haberal (2011). "Effect of strontium ranelate on fracture healing in the osteoporotic rats." J Orthop Res **29**(1): 138-142.

Paridis, D. and T. Karachalios (2011). "Atrophic femoral bone nonunion treated with 1-84 PTH." J Musculoskelet Neuronal Interact **11**(4): 320-322; quiz 323.

Parisien, M., S. J. Silverberg, E. Shane, L. de la Cruz, R. Lindsay, J. P. Bilezikian and D. W. Dempster (1990). "The histomorphometry of bone in primary hyperparathyroidism: preservation of cancellous bone structure." J Clin Endocrinol Metab **70**(4): 930-938.

Perumal, V. and C. S. Roberts (2007). "(ii) Factors contributing to non-union of fractures." Current Orthopaedics **21**(4): 258-261.

Potts, J. T., Jr., H. M. Kronenberg and M. Rosenblatt (1982). "Parathyroid hormone: chemistry, biosynthesis, and mode of action." Adv Protein Chem **35**: 323-396.

Rai, B., M. E. Oest, K. M. Dupont, K. H. Ho, S. H. Teoh and R. E. Guldberg (2007). "Combination of platelet-rich plasma with polycaprolactone-tricalcium phosphate scaffolds for segmental bone defect repair." J Biomed Mater Res A **81**(4): 888-899.

Reed, A. A., C. J. Joyner, S. Isefuku, H. C. Brownlow and A. H. Simpson (2003). "Vascularity in a new model of atrophic nonunion." J Bone Joint Surg Br **85**(4): 604-610.

Reynolds, D. G., M. Takahata, A. L. Lerner, R. J. O'Keefe, E. M. Schwarz and H. A. Awad (2011). "Teriparatide therapy enhances devitalized femoral allograft osseointegration and biomechanics in a murine model." Bone **48**(3): 562-570.

Ring, D., W. T. Barrick and J. B. Jupiter (1997). "Recalcitrant nonunion." Clin Orthop Relat Res(340): 181-189.

Rüedi, T. P. and W. M. Murphy (2000). AO principles of fracture management. Stuttgart ; New York

Davos Platz, Switzerland, Thieme ;

AO Pub.

Schiller, P. C., G. D'Ippolito, B. A. Roos and G. A. Howard (1999). "Anabolic or catabolic responses of MC3T3-E1 osteoblastic cells to parathyroid hormone depend on time and duration of treatment." J Bone Miner Res **14**(9): 1504-1512.

Schindeler, A., M. M. McDonald, P. Bokko and D. G. Little (2008). "Bone remodeling during fracture repair: The cellular picture." Semin Cell Dev Biol **19**(5): 459-466.

Schmitz, J. P. and J. O. Hollinger (1986). "The critical size defect as an experimental model for craniomandibulofacial nonunions." Clin Orthop Relat Res(205): 299-308.

Seebach, C., R. Skripitz, T. T. Andreassen and P. Aspenberg (2004). "Intermittent parathyroid hormone (1-34) enhances mechanical strength and density of new bone after distraction osteogenesis in rats." J Orthop Res **22**(3): 472-478.

Silverberg, S. J., E. Shane, L. de la Cruz, D. W. Dempster, F. Feldman, D. Seldin, T. P. Jacobs, E. S. Siris, M. Cafferty, M. V. Parisien and et al. (1989). "Skeletal disease in primary hyperparathyroidism." J Bone Miner Res **4**(3): 283-291.

Silverberg, S. J., M. D. Walker and J. P. Bilezikian (2013). "Asymptomatic primary hyperparathyroidism." J Clin Densitom **16**(1): 14-21.

Singh, R., S. Bleibleh, N. K. Kanakaris and P. V. Giannoudis (2016). "Upper limb non-unions treated with BMP-7: efficacy and clinical results." Injury **47 Suppl 6**: S33-S39.

Skripitz, R., T. T. Andreassen and P. Aspenberg (2000). "Strong effect of PTH (1-34) on regenerating bone: a time sequence study in rats." Acta Orthop Scand **71**(6): 619-624.

Stein, E. M., D. W. Dempster, J. Udesky, H. Zhou, J. P. Bilezikian, E. Shane and S. J. Silverberg (2011). "Vitamin D deficiency influences histomorphometric features of bone in primary hyperparathyroidism." Bone **48**(3): 557-561.

Stein, E. M., B. C. Silva, S. Boutroy, B. Zhou, J. Wang, J. Udesky, C. Zhang, D. J. McMahon, M. Romano, E. Dworakowski, A. G. Costa, N. Cusano, D. Irani, S. Cremers, E. Shane, X. E. Guo and J. P. Bilezikian (2013). "Primary hyperparathyroidism is associated with abnormal cortical and trabecular microstructure and reduced bone stiffness in postmenopausal women." J Bone Miner Res **28**(5): 1029-1040.

Stevenson, S., S. E. Emery and V. M. Goldberg (1996). "Factors affecting bone graft incorporation." Clin Orthop Relat Res(324): 66-74.

Stevenson, S. and M. Horowitz (1992). "The response to bone allografts." J Bone Joint Surg Am **74**(6): 939-950.

Street, J. T., J. H. Wang, Q. D. Wu, A. Wakai, A. McGuinness and H. P. Redmond (2001). "The angiogenic response to skeletal injury is preserved in the elderly." J Orthop Res **19**(6): 1057-1066.

Stuermer, E. K., S. Sehmisch, T. Rack, E. Wenda, D. Seidlova-Wuttke, M. Tezval, W. Wuttke, K. H. Frosch and K. M. Stuermer (2010). "Estrogen and raloxifene improve metaphyseal fracture healing in the early phase of osteoporosis. A new fracture-healing model at the tibia in rat." Langenbecks Arch Surg **395**(2): 163-172.

Tagil, M., M. M. McDonald, A. Morse, L. Peacock, K. Mikulec, N. Amanat, C. Godfrey and D. G. Little "Intermittent PTH(1-34) does not increase union rates in open rat femoral fractures and exhibits attenuated anabolic effects compared to closed fractures." Bone **46**(3): 852-859.

Takahata, M., E. M. Schwarz, T. Chen, R. J. O'Keefe and H. A. Awad (2012). "Delayed short-course treatment with teriparatide (PTH1-34) improves femoral allograft healing by enhancing intramembranous bone formation at the graft-host junction." Journal of Bone and Mineral Research **27**(1): 26-37.

Tam, C. S., J. N. M. Heersche, T. M. Murray and J. A. Parsons (1982). "Parathyroid-Hormone Stimulates the Bone Apposition Rate Independently of Its Resorptive Action - Differential-Effects of Intermittent and Continuous Administration." Endocrinology **110**(2): 506-512.

Tang, X. J. and Q. Y. Wu (2006). "Mesenchymal stem cellular adhesion and cytotoxicity study of random biopolyester scaffolds for tissue engineering." J Mater Sci Mater Med **17**(7): 627-632.

Tian, Y., Y. Xu, Q. Fu and M. He (2011). "Parathyroid hormone regulates osteoblast differentiation in a Wnt/beta-catenin-dependent manner." Mol Cell Biochem **355**(1-2): 211-216.

Tiedeman, J. J., K. L. Garvin, T. A. Kile and J. F. Connolly (1995). "The role of a composite, demineralized bone matrix and bone marrow in the treatment of osseous defects." Orthopedics **18**(12): 1153-1158.

Tiyapatanaputi, P., P. T. Rubery, J. Carmouche, E. M. Schwarz, J. O'Keefe R and X. Zhang (2004). "A novel murine segmental femoral graft model." J Orthop Res **22**(6): 1254-1260.

Tsunori, K., S. Sato, A. Hasuike, S. Manaka, H. Shino, N. Sato, T. Kubota, Y. Arai, K. Ito and M. Miyazaki (2015). "Effects of Intermittent Administration of Parathyroid Hormone on Bone Augmentation in Rat Calvarium." Implant Dentistry **24**(2): 142-148.

Tuli, S. M. and A. D. Singh (1978). "The osteoninductive property of decalcified bone matrix. An experimental study." J Bone Joint Surg Br **60**(1): 116-123.

Tuominen, T., T. Jamsa, J. Oksanen, J. Tuukkanen, T. J. Gao, T. S. Lindholm and P. Jalovaara (2001). "Composite implant composed of hydroxyapatite and bone morphogenetic protein in the healing of a canine ulnar defect." Ann Chir Gynaecol **90**(1): 32-36.

Tzioupis, C. and P. V. Giannoudis (2007). "Prevalence of long-bone non-unions." Injury **38 Suppl 2**: S3-9.

Uzawa, T., M. Hori, S. Ejiri and H. Ozawa (1995). "Comparison of the effects of intermittent and continuous administration of human parathyroid hormone(1-34) on rat bone." Bone **16**(4): 477-484.

Vaccaro, A. R. (2002). "The role of the osteoconductive scaffold in synthetic bone graft." Orthopedics **25**(5 Suppl): s571-578.

Vehof, J. W., J. P. Fisher, D. Dean, J. P. van der Waerden, P. H. Spauwen, A. G. Mikos and J. A. Jansen (2002). "Bone formation in transforming growth factor beta-1-coated porous poly(propylene fumarate) scaffolds." J Biomed Mater Res **60**(2): 241-251.

Walker, M. D., K. K. Nishiyama, B. Zhou, E. Cong, J. Wang, J. A. Lee, A. Kepley, C. Zhang, X. E. Guo and S. J. Silverberg (2016). "Effect of Low Vitamin D on Volumetric Bone Mineral Density, Bone Microarchitecture, and Stiffness in Primary Hyperparathyroidism." J Clin Endocrinol Metab **101**(3): 905-913.

Wheeler, D. L. and W. F. Enneking (2005). "Allograft bone decreases in strength in vivo over time." Clin Orthop Relat Res(435): 36-42.

Wilson, R. J., S. Rao, B. Ellis, M. Kleerekoper and A. M. Parfitt (1988). "Mild asymptomatic primary hyperparathyroidism is not a risk factor for vertebral fractures." Ann Intern Med **109**(12): 959-962.

Wojtowicz, A. M., K. L. Templeman, D. W. Hutmacher, R. E. Guldberg and A. J. Garcia (2010). "Runx2 overexpression in bone marrow stromal cells accelerates bone formation in critical-sized femoral defects." Tissue Eng Part A **16**(9): 2795-2808.

Woo, E. J. (2013). "Adverse events after recombinant human BMP2 in nonspinal orthopaedic procedures." Clin Orthop Relat Res **471**(5): 1707-1711.

Yasuda, H., N. Shima, N. Nakagawa, K. Yamaguchi, M. Kinosaki, S. Mochizuki, A. Tomoyasu, K. Yano, M. Goto, A. Murakami, E. Tsuda, T. Morinaga, K. Higashio, N. Udagawa, N. Takahashi and T. Suda (1998). "Osteoclast differentiation factor is a ligand for osteoprotegerin/osteoclastogenesis-inhibitory factor and is identical to TRANCE/RANKL." Proc Natl Acad Sci U S A **95**(7): 3597-3602.

Yaszemski, M. J., R. G. Payne, W. C. Hayes, R. Langer and A. G. Mikos (1996). "Evolution of bone transplantation: molecular, cellular and tissue strategies to engineer human bone." Biomaterials **17**(2): 175-185.

Zaruba, M. M., B. C. Huber, S. Brunner, E. Deindl, R. David, R. Fischer, G. Assmann, N. Herbach, S. Grundmann, R. Wanke, J. Mueller-Hoecker and W. M. Franz (2008). "Parathyroid hormone treatment after myocardial infarction promotes cardiac repair by enhanced neovascularization and cell survival." Cardiovasc Res **77**(4): 722-731.

Zimmermann, G., C. Wagner, K. Schmeckenbecher, A. Wentzensen and A. Moghaddam (2009). "Treatment of tibial shaft non-unions: bone morphogenetic proteins versus autologous bone graft." Injury **40 Suppl 3**: S50-53.

Chapter 2: Aim 1: **Examine concentration dependent osteogenic responses to PTH in osteoblastic cells in culture.**

Synopsis.

It is well accepted that intermittent (daily injections) of PTH result in a net anabolic effect on bone. However, the impacts of continuously elevated PTH levels are less clear. Generally, continuously elevated serum PTH levels are considered to have catabolic effects in bone. However, there is some inconsistency observed, particularly in humans with mild primary hyperparathyroidism. The factors responsible for the variability in skeletal response to continuously elevated PTH are not entirely clear. It is possible there is a threshold above which continuously elevated PTH is catabolic and below which it is anabolic. Understanding these differences may have implications for improving bone regeneration techniques utilizing locally delivered PTH. A number of studies have demonstrated positive outcomes of daily injections of PTH (intermittent) in bone regeneration/fracture healing studies. However, the skeleton is not the only organ affected by PTH. Thus local delivery of PTH to a fracture site may be desirable in order to avoid systemic effects on organs like the kidneys. Studies examining the effects of locally delivered PTH for bone regeneration applications are relatively limited, but indicate a generally positive result with locally delivered PTH; even though the release of PTH from the biomaterial carriers results in a continuous delivery of PTH. An improved understanding of this observation would be beneficial to the progression of improved therapies for bone regeneration. The goal of this study was to examine concentration dependent osteogenic responses to PTH in osteoblastic cells in culture at lower concentrations than typically studied. MC3T3-E1 osteoblastic cells were cultured untreated or treated with varying concentrations of PTH (0.00001 - 100nM)

continuously or intermittently 100(nM) and quantifying alkaline phosphatase (ALP) activity and mineralization (alizarin red staining) over 28 days in culture (timepoints: 3, 7, 14, 21 and 28 days). Alkaline phosphatase activity was not significantly different ($p > 0.999$) between treatment groups, or timepoints. Interestingly differences with both timepoint and PTH concentration were observed with alizarin red staining for mineralization. Over the timecourse of the study 0 – 0.01 nM PTH treatment resulted in the expected increase in mineralization, with the first significant increase detected by day 14. However, treatment with higher concentrations of PTH (0.1-100 nM) as well as intermittent treatment did not result in an increase in mineralization over 28 days. At days 3, 7, and 14 no difference between treatment groups was observed. However, by day 28 higher concentration treatment groups (0.1 – 100 nM) had significantly less mineralization than lower (0 – 0.01 nM) concentrations ($p < 0.0018$). These results contribute a fundamental understanding of the effects of continuous low dose PTH stimulation on osteoblastic cells. This study indicates a lack of observed negative effect of low dose continuously administered PTH on mineralization of osteoblastic cells. Alkaline phosphatase activity is variable, but not negatively affected at any examined concentration. Though this is not necessarily indicative of potential for improved healing, it lays ground work for in vivo studies to examine whether this effect is observed, or possibly even improved when signals from other cell types come into play. This is important for further development of bone regeneration therapies utilizing continuous PTH release from local delivery systems. Furthermore, it increases the understanding of how various degrees of hyperparathyroidism affect bone metabolism as well as provide a more informed basis for conducting in vivo studies aimed at investigating the mechanism behind the anabolic and catabolic responses to PTH.

2.1 Introduction.

It is well accepted that intermittent (daily injections) of PTH result in a net anabolic effect on bone. PTH decreases the risk of fragility fractures, increases cortical thickness and improves trabecular bone architecture in the ilium of postmenopausal women (Dempster, Cosman et al. 2001, Neer, Arnaud et al. 2001, Black, Greenspan et al. 2003, Jiang, Zhao et al. 2003). The anabolic effect of daily injections of PTH on the skeletal system is fairly well characterized. To the extent recombinant PTH 1-34 is FDA approved for use as an anabolic therapy for osteoporosis. However, the impacts of continuously elevated PTH levels are less clear. Generally, continuously elevated serum PTH levels are considered to have catabolic effects in bone. This effect is observed in both animal and human models (Tam, Heersche et al. 1982, Uzawa, Hori et al. 1995). However, in male Sprague Dawley rats infused continuously with PTH 1-34 for 12 days (4 µg/100g/day) the effect of PTH was inconsistent. One of the three experiments showed bone formation was increased with continuous infusion of PTH (n = 7 per group) over that of vehicle treated animals. However, the other two experiments showed no difference between animals receiving vehicle treatment versus continuous PTH 1-34 treatment (Hock and Gera 1992). In humans cortical bone loss is characteristic of primary hyperparathyroidism, however trabecular bone may be preserved or even enhanced (Silverberg, Shane et al. 1989, Parisien, Silverberg et al. 1990). Patients with asymptomatic PHPT demonstrated reduced bone mineral density at cortical sites, but at more trabecular sites (like the lumbar spine) it was preserved (Silverberg, Walker et al. 2013). Similarly, postmenopausal women with mild primary hyperparathyroidism (normal: 10-65 pg/mL, elevated: 116 +/- 19 pg/mL), have demonstrated a preservation of trabecular bone compared to the normal bone loss observed in postmenopausal women (Dempster, Parisien et al. 1999,

Dempster, Muller et al. 2007). The factors responsible for this variability in skeletal response to continuously elevated PTH are not entirely clear. Studies have examined the correlation of demographic factors as well as co-existing deficiencies (i.e. serum 25-hydroxyvitamin D (25OHD)) with severity of PHPT as well as the impact on BMD and bone turnover (Grey, Lucas et al. 2005, Moosgaard, Christensen et al. 2008, Stein, Dempster et al. 2011, Walker, Nishiyama et al. 2016, Makras and Anastasilakis 2017). However, no clear explanation stands out. Perhaps there is a threshold above which continuously elevated PTH is catabolic and below which it is anabolic.

These differences are of particular interest for bone regeneration applications. A number of studies have demonstrated positive outcomes of daily injections of PTH (intermittent) in bone regeneration/fracture healing studies (Skripitz, Andreassen et al. 2000, Andreassen and Cacciafesta 2004, Reynolds, Takahata et al. 2011, Kumabe, Lee et al. 2017). However, the skeleton is not the only organ affected by PTH (Bilezikian, Raisz et al. 2008). Thus local delivery of PTH to a fracture site may be desirable in order to avoid systemic effects on organs like the kidneys. Studies examining the effects of locally delivered PTH for bone regeneration applications are relatively limited. Published studies show a generally positive result with locally delivered PTH even though the release of PTH from the biomaterial carriers results in a continuous delivery of PTH. For example, PTH delivered via polyethylene glycol (PEG) matrix resulted in an approximately 2 fold increase in mineralized bone and area of regeneration in bone chambers in rabbit calvaria (Jung, Hammerle et al. 2007) and comparable healing to autograft when used in a cylindrical drill defect in canine mandibles (Jung, Cochran et al. 2007). Accelerated healing of drill defects in sheep was also observed with local PTH administration (Arrighi, Mark et al. 2009). A better understanding of whether or not this observation is due to something as straightforward

as there being a threshold above which continuously delivered PTH is catabolic and below which it is anabolic or a more involved mechanism would be beneficial to the progression of improved therapies for bone regeneration.

Though in vitro studies only demonstrate part of what occurs in vivo, as the complexities of the in vivo remodeling and healing mechanisms have yet to be duplicated in vitro, they do provide a good baseline for in vivo mechanistic studies. Cell culture experiments have contributed to the understanding of the pathways that lead to the functional outcomes of PTH treatment and may also lay groundwork in understanding differences between treatment regimens (i.e. intermittent vs continuous). PTH acts in large part through a g-protein coupled receptor on osteoblasts (Jilka 2007). Studies in MC3T3-E1 (osteoblastic) cells indicate the receptor for PTH and PTH related protein (PTH1R) mRNA is detected early in the differentiation timeline (steady-state by 5 days), by 12-14 days PTH1R mRNA increased 2 fold and remained elevated (Schiller, D'Ippolito et al. 1999). Differentiation and bone formation markers are upregulated in MC3T3-E1 (osteoblastic) cells treated with intermittent PTH 1-34 (8M concentration for the first 6 hours of each 48 hour cycle) (Tian, Xu et al. 2011). Similarly, cells isolated from newborn rat calvaria exhibited an increase in alkaline phosphatase (ALP, a phenotypic marker for osteoblast cell maturation), calcium content, and number of mineralized bone nodules with intermittent exposure to PTH (the first 6 hours of each 48 hour cycle). Continuous treatment (PTH 1-34 50 ng/mL), however, resulted in an observed decrease in ALP on day 5 (first day sampled) that remained for the remainder of the period. Calcium content and number of mineralized bone nodules were suppressed as well (Ishizuya, Yokose et al. 1997). Though there is a base understanding of the effects of PTH on osteoblasts in vitro, there is little

literature on the effects of low concentrations of continuously delivered PTH on osteoblasts and whether or not that changes the outcome.

This study examined the dose response of osteoblastic cells to continuous PTH stimulation through examining the effects of subjecting cultured osteoblastic cells to continuous PTH stimulation on alkaline phosphatase activity and mineralization over the course of 28 days. It was hypothesized low concentrations of continuous PTH stimulation would result in osteoblastic cell activity favorable to bone formation, whereas continuous stimulation with higher concentrations would not. The results found in this study contribute a fundamental understanding of the effects of continuous low dose PTH stimulation on osteoblastic cells. Understanding of whether or not there is a threshold below which continuous PTH elicits anabolic activity from osteoblasts is important for further development of bone regeneration therapies utilizing continuous PTH release from local delivery systems. Furthermore, it increases our understanding of how various degrees of hyperparathyroidism affect bone metabolism as well as provide a more informed basis for conducting in vivo studies aimed at investigating the mechanism behind the anabolic and catabolic responses to PTH.

2.2 Methods.

Proliferation.

Alkaline phosphatase and mineralization studies examined cells exposed to continuous concentrations of 0 (no treatment control), 0.00001, 0.0001, 0.001, 0.01, 0.1, 1, 10, or 100 nM PTH 1-84 as well as an intermittent treatment group at the highest concentration (100nM). As one treatment group (intermittently treated cells) was subject to daily media changes vs. every 72 hours, preliminary proliferation studies were done to determine if daily media changes

affected proliferation of MC3T3-E1 osteoblastic cells. MC3T3-E1 subclone 4 (pre-osteoblast) cells were acquired from ATCC. Cells were seeded, 1000 cells/well in 96 well plates, in growth medium and switched to differentiation media (α-MEM + 10% FBS + 1% Pen Strep + 100mM β-glycerophosphate + 50 μg/mL L-ascorbic acid) 24 hours later and treated per experiment details (5 replicates – 5 wells of each treatment) and the experiment was repeated 3 times. Wells for each treatment group were either given fresh media with PTH and left alone for 72 hours, or media and the appropriate amount of PTH were renewed every 24 hours. Cells were treated with varying concentrations (0, 0.000001, 0.00001, 0.0001, 0.001, 0.01, 0.1, 1, 10, 100 and 1000 nM) of PTH continuously for 72 hours. For comparing daily media changes vs. every 72 hours for the intermittent PTH treatment group, the cells were treated with 100nM PTH for either 2.5 hours daily for 3 days, or cells were treated once for 2.5 hours and then left for 72 hours. After 72 hours alamar blue (reasazurin 200 μg/mL in PBS, filtered through a 0.2 μm filter) was added to each well, 10% of total volume in well (18 μL to the 180 μL of media). Plates were placed in an incubator (37° C with 5% CO_2) for 1 hour and read at 530/590 nm. Proliferation was compared between treatment groups (both concentration and media change frequency) by two way ANOVA, a p-value of less than 0.05 was considered significant.

ALP activity:

MC3T3-E1 subclone 4 (pre-osteoblast) cells, acquired from ATCC, were seeded at 15,000 cells/cm^2 in 6 well plates in basal medium (α-MEM, supplemented with 10% fetal bovine serum, 1% penicillin/streptomycin solution). Cells were incubated at 37 °C with 5% CO_2 for 24 hours. Basal medium was then changed to osteogenic medium (basal + 50 μg/mL L-Ascorbic Acid + 10mM β-glycerophosphate). Osteogenic medium changes occurred every 72 hours. PTH has been

shown to be stable in culture with or without cells without decreasing concentration significantly for up to 72 hours (Rickard, Wang et al. 2006). Cells were exposed to continuous concentrations of 0 (no treatment control), 0.00001, 0.0001, 0.001, 0.01, 0.1, 1, 10, or 100 nM PTH 1-84 as well as an intermittent treatment group at the highest concentration (100nM). Cells exposed to continuous concentrations of PTH had the appropriate concentration of PTH combined with the media at each change (every 72 hours). Cells exposed to intermittent PTH, were exposed to media with PTH for 2.5 hours daily 5 days/week. Cell lysate was collected at days 3, 7, 14, 21, and 28 and used to quantify protein and ALP. The experiment was repeated 9 times (9 different passages of MC3T3-E1 cells).

The protein concentration of each sample (well) was determined using a BCA Protein Assay Kit (Pierce Thermo Scientific). Alkaline phosphatase activity was determined using an ALP kit (abcam Cambridge, MA ab83369). Briefly, media was aspirated from wells, and wells were washed with 2-3 mL PBS. ALP buffer (200 µL) was added to each well. Cells were scraped from each well using a cell scraper and collected. Cells were sonicated 3 times: 2-3 seconds of sonication with 20 seconds between cycles. All samples were centrifuged at 13,000 G for 3 minutes at 4°C. The supernatant was collected and stored at -80 °C until all samples for all timepoints were collected. BCA (pierce) and ALP (abcam) analyses were performed per kit instructions. Alkaline phosphatase activity was normalized by total protein and expressed as p-nitrophenyl phosphate in nmol/min/mg protein.

Alizarin Red Staining:

MC3T3-E1 subclone 4 (pre-osteoblast) cells, acquired from ATCC, were seeded at 15,000 cells/cm^2 in 12 well plates in basal medium (α-MEM, supplemented with 10% fetal bovine serum, 1% penicillin/streptomycin solution). Cells were incubated at 37° C with 5% CO_2 for 24 hours. Basal medium was then changed to osteogenic medium (basal + 50 μg/mL L-Ascorbic Acid + 10 mM β-glycerophosphate) (Day 0). Osteogenic medium changes occurred every 72 hours. Cells were exposed to continuous concentrations of 0 (no treatment control), 0.00001, 0.0001, 0.001, 0.01, 0.1, 1, 10, or 100 nM PTH 1-84 as well as an intermittent treatment group at the highest concentration (100nM).Cells exposed to continuous concentrations of PTH had the appropriate amount of PTH combined with the media at each change. Cells exposed to intermittent PTH, were exposed to media with PTH for 2.5 hours daily 5 days/week. The experiment was repeated 5 times (5 different passages of MC3T3-E1 cells).

At days 3, 7, 14, 21, and 28 cells were fixed in formalin and stained with Alizarin Red. Media was aspirated from each well and each well was rinsed with 2 mL PBS followed by addition of 2 mL neutral buffered formalin (NBF) to each well. After one hour at room temperature, NBF was aspirated and each well was rinsed with 2mL PBS. Alizarin red (1g alizarin red S (sigma: #A5533): 100mL DI water) was added to each well (2 mL/well). Alizarin red was aspirated after 20 minutes at room temperature and wells were rinsed 2-3 times with PBS (until background was clear). Once the background was clear a final 2 mL of DI water was added to stained wells and wells were examined under inverted microscope and digitized for mineralized area analysis in Bioquant Osteo (Nashville, TN). As mineralized area stains a vibrant red, as shown in Figure 2. 1, thresholding to measure mineralized area was utilized to obtain mineralized area/total area.

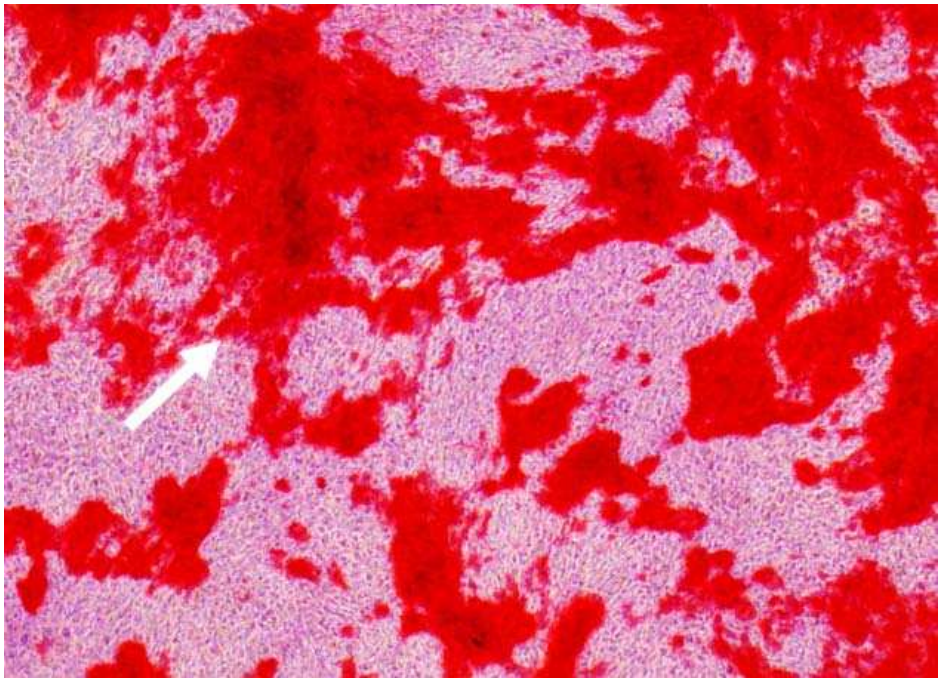

Figure 2. 1 : Alizarin Red staining of MC3T3-E1 cells, mineralization stains red (indicated by the white arrow).

Statistics:

Two way analysis of variance (ANOVA), for timepoint and treatment group, and Tukey post hoc test were used to determine differences in the outcome variables between the treatment groups and the control. A p-value of less than 0.05 was considered significant.

2.3 Results.

No differences in proliferation were observed due to frequency of media change (daily vs. renewed every 72 hours) (Figure 2. 2). Similarly, there were no significant effects of treatment group on proliferation ($p > 0.2787$).

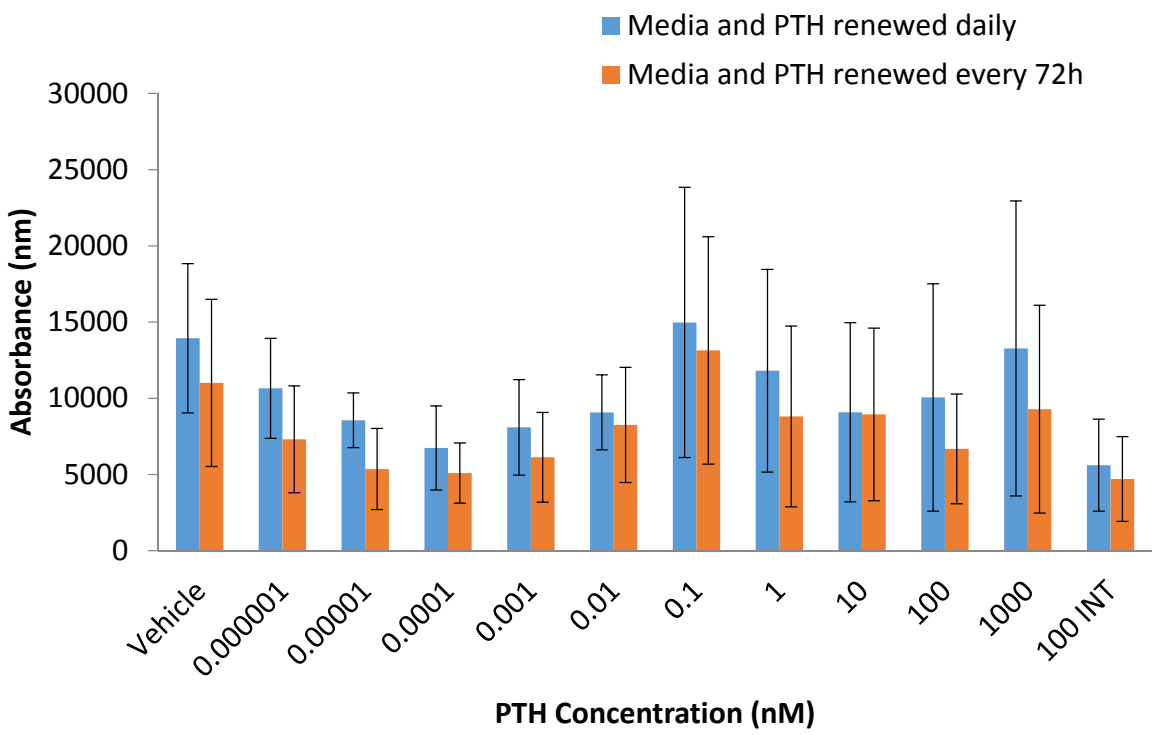

Figure 2. 2: Proliferation data showed no differences between treatment group or media change schedule ($p > 0.2787$).

ALP Activity:

When data from all nine passages (experiments) were averaged alkaline phosphatase activity (Figure 2. 3) did not show any significant differences between treatment concentrations or timepoint over the course of 28 days (2 way ANOVA $p > 0.999$). In individual experiments some trends seemed to appear, however, variability of results between the 9 passages was high. In 2 passages (experiments 4 and 5) an increasing trend in ALP activity over the course of 28 days (within each treatment group) was observed, however this result was not consistent or repeatable. In 2 passages (experiments 1 and 3) an increase in ALP activity between days 3 and 28 was observed in all treatment groups, as well as increased ALP activity with continuous treatment of 1 or 10 nM PTH or intermittent treatment with 100 nM PTH. Contrarily, one passage

(experiment 4) indicated treatment with 0, 0.00001, 0.0001 and 100 nM Intermittent PTH resulted in increased ALP activity at days 21 and 28. No trends were observed between treatment group or timepoint in any other experiments.

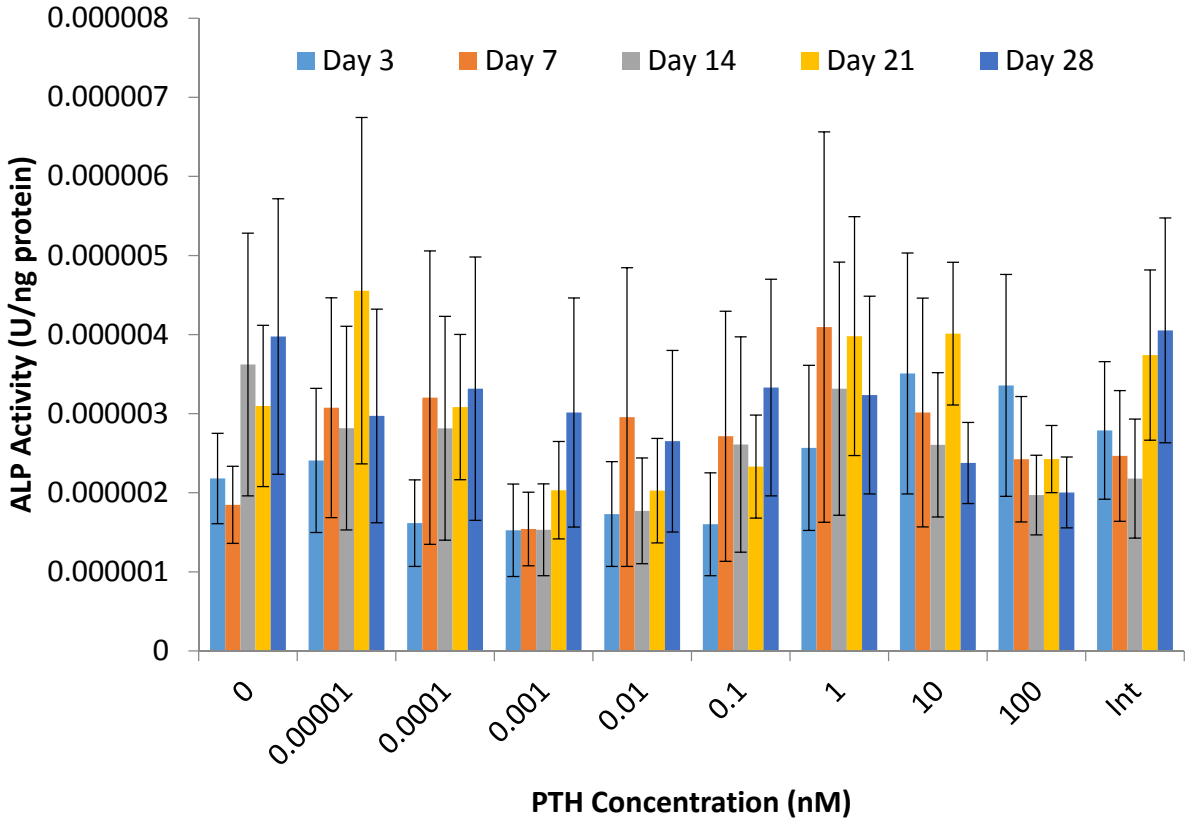

Figure 2. 3: ALP activity (combined data, n = 9) was not different between treatment groups or timepoints ($p > 0.999$).

Alizarin Red staining:

Contrary to findings with ALP, Alizarin Red data indicated consistent differences both between timepoint and treatment group (2-way ANOVA p = 0.0002). At days 3, 7, and 14 no difference in mineralization was observed between different treatment groups (Figure 2. 4).

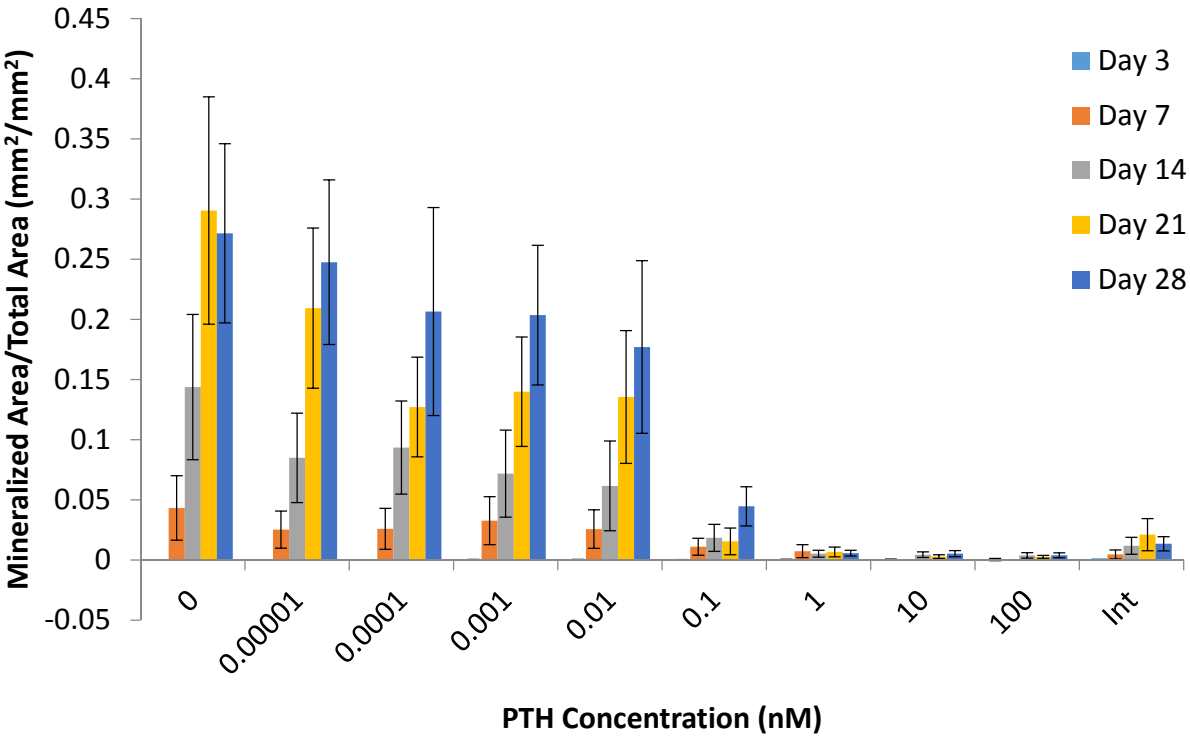

Figure 2. 4 : Alizarin Red staining indicated increased mineralization at later timepoints as well as decreased mineralization at higher PTH treatment concentrations.

However, by day 21 0.00001, 0.1, 1, 10, 100 nM, and intermittent 100nM had less mineralization than control (0 nM PTH) ($p < 0.0001$). By day 28 the lower treatment concentrations (0, 0.00001, 0.0001, 0.001, 0.01 nM) had significantly more mineralization than higher concentrations (0.1, 1, 10, 100 nM) and 100nM intermittent treatment ($p < 0.0018$) (Figure 2. 5). Over the timecourse

of the study, 0, 0.00001, 0.0001, 0.001, 0.01 nM PTH treatments all showed increasing mineralization. In cells without PTH treatment, mineralization was significantly increased by day 14 ($p < 0.0283$) and continued to increase out to 21 days, after which it leveled off. Treatment with concentrations of 0.00001, 0.0001, 0.001, 0.01 nM PTH showed significant increases in mineralization by day 21 ($p < 0.0359$). The higher PTH concentrations (0.1, 1, 10, 100 nM) as well as intermittent treatment did not show any clear trends over the 28 days.

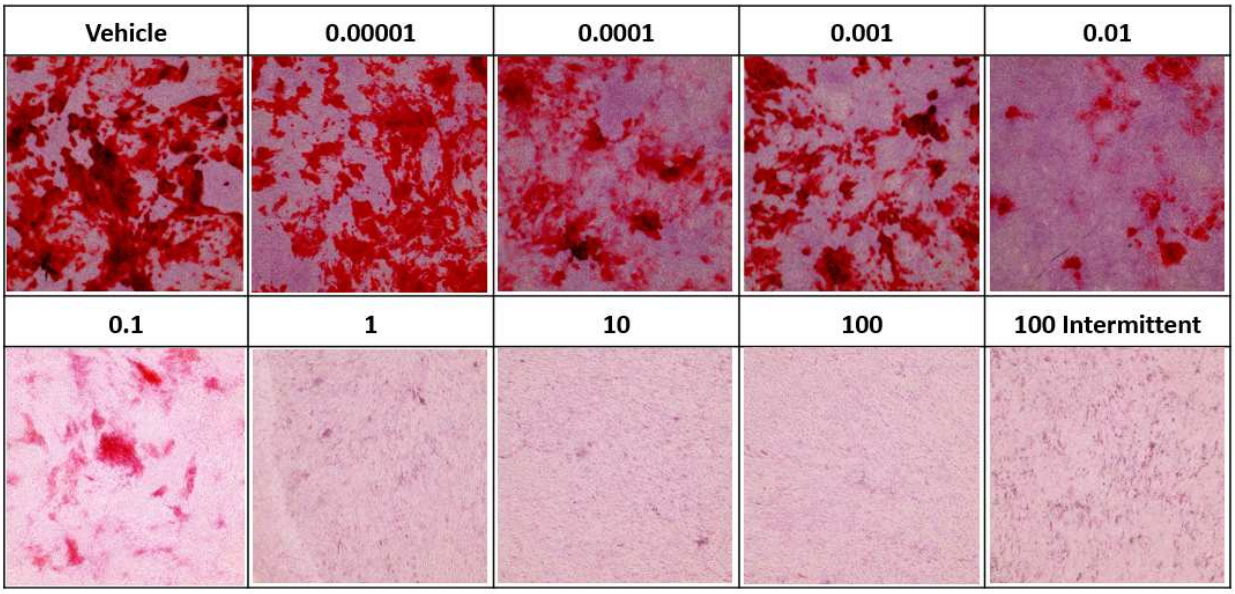

Figure 2. 5: Alizarin Red staining of MC3T3-E1 cells at day 28 (10X magnification), mineralized area stains red. Treatment with lower concentrations of continuous PTH (0 - 0.01 nM) resulted in significantly more mineralization than higher concentrations (0.1 - 100 nM), as well as the intermittent treatment.

2.4 Discussion.

The goal of this study was to examine concentration dependent osteogenic responses to PTH in osteoblastic cells in culture. Though the effect of PTH on osteoblastic cells in culture has been examined, literature examining low doses of continuously administered PTH is limited.

Understanding of whether or not there is a threshold below which continuous PTH elicits anabolic activity from osteoblasts is important for further development of bone regeneration therapies utilizing continuous PTH release from local delivery systems. Furthermore, it may add understanding of how various degrees of hyperparathyroidism affect bone metabolism as well as provide a more informed basis for conducting in vivo studies aimed at investigating the mechanism behind the anabolic and catabolic responses to PTH. This study examined ALP, a phenotypic marker of osteoblastic maturation, and mineralization in MC3T3-E1 osteoblastic cells. MC3T3-E1 cells are well characterized and have been used in a number of studies examining the effects of PTH on osteoblasts. In differentiating MC3T3-E1 cells ALP is detectable by 9 days, and increases dramatically between days 9 and 15. Similarly, matrix calcium content significantly increases between days 14 and 20 (Schiller, D'Ippolito et al. 1999). Intermittent exposure of PTH has been shown to result in an increase in ALP and matrix mineralization, whereas continuous exposure resulted in suppression (Ishizuya, Yokose et al. 1997, Tian, Xu et al. 2011). To add to the knowledge base surrounding the understanding of continuous exposure to PTH this study examined lower concentrations than typically explored in literature.

In vitro proliferation was examined in this work at an early timepoint (prior to estimated completion of differentiation of the cells). The goal was to gain insight as to whether PTH concentration or daily media changes would have an effect on the longer term cultures to consider when examining ALP activity and mineralization data. Daily media changes have been a suggested reason for inconsistent results with studies utilizing intermittent PTH delivery; as more frequent media changes may result in premature removal of factors excreted by cells that are necessary for a more representative progression of their cycle (Schiller, D'Ippolito et al. 1999). In

vivo work has shown intermittent administration of PTH stimulates bone formation on the surface of periosteal and trabecular bone by increasing osteoblast number (Jilka, O'Brien et al. 2009). However, data suggested PTH exerts pro-differentiating and/or pro-survival effects on pre-osteoblasts. The findings in this study of a lack of effect of PTH treatment at any concentration in vitro are consistent with previous in vivo literature indicating PTH is not increasing osteoblast number in the proliferation phase. Similarly, the lack of effect of frequency of media change on proliferation indicates administration pattern is likely not a primary cause of variability observed in ALP activity or mineralization experiments.

Ishizuya et al reported continuous exposure to PTH in long term cultures resulted in decreased levels of mineralization compared with controls (Ishizuya, Yokose et al. 1997). The same result was observed by Schiller et al (as long as treatment was initiated on or before day 15) (Schiller, D'Ippolito et al. 1999). In cell cultures continuously exposed to PTH (starting prior to day 14) mineralization was inhibited (~60%) compared to cultures where PTH treatment was initiated on day 20 or later. Cells exposed to 10nM PTH from days 20 - 25 showed an approximately 5 fold increase in matrix mineralization (Schiller, D'Ippolito et al. 1999). However, these studies utilized higher concentrations than the present study. Similarly, as the basis of this research is bone regeneration applications, many cells in the defect area may be exposed to PTH the entire duration of their maturation cycle, thus understanding the implications for low concentrations of PTH starting at day 0 in this study is still of interest. At concentrations above 0.01 nM PTH, a similar result to Schiller et al. and Ishizuya et al. was observed in this study. Mineralization was significantly decreased when compared to controls (no PTH treatment). However, lower concentrations resulted in similar mineralization levels to control. The

anticipated increase in mineralization with time (as is typically observed in differentiation MC3T3 cells) was also evident at lower concentrations. The potential inhibitory effect PTH seems to have on mineralization of MC3T3 cells in culture appears to exist with concentrations of 0.1 nM or above. Interestingly, intermittent treatment did not result in the expected increases in mineralization over control or over the timecourse of the study. Previous studies in MC3T3-E1 cells have shown more than 90 minutes of PTH exposure was necessary to observe the stimulatory effects of PTH (Schiller, D'Ippolito et al. 1999). However, with 2.5 hours of treatment, this stipulation was met. A similar result was recently observed by Milstrey et al. Osteoblasts from calvaria of mice were treated with PTH for 6 hours and incubated for 42 hours in differentiation medium. Mineralization was diminished with higher concentrations of PTH treatment (10 and 50nM), but not with lower concentrations (10^{-5} – 1 nM). Treatment with 10^{-5} and 10^{-3} nM tended to increase mineralization (Milstrey, Wieskoetter et al. 2017). Authors suggested, as bone remodeling is dependent on an initiation phase with osteoclast recruitment (Matsuo and Irie 2008), perhaps the lack of coupling factors are responsible for the inhibitory effects of PTH at higher concentrations. The inhibitory effect may also be due to the traditionally accepted concept that continuous PTH is catabolic. Perhaps at these higher concentrations an inhibitory effect is part of the catabolic effect PTH can have on bone. Though lower concentrations may not result in increased mineralization over control, the lack of negative effect is promising. Perhaps coupling factors from other cell types or upregulation of other functional outcomes resulting from treatment with lower concentrations of PTH, a net anabolic effect would be observed.

Results from the ALP activity study are difficult to interpret. As ALP is a phenotypic marker of osteoblast differentiation, it was expected increases would have at least been observed throughout the timecourse of the study in the control group. The lack of this observation is especially surprising given the anticipated increase in mineralization with time was observed in control cells and with lower PTH treatment concentrations. Research has shown different subclones of cell lines, characterized with regard to ability to mineralize a collagen extracellular matrix express different mRNAs. Mineralizing subclones selectively expressed mRNAs for osteoblast markers as compared to non-mineralizing subclones. Alkaline phosphatase mRNA was present in certain nonmineralizing as well as mineralizing subclones, suggesting ALP expression is perhaps subject to controls from other osteoblast markers (Wang, Christensen et al. 1999). However, a good correlation between the ability of a particular MC3T3 subclone to mineralize and is activity in an in vivo ostoegenesis assay was observed. Which would indicate, as our cells were mineralizing as expected, other osteogenic markers would theoretically be evident and show the anticipated trends. Consistent observations of alkaline phosphatase activity could also be dependent on signals from other cell types not received in culture. In vivo work indicates even though osteoblasts are target cells for PTH, continuous elevation of PTH stimulates osteoclast-dependent as well as osteoclast independent (Wnt signaling) pro-osteoblastogenic pathways. Both of which are required for balanced bone remodeling in trabecular bone (Jilka, O'Brien et al. 2010). Similarly, Bellido et al noted continuous PTH 1-84 treatment for 7 days in mice resulted in an increase in osteoclast number at day 2 followed by an increase in osteoblast number at day 4 (Bellido, Ali et al. 2003). Perhaps, though ALP activity and mineralization are both indicators of

osteoblast differentiation the interactions with other cells types are vital to consistent outcomes in ALP activity.

The lack of increase in ALP activity in cells treated intermittently with PTH is similarly difficult to explain. Similar to mineralization measures, the 2.5 hour treatment met previously published literature indications of a minimum of 90 minutes of treatment to observe stimulatory effects in MC3T3 (Ishizuya, Yokose et al. 1997, Schiller, D'Ippolito et al. 1999). Ishizuya et al found PTH exposure (50 ng/mL) for the first 6 hours of each 48 hour cycle stimulated osteoblast differentiation as indicated by ALP measures. Whereas continuous exposure during the 48 hour cycle inhibited osteoblast differentiation (Ishizuya, Yokose et al. 1997). Thus, an increase in ALP activity in the intermittent treatment group was expected. However, recently, similar findings in MC3T3s exposed to low concentrations of PTH have been made. Alkaline phosphatase activity was not changed in osteoblasts from calvaria of mice treated with PTH concentrations of 10^{-5} – 1 nM for the first 6 hours of each treatment cycle and incubated for 42 hours. ALP activity increased from day 12-26 in the control group and lower concentrations of PTH (up to 1nM). Higher PTH concentrations (10 and 50 nM) lead to decreased ALP activity at day 26 compared to others (Milstrey, Wieskoetter et al. 2017).

Consistent anabolic effects of PTH in osteoblastic cell cultures have been difficult to demonstrate in vitro for a number of researchers (Choudhary, Huang et al. 2008). Differences in confluency or maturity of cells in cultures may play a role in unexpected, or inconsistent results (Kondo, Ohyama et al. 1997). In vitro studies have demonstrated maturity and confluency of osteoblasts may affect the outcome of PTH treatment. Bone marrow cells isolated from femora and tibiae of PTH or vehicle treated rats (30 µg/kg s.c.) and cultured at a high density,

demonstrated a significant increase ALP expression (ALP was measured at 4, 7, 10, 13, 16 days). When cultured at a low density to generate colonies (colony forming unit-fibroblastic (CFU-F)) PTH induced apparent increases in CFU-F and the number of ALP-positive CFU-F (Nishida, Yamaguchi et al. 1994). Subconfluent primary osteoblast-like cells (isolated from mouse calvaria) exposed to PTH for 7 days stimulated ALP in a dose-dependent manner. However, in cells that reached confluency prior to the end of the 7 days, PTH dose dependently inhibited ALP production (Isogai, Akatsu et al. 1996). These findings, in combination with Schiller et al suggest PTH treatment starting at different timepoints affects outcome measures indicate variability in osteoblast responsiveness to PTH depending on different stages of osteoblast development.

The variable response observed in tissue culture may not be as evident in vivo. However, establishment of a base understanding of how osteoblasts react to varying PTH treatments in vitro provides an important baseline for understanding what it observed in vivo. Tissue engineering/regenerative medicine is a very complex field. The healing response of a living being is a multi-faceted event. Osteoblasts of every stage of maturation will be present throughout the healing process. In vivo studies thus far indicate local continuous delivery of PTH via biomaterial scaffold is effective for bone regeneration. In vitro models can lay very important groundwork and supplementation for in vivo mechanistic studies aimed at optimizing treatment results. This study indicates a lack of observed negative effect of low dose continuously administered PTH on mineralization of osteoblastic cells. Alkaline phosphatase activity is variable, but not negatively affected at any examined concentration. Though this is not necessarily indicative of potential for improved healing, it lays ground work for in vivo studies to examine whether this effect is observed, or possibly even improved when signals from other cell types come into play.

References.

Andreassen, T. T. and V. Cacciafesta (2004). "Intermittent parathyroid hormone treatment enhances guided bone regeneration in rat calvarial bone defects." J Craniofac Surg **15**(3): 424-427; discussion 428-429.

Arrighi, I., S. Mark, M. Alvisi, B. von Rechenberg, J. A. Hubbell and J. C. Schense (2009). "Bone healing induced by local delivery of an engineered parathyroid hormone prodrug." Biomaterials **30**(9): 1763-1771.

Bellido, T., A. A. Ali, L. I. Plotkin, Q. Fu, I. Gubrij, P. K. Roberson, R. S. Weinstein, C. A. O'Brien, S. C. Manolagas and R. L. Jilka (2003). "Proteasomal degradation of Runx2 shortens parathyroid hormone-induced anti-apoptotic signaling in osteoblasts. A putative explanation for why intermittent administration is needed for bone anabolism." J Biol Chem **278**(50): 50259-50272.

Bilezikian, J. P., L. G. Raisz and T. J. Martin (2008). Principles of bone biology. San Diego, Calif., Academic Press/Elsevier.

Black, D. M., S. L. Greenspan, K. E. Ensrud, L. Palermo, J. A. McGowan, T. F. Lang, P. Garnero, M. L. Bouxsein, J. P. Bilezikian and C. J. Rosen (2003). "The effects of parathyroid hormone and alendronate alone or in combination in postmenopausal osteoporosis." N Engl J Med **349**(13): 1207-1215.

Choudhary, S., H. Huang, L. Raisz and C. Pilbeam (2008). "Anabolic effects of PTH in cyclooxygenase-2 knockout osteoblasts in vitro." Biochem Biophys Res Commun **372**(4): 536-541.

Dempster, D. W., F. Cosman, E. S. Kurland, H. Zhou, J. Nieves, L. Woelfert, E. Shane, K. Plavetic, R. Muller, J. Bilezikian and R. Lindsay (2001). "Effects of daily treatment with parathyroid hormone on bone microarchitecture and turnover in patients with osteoporosis: a paired biopsy study." J Bone Miner Res **16**(10): 1846-1853.

Dempster, D. W., R. Muller, H. Zhou, T. Kohler, E. Shane, M. Parisien, S. J. Silverberg and J. P. Bilezikian (2007). "Preserved three-dimensional cancellous bone structure in mild primary hyperparathyroidism." Bone **41**(1): 19-24.

Dempster, D. W., M. Parisien, S. J. Silverberg, X. G. Liang, M. Schnitzer, V. Shen, E. Shane, D. B. Kimmel, R. Recker, R. Lindsay and J. P. Bilezikian (1999). "On the mechanism of cancellous bone preservation in postmenopausal women with mild primary hyperparathyroidism." J Clin Endocrinol Metab **84**(5): 1562-1566.

Grey, A., J. Lucas, A. Horne, G. Gamble, J. S. Davidson and I. R. Reid (2005). "Vitamin D repletion in patients with primary hyperparathyroidism and coexistent vitamin D insufficiency." J Clin Endocrinol Metab **90**(4): 2122-2126.

Hock, J. M. and I. Gera (1992). "Effects of continuous and intermittent administration and inhibition of resorption on the anabolic response of bone to parathyroid hormone." J Bone Miner Res **7**(1): 65-72.

Ishizuya, T., S. Yokose, M. Hori, T. Noda, T. Suda, S. Yoshiki and A. Yamaguchi (1997). "Parathyroid hormone exerts disparate effects on osteoblast differentiation depending on exposure time in rat osteoblastic cells." J Clin Invest **99**(12): 2961-2970.

Isogai, Y., T. Akatsu, T. Ishizuya, A. Yamaguchi, M. Hori, N. Takahashi and T. Suda (1996). "Parathyroid hormone regulates osteoblast differentiation positively or negatively depending on the differentiation stages." J Bone Miner Res **11**(10): 1384-1393.

Jiang, Y., J. J. Zhao, B. H. Mitlak, O. Wang, H. K. Genant and E. F. Eriksen (2003). "Recombinant human parathyroid hormone (1-34) [teriparatide] improves both cortical and cancellous bone structure." J Bone Miner Res **18**(11): 1932-1941.

Jilka, R. L. (2007). "Molecular and cellular mechanisms of the anabolic effect of intermittent PTH." Bone **40**(6): 1434-1446.

Jilka, R. L., C. A. O'Brien, A. A. Ali, P. K. Roberson, R. S. Weinstein and S. C. Manolagas (2009). "Intermittent PTH stimulates periosteal bone formation by actions on post-mitotic preosteoblasts." Bone **44**(2): 275-286.

Jilka, R. L., C. A. O'Brien, S. M. Bartell, R. S. Weinstein and S. C. Manolagas (2010). "Continuous elevation of PTH increases the number of osteoblasts via both osteoclast-dependent and -independent mechanisms." J Bone Miner Res **25**(11): 2427-2437.

Jung, R. E., D. L. Cochran, O. Domken, R. Seibl, A. A. Jones, D. Buser and C. H. Hammerle (2007). "The effect of matrix bound parathyroid hormone on bone regeneration." Clin Oral Implants Res **18**(3): 319-325.

Jung, R. E., C. H. F. Hammerle, V. Kokovic and F. E. Weber (2007). "Bone regeneration using a synthetic matrix containing a parathyroid hormone peptide combined with a grafting material." International Journal of Oral & Maxillofacial Implants **22**(2): 258-266.

Kondo, H., T. Ohyama, K. Ohya and S. Kasugai (1997). "Temporal changes of mRNA expression of matrix proteins and parathyroid hormone and parathyroid hormone-related protein (PTH/PTHrP) receptor in bone development." J Bone Miner Res **12**(12): 2089-2097.

Kumabe, Y., S. Y. Lee, T. Waki, T. Iwakura, S. Takahara, M. Arakura, Y. Kuroiwa, T. Fukui, T. Matsumoto, T. Matsushita, K. Nishida, R. Kuroda and T. Niikura (2017). "Triweekly administration of parathyroid hormone (1-34) accelerates bone healing in a rat refractory fracture model." BMC Musculoskelet Disord **18**(1): 545.

Makras, P. and A. D. Anastasilakis (2017). "Bone Disease in Primary Hyperparathyroidism." Metabolism.

Matsuo, K. and N. Irie (2008). "Osteoclast-osteoblast communication." Arch Biochem Biophys **473**(2): 201-209.

Milstrey, A., B. Wieskoetter, D. Hinze, N. Grueneweller, R. Stange, T. Pap, M. Raschke and P. Garcia (2017). "Dose-dependent effect of parathyroid hormone on fracture healing and bone formation in mice." J Surg Res **220**: 327-335.

Moosgaard, B., S. E. Christensen, P. Vestergaard, L. Heickendorff, P. Christiansen and L. Mosekilde (2008). "Vitamin D metabolites and skeletal consequences in primary hyperparathyroidism." Clin Endocrinol (Oxf) **68**(5): 707-715.

Neer, R. M., C. D. Arnaud, J. R. Zanchetta, R. Prince, G. A. Gaich, J. Y. Reginster, A. B. Hodsman, E. F. Eriksen, S. Ish-Shalom, H. K. Genant, O. Wang and B. H. Mitlak (2001). "Effect of parathyroid hormone (1-34) on fractures and bone mineral density in postmenopausal women with osteoporosis." N Engl J Med **344**(19): 1434-1441.

Nishida, S., A. Yamaguchi, T. Tanizawa, N. Endo, T. Mashiba, Y. Uchiyama, T. Suda, S. Yoshiki and H. E. Takahashi (1994). "Increased bone formation by intermittent parathyroid hormone administration is due to the stimulation of proliferation and differentiation of osteoprogenitor cells in bone marrow." Bone **15**(6): 717-723.

Parisien, M., S. J. Silverberg, E. Shane, L. de la Cruz, R. Lindsay, J. P. Bilezikian and D. W. Dempster (1990). "The histomorphometry of bone in primary hyperparathyroidism: preservation of cancellous bone structure." J Clin Endocrinol Metab **70**(4): 930-938.

Reynolds, D. G., M. Takahata, A. L. Lerner, R. J. O'Keefe, E. M. Schwarz and H. A. Awad (2011). "Teriparatide therapy enhances devitalized femoral allograft osseointegration and biomechanics in a murine model." Bone **48**(3): 562-570.

Rickard, D. J., F. L. Wang, A. M. Rodriguez-Rojas, Z. Wu, W. J. Trice, S. J. Hoffman, B. Votta, G. B. Stroup, S. Kumar and M. E. Nuttall (2006). "Intermittent treatment with parathyroid hormone (PTH) as well as a non-peptide small molecule agonist of the PTH1 receptor inhibits adipocyte differentiation in human bone marrow stromal cells." Bone **39**(6): 1361-1372.

Schiller, P. C., G. D'Ippolito, B. A. Roos and G. A. Howard (1999). "Anabolic or catabolic responses of MC3T3-E1 osteoblastic cells to parathyroid hormone depend on time and duration of treatment." J Bone Miner Res **14**(9): 1504-1512.

Silverberg, S. J., E. Shane, L. de la Cruz, D. W. Dempster, F. Feldman, D. Seldin, T. P. Jacobs, E. S. Siris, M. Cafferty, M. V. Parisien and et al. (1989). "Skeletal disease in primary hyperparathyroidism." J Bone Miner Res **4**(3): 283-291.

Silverberg, S. J., M. D. Walker and J. P. Bilezikian (2013). "Asymptomatic primary hyperparathyroidism." J Clin Densitom **16**(1): 14-21.

Skripitz, R., T. T. Andreassen and P. Aspenberg (2000). "Strong effect of PTH (1-34) on regenerating bone: a time sequence study in rats." Acta Orthop Scand **71**(6): 619-624.

Stein, E. M., D. W. Dempster, J. Udesky, H. Zhou, J. P. Bilezikian, E. Shane and S. J. Silverberg (2011). "Vitamin D deficiency influences histomorphometric features of bone in primary hyperparathyroidism." Bone **48**(3): 557-561.

Tam, C. S., J. N. M. Heersche, T. M. Murray and J. A. Parsons (1982). "Parathyroid-Hormone Stimulates the Bone Apposition Rate Independently of Its Resorptive Action - Differential-Effects of Intermittent and Continuous Administration." Endocrinology **110**(2): 506-512.

Tian, Y., Y. Xu, Q. Fu and M. He (2011). "Parathyroid hormone regulates osteoblast differentiation in a Wnt/beta-catenin-dependent manner." Mol Cell Biochem **355**(1-2): 211-216.

Uzawa, T., M. Hori, S. Ejiri and H. Ozawa (1995). "Comparison of the effects of intermittent and continuous administration of human parathyroid hormone(1-34) on rat bone." Bone **16**(4): 477-484.

Walker, M. D., K. K. Nishiyama, B. Zhou, E. Cong, J. Wang, J. A. Lee, A. Kepley, C. Zhang, X. E. Guo and S. J. Silverberg (2016). "Effect of Low Vitamin D on Volumetric Bone Mineral Density, Bone Microarchitecture, and Stiffness in Primary Hyperparathyroidism." J Clin Endocrinol Metab **101**(3): 905-913.

Wang, D., K. Christensen, K. Chawla, G. Xiao, P. H. Krebsbach and R. T. Franceschi (1999). "Isolation and characterization of MC3T3-E1 preosteoblast subclones with distinct in vitro and in vivo differentiation/mineralization potential." J Bone Miner Res **14**(6): 893-903.

Chapter 3: Aim 2: Characterize in vitro PTH release from thiol-ene hydrogel and in vivo thiol-ene hydrogel degradation.

Synopsis.

Understanding and optimizing biomaterial/biomolecule delivery systems is essential for their use in regenerative medicine. The mechanical properties, degradation rate, and mode of delivery of bioactive molecules of hydrogels are all tailorable making them good options for delivery of bioactive molecules. Hydrogels may be used alone, or in combination with more rigid scaffolds when a more rigid structure is desirable (ie. use in combination with a rigid scaffold to bridge a segmental defect in bone). The chemical cross linking in hydrogels allows them to remain insoluble when placed in aqueous environments, which allows for control of drug delivery. One strategy for controlling the release of a biomolecule is entrapping the molecule within the hydrogel matrix. This approach is somewhat dependent on the molecular weight of the entrapped molecule relative to the network structure, making it a useful approach for use with relatively high molecular weights. Entrapping the molecules within the matrix allows them to slowly diffuse out, thus controlling their delivery and therefore their impact on the extracellular environment. For example Mariner et al. utilized a synthetic hydrogel scaffold to deliver rhBMP-2 to critical sized calvarial defects, resulting in better healing than the commercially available (and FDA approved) carrier for BMP-2. Another approach is to tether the biomolecule to the hydrogel matrix. This allows for controlling release through degradation of those bonds instead of relying on diffusion. Degradation of hydrogels may be controlled by different mechanisms like hydrolysis or proteases (i.e. matrix metalloproteinases (MMPs)) released by cells, thus allowing tailorability of release, depending on environment and desired release profile. How biomolecules

are delivered can affect both bioactivity and release profile, both of which may affect healing. For many novel bioactive molecules, like parathyroid hormone (PTH), being explored for bone regeneration applications the ideal release profile is unknown. Thus, characterization of the release profile for materials used in efficacy studies examining the effect of locally delivered PTH on bone regeneration is important for understanding and optimizing the observed healing response. This study characterized in vitro PTH release from thiol-ene hydrogels when PTH was either entrapped within the hydrogel matrix, as well as the in vitro release from thiol-ene hydrogels containing PTH cross-linked to the matrix. In vivo degradation of thiol-ene hydrogels and thiol-ene hydrogels surrounding a rigid PPF scaffold in a subcutaneous pocket was also characterized.

3.1 Introduction.

The skeletal system is capable of self-repair when damaged. This not only applies to microdamage, but also to macrostructural fractures and breaks (Einhorn 1998). However, cases arise where extenuating circumstances or extent of damage result in delayed or non-union (Karladani, Granhed et al. 2001, Harris, Althausen et al. 2009). Though autograft and allograft are treatment options for bone defects complicated by segmental bone loss (Mahendra and Maclean 2007, Jahangir, Nunley et al. 2008), their limitations have led to further research of biomaterials alternatives as well as bioactive molecules for bone regeneration applications. Thus, as the field of tissue engineering/regenerative medicine progresses, more biodegradable materials are being used as scaffolds and/or delivery systems for drugs, cells, or other bioactive molecules. Hydrogels are promising scaffolds for these applications. The mechanical properties, degradation rate, and mode of delivery of bioactive molecules of hydrogels may be tailored. Hydrogels may be used

alone, or in combination with more rigid scaffolds. For example, when treating a segmental bone defect it may be desirable or necessary to have a rigid scaffold to bridge the defect area.

The chemical cross linking in hydrogels allows them to remain insoluble when placed in aqueous environments, which allows for control of drug delivery. One strategy for controlling the release of a biomolecule is entrapping the molecule within the hydrogel matrix (Mellott, Searcy et al. 2001, Lin and Metters 2006). This approach is somewhat dependent on the molecular weight of the entrapped molecule relative to the network structure, making it a particularly useful approach for use with relatively high molecular weight proteins. Entrapping the molecules within the matrix allows them to slowly diffuse out, thus controlling their delivery and, therefore, their impact on the extracellular environment. For example, Mariner et al. utilized a synthetic hydrogel scaffold to deliver rhBMP-2 (by diffusion out of the hydrogel matrix) to critical sized calvarial defects, resulting in better healing than the commercially available (and FDA approved) carrier for BMP-2. Another approach is to tether the biomolecule to the hydrogel matrix (Grim, Marozas et al. 2015). This allows for controlling release through degradation of chemical bonds instead of relying on diffusion. Degradation of hydrogels may be controlled by different mechanisms like hydrolysis or proteases (like MMPs) released by cells (Wong and Bronzino 2007), thus allowing tailorability of release, depending on environment and desired release profile.

How biomolecules are delivered can affect both bioactivity and release profile, both of which may affect healing. Understanding and optimizing biomaterial/biomolecule delivery systems is essential for their use in regenerative medicine. For example, BMP-2 delivered via a burst release from a material followed by sustained release resulted in more new bone formation than other release profiles in a bone regeneration model (Brown, Li et al. 2011). Other molecules,

like parathyroid hormone (PTH), could similarly be incorporated into hydrogels or other biomaterial scaffolds to promote bone healing. However, for PTH (and many novel alternatives to grafting or BMP use) the ideal release profile is unknown. Thus, characterization of the release profile for materials used in efficacy studies examining the effect of locally delivered PTH on bone regeneration is important for understanding and optimizing the observed healing response. In recent years PTH has become a molecule of interest for bone regeneration applications. Daily injections of PTH, an 84 amino acid peptide is a key regulator of calcium homeostasis in the body (Habener, Rosenblatt et al. 1984), is presently FDA approved as an anabolic treatment for osteoporosis. When administered as daily injections PTH treatment results in an increase in bone volume and bone mineral density in women with osteoporosis (Hock and Gera 1992, Ejersted, Andreassen et al. 1993, Mosekilde 1995, Jiang, Zhao et al. 2003). When systemic PTH levels are continuously elevated, as in hyperparathyroidism, it is generally accepted PTH has a catabolic effect (Tam, Heersche et al. 1982, Uzawa, Hori et al. 1995). However, there is some variability observed with continuously elevated PTH. Cortical bone loss is characteristic of primary hyperparathyroidism, however trabecular bone is preserved or enhanced (Silverberg, Shane et al. 1989, Parisien, Silverberg et al. 1990, Silverberg, Walker et al. 2013). There is also anecdotal evidence indicating mild primary hyperparathyroidism has a protective effect against post-menopausal osteoporosis (Dempster, Parisien et al. 1999, Dempster, Muller et al. 2007). The anabolic effect PTH has on bone makes it a molecule of interest for bone regeneration applications. A number of studies have shown PTH to have beneficial effects on bone healing when given as daily injections (Skripitz, Andreassen et al. 2000, Andreassen and Cacciafesta 2004, Milstrey, Wieskoetter et al. 2017). The inconsistent observations surrounding continuously

elevated systemic PTH may indicate the usefulness of PTH for bone regeneration applications is not limited to daily injections. Delivery of PTH locally for bone regeneration may allow the ability to optimize delivery profile for healing response while decreasing or eliminating systemic exposure and overall skeletal effects. In the case of continuously delivered PTH, this is beneficial, as the effect can be limited to the site of high remodeling (defect site), as continuous PTH does not have the same catabolic effect at these sites (Silverberg, Shane et al. 1989, Parisien, Silverberg et al. 1990).

The use of a biomaterial scaffold system to deliver PTH locally to enhance fracture healing is a relatively new pursuit. The few animal studies that have been conducted show promising results (Fuerst, Derungs et al. 2007, Jung, Cochran et al. 2007, Arrighi, Mark et al. 2009). The optimal release profile of PTH from a scaffold necessary to achieve an anabolic response in bone regeneration applications is presently unclear. Thus, understanding the profile of PTH released from biomaterial scaffolds used in bone regeneration studies is critical to understanding efficacy. The objective of this aim was to characterize in vitro PTH release from MMP degradable thiol-ene hydrogels when PTH is either entrapped within the hydrogel matrix, or cross-linked to the matrix. As well as to characterize the in vivo thiol-ene hydrogel degradation when used alone or in conjunction with a rigid poly(propylene fumarate) (PPF) scaffold. Understanding the release profile of the PTH from the thiol-ene gel, as well as in vivo degradation aids understanding the impacts of PTH on bone regeneration when delivered via thiol-ene hydrogel.

3.2 Methods.

Poly(propylene fumarate) scaffold preparation:

Poly(propylene fumarate) scaffolds were fabricating using stereolithography as previously described (Lee, Wang et al. 2007) and coated with Synthetic Bone Mineral (SBM) coating (Dadsetan, Guda et al. 2015) courtesy of Dr. Michael Yaszemski's Biomaterials and Tissue Engineering Laboratory at Mayo Clinic. The CAD designed scaffolds were cylinders with square pores. The external dimensions were 6 mm in length and 3 mm in outer diameter (Figure 3. 1). The pores throughout the scaffold are 1 mm x 1 mm and the strut thickness was 500 µm.

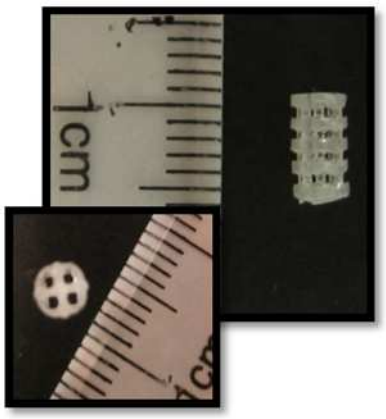

Figure 3. 1 : PPF scaffold

Hydrogel preparation:

Monomer solutions for the hydrogels were prepared with assistance from Dr. Kristi Anseth's lab at CU Boulder, as previously described (Fairbanks, Schwartz et al. 2009). Briefly, Monomer solutions were: 6 wt%/vol 10K 4-arm poly(ethylene glycol)-norbornene (PEG-NB), 1mM adhesion peptide (CRGDS), 5.5 mM di-cysteine MMP-degradable crosslinker peptide (KCGPQGIAGQCK), and 0.01% of the photoinitiator lithium phenyl-2,4,6-trimethylbenzoylphosphinate (LAP). A 1mL syringe was used as a mold to create 90µl gels

(diameter: ~4mm. Height: ~5mm). Gels were polymerized by placing the solution in molds under a 2.5 mW/cm^2 UV lamp (365 nm) for 2.5 minutes. In samples were the hydrogel was combined with a PPF scaffold, the rigid PPF scaffold was placed in the mold and the hydrogel solution was pipetted into the mold, filling the pores of the scaffold as seen in Figure 3. 2. The solution was then polymerized around the scaffold utilizing the same UV light as samples without PPF.

Figure 3. 2 : Left: Thiol-ene hydrogel. Right: PPF scaffold surrounded by thiol-ene hydrogel

Thiolation of bb-PTH 1-84 for cross-linking to thiol-ene gels:

In samples where bbPTH 1-84 was cross-linked to the hydrogel matrix, PTH was modified by adding a sulfhydryl group to accommodate cross-linking. PTH was thiolated using trauts reagent (2-iminothiolene-HCL). PTH was exposed to a 20 x molar excess of Trauts reagent (2-iminothiolene-HCL) and 3mM EDTA and incubated at room temperature for 2 hours. Excess trauts reagent was removed via a desalting column. Thiolaton of PTH was verified by high performance liquid chromatography (HPLC), and thiolated PTH was stored at -80°C until use.

In vitro release:

In vitro release of PTH from hydrogels was determined for n = 5 thiol-ene hydrogels with bbPTH 1-84 entrapped within the hydrogel matrix (not cross-linked to the gel), as well as n = 5 thiol-ene hydrogels with bbPTH 1-84 cross-linked to the hydrogel matrix, as represented in Figure 3. 3 To determine release profiles of PTH entrapped within vs. cross linked to hydrogels, hydrogels containing no PTH (control), 30 µg bbPTH 1-84 or 30 µg thiolated bbPTH 1-84 were placed in 1mL of dPBS and stored at 37°C. Samples (n = 5) were collected at day 3, 7, 14, 21, and 28, and stored at -80 °C until the last sample was collected. After all samples were collected the supernatant was assayed by µBCA to determine the amount of PTH released from the hydrogels at each time point. A second set of hydrogels (n = 3/ group), containing PTH or thiolated PTH were polymerized within the pores/around PPF scaffolds to determine if PPF affected PTH release.

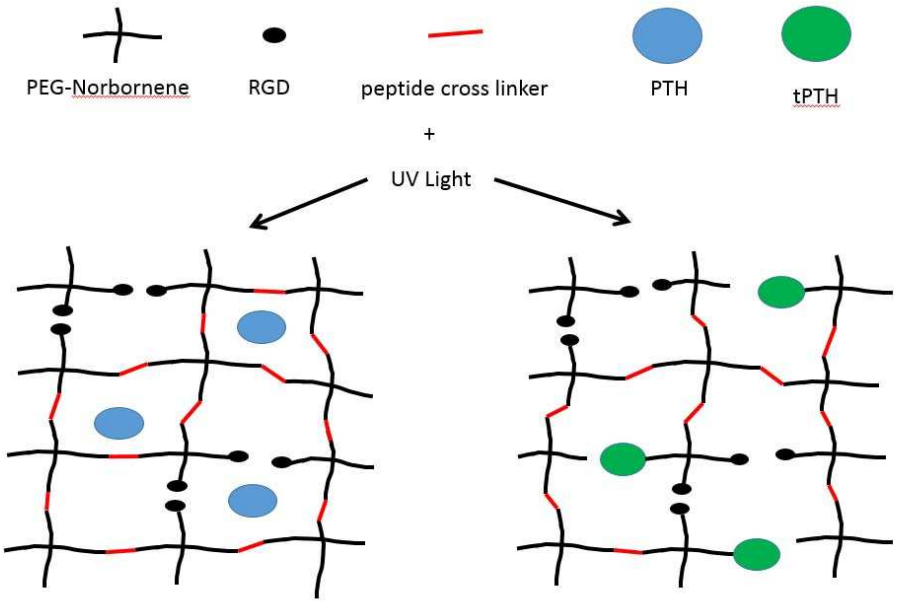

Figure 3. 3 : (Left) visual representation of PTH entrapped within the thiol-ene hydrogel matrix, (Right) PTH tethered to the thiol-ene hydrogel matrix

Verification of bioactivity:

To assess and verify bioactivity of bbPTH 1-84 released from hydrogels, MC3T3 cells were seeded in 6 well plates in basal medium (α-MEM, supplemented with 10% fetal bovine serum, 1% penicillin/streptomycin solution). After 24 hours, the basal medium was changed to osteogenic medium (basal + 50 μg/mL L-Ascorbic Acid+ 10 mM β-glycerophosphate) (Day 0). On day 3 medium was replaced. On day 5 cells were stimulated for 10 minutes with PTH released from gels (collected as described for release studies), or a control treatment as follows:

- Forskolin (positive control)
- Vehicle (slightly acidic saline - control)
- 100 nM bbPTH 1-84 solution prepared from lyophilized bbPTH 1-84 (positive control)
- 100 nM thiolated bbPTH 1-84 solution prepared as described above
- PTH released from hydrogels containing 30 μg bbPTH 1-84
- PTH released from hydrogels containing 30 μg thiolated bbPTH 1-84
- Hydrogels containing only PTH vehicle solution

Cyclic AMP was measured in duplicate for each sample by ELISA (Cayman Chemical) to determine if the PTH released from the scaffolds was bioactive. Bioactivity was assessed using the same methodology for hydrogels surrounding PPF scaffolds out to 21 days.

In vivo degradation.

Thiol-ene hydrogel preparation.

Thiol-ene hydrogels were prepared as described for in vitro studies, with the addition of a fluorphore (Alexa Fluor 680) cross linked to the matrix. Alexa Fluor 680 was modified to contain a sulfhydryl group in order to allow cross-linking to the hydrogel matrix.

Surgery.

All procedures were approved by the Institutional Animal Care and Use Committee (IACUC protocol number 15-555A). Twelve male Sprague Dawley rats (~350g) were anesthetized by isoflurane inhalation (2-3%, to effect). Animals received buprenorphine SR (0.6-0.8mg/kg) and cefazolin (20 mg/kg) subcutaneously 20-30 minutes prior to surgery, for pain management and prophylactic antibiotic respectively. After anesthesia the rat's fur was clipped to remove hair at the incision site. An incision was be made in the skin, a pocket under the skin was made and the gels were placed in the pocket and the skin was stapled to close. Four rats received Alexa Fluor 680 labeled thiol-ene hydrogels. Eight rats received PPF scaffolds surrounded by Alexa Fluor 680 labeled thiol-ene hydrogels. Animals were imaged daily for the first 10 days, then every other day until the assigned time point.

Animals with hydrogels (not surrounding PPF) were imaged until fluorescence from the gel could no longer be distinguished from fluorescence of the surrounding skin. When fluorescence from the gel could no longer be detected, the implant site was opened and examined to qualitatively assess hydrogel degradation. In animals with hydrogels + PPF scaffolds, time points were 10 (n = 2), 20 (n = 2), 40 (n = 2) and day 56 (n = 2). At each time point the implant site was opened and examined to qualitatively assess hydrogel degradation.

Imaging.

Preliminary ex-vivo imaging was performed to verify no components of the system fluoresced at the utilized excitation/emission wavelengths for Alexa Fluor 680 (excitation wavelength: 679 and emission wavelength: 702). The PPF scaffold, thiol-ene hydrogels, thiol-ene hydrogels surrounding PPF scaffolds, and suture were all imaged. Poly(ether-ether) ketone

(PEEK) plates and titanium k-wires utilized in femur defect models were also imaged to determine whether or not they fluoresced at the excitation and emission wavelengths for Alexa Fluor 680 to determine whether or not fluorescence of any components would interfere with fluorescence detected from the hydrogels if they were to be implemented in a femur defect model in future studies.

At each measurement timepoint, rats were anesthetized by isoflurane inhalation (2-3%, to effect). Rats were then placed in the light-tight, heated chamber; anesthesia continued during the procedure with 2% isoflurane introduced via nose cone. As fur and organs also fluoresce at similar wavelengths, and at times it may make it difficult to distinguish the gel, the subcutaneous pocket was isolated using black paper to cover the rat and imaged as well in the event gel fluorescence needed to be confirmed (was not obvious in the whole animal image). An example of a rat imaged as well as the isolated gel pocket are shown in Figure 3. 4. The fluorescent label from the gel was detected by the IVIS spectrum system (excitation wavelength: 679 and emission wavelength: 702), integrated, digitized and displayed. Fluorescence was analyzed for a 4mm circular ROI, centered in the gel area, using Living Image software

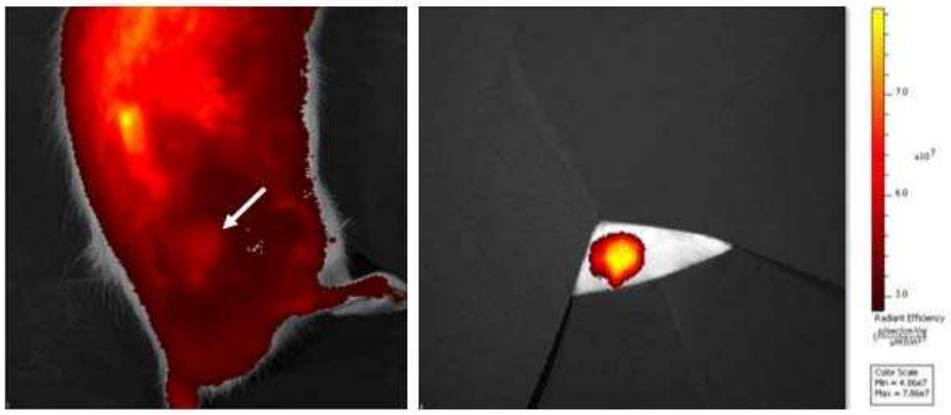

Figure 3. 4 : (Left) IVIS imaging of rat with fluorophore labeled thiol-ene hydrogel, indicated by the white arrow. (Right) IVIS imaging of implanted thiol-ene hydrogels isolated using black paper.

3.3 Results.

In vitro release.

No difference was observed in PTH or thiolated PTH released from gels with or without PPF scaffolds ($p > 0.24$), thus 28 day release studies were carried out without PPF scaffolds. Figure 3. 5 shows the differing release profiles between gels containing PTH (entrapped in the matrix) and those containing thiolated PTH (cross-linked to the matrix). Parathyroid hormone entrapped in the matrix of thiol-ene gels diffused out rapidly, with 80% being released by day 3, and 100% by day 14. Gels containing thiolated PTH (PTH tethered to the hydrogel), showed retention of the bulk of PTH with only 8 % of the PTH released by day 14. Between days 14 and 21 80% of the PTH was released, and by day 28 and 100% of the PTH was released.

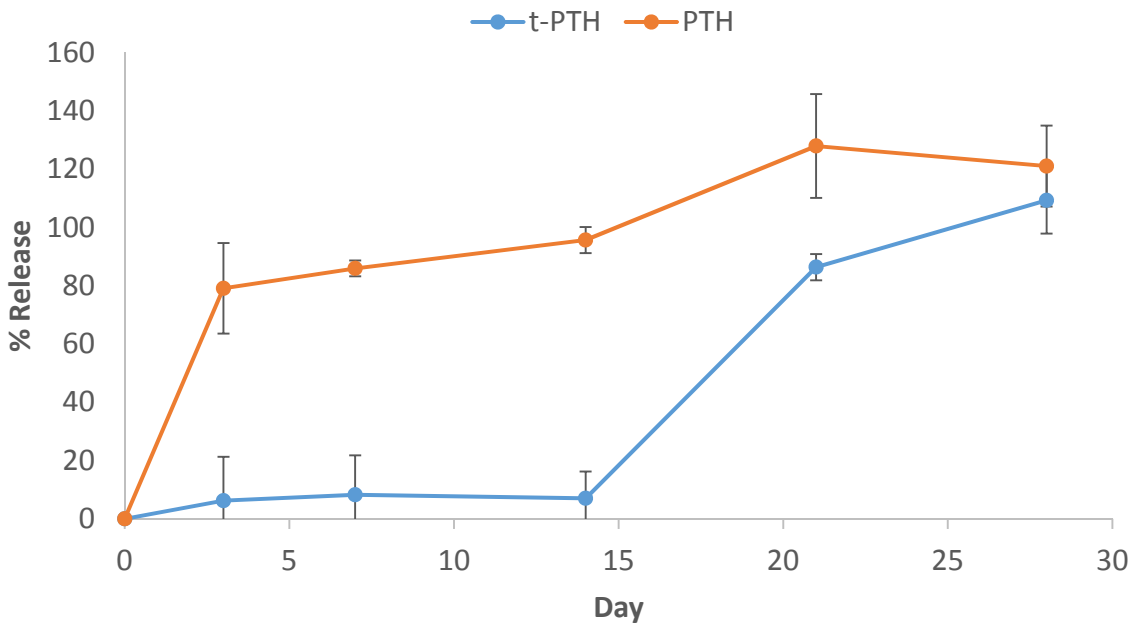

Figure 3. 5 : Thiol-ene hydrogel release profile data for gels containing PTH entrapped in the matrix (orange), and PTH tethered to the matrix (blue).

Verification of bioactivity.

Cyclic AMP activity was significantly higher in all PTH groups and forskolin than vehicle and hydrogel controls ($p > 0.003$) Bioactivity of PTH released from hydrogels was confirmed at days 7, 14 and 21 with no significant differences detected as compared to PTH reconstituted the day of treatment ($p > 0.554$) (Figure 3. 6).

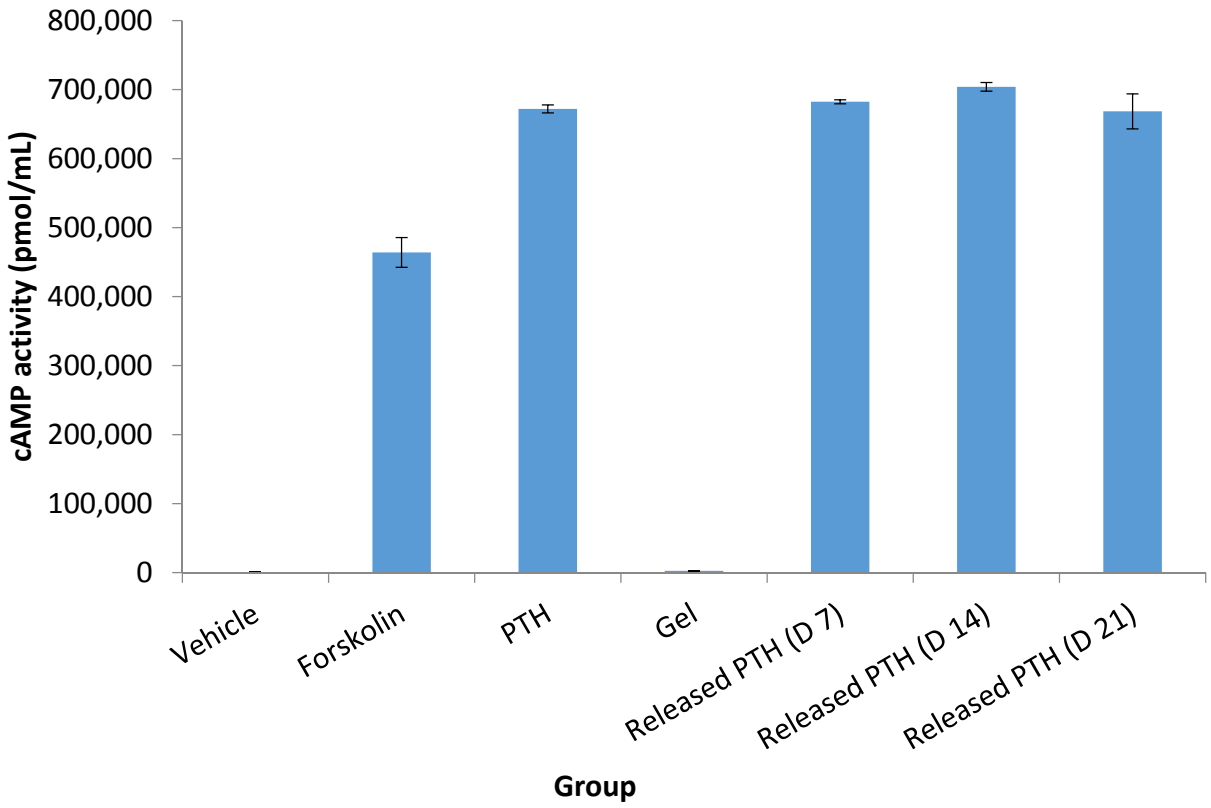

Figure 3. 6 : Bioactivity of PTH released from hydrogels at day 7, 14, and 21 was retained.

In vivo degradation.

Preliminary ex vivo imaging of thiol-ene gels, PPF scaffolds, and the combination of the PPF scaffold and thiol-ene gel confirmed the gels and scaffolds did not fluoresce. The titanium k-wires utilized for femur defect studies similarly did not fluoresce, however, the PEEK fixation plates did fluoresce.

Alexa Fluor 680 gels (no PPF scaffold) were detectable until between day 8 and 21. Fluorescence could no longer be detected in two rats at day 8, one rat at day 18, and one rat at day 21. Detected fluorescence is shown in Figure 3. 7. Over the first 5 days there was an initial decrease in the amount of fluorescence detected followed by a leveling off at an average radiant efficiency of approximately 6E7 $(p/s/cm^2/sr)/(\mu W/cm^2)$. Detectable fluorescence remained at that level until gels were no longer detectable. Upon dissection of the subcutaneous pocket where gels were located, no evidence of gel could be detected at day 18 or 21, in the two rats sacrificed at day 8 there was still a small amount of fluid in the pocket that fluoresced when imaged.

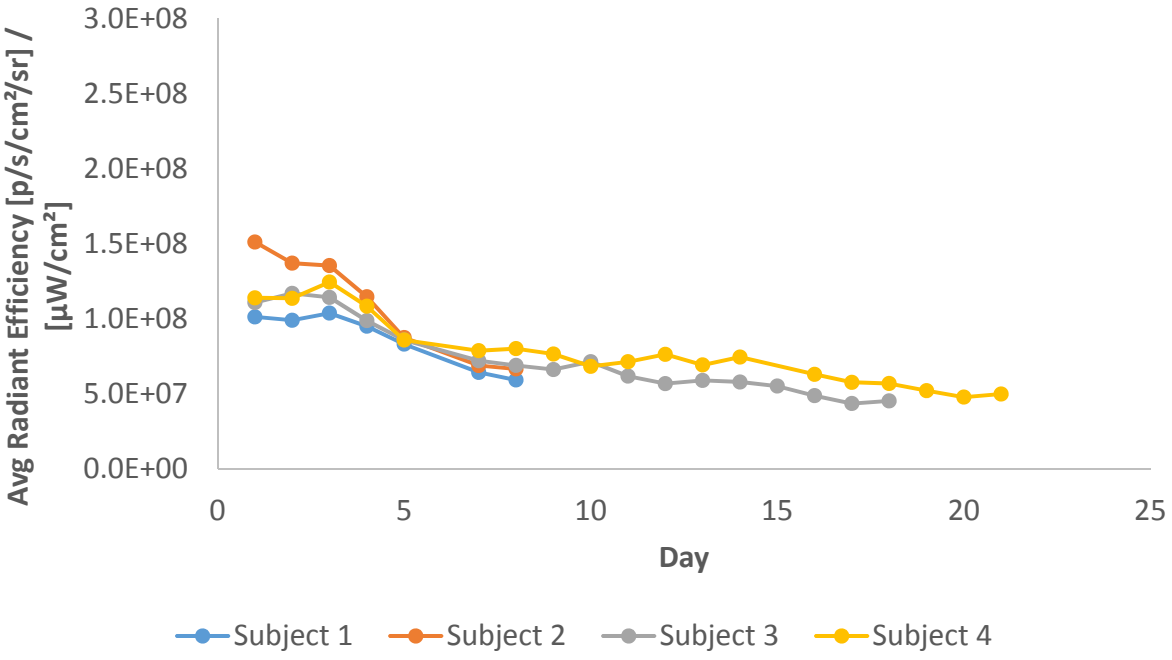

Figure 3. 7 : In vivo fluorescence of thiol-ene hydrogels labeled with Alexa Fluor 680. Gels were detectable until between days 8 and 21. Upon resection of the implant site, some fluid was visible in animals euthanized at day 8, and there was no evidence of gel or fluorescence at day 21.

Alexa Fluor 680 labeled hydrogels surrounding PPF scaffolds remained detectable up to 8 weeks (the latest timepoint in the study, Figure 3. 8). The amount of detected fluorescence is shown in Figure 3. 8.

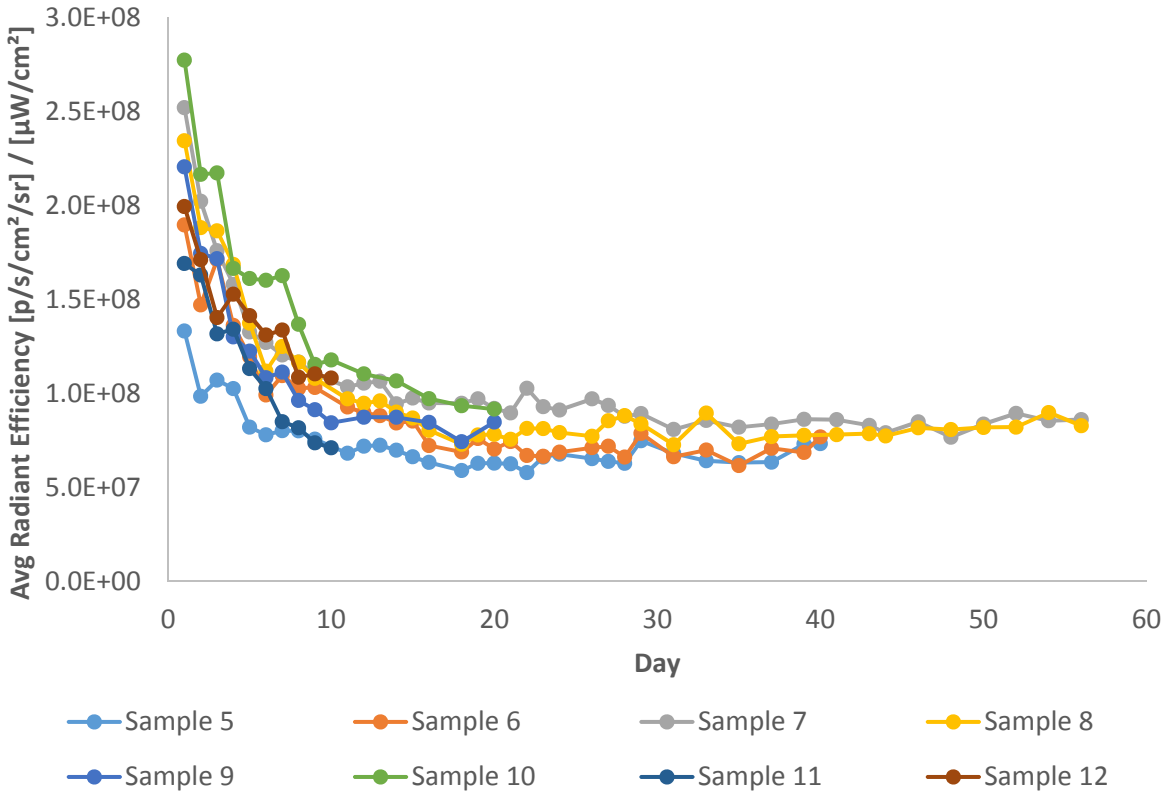

Figure 3. 8 : In vivo fluorescence of PPF scaffolds and thiol-ene hydrogels labeled with Alexa Fluor 680. Fluorescence from the gels was detectable until day 56 when animals were euthanized. Upon resection of the implant site, gels surrounding PPF scaffolds were evident in the subcutaneous pocket.

Representative images of rats with labeled gels and gels isolated using black paper over the timecourse of the study are shown in Figure 3. 9 and Figure 3. 10. There was more variability observed in the initial amount of fluoresce detected in hydrogels surrounding PPF scaffolds. However, like Alexa Fluor 680 labeled hydrogels without PPF scaffolds an initial drop in fluoresce over the first 5 days was followed by a leveling off at an average radiant efficiency of approximately 6E7 $(p/s/cm^2/sr)/(\mu W/cm^2)$. This fluorescence level persisted until week 8 when the study was terminated.

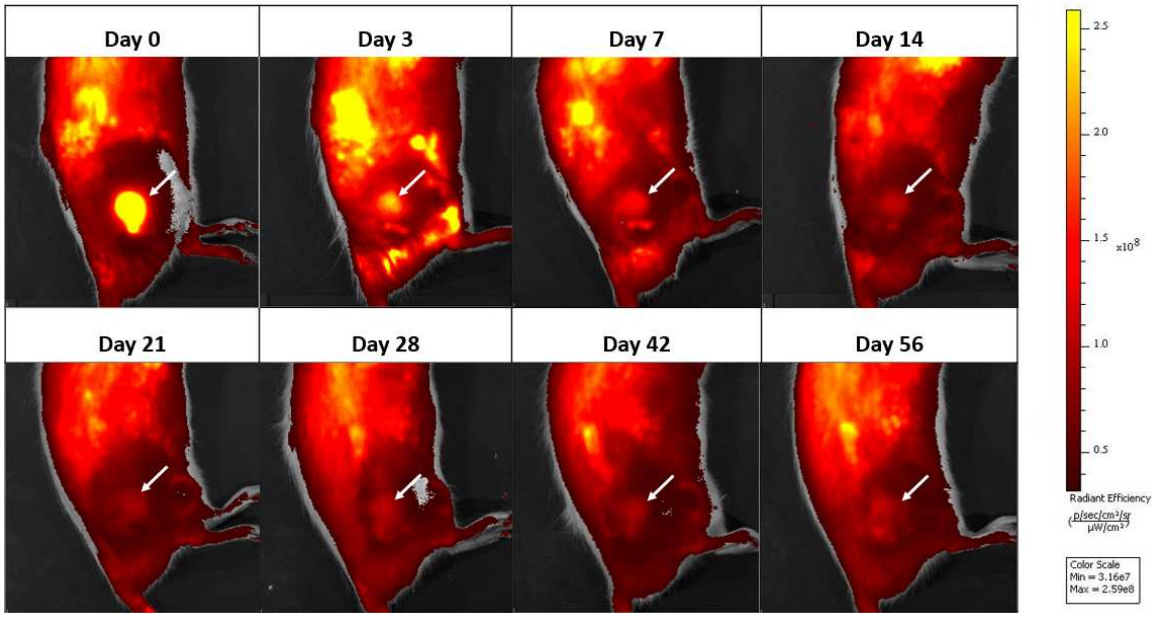

Figure 3. 9 : IVIS imaging of fluorophore cross linked to a thiol-ene hydrogel surrounding a PPF scaffold over the course of 8 weeks.

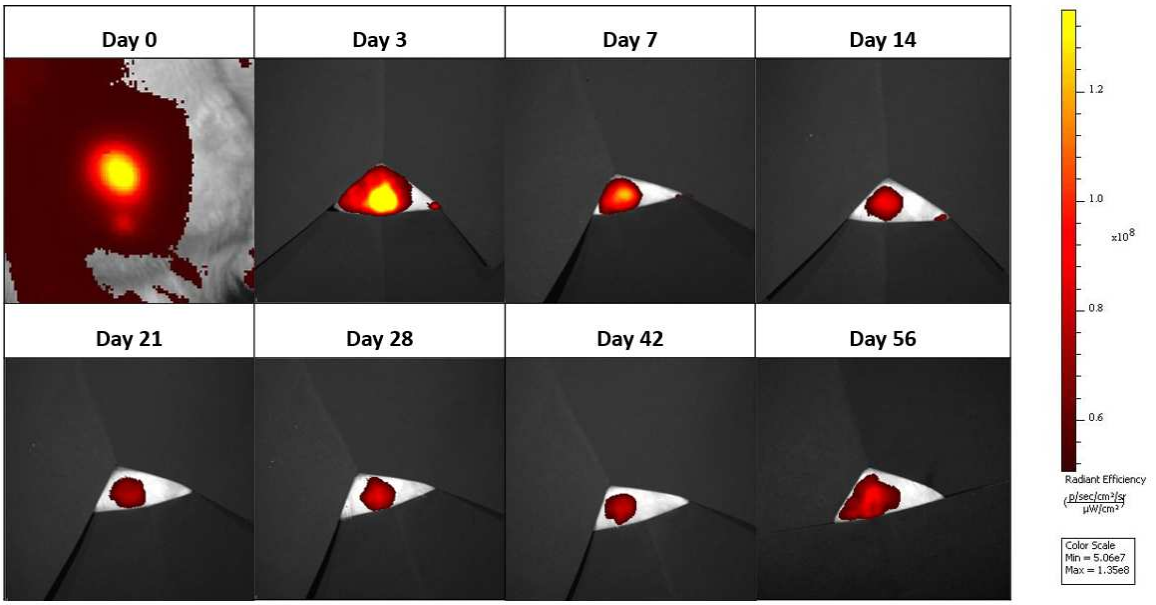

Figure 3. 10 : IVIS imaging of fluorophore cross linked to a thiol-ene hydrogel surrounding a PPF scaffold for 8 weeks. The subcutaneous implant is isolated using black paper to mitigate any autofluorescence from the rat to verify location and fluorescence.

Upon dissection of the subcutaneous pocket, gel surrounding and within the PPF scaffold was evident at all timepoints examined (Figure 3. 11). At days 10 and 20, the gel and scaffold were easily removed from the pocket in one piece. At day 40 gel removal from the pocket in one piece was more difficult (the gel fell apart more easily) than earlier timepoints.

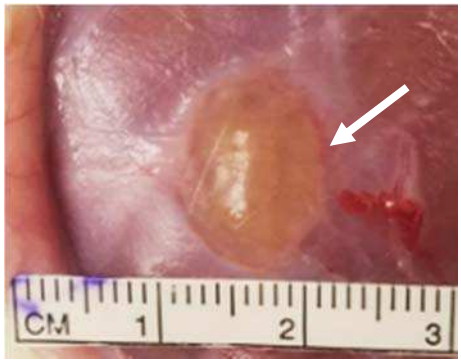

Figure 3. 11 : Thiol-ene hydrogel surrounding a PPF scaffold, subcutaneous implant at day 56.

3.4 Discussion.

Hydrogels are an effective and tailorable mode of bioactive molecule, drug, or cell delivery for tissue engineering/regenerative medicine applications. Release profile of molecules from hydrogels can impact the healing response from surrounding tissue. Thus characterization of the release profile and degradation of hydrogels is integral to understanding and interpreting any healing response, or lack thereof, when the hydrogel is used in regenerative medicine applications. PTH delivered via polyethylene glycol (PEG) matrix resulted in increased bone formation in bone chambers in rabbits as well as cylindrical defects around titanium implants in dog mandibles (Jung, Cochran et al. 2007, Jung, Hammerle et al. 2007). However, the release profile of PTH released from this delivery system was not reported in either study. PTH delivered via fibrin hydrogel also resulted in increased healing compared to controls, in vitro PTH release

was tracked out to 72 hours. In the first 72 hours only 11.6% of the loaded PTH was released from the hydrogel (Arrighi, Mark et al. 2009). These studies characterized the release of PTH from thiol-ene hydrogels when entrapped within the hydrogel matrix or tethered to the hydrogel matrix as well as in vivo degradation of hydrogels alone or in combination with a rigid PPF scaffold in a subcutaneous implant model.

In vitro release data confirm different release profiles when PTH is entrapped within the hydrogel matrix as compared to when it is tethered to the hydrogel matrix. The release profile of PTH released from hydrogels with PTH entrapped in the matrix is comparable to what is seen with collagen sponges used to deliver BMP clinically. The in vitro release data showed rapid diffusion of PTH out of the thiol-ene gel when it is entrapped within the matrix. The majority (80%) of the PTH had been released by 72 hours. This is likely due to the small size of PTH, and not entirely unexpected. More sustained release from the gel may occur for larger molecules like BMP, hydrophobic and insoluble proteins may also get trapped in the matrix until degradation as well (Mariner, Wudel et al. 2013, Grim, Marozas et al. 2015). The remainder of PTH entrapped within the hydrogel matrix was released by day 21. Notably the measures for days 21 and 28 are slightly higher than 100% release. As a fixed amount of PTH was entrapped within the matrix, this is likely due to variability in hydrogel breakdown affecting protein measures. The use of a μBCA assay to measure PTH released from scaffolds is a limitation of this study as the assay is not specific to PTH. Thus if the bond between an RGD peptide and the PEG backbone was broken down by hydrolysis and liberated from the hydrogel matrix, it may have been picked up by the assay. This was addressed by utilizing hydrogels with no PTH as controls (or blanks) to be subtracted off at each timepoint. However, variability in breakdown likely still contributes a small

amount to overall variability in protein measures. Ideally a PTH specific assay would have been used. However, after multiple trials utilizing a PTH specific assay, it was discovered a component of the gel was causing nonspecific binding in the assay giving far more variable and unreliable results than examining protein content in general. The release profile of PTH released from hydrogels with PTH tethered to the matrix is more comparable to that observed by Arrighi et al in the fibrin hydrogel used to deliver PTH to drill defects in sheep (Arrighi, Mark et al. 2009). Tethering PTH to the thiol-ene hydrogel matrix successfully mitigated the rapid release of the majority of PTH until day 14. Interestingly, between days 14 and 21 80% of the tethered PTH was released from the hydrogel. PTH can be liberated from the hydrogel matrix either by hydrolysis or MMP activity. As the in vitro studies did not contain any MMPs, the release observed between days 14 and 21 is indicative of the timepoint at which those bonds are broken down by hydrolysis and liberated from the hydrogel matrix.

The information obtained from in vitro release experiments are limited to contributing to the understanding of PTH liberated from the hydrogel matrix by either diffusion or hydrolysis. Addition of MMPs to the experiment in attempt to mimic the in vivo environment more completely would not be expected to have a drastic impact on the release of PTH when it is entrapped within the matrix. PTH diffuses easily from the hydrogel matrix at an early timepoint. The hydrogel breaking down, or mesh size increasing beyond that caused by swelling from the surrounding PBS does not appear necessary for PTH diffusion. Introduction of MMPs would result in a more rapid breakdown of the hydrogel matrix, perhaps allowing for 100% of the PTH to be released prior to day 21. However, the diffusion resulting in the early burst release would persist. Contrarily, when PTH is tethered to the hydrogel matrix, the release profile would likely be

slightly different than what was observe in this study if MMPs were added or when the hydrogel is placed in vivo. In gels were PTH is tethered to the matrix, PTH can be liberated by hydrolysis (as observed in this study) or by MMP degradation of the hydrogels. In an in vivo environment, or if MMPs were introduced the breakdown of the hydrogel matrix would be expected to result in release of more than 8% of PTH at earlier timepoints than day 14 as there would be a second mechanism by which PTH could be liberated. It is difficult to define a physiologically relevant value for addition of MMPs to in vitro studies. However, understanding in vivo degradation of these gels and combining that information with the in vitro release profile can lend greater insight into an anticipated in vivo release profile. In vivo degradation studies indicated thiol-ene hydrogels breakdown in a subcutaneous implant model between 8 and 21 days. Thus all PTH (whether entrapped within he matrix, or tethered to it) would be released by 21 days. This would likely have a noticeable impact on the release profile for hydrogels with PTH tethered to the matrix. As the matrix is degraded more PTH would be released at earlier timepoints than the 14 -21 day release observed in vitro. Interestingly, when the thio-ene hydrogels were used with rigid PPF scaffolds in vivo degradation did not occur as rapidly. In these cases, it seems the in vitro release profile observed for PTH tethered to the matrix may be comparable to what would be observed in vivo.

In vivo degradation of thiol-ene hydrogels has not been examined previously. Though there are some limitations to this study, it provides useful information for understanding how the in vitro release profiles may more directly relate to in vivo modes as an important aspect of the thiol-ene hydrogel degradation is MMPs. Ultimately the application for this PTH delivery system is a femur defect model to study bone regeneration applications. However, as

degradation of thiol-ene hydrogels has not been performed in this manner previously a more straightforward model was chosen for these studies. The chosen subcutaneous model provides a physiologically relevant biological component to the degradation study. In comparison to a femur defect however, the amount of damage at the implant site as well as fluid flow are less thus the amount of MMPs infiltrating the hydrogels are likely less. The cells/MMPs that are present in the subcutaneous model result in faster degradation than an environment without them as expected. Thiol-ene hydrogels labeled with Alexa Fluor 680 were completely broken down in subcutaneous pockets between 8 and 21 days. Whereas the gels used for in vitro release remained in PBS at 37 °C for 28 days with no visible evidence of degradation. Interestingly when the labeled thoil-ene gel was combined with the PPF scaffold, in vivo degradation did not occur as rapidly. In fact, gels were still present at 8 weeks. This may be due in part to the PPF scaffold playing a role in decreasing fluid flow through the scaffold, slowing breakdown. It may also provide a more mechanically protected environment in general. The rats used in these studies were not restricted in their daily activities in any way. It is possible degradation of hydrogels was influenced by grooming or playing/interacting with cage mates. Incorporation of the PPF scaffold may have helped mitigate any outside mechanical influences. It seems likely degradation would occur more rapidly in a femur defect model as the damage level and amount MMPs and fluid present at the implant site would be higher.

Labeling with Alexa Fluor 680 allowed in vivo tracking of the hydrogels in these studies. An initial drop in detectable fluorescence over the first 3 – 5 days was observed followed by a leveling off for the duration of the study. The initial drop observed is likely due, at least in part, to diffusion of unbound fluorophore out of the matrix. Though an excess of binding sites for the

fluorophore were available, that does not guarantee all will bind during photo-polymerization. It is important to note, the location of binding of Alexa Fluor 680 to the hydrogels is to the PEG-Nb backbone. Thus Alexa Fluor 680 can be liberated form the hydrogel matrix by either hydrolysis or MMP degradation. If the MMP degradable cross-linker were labeled instead the leveling off in fluorescence may not have been observed. However, hydrogels being detected at a consistent level of fluorescence until there was no longer evidence of the hydrogels in the subcutaneous pocket may also be due to the degradation characteristics of the hydrogels as a whole (not just the link between Alexa Fluor 680 and PEb-Nb). The effect seen may also be influenced by the model. As gels are in a subcutaneous pocket, perhaps there is not enough cellular activity to remove liberated fluorophore from the implant area. Whereas in a higher damage model, like a femur defect, perhaps liberated fluorophore could be more readily removed.

In vitro release of PTH from thiol-ene scaffolds was characterized for two different release profiles. This information can be utilized to help understand healing response when thiol-ene gels are used for bone regeneration applications. Similarly, some important difference were noticed in in vivo studies. Firstly, tagging the gel with Alexa Fluor 680 was an effective means by which to track in vivo degradation. Secondly, incorporation of the PPF scaffold prolonged the degradation process. Though observations may not be fully representative of thiol-ene hydrogel degradation in a femur defect model, the general timeline of thiol-ene hydrogel degradation as well as differing degradation timelines resulting from including a rigid PPF scaffold are novel and important findings for understanding how PTH delivered via these hydrogels may affect healing in a bone defect.

References.

Andreassen, T. T. and V. Cacciafesta (2004). "Intermittent parathyroid hormone treatment enhances guided bone regeneration in rat calvarial bone defects." J Craniofac Surg **15**(3): 424-427; discussion 428-429.

Arrighi, I., S. Mark, M. Alvisi, B. von Rechenberg, J. A. Hubbell and J. C. Schense (2009). "Bone healing induced by local delivery of an engineered parathyroid hormone prodrug." Biomaterials **30**(9): 1763-1771.

Brown, K. V., B. Li, T. Guda, D. S. Perrien, S. A. Guelcher and J. C. Wenke (2011). "Improving bone formation in a rat femur segmental defect by controlling bone morphogenetic protein-2 release." Tissue Eng Part A **17**(13-14): 1735-1746.

Dadsetan, M., T. Guda, M. B. Runge, D. Mijares, R. Z. LeGeros, J. P. LeGeros, D. T. Silliman, L. Lu, J. C. Wenke, P. R. Brown Baer and M. J. Yaszemski (2015). "Effect of calcium phosphate coating and rhBMP-2 on bone regeneration in rabbit calvaria using poly(propylene fumarate) scaffolds." Acta Biomater **18**: 9-20.

Dempster, D. W., R. Muller, H. Zhou, T. Kohler, E. Shane, M. Parisien, S. J. Silverberg and J. P. Bilezikian (2007). "Preserved three-dimensional cancellous bone structure in mild primary hyperparathyroidism." Bone **41**(1): 19-24.

Dempster, D. W., M. Parisien, S. J. Silverberg, X. G. Liang, M. Schnitzer, V. Shen, E. Shane, D. B. Kimmel, R. Recker, R. Lindsay and J. P. Bilezikian (1999). "On the mechanism of cancellous bone preservation in postmenopausal women with mild primary hyperparathyroidism." J Clin Endocrinol Metab **84**(5): 1562-1566.

Einhorn, T. A. (1998). "The cell and molecular biology of fracture healing." Clin Orthop Relat Res(355 Suppl): S7-21.

Ejersted, C., T. T. Andreassen, H. Oxlund, P. H. Jorgensen, B. Bak, J. Haggblad, O. Torring and M. H. Nilsson (1993). "Human parathyroid hormone (1-34) and (1-84) increase the mechanical strength and thickness of cortical bone in rats." J Bone Miner Res **8**(9): 1097-1101.

Fairbanks, B. D., M. P. Schwartz, C. N. Bowman and K. S. Anseth (2009). "Photoinitiated polymerization of PEG-diacrylate with lithium phenyl-2,4,6-trimethylbenzoylphosphinate: polymerization rate and cytocompatibility." Biomaterials **30**(35): 6702-6707.

Fuerst, A., S. Derungs, B. von Rechenberg, J. A. Auer, J. Schense and J. Watson (2007). "Use of a parathyroid hormone peptide (PTH(1-34))-enriched fibrin hydrogel for the treatment of a subchondral cystic lesion in the proximal interphalangeal joint of a warmblood filly." J Vet Med A Physiol Pathol Clin Med **54**(2): 107-112.

Grim, J. C., I. A. Marozas and K. S. Anseth (2015). "Thiol-ene and photo-cleavage chemistry for controlled presentation of biomolecules in hydrogels." J Control Release **219**: 95-106.

Habener, J. F., M. Rosenblatt and J. T. Potts, Jr. (1984). "Parathyroid hormone: biochemical aspects of biosynthesis, secretion, action, and metabolism." Physiol Rev **64**(3): 985-1053.

Harris, A. M., P. L. Althausen, J. Kellam, M. J. Bosse and R. Castillo (2009). "Complications following limb-threatening lower extremity trauma." J Orthop Trauma **23**(1): 1-6.

Hock, J. M. and I. Gera (1992). "Effects of continuous and intermittent administration and inhibition of resorption on the anabolic response of bone to parathyroid hormone." J Bone Miner Res **7**(1): 65-72.

Jahangir, A. A., R. M. Nunley, S. Mehta and A. Sharan (2008) "Bone-graft substitutes in orthopaedic surgery." AAOS Now.

Jiang, Y., J. J. Zhao, B. H. Mitlak, O. Wang, H. K. Genant and E. F. Eriksen (2003). "Recombinant human parathyroid hormone (1-34) [teriparatide] improves both cortical and cancellous bone structure." J Bone Miner Res **18**(11): 1932-1941.

Jung, R. E., D. L. Cochran, O. Domken, R. Seibl, A. A. Jones, D. Buser and C. H. Hammerle (2007). "The effect of matrix bound parathyroid hormone on bone regeneration." Clin Oral Implants Res **18**(3): 319-325.

Jung, R. E., C. H. F. Hammerle, V. Kokovic and F. E. Weber (2007). "Bone regeneration using a synthetic matrix containing a parathyroid hormone peptide combined with a grafting material." International Journal of Oral & Maxillofacial Implants **22**(2): 258-266.

Karladani, A. H., H. Granhed, J. Karrholm and J. Styf (2001). "The influence of fracture etiology and type on fracture healing: a review of 104 consecutive tibial shaft fractures." Arch Orthop Trauma Surg **121**(6): 325-328.

Lee, K. W., S. Wang, B. C. Fox, E. L. Ritman, M. J. Yaszemski and L. Lu (2007). "Poly(propylene fumarate) bone tissue engineering scaffold fabrication using stereolithography: effects of resin formulations and laser parameters." Biomacromolecules **8**(4): 1077-1084.

Lin, C. C. and A. T. Metters (2006). "Hydrogels in controlled release formulations: network design and mathematical modeling." Adv Drug Deliv Rev **58**(12-13): 1379-1408.

Mahendra, A. and A. D. Maclean (2007). "Available biological treatments for complex non-unions." Injury **38 Suppl 4**: S7-12.

Mariner, P. D., J. M. Wudel, D. E. Miller, E. E. Genova, S. O. Streubel and K. S. Anseth (2013). "Synthetic hydrogel scaffold is an effective vehicle for delivery of INFUSE (rhBMP2) to critical-sized calvaria bone defects in rats." J Orthop Res **31**(3): 401-406.

Mellott, M. B., K. Searcy and M. V. Pishko (2001). "Release of protein from highly cross-linked hydrogels of poly(ethylene glycol) diacrylate fabricated by UV polymerization." Biomaterials **22**(9): 929-941.

Milstrey, A., B. Wieskoetter, D. Hinze, N. Grueneweller, R. Stange, T. Pap, M. Raschke and P. Garcia (2017). "Dose-dependent effect of parathyroid hormone on fracture healing and bone formation in mice." J Surg Res **220**: 327-335.

Mosekilde, L. (1995). "Assessing bone quality--animal models in preclinical osteoporosis research." Bone **17**(4 Suppl): 343S-352S.

Parisien, M., S. J. Silverberg, E. Shane, L. de la Cruz, R. Lindsay, J. P. Bilezikian and D. W. Dempster (1990). "The histomorphometry of bone in primary hyperparathyroidism: preservation of cancellous bone structure." J Clin Endocrinol Metab **70**(4): 930-938.

Silverberg, S. J., E. Shane, L. de la Cruz, D. W. Dempster, F. Feldman, D. Seldin, T. P. Jacobs, E. S. Siris, M. Cafferty, M. V. Parisien and et al. (1989). "Skeletal disease in primary hyperparathyroidism." J Bone Miner Res **4**(3): 283-291.

Silverberg, S. J., M. D. Walker and J. P. Bilezikian (2013). "Asymptomatic primary hyperparathyroidism." J Clin Densitom **16**(1): 14-21.

Skripitz, R., T. T. Andreassen and P. Aspenberg (2000). "Strong effect of PTH (1-34) on regenerating bone: a time sequence study in rats." Acta Orthop Scand **71**(6): 619-624.

Tam, C. S., J. N. M. Heersche, T. M. Murray and J. A. Parsons (1982). "Parathyroid-Hormone Stimulates the Bone Apposition Rate Independently of Its Resorptive Action - Differential-Effects of Intermittent and Continuous Administration." Endocrinology **110**(2): 506-512.

Uzawa, T., M. Hori, S. Ejiri and H. Ozawa (1995). "Comparison of the effects of intermittent and continuous administration of human parathyroid hormone(1-34) on rat bone." Bone **16**(4): 477-484.

Wong, J. Y. and J. D. Bronzino (2007). Biomaterials, CRC Press.

Chapter 4: Aim 3: Quantification of dose dependent effects of locally delivered PTH on bone regeneration in a rat critical size bone defect model.

Synopsis.

Segmental defects in bone commonly have complications or fail to heal properly on their own resulting in the use of around 2.2 million autografts or allografts each year in orthopaedic procedures. Disability due to orthopaedic injury has a significant impact on both the patient and the healthcare system. Limitations of autograft and allograft have led to research into bone graft substitutes. Parathyroid hormone has an anabolic effect on bone and may be combined with a biomaterial scaffold in order to promote bone regeneration and provide an alternative to autograft for treatment of large segmental defects and non-unions. Systemic administration of PTH has been shown to enhance bone regeneration in a variety of research models as well as off label use in a human case. Continuously released, locally delivered PTH has been shown to improve healing/formation around dental implants in dogs and drill defects in sheep. However, dose response to local continuously delivered PTH is still unknown. Whether or not the benefits of PTH treatment observed in these models translate to critical size defect models is also unknown. The objective of this aim was to quantify bone healing induced by locally delivered PTH in a critical size defect model in rats. Efficacy of locally delivered PTH for bone regeneration in a critical size defect was assessed by micro computed tomography at 12 weeks. Bridging of the defect by a rigid poly(propylene fumarate) scaffold and delivery of 3 or 10 μg bbPTH 1-84 via a thiol-ene hydrogel surrounding the rigid scaffold tended to increase bridging of critical size defects. Whereas treatment with higher doses of PTH appeared to result in less bone ingrowth in the defect area supporting the idea there may be a threshold below which local continuously

delivered PTH may be anabolic. Though a robust healing response was not observed as compared to controls; full bridging of critical size defects in some samples was achieved, and a tendency of treatment with 3µg PTH per hydrogel to improve healing was observed. Continued development of the approaches described herein could lead to improved therapies for treatment of non-union and critical size defects in bone. Bone regeneration through locally delivered parathyroid hormone has the potential to improve functional restoration, even beyond that of allografts and without the drawbacks of current treatments, which would improve the quality of life for patients.

4.1 Introduction.

Systemic administration of PTH has been shown to enhance bone regeneration in a variety of research models as well as off label use in a human case (Skripitz, Andreassen et al. 2000, Seebach, Skripitz et al. 2004, O'Loughlin, Cunningham et al. 2009). In closed fracture models PTH treatment results in increased bone formation in the fracture callus (Andreassen, Ejersted et al. 1999, Hamann, Picke et al. 2014, Milstrey, Wieskoetter et al. 2017). PTH similarly increases bone formation in bone chambers and calvarial defects (Andreassen and Cacciafesta 2004, Tsunori, Sato et al. 2015). However, fractures complicated by segmental bone loss do not heal as readily as closed fractures. Healing of a segmental defect model is more difficult to achieve than a closed fracture or drill defect model. PTH treatment (100 µg/kg 3x per week, for 8 weeks) resulted in increased union rate and accelerated healing in a refractory fracture model in rats (Kumabe, Lee et al. 2017). Research utilizing PTH for treatment of segmental bone loss is limited. However, osseointegration of devitalized allografts in a critical size defect was observed in mice with PTH treatment (40 µg/kg/d) in mice (Reynolds, Takahata et al. 2011). Off label PTH

use enhanced healing sufficient to regain use in a human patient with femoral nonunion that failed to heal despite autograft and BMP-7 treatment (Paridis and Karachalios 2011).

The current gold standard for treatment of a critical size defect is autograft (Livingston, Gordon et al. 2003). However, due to limited availability and the potential for donor site morbidity it is not always the best (or a viable) option. Local delivery of PTH may provide an alternative to autograft, allograft and other bone graft substitutes. The anabolic effect PTH has on bone may provide a comparable healing response to allograft. Local delivery gives the potential for reducing systemic exposure to exogenous hormone which may reduce any side effects or risks associated as well as decrease costs. Similarly, if local delivery were achievable in conjunction with an osteoconductive biomaterial scaffold the potential for promotion of healing may be further increased. The effect of localized delivery of PTH on fracture healing and bone regeneration has not been extensively investigated. Though, there are only a handful of in vivo studies investigating the use of locally delivered PTH for bone regeneration, the results are promising (Fuerst, Derungs et al. 2007, Jung, Cochran et al. 2007, Arrighi, Mark et al. 2009).

Polyethylene glycol matrices (PEG) infused with PTH 1-34 (20 μg/mL) were found to be just as effective as autograft when used to fill the defect around a titanium implant (Jung, Cochran et al. 2007). Similarly, fibrin gel delivery of 100 μg/mL PTH 1-34 has produced increased bone volume fraction in femoral drill defects (8 mm diameter, 13 mm depth) in sheep at 8 weeks (Arrighi, Mark et al. 2009). A combination of local delivery of PTH via a gene activated matrix and systemic (40 μg/kg/day) has also been shown to provide improved healing in a segmental defect model in what animal and bone (Chen, Frankenburg et al. 2003). These studies indicate that PTH delivered locally via biomaterials scaffold may be an alternative to for bone grafts for the

treatment of open fractures or critical size bone defects.

The objective of this aim was to quantify bone healing induced by locally delivered PTH in a critical size defect model in rats. This established a base knowledge of the effects of locally delivered PTH on segmental defect healing. This knowledge is critical to future development and improvement of therapies to treat segmental bone defects and non-union fractures. It was hypothesized that PTH would enhance bone healing in a critical size defect model; the goal was to find the minimum effective dose that results in defect bridging and functional restoration of the femur.

The goal was to characterize healing induced by local delivery of PTH, thus a novel scaffold material was not pursued. Instead scaffolds designed by collaborating research groups for bioactive molecule delivery were tailored to incorporate PTH and utilized. The first 5 studies completed were pilot studies examining the effects of locally delivered PTH via 5 different biomaterial scaffolds. The ideal release profile and timing of locally delivered PTH is unknown. Thus since each scaffold had different structural properties as well as methods by which PTH was incorporated, this allowed a general assessment and basis of knowledge to build off of for larger more directed studies. The first pilot study utilized a Methylcellulose hydrogel to entrap and deliver PTH. Studies utilizing an electrospun scaffold (10% poly(lactic-co-glycolic) acid (PLGA, 5% hydroxyapatite nanoparticles, 0.5% polyethylene oxide), HydroxyColl (a hydroxyapatite-collagen sponge), and poly(propylene fumarate) scaffold with PLGA microspheres and a PEG based thiol-ene hydrogel followed. Each of these materials had been used by collaborating research groups as a biomolecule delivery system and represented a different aspect of material options for delivery of PTH for bone regeneration applications. Thus, in the pilot studies, there was not

always a progression leading from one to the other, but a trial of a variety of materials designed for delivery of bioactive molecules.

Hydrogels are promising vehicles for drug and bioactive molecule delivery. There are a variety of options that create delivery systems that have potential to be tailored to enable different release profiles. For example, Chitosan hydrogel composites and hyaluronic acid hydrogels have been explored as a potential injectable rhBMP-2 carrier (Luca, Rougemont et al. 2011, Martinez-Sanz, Ossipov et al. 2011). Agarose and methylcellulose hydrogels have also been successfully used for delivery of glutathione or IL-10 (Martin, Minner et al. 2008). Poly(ethylene glycol) (PEG) based hydrogels have shown promise for delivery of a variety of bioactive molecules, including BMP and PTH (Jung, Cochran et al. 2007, Kim, Hefferan et al. 2009). Preliminary studies in our lab (unpublished data) utilizing a 1.5% agarose, 7% methylcellulose, 1% chitosan hydrogel to deliver 40μg of PTH to a critical size defect in a rat model demonstrated an increase in bone volume in the defect area with PTH treatment compared to both the empty and vehicle groups after 7 weeks of healing. However, full bridging of the defect was not observed in any samples. Based on the findings in the preliminary study the methylcellulose hydrogel was modified slightly to increase viscosity and electrospun fibers were added prior to use in pilot study 1 discussed here. The effect of PTH treatment was not observed in the pilot study reported here however, and the options for improving mechanical integrity of the hydrogel and potential for modified release seemed limited. Thus, this hydrogel was not pursued further in order to test materials with the ability to bridge the defect area and provide modifiable PTH release.

Electrospun scaffolds provide customizable potential for PTH delivery as well as a physical network for potential guided regeneration. The electrospinning process has the benefit of being

able to add bioactive molecules to the scaffold for delivery. The release of PTH can be varied by degradation properties of the scaffold as well as amount added in to the scaffold. Electrospun poly (lactic acid) membranes have shown promise as potential material for enhancing bone regeneration (Kim, Lee et al. 2006). Electrospun PLGA-HA membranes have been shown to have a positive effect of cells, increasing proliferation and ALP expression (Ngiam, Liao et al. 2009). In these studies (study 2) a 10% poly(lactic-co-glycolic) acid (PLGA), 5% Hydroxyapatite nanoparticles (Hap), 0.5% polyethylene oxide electrospun scaffold (Electrospun PLGA/HA/PTH) was used.

Hydroxyapatite-collagen sponges have shown good bioactivity in vitro when cultured with MC3T3-E1 cells for 28 days as well as improved healing in a critical size calvarial defect model in Wistar rats (Cunniffe, Dickson et al. 2010, Gleeson, Plunkett et al. 2010). Increasing bioactivity of scaffolds of this nature have also been successful though addition of bioactive molecules like BMP-2 (Curtin, Cunniffe et al. 2012). The HydroxyColl sponge is similar to the collagen sponge used in Infuse™ to deliver BMP-2 for spinal fusion and recalcitrant non-union applications. This scaffold give provides the benefits of a scaffold that has previously been shown to be bioactive in critical size defects as well as providing a straightforward method for local delivery of PTH (soaking the sponge in PTH solution). The HydroxyColl sponge used in study 3 also has the benefit of being a natural material, versus a synthetic polymer thus making it easier for the body to break down and decreasing concerns of unfavorable degradation characteristics.

Poly(propylene fumarate) (PPF) is an osteoconductive and biodegradable polymer that has been studied both as a scaffold for bone ingrowth as well as a method by which to deliver bioactive molecules (Kempen, Lu et al. 2006, Lee, Wang et al. 2007) and is vastly customizable.

As a scaffold for bone regeneration applications, PPF has been utilized in the form of an injectable foaming cement (Lewandrowski, Cattaneo et al. 1999) as well as a preformed scaffold (Lee, Wang et al. 2007). As a mode of bioactive molecule delivery preformed PPF scaffolds may be coated with the desired bioactive molecule (Vehof, Fisher et al. 2002), or it may be incorporated into the structure of the scaffold. For example, controlled release of BMP-2 from injectable PPF was achieved by incorporating PLGA and PPF microspheres that contained BMP-2 in the scaffold itself. By adjusting the ratio of PLGA and PPF making up the microspheres, release of BMP-2 could be modified (Kempen, Lu et al. 2006). The preformed PPF scaffold used in study 4 has been shown to aid in bone regeneration applications when delivering BMP-2 (Kempen, Yaszemski et al. 2009, Kempen, Lu et al. 2010). The PPF scaffold fabrication process allows a customizable geometry as well as tailorable mechanical properties. The PPF scaffold can more readily be fabricated with mechanical properties comparable to those of bone than can any other scaffolds used in these studies (Lee, Wang et al. 2007). Study 4 utilized a preformed PPF scaffold to bridge the defect area, the pores of the scaffold were filled with PLGA microspheres containing PTH. The PPF scaffold and PLGA microspheres have been shown to be effective in delivery of BMP-2 for bone regeneration applications (Kempen, Lu et al. 2006, Kempen, Lu et al. 2008).

As hydrogels are tailorable candidates for biomolecule delivery, a second hydrogel was also explored. PEG based thiol-ene hydrogels have previously been shown to promote better healing when used to deliver BMP-2 in calvarial defects than the commercially available collagen sponge for BMP delivery (Mariner, Wudel et al. 2013). In comparison to the methylcellulose hydrogel used in study 1, the thiol-ene hydrogel (study 5) retained a shape and could be

confidently placed in the bone defect. It also allowed straightforward modifications to alter the PTH release profile (Grim, Marozas et al. 2015).

Upon completion of these pilots, the thiol-ene hydrogel was utilized in two larger scale follow-up studies further examining the effects of local delivery on bone regeneration in a critical size defect. The thiol-ene hydrogel provided the most straightforward modifications for varying PTH release profile. However, though the hydrogels have sufficient mechanical integrity to bridge the defect area, degradation seemed relatively fast compared to healing time, thus for the two larger scale studies the thiol-ene hydrogels were utilized with the rigid PPF scaffolds from study 4. Through the use of thiol-ene hydrogels in combination with PPF scaffolds, the effects of two different release profiles of locally delivered PTH on bone regeneration in a critical size defect model in rats was examined.

4.2: Study 1: Methylcellulose Hydrogel (1.5% Agarose, 9% Methylcellulose, 1 % Chitosan, poly (L-lactic) acid (PLLA) fibers)

Study 1: Scaffold preparation.

A Methylcellulose Hydrogel (1.5% Agarose, 9% Methylcellulose, 1 % Chitosan, poly (L-lactic) acid (PLLA) fibers) was created in the laboratory of Dr. Ryan Gilbert at Rensselaer Polytechinic Institute (RPI). Parathyroid hormone was reconstituted in sterile PBS in the appropriate concentration to allow for gels to contain either 40 μg or 120 μg and mixed with the remaining hydrogel reagents from Dr. Gilbert's lab. Concentration of PTH per gel was based on preliminary studies with a similar hydrogel. To mix, a 1 mL syringe was used to draw as much PBS/PTH solution and hydrogel as possible into the syringe and then back out a minimum of 10 times. After mixing, air bubbles were removed by centrifuging samples at 2000 rpm for 2 minutes.

Study 1: Surgery.

Female Sprague Dawley rats (240-300g, ~16 weeks old) underwent surgery to create a 5mm segmental defect in the femur. Surgeon and animal aseptic preparation prior to the surgery was according to the Institutional Animal Care and Use Committee (IACUC) Guidelines for Rodent Survival Surgery. Rats were anesthetized by isoflurane inhalation (2-3%, to effect). After anesthesia the rat's fur was clipped to remove hair at the incision site. An incision was made over the lateral aspect of the femur. The diaphysis of the femur was approached, clearing away soft tissue with a combination of sharp and blunt dissection. A 4 pin internal fixation plate (as shown in **Error! Not a valid bookmark self-reference.**) was attached to the femur with 0.035" threaded k-wires and a 5mm defect was created using a dremel saw. After the defect was created a small muscle pocket was made using sutures to hold the muscle close to the bone in attempt to prevent the hydrogel from moving away from the defect area. Then one of 4 treatments (n = 5/group)

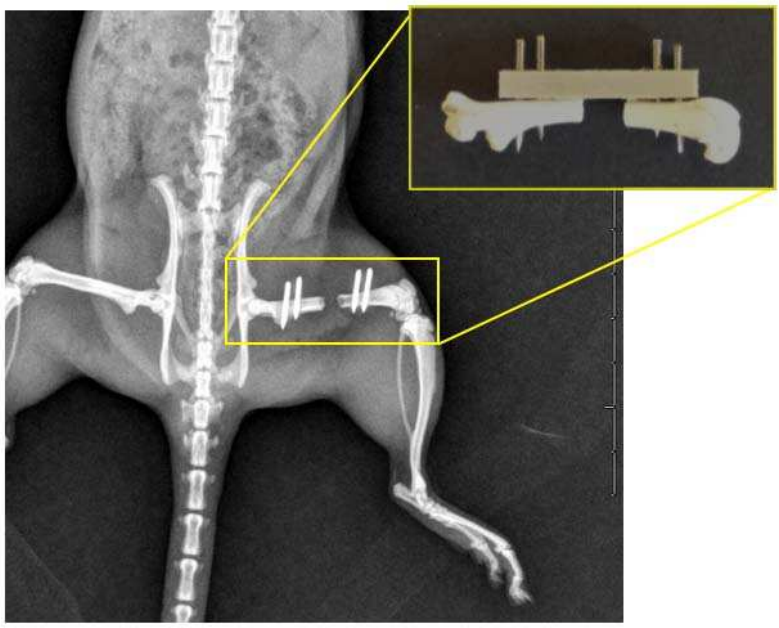

Figure 4. 1 : Femur defect with fixation plate model.

was placed in the defect area; the defect was left empty, a hydrogel (vehicle) containing no PTH

was placed, a hydrogel + 40 µg bbPTH 1-34 was placed, or a hydrogel + 120 µg bbPTH 1-34 treatment. The soft tissue was then sutured closed and wound clip staples were placed over the incision to help protect the incision. Animals received morphine (0.01 mg/kg) subcutaneously 20-30 minutes prior to surgery and cefazolin (20 mg/kg) as a prophylactic antibiotic. Rats were allowed to recover and were observed daily for evidence of wound problems such as swelling or drainage. One rat was sacrificed 24 hours post-op to observe whether or not the hydrogel was still apparent in the defect area. For all other rats healing was monitored via x-ray at 6, 10 and 12 weeks. At the end of the study animals were sacrificed and femurs were fixed in neutral buffered formalin for 72 hours then stored in 70% ethanol. Healing was assessed via 2-D measurement of new bone ingrowth on faxitron images.

Study 1: Radiographs.

At weeks 6 and 10 rats were anesthetized with ketamine/xylazine (50 mg/kg) and radiographed to monitor healing progress. A minimum of 5 length measurements between bone ends in the defect area were collected, as indicated by the red arrows in Figure 4. 2.

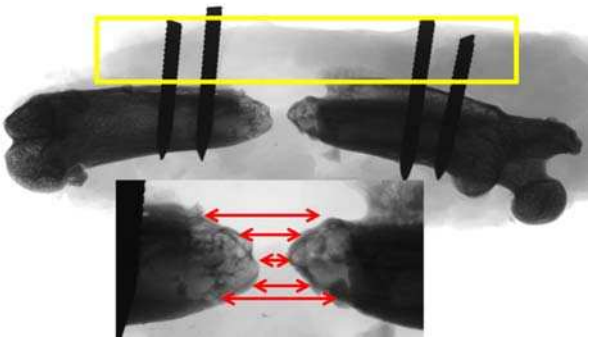

Figure 4. 2 : Faxitron image representative of % defect bridged measure performed on radiographs. The yellow box indicates the location of the fixation plate, % Defect bridged measurement examples - indicated by red arrows.

The percent of the defect area that had bridged with new bone was calculated as original defect size (5mm) minus average length between bone ends (measured in mm), divided by original defect size x 100% (equation 1).

$$\%\, defect\ bridged\ = \left(\frac{5\ mm - length\ between\ bone\ ends}{5\ mm}\right) * 100 \qquad (1)$$

Study 1: Faxitron image analysis.

Faxitron images of the femur were used to obtain 2-D measurements of bone ingrowth into the defect area. New bone in the defect area, as well as the percent of the defect that had bridged were measured using Bioquant Osteo software. Figure 4. 3 shows a faxitron image with the defect area expanded to demonstrate where the defect area was defined. Percent defect bridged was determined as described for week 6 and 10 (Figure 4. 2).

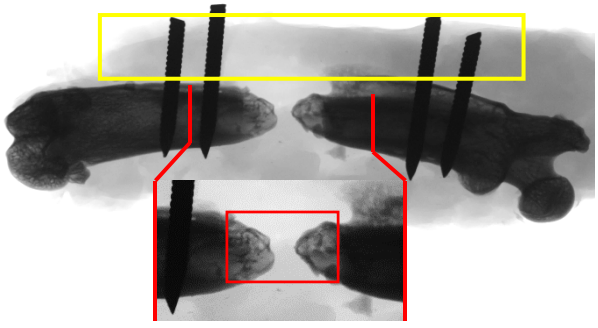

Figure 4. 3 : Faxitron image used for 2-D bone measurements. Area in which new bone ingrowth into the defect area is indicated with the red box.

Study 1: Statistics.

One way analysis of variance (ANOVA) was used to determine differences between treatment groups, a p-value of less than 0.05 was be considered significant. If significant differences were detected by ANOVA, a Tukey post-hoc test was compare individual groups to one another.

Study 1: Results.

One rat was sacrificed 24 hours post op to assess whether or not the gel was still observable in the defect area. At 24 hours post op, there was no evidence of the hydrogel still being present in the defect area. Four rats were lost to surgery/recovery complications, in all other animals there were no complications. At 6 or 10 weeks no differences were observed in bone area or percent defect bridged ($p > 0.169$). Similarly at 12 weeks, there were no significant differences in new bone in the defect ($p = 0.481$) (Figure 4. 4) or in percent defect bridged measures ($p = 0.216$). When femurs were excised, the defect area of all samples were bridged by a fibrous capsule.

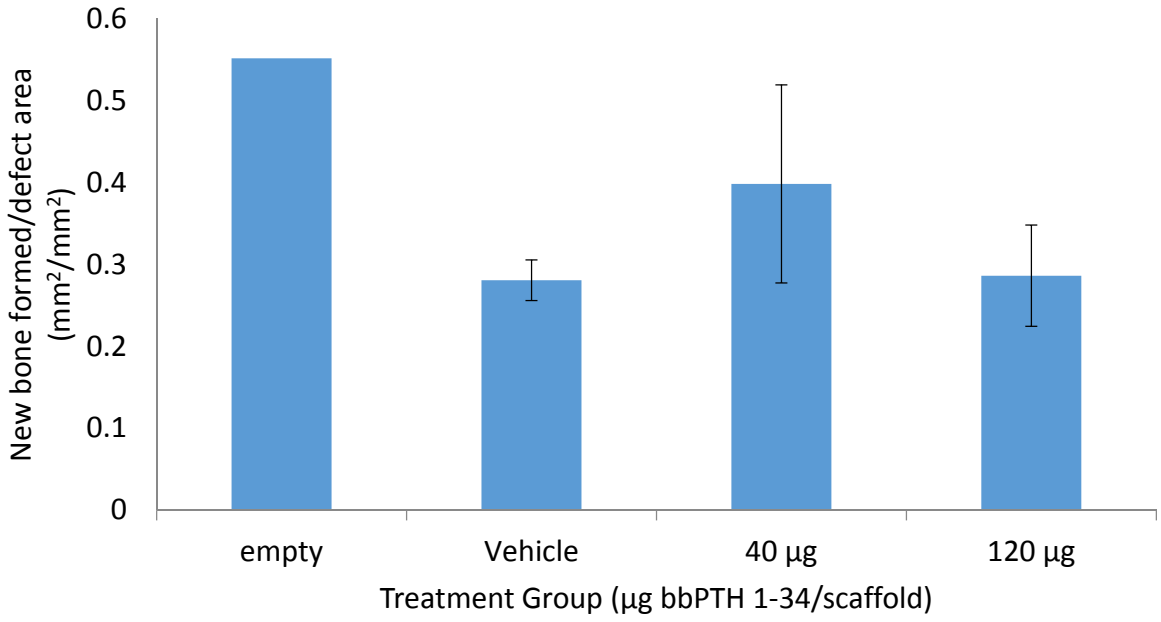

Figure 4. 4 : New bone ingrowth into to the defect area for Study 1 - Methylcellulose hydrogel. No differences between treatment group were observed.

Study 1: Discussion.

Results of the study utilizing the methylcellulose hydrogel did not show any difference between treatment groups. This material was chosen based on preliminary (unpublished) data from our laboratory that showed an increase in bone volume in the defect area when 40 µg PTH was delivered via a 1.5% agarose, 7% methylcellulose, 1% chitosan hydrogel. Differences in results between the studies could be due to a variety of factors. The preliminary data was collected at week 7, whereas this study was terminated at week 12. It is possible that differences detectable at earlier time points may not be by week 12. There were also changes in the fixation method in the defect model between the two studies to eliminate fixation instability observed in the pilot. The instability in the preliminary study may have confounded results observed. Finally, the addition of PLLA fibers into the gel may have had an undesired impact on healing or PTH

release. When grossly examining the defect area, clearing away as much soft tissue as possible without disrupting the healing site, a soft tissue callus bridging every defect was observed. Full bridging of the defect is desirable, but only if it is bone, or a precursor to bone. However, in these samples the callus was fibrous in nature. This could potentially indicate an inflammatory response beyond that desired for a normal bone healing situation. It is possible that, though similar hydrogels without PTH have been used for nerve regeneration applications (Martin, Minner et al. 2008), that the material is not favorable to a critical size bone defect environment. Lastly, differences may not have been observed between groups simply because the gel did not remain in the defect area well. The gel lacked mechanical integrity. A muscle pocket was formed around the femur in attempt to keep the gel in place. However, at 24 hours post op no obvious evidence of the gel was observed. Thus this particular carrier was abandoned in pursuit of carriers with the ability to bridge the defect area and provide more modifiable PTH release.

4.3: Study 2: 10% poly(lactic-co-glycolic) acid (PLGA), 5% Hydroxyapatite nanoparticles (Hap), 0.5% polyethylene oxide electrospun scaffold (Electrospun PLGA/HA/PTH)

Study 2: Scaffold preparation.

Scaffolds were a gift from Dr. Ryan Gilbert at Renassler Polytechnic Institute by Shreel Joshi. Briefly, rectangular arrangements of fibers (10%PLGA (50:50), 5%Hap nanoparticles, 0.5% PEO (polyethylene oxide) were created. From this, an area of fiber measured 5 mm x 80 mm was cut out. The arrangements of fibers were then folded over 8 times, wrapped around a steel needle of 2 mm diameter and the ends were sealed with dichloromethane. Holes of diameter 0.75 mm at an even spacing of 1 mm were then created in the scaffold (Figure 4. 5). Accommodation of varying amounts of PTH was done during the electrospinning process. To

increase the amount of PTH in each fiber the absorption time for PTH to adsorb onto hydroxyapatite nanoparticles was increased. Unadsorbed PTH was also electrospun into the fiber, to ensure that no PTH was lost in the process. Scaffolds were created to incorporate no PTH, 50 µg hPTH 1-34, 100 µg hPTH 1-34, or 200 µg hPTH 1-34 into the fibers (n = 3/group). Though the result would not be expected to be drastically different than what would be observed with bbPTH, in the interest of outcomes being directly comparable to literature and commercially available PTH human PTH was utilized in this study. Scaffolds were stored in 15 mL microcentrifuge tubes. The scaffolds were sterilized with the caps open within the ethylene oxide sealed bag. Tubes were capped within the hood after sterilization and stored in a -80^0 C freezer until use (shelf life ~6 months, stored at -80^0 C).

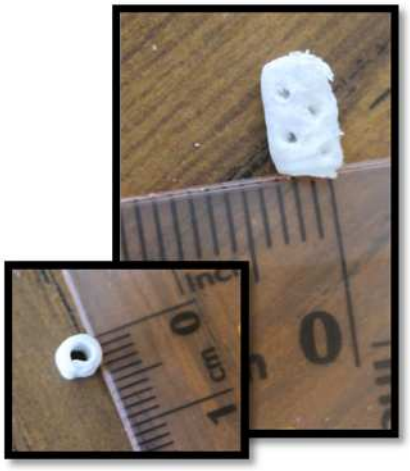

Figure 4. 5 : 10% poly(lactic-co-glycolic) acid (PLGA), 5% Hydroxyapatite nanoparticles (Hap), 0.5% polyethylene oxide electrospun scaffold (Electrospun PLGA/HA/PTH)

Study 2: Surgery.

Male Sprague Dawley rats (250-300g) underwent surgery to create a 5mm segmental defect in the femur. Surgeon and animal aseptic preparation prior to the surgery was according to the Institutional Animal Care and Use Committee (IACUC) Guidelines for Rodent Survival Surgery. Rats were anesthetized by isoflurane inhalation (2-3%, to effect). After anesthesia the rat's fur was clipped to remove hair at the incision site. An incision was made over the lateral aspect of the femur. The diaphysis of the femur was approached, clearing away soft tissue with a combination of sharp and blunt dissection. A 4 pin, raised, internal fixation plate (Figure 4. 6) was attached to the femur with 0.9 mm threaded k-wires and a 5 mm defect was created using

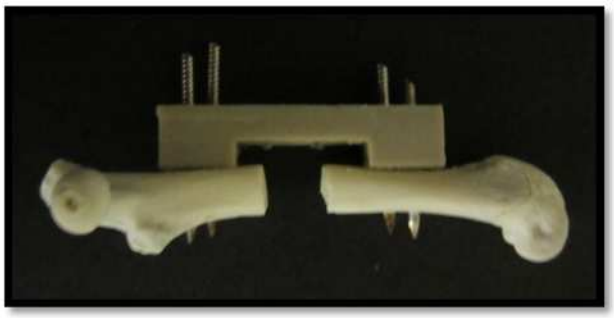

Figure 4. 6 : Raised fixation plate model used for Electrospun scaffold, HydroxyColl, and PPF scaffold with microspheres studies.

gigli wire. Pilot studies 2, 3, and 4 utilized a raised plate model to avoid the possibility bone growth along the fixation plate would confound results. After the defect was created the treatment was placed. Treatment consisted of the given material scaffold (vehicle) or the material scaffold containing 50, 100 or 200 µg PTH. The soft tissue was then sutured closed and wound clip staples were placed over the incision to help protect the incision. Animals received buprenorphine SR (0.6-0.8 mg/kg) subcutaneously 20-30 minutes prior to surgery. Rats were allowed to recover and were observed daily for evidence of wound problems such as swelling or drainage. As limited information was gained from longitudinal x-rays in the previous studies,

defects were not radiographed at timepoints prior to 12 weeks. At 12 weeks animals were sacrificed and healing was assessed via micro computed tomography.

Study 2: µCT.

Bone volume and mineral density were assessed by micro computed tomography. The defect area of each femur was scanned at medium resolution (µCT 80, Scanco Medical). During scans samples were held in a 35 mm tube surrounded by 70% ethanol. The area between the two inner fixation pins (Figure 4. 7) was scanned at 70 kVp, 114 µA, 8 W, FOV/diameter of 36.9 mm. The area of the scan evaluated was limited to new bone ingrowth into the defect area and was evaluated with a lower threshold of 220, gauss support = 1 and sigma = 0.8.

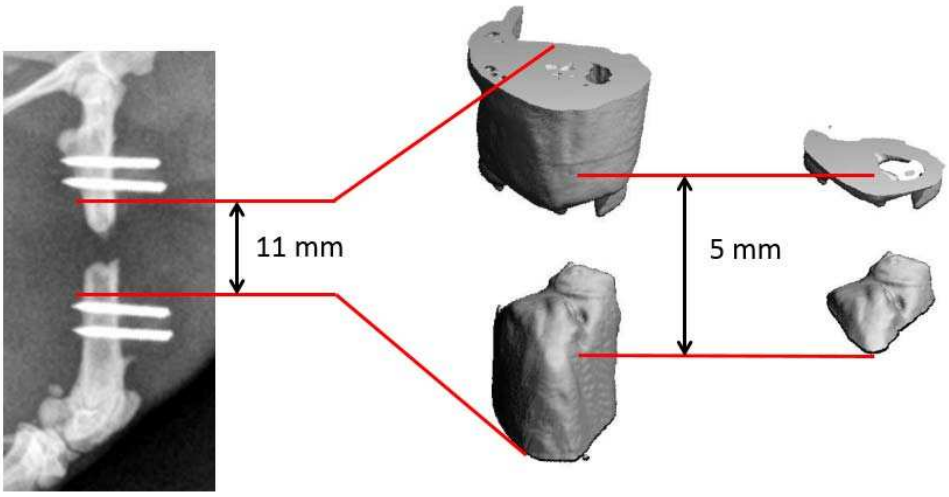

Figure 4. 7 : MicroCT scan region (11 mm) and region that was analyzed for comparison between groups (5 mm).

Statistics.

One way analysis of variance (ANOVA) was used to determine differences between treatment groups within each study. The different carriers were not compared to one another. A p-value of less than 0.05 was considered significant. If significant differences were detected by ANOVA, a Tukey post hoc test was used compare individual groups to one another.

Study 2: Results.

Four samples had to be omitted from analyses due to plate fixation failure (Figure 4. 8). This severely decreased the sample size, leaving n = 1 in the 50 and 200 µg groups and n = 1 in the 100 µg group. Thus, making it difficult to draw conclusions from the study. However, with the samples that remained usable, no significant effect of treatment was observed in measures of bone volume in the defect area (p = 0.890) or mineral density of new bone in the defect area (p = 0.694).

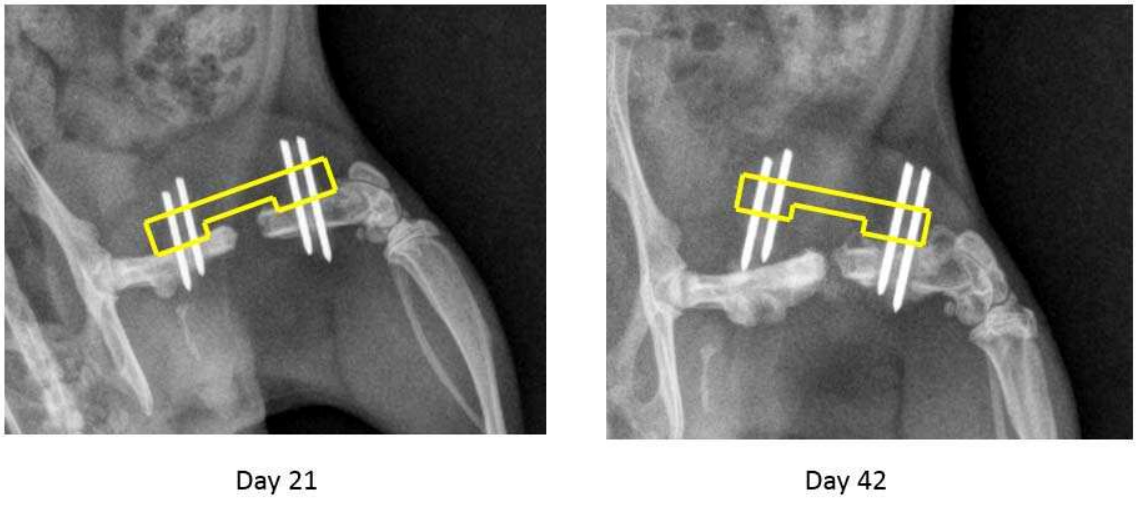

Figure 4. 8 : Example radiograph images of fixation issues. Plate is outlined in yellow.

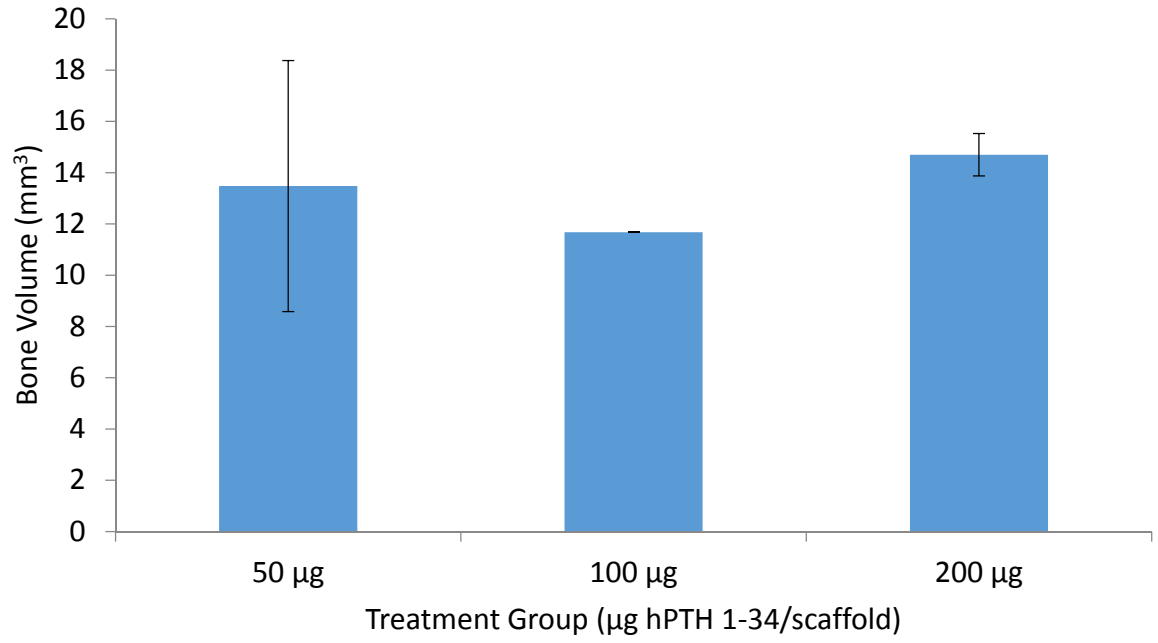

Figure 4. 9 : Bone volume in the defect area 10% poly(lactic-co-glycolic) acid (PLGA), 5% Hydroxyapatite nanoparticles, 0.5% polyethylene oxide electrospun scaffold (Electrospun PLGA/HA/PTH)

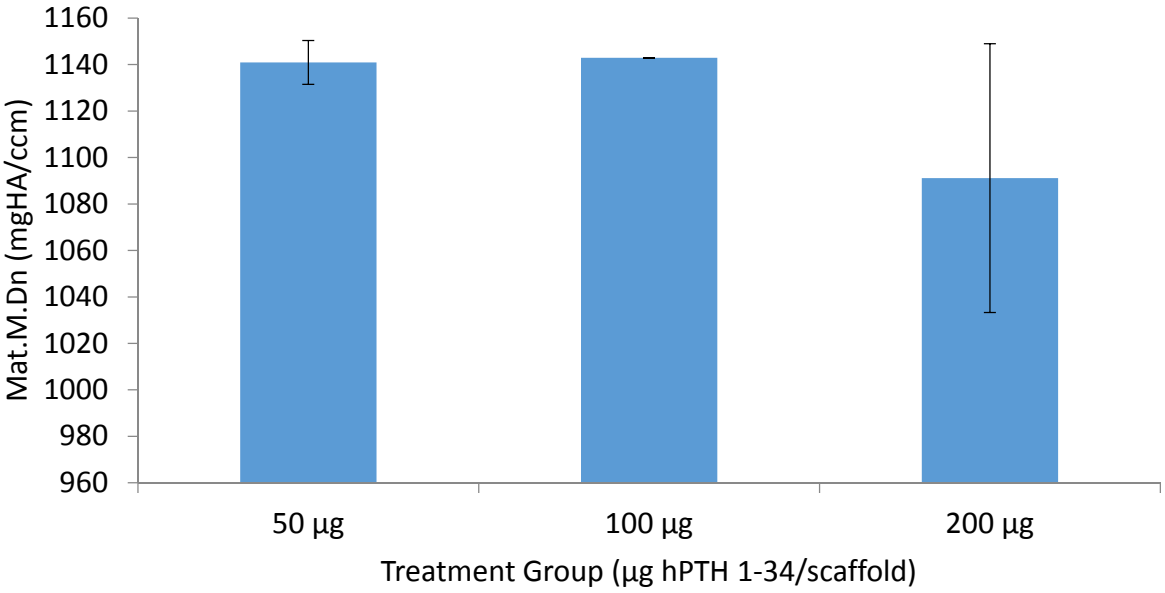

Figure 4. 10 : Bone mineral density of new bone formed in the defect area 10% poly(lactic-co-glycolic) acid (PLGA), 5% Hydroxyapatite nanoparticles, 0.5% polyethylene oxide electrospun scaffold (Electrospun PLGA/HA/PTH)

No difference in the amount of bone in the defect area was observed, and no samples showed full bridging of the defect area. However, µCT scans did show bone formation "scattered" throughout the defect area as shown in Figure 4. 11.

Figure 4. 11 : Bone formation throughout the defect area - regardless of lack of full bridging. 10% poly(lactic-co-glycolic) acid (PLGA), 5% Hydroxyapatite nanoparticles, 0.5% polyethylene oxide electrospun scaffold (Electrospun PLGA/HA/PTH)

Study 2: Discussion.

Unfortunately, the fixation issues resulting from use of the raised fixation plate resulted in loss of too many samples to draw conclusions regarding the effects of PTH on healing from this study. The raised fixation plate was utilized in order to prevent the plate acting as a surface for bone growth, and potentially confounding or inadvertently supplementing any response as a result of PTH or scaffold use (Oest, Dupont et al. 2007). Similar plates have been used by other research groups with success, however fixation failure was problematic in this study. Though effects of locally delivered PTH could not be concluded from this study, the elctrospun scaffold was easy to work with, provided a variety of dose options for PTH and had potential for

customizability. Likewise bone formation in the center of the defect area may indicate promise for the scaffold for bone regeneration applications in general. Fixation failure did not result until a later timepoint and was not observed with sufficient time to change the surgical model for pilots with the HydroxyColl sponge or PPF scaffolds as there was some overlap.

4.4: Study 3: HydroxyColl Sponge

Study 3: Scaffold preparation.

Scaffolds were a gift from Dr. Fergal O'Brien at the Royal College of Surgeons Ireland. A 5 x 5 x 3 mm cube of HydroxyColl sponge (Figure 4. 12) was utilized for PTH delivery. Size was based

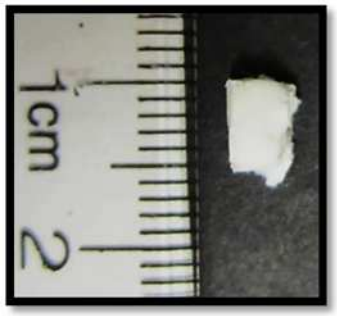

Figure 4. 12 : HydroxyColl scaffold

on 5 mm length of defect, ~4 mm diameter of femur and the 3mm thickness the scaffold material was made at. 30 µL of the appropriate bbPTH 1-84 solution or vehicle was added to each scaffold 20 min prior to implantation. As the ability to synthesize full length bbPTH 1-84 became available, all studies moving forward utilized bbPTH 1-84. Groups were as follows: Vehicle, 50 µg bbPTH 1-84, 100 µg bbPTH 1-84, 200 µg bbPTH 1-84, 400 µg bbPTH 1-84 (n = 3/group).

Study 3: Surgery.

Surgical procedure for study 3 was the same as that used for study 2.

Study 3: µCT.

Microcomputed tomography scanning and analyses were the same as those used for study 2.

Study 3: Statistics.

One way analysis of variance (ANOVA) was used to determine differences between treatment groups within each study. A p-value of less than 0.05 was be considered significant. If significant differences were detected by ANOVA, a Tukey post hoc test was used compare individual groups to one another.

Study 3: Results.

Only 2 samples in study 3 were lost due to fixation problems. Vehicle, HydroxyColl with 50 and 100 µg PTH had a final sample size of 3 rats per group and the 200 µg group had a sample size of 2. Even though fewer samples were lost in this study, no significant differences in bone volume in the defect area (p = 0.491) or mineral density of new bone (p = 0.790) was observed between treatment groups.

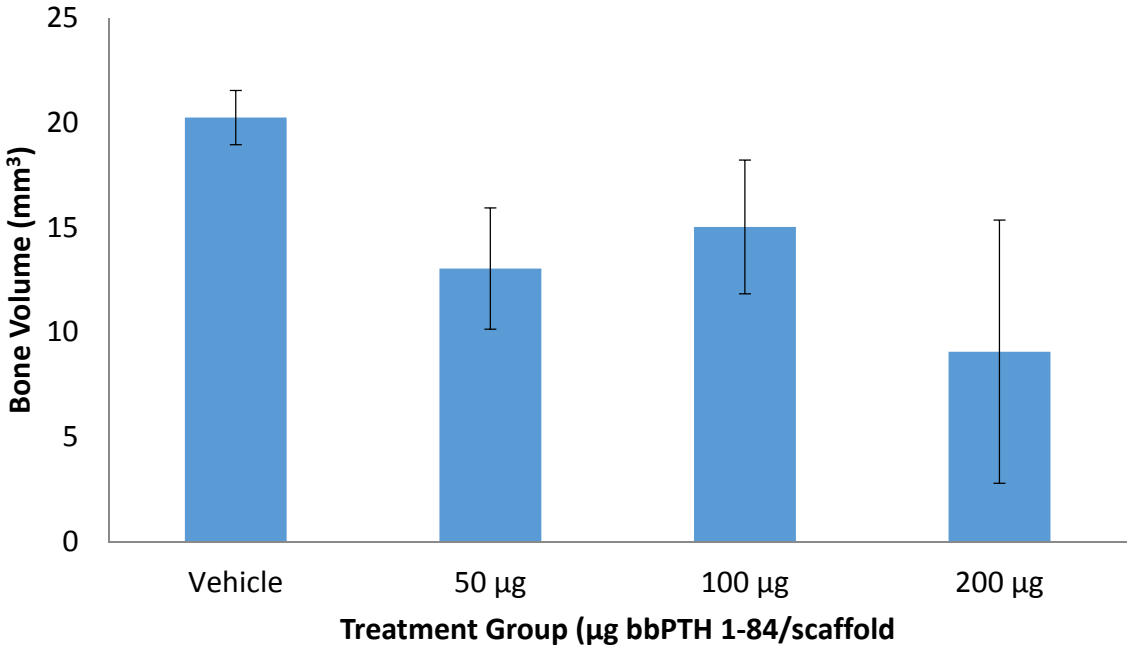

Figure 4. 13 : New bone ingrowth in the defect area of samples in the HydroxyColl study

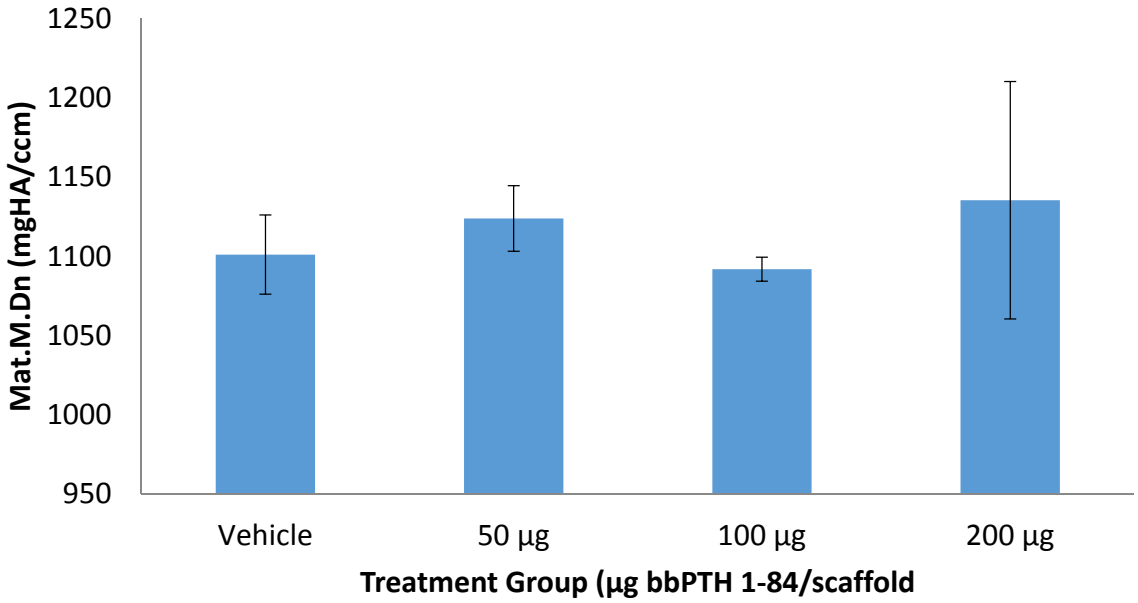

Figure 4. 14: Bone mineral density of new bone in the defect area of samples in the HydroxyColl study.

Study 3: Discussion.

The fixation issues that plagued study 2 (electrospun scaffolds) were not observed as readily in the HydroxyColl study. The lack of difference between groups observed in the HydroxyColl study could potentially be due to a lack of effect of PTH on bone regeneration or due to an aspect of the delivery of PTH. Brown et al demonstrated the importance of being able to modulate the release of bioactive molecules from scaffolds, as there is likely an optimal release profile for healing response. For example, analysis of segmental defect model indicated burst followed by sustained release of rhBMP-2 regenerated more new bone than other release profiles (Brown, Li et al. 2011). In vitro release of PTH from the HydroxyColl scaffolds yields a burst release with the majority of released PTH coming out in the first day and then a much lower sustained release. Though the burst release profile is effective for delivery of BMP-2, it may not be for PTH. The ideal release profile for delivery of PTH in bone regeneration applications is

presently unknown. Based on the increased healing observed as a result of local PTH delivery (released in a sustained fashion without the large burst release) by Arrighi et al a more sustained release may be desirable. (Jung, Cochran et al. 2007, Arrighi, Mark et al. 2009). Another challenge to healing response was when the PTH solution was added to the sponges, mechanical integrity was lost. In its dry form, the collagen sponge holds shape nicely, once wet, however it held very little form and it was difficult to ensure the sponge would stay in place in the defect area. For other models this would likely not be an issue, however with the segmental defect model methods by which to keep a scaffold in place are limited.

4.5: Study 4: Poly(propylene fumarate) scaffold and PLGA microspheres

Study 4: Scaffold preparation.

Poly(propylene fumarate) scaffolds and PLGA microspheres were provided by Dr. Michael Yaszemski's Biomaterials and Tissue Engineering Laboratory at Mayo Clinic. PPF scaffolds were fabricated via steriolithography as previously described (Lee, Wang et al. 2007) and coated with Synthetic Bone Mineral (SBM) coating (Dadsetan, Guda et al. 2015). The CAD designed scaffolds

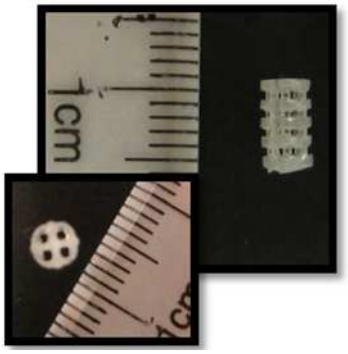

Figure 4. 15 : Poly(propylene fumarate) scaffold, longitudinal and cross sectional views

were cylinders with square pores, shown in Figure 4. 15. The external dimensions were 6 mm in

length and 3 mm in outer diameter. The pores throughout the scaffold were 1 mm x 1 mm and the strut thickness was 500 µm.

PLGA microspheres were originally fabricated to encapsulate bbPTH 1-84. PTH was reconstituted in 1% BSA for encapsulation and encapsulated at 10 µg PTH/mg microspheres. Upon using these microspheres with the PPF scaffold, the encapsulation concentration of 10 µg PTH/mg required too many microspheres to cleanly fit in the defect area. Microspheres were re-made at 30 µg/mg. Bioactivity of PTH released from the microspheres was verified by treating MC3T3-E1 cells with released PTH and performing a cyclic AMP assay prior to use. Immediately prior to surgery; the appropriate amount of microspheres for each group were incorporated into the PPF scaffold by making a "putty" of microspheres by adding 70 µL collagen, PureCol (Advanced BioMatrix, Carlsbad, CA) to the appropriate amount of microspheres for the given dose, then transferred to the scaffold and pasted into the pores with a spatula. Doses for this study were vehicle, 50 µg bbPTH 1-84, 100 µg bbPTH 1-84, and 200 µg bbPTH 1-84 (n = 3/group).

Study 4: Surgery.

Surgical procedure was the same as that used for study 2.

Study 4: µCT.

Microcomputed tomography scanning and analyses were the same as those used for study 2.

Study 4: Statistics.

One way analysis of variance (ANOVA) was used to determine differences between treatment groups within each study. A p-value of less than 0.05 was considered significant. If significant differences were detected by ANOVA, a Tukey post hoc test was used compare individual groups to one another.

Study 4: Results.

Six samples were lost due complications, 3 to plate fixation failure, 2 died in surgery, and 1 had to be euthanized due to formation of infection/absess. This resulted in n = 2 in the vehicle and 100 µg groups and n = 1 in the 50 and 200 µg groups, limiting the ability to draw concrete conclusions from this pilot study. However, no significant differences were observed in bone volume in the defect area (p = 0.429) or mineral density of new bone in the defect area (p = 0.665) between groups.

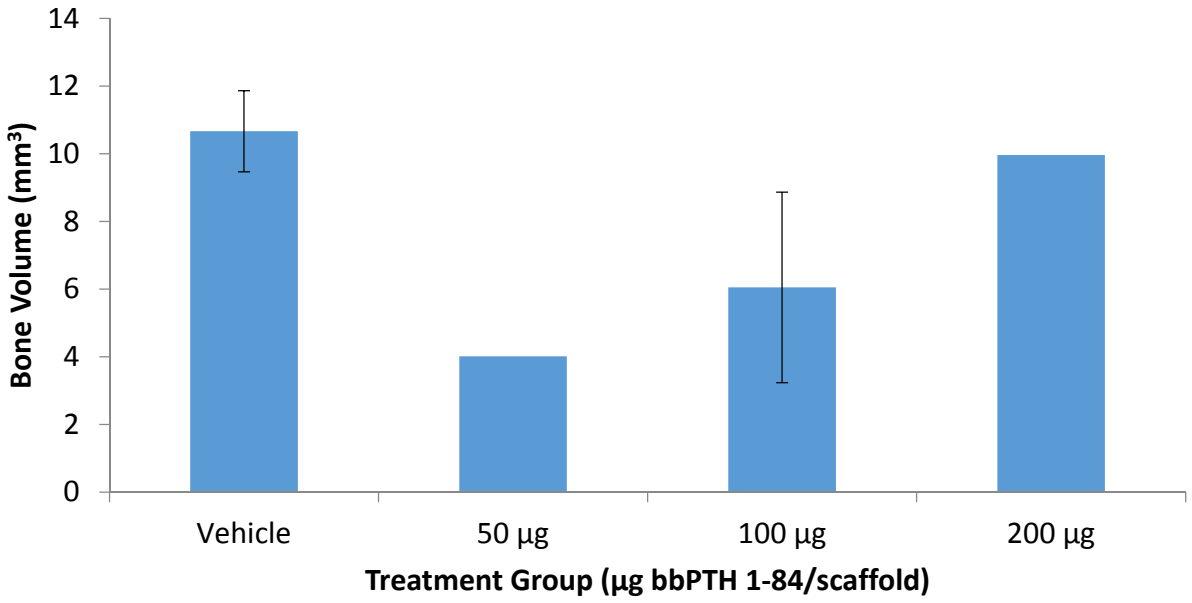

Figure 4. 16 : New bone ingrowth in the defect area of samples with PPF scaffolds and PLGA microspheres containing varying amounts of PTH.

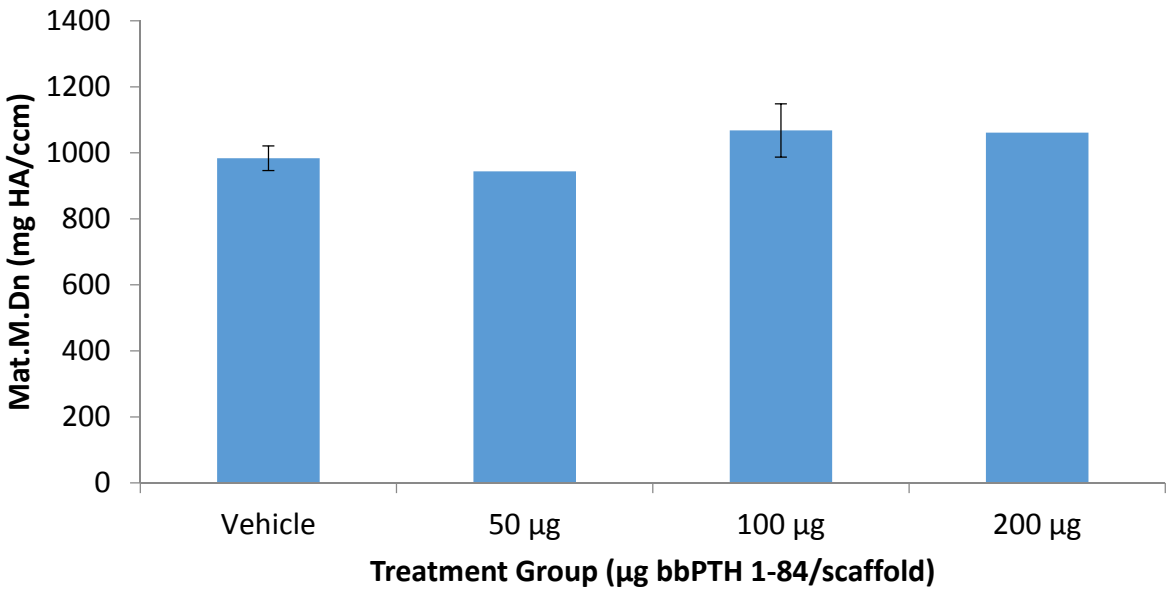

Figure 4. 17: Mineral density of new bone in the defect area for samples treated with PPF scaffolds and PLGA microspheres containing varying amounts of PTH.

Study 4: Discussion.

Similar to the study utilizing the electrospun scaffolds, the fixation issues resulting from use of the raised fixation plate resulted in loss of too many samples to draw concrete conclusions from the studies utilizing PPF/microspheres. Fixation with a raised plate was utilized in order to prevent the plate acting as a surface for bone growth, and potentially confounding or inadvertently supplementing any response as a result of PTH or scaffold use (Oest, Dupont et al. 2007). Similar plates have been used by other research groups with success, and observed minimal fixation failure in the study examining PTH released from HydroxyColl scaffolds. However, based on observations in the studies utilizing the electrospun scaffolds and this study (PPF scaffold with microspheres), the inconsistency in successful long term fixation was too risky to proceed with this fixation method. All studies following utilized a fixation plate, fixed flat along

the bone. Though concrete observations on the effects of PTH could not be made from this study, observations on usability and customizability of the scaffold and microspheres, could be. The PPF scaffold fit snugly into the defect area and there was no concern of it moving from the defect site. Though the microspheres were effective at encapsulating and releasing bioactive PTH, they were rather difficult to work with and not the most practical option when it came to prepping scaffolds for use in surgery.

4.6: Study 5: Thiol-ene Hydrogel

Study 5: Scaffold preparation.

Monomer solutions for the hydrogels were prepared courtesy of Dr. Kristi Anseth's lab at CU Boulder as previously described (Fairbanks, Schwartz et al. 2009). Briefly, Monomer solutions were: 6 wt%/vol 10K 4-arm poly(ethylene glycol)-norbornene (PEG-NB), 1mM adhesion peptide (CRGDS), 5.5 mM di-cysteine MMP-degradable crosslinker peptide (KCGPQGIAGQCK), and 0.01% of the photoinitiator lithium phenyl-2,4,6-trimethylbenzoylphosphinate (LAP). The appropriate amount of PTH for the given treatment group was reconstituted in dPBS to be incorporated into the gel. A 1mL syringe was used as a mold to create 90 µL gels (diameter: ~4 mm, height: ~5 mm) (Figure 4. 18). Hydrogels were polymerized by placing the solution in molds under a 2.5 mW/cm^2 UV lamp (365 nm) for 2.5 minutes.

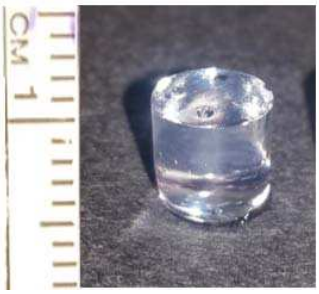

Figure 4. 18 : Thiol-ene hydrogel used in study 5.

Study 5: Surgery.

Female Sprague Dawley rats (240-300 g, ~16 weeks old) underwent surgery to create a 5mm segmental defect in the femur. Surgeon and animal aseptic preparation prior to the surgery was according to the Institutional Animal Care and Use Committee (IACUC) Guidelines for Rodent Survival Surgery. Rats were anesthetized by isoflurane inhalation (2-3%, to effect). After anesthesia the rat's fur was clipped to remove hair at the incision site. An incision was made over the lateral aspect of the femur. The diaphysis of the femur was approached, clearing away soft tissue with a combination of sharp and blunt dissection. A 4 pin internal fixation plate (as was used in study 1, **Error! Not a valid bookmark self-reference.**) was attached to the femur with threaded k-wires and a 5 mm defect was created using gigli wire. After the defect is created one of 5 treatments (n = 5/group) was placed; the defect was left empty, a hydrogel (vehicle) containing no PTH was placed, a hydrogel + 3 µg bbPTH 1-84 was placed, a hydrogel + 30 µg bbPTH 1-84, or a hydrogel + 300 µg bbPTH 1-84. The soft tissue was then sutured closed and wound clip staples were placed over the incision to help protect the incision. Animals received buprenorphine SR (0.06-0.8mg/kg) subcutaneously 20-30 minutes prior to surgery. Animals also received cefazolin (20 mg/kg) at the end of surgery as a prophylactic antibiotic. Rats were allowed to recover and were observed daily for evidence of wound problems such as swelling or drainage. As previous studies had fixation issues healing was monitored via x-ray at 3, 6, 9, and 12 weeks. At the end of the study (12 weeks) animals were sacrificed and femurs were fixed in neutral buffered formalin for 72 hours then stored in 70% ethanol.

Study 5: Radiography.

At weeks 3, 6, 9, and 12 rats were anesthetized for radiograph analaysis. Rats were anesthetized by isoflurane inhalation (2-3% to effect). Rats were radiographed using a MinXray TR90 (Northbrook, Illinois) to document healing progression as assessed by % bridging measures (described in study 1). Rats were positioned in a supine position with the affected leg secured at ~90 degrees to the body. Images were acquired with settings of 40kV and 3.72 mA at 0.14 seconds, and stored electronically for comparison and analysis.

Study 5: µCT.

Bone volume and mineral density were assessed by micro computed tomography. The defect area of each femur was scanned at medium resolution (µCT 80, Scanco Medial). During scans samples were held in a 35mm tube surrounded by 70% ethanol. The area between the two inner fixation pins was scanned at 70 kVp, 114 µA, 8 W, FOV/diameter (mm) of 36.9. The area of the scan evaluated was limited to new bone ingrowth into the defect area (Figure 4. 7) and was evaluated with a lower threshold of 220, gauss support = 1 and sigma = 0.8.

Study 5: Statistics.

One way analysis of variance (ANOVA) was used to determine differences between treatment groups, a p-value of less than 0.05 was be considered significant. If significant differences were detected by ANOVA, a Tukey post-hoc test was compare individual groups to one another.

Study 5: Results.

Two samples were lost due to bone fixation issues in the 3µg treatment group around week 3. Upon dissection of the defect site, no evidence of the hydrogel in the defect area was

observed. No differences in % defect bridged between treatment groups at week 3, 6, or 9. Week 12 µCT data showed treatment with 300 µg bbPTH 1-84 resulted in significantly lower bone volume in the defect area than the vehicle group ($p = 0.039$). Treatment with 3 µg PTH tended to result in increased bone volume in the defect area as compared to treatment with 300 µg ($p = 0.0505$) as well (Figure 4. 19). No other significant differences between groups were observed ($p > 0.14$). No differences were observed in mineral content (Figure 4. 20) in the region of interest ($p = 0.526$).

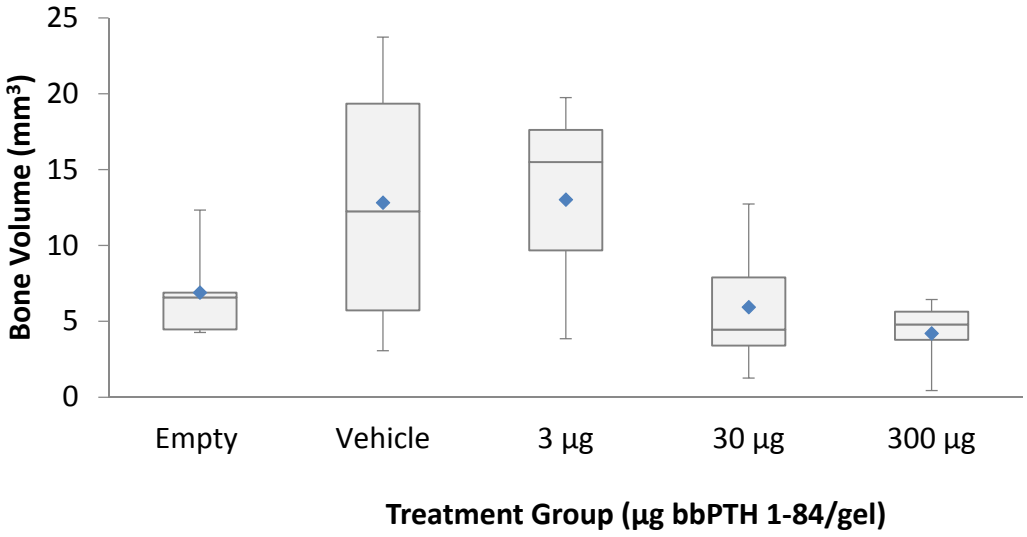

Figure 4. 19 : Bone Volume of new bone in the defect area in rats treated with PTH delivered via thiol-ene hydrogel.

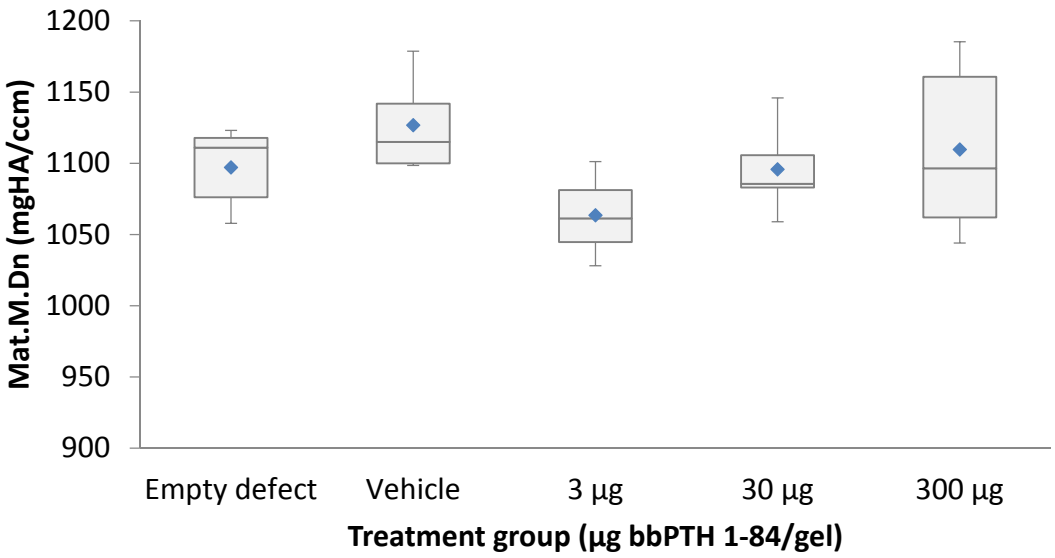

Figure 4. 20 : Mineral density of new bone formed in the defect area in rats treated with PTH delivered via thiol-ene hydrogel.

Though full bridging was no observed in any samples, when bridging was more qualitatively evident, it seemed to happen primarily along the fixation plate (Figure 4. 21).

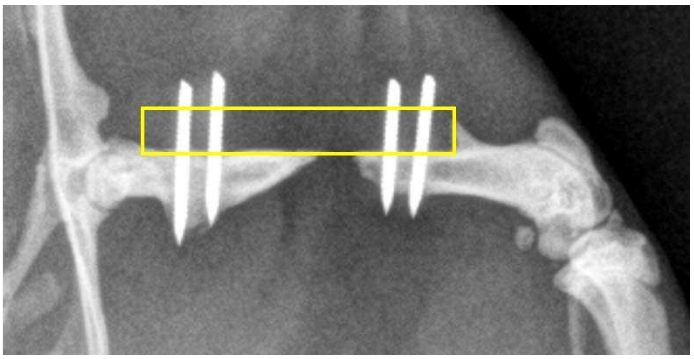

Figure 4. 21: Example radiograph of bridging along the fixation plate

Study 5: Discussion.

Some interesting results were found with the thiol-ene hydrogel pilot. Most notably, treatment with, 300 µg PTH resulted in less healing than the vehicle and 3 µg treatment groups.

Indicating, as theorized, there may be limit, above which PTH does not have a positive impact on bone regeneration. However, no treatment groups performed better than the vehicle, and no samples achieved complete bridging of the defect by week 12. A different result may be observed if a rigid scaffold (like PPF) were used in combination with the hydrogel. In the two animals that had to be prematurely euthanized, no evidence of the hydrogel was detectable. Indicating it likely is not present in the defect area beyond 3 weeks. Because the hydrogel is not a rigid scaffold and breaks down more rapidly, the lack of something bridging the defect for a longer period of time may be problematic for the healing response.

Moving forward, to best test the hypothesis, one scaffold was chosen based on results found in these pilots, ease of use, ability to bridge the defect area, and customizability. The methylcellulose hydrogel, was difficult to use based on its lack of mechanical integrity. HydroxyColl was easy to use but not as effective at bridging the defect gap as desired and lacked the same customizability in release profile of PTH as the other materials. The electrospun scaffold bridged the defect sufficiently and can be made with varying doses of PTH. Release profile of PTH from this scaffold is potentially customizable. The PPF scaffold does an excellent job of bridging the defect area and though the microspheres are not overwhelmingly convenient to work with may also be incorporated with another method of PTH delivery. Even though the materials used in studies 2, 3, 4, and 5 bridged the defect area, complete bony bridging was not observed in any studies at 12 weeks. Representative μCT scan can be seen in (Figure 4. 22). In samples treated with electrospun scaffolds or HydroxyColl sponges some bone formation in the center of the defect area was apparent, but complete bridging was not.

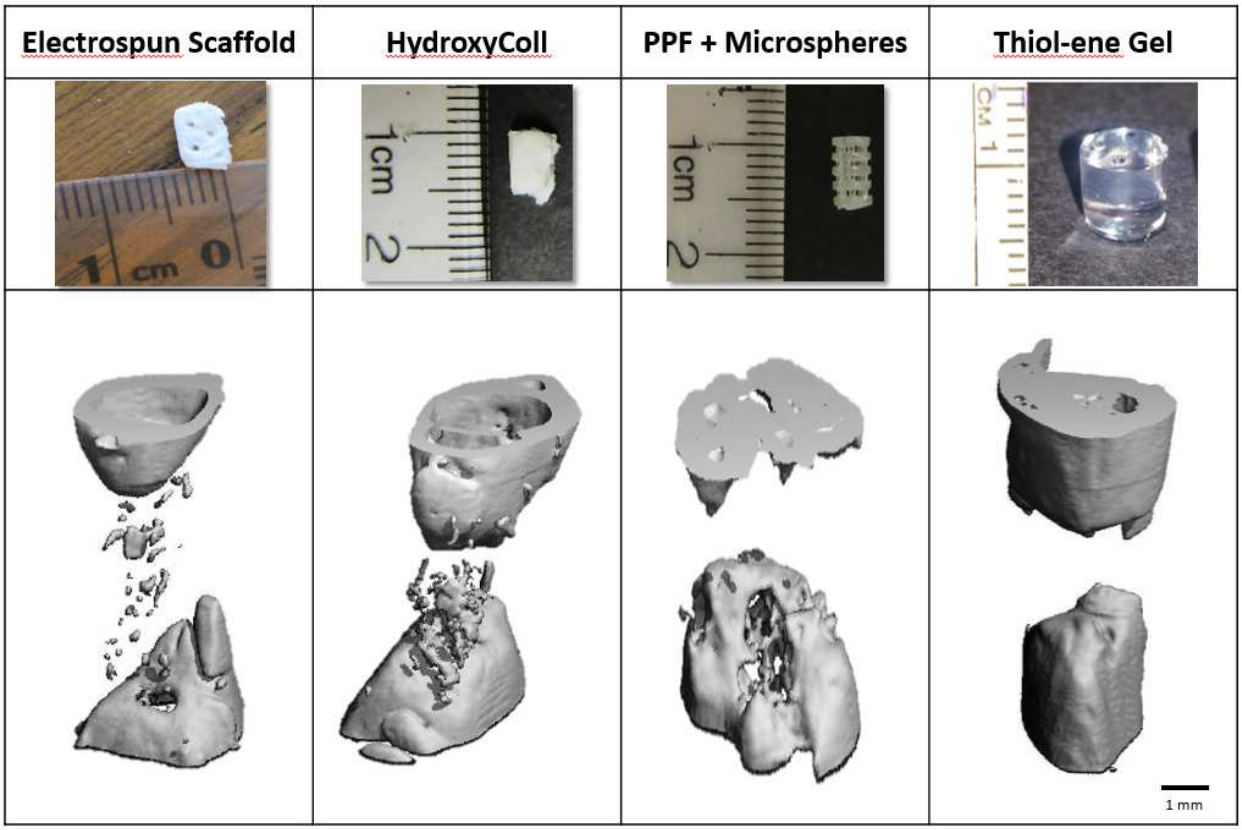

Figure 4. 22: Representative µCT scans at week 12 for each biomaterial type. Some bone formation was observed in the middle of the defect area in samples with electrospun scaffolds and HydroxyColl sponges, however, complete bony bridging was not observed with any materials.

The thiol-ene hydrogel is very easy to work with and customizable in both release and degradation (Grim, Marozas et al. 2015). The pilot utilizing the thiol-ene gel also provided the most insight for selection of PTH doses for larger scale studies. Thus, for the more in depth studies examining the effects of PTH on bone regeneration the thiol-ene hydrogel in conjunction with the PPF scaffold were used. The pilots were followed by two studies combining the thiol-ene hydrogel and PPF scaffold; one with PTH entrapped within the hydrogel matrix, the other with PTH tethered to the hydrogel matrix.

Study 6: Thiol-ene hydrogel with PTH entrapped within the matrix and PPF scaffold

Study 6: Scaffold preparation.

Monomer solutions for the hydrogels were prepared courtesy of Dr. Kristi Anseth's lab at CU Boulder as previously described (Fairbanks, Schwartz et al. 2009). The appropriate amount of PTH for the given treatment group was reconstituted in dPBS to be incorporated into the gel. Monomer solutions were combined and pipetted into the mold with the PPF scaffold. Gels were polymerized around the scaffolds by placing the molds under a 2.5 mW/cm^2 UV lamp (365 nm) for 2.5 minutes.

Study 6: Surgery.

Male Sprague Dawley rats (240-300g) underwent surgery to create a >5mm segmental defect in the femur. Surgeon and animal aseptic preparation prior to the surgery was according to the Institutional Animal Care and Use Committee (IACUC) Guidelines for Rodent Survival Surgery. Rats were anesthetized by isoflurane inhalation (2-3%, to effect). After anesthesia the rat's fur was clipped to remove hair at the incision site. An incision was made over the lateral aspect of the femur. The diaphysis of the femur was approached, clearing away soft tissue with a combination of sharp and blunt dissection. A 4 pin internal fixation plate was attached to the femur with 0.045" threaded stainless steel k-wires and a >5 mm defect was created using gigli wire. After the defect is created one of 6 treatments (n = 7/group) was placed; the defect was left empty, a PPF + thiol-ene hydrogel (vehicle) containing no PTH was placed, a PPF + thiol-ene hydrogel + 1 µg bbPTH 1-84 was placed, a PPF + thiol-ene hydrogel + 3 µg bbPTH 1-84, a PPF + thiol-ene hydrogel + 10µg bbPTH 1-84 treatment was placed, or a PPF + thiol-ene hydrogel + 30 µg bbPTH 1-84 treatment was placed. The soft tissue was then sutured closed and wound clip

staples were placed over the incision to help protect the incision. Animals received buprenorphine SR (0.6 - 0.8 mg/kg) subcutaneously 20-30 minutes prior to surgery. Animals also received cefazolin (20 mg/kg) at the end of surgery as a prophylactic antibiotic. Rats were allowed to recover and were observed daily for evidence of wound problems such as swelling or drainage. Healing was monitored via x-ray at 4, and 8 weeks. At the end of the study (12 weeks) animals were sacrificed, femurs were fixed in neutral buffered formalin for 72 hours then stored in 70% ethanol and healing was assessed via micro computed tomography.

Study 6: Radiography.

At weeks 4 and 8 rats were radiographed using a MinXray TR90 (Northbrook, Illinois) to document healing progression. Rats were anesthetized by isoflurane inhalation (2-3% to effect). Rats were positioned in a supine position with the affected leg secured at approximately 90 degrees to the body. Images were acquired with settings of 40kV and 3.72 mA at 0.14 seconds, and stored electronically for comparison and analysis. Radiographs were used to calculate the percent of the defect area that had bridged with new bone was calculated as original defect size (5mm) minus length between bone ends (measured in mm), divided by original defect size, as previously described (Equation 1).

Study 6: µCT.

Bone volume and mineral density were assessed by micro computed tomography. The defect area of each femur was scanned at medium resolution (µCT 80, Scanco Medial). During scans samples were held in a 35 mm tube surrounded by 70% ethanol. The area between the two inner fixation pins was scanned at 70 kVp, 114 µA, 8 W, FOV/diameter 36.9 mm. Because there was enough healing that native bone ends could not be easily discerned, the area of the scan

evaluated was limited to the middle 3.5 mm of the defect area (Figure 4. 23). Bone was evaluated with a lower threshold of 220, gauss support = 1 and sigma = 0.8.

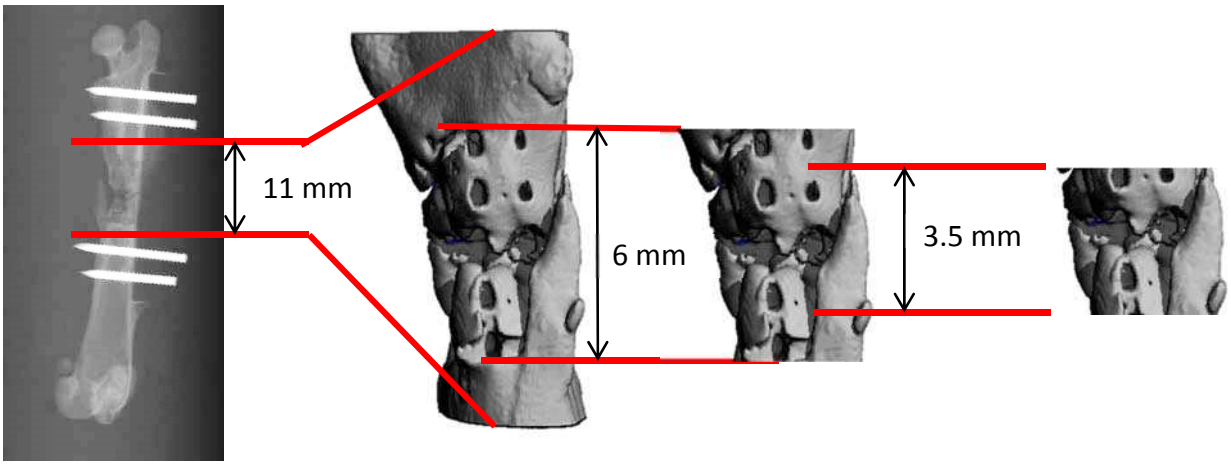

Figure 4. 23 : MicroCT scans region (11 mm), the entire defect area (6 mm), and the analysis region (3.5 mm).

Samples were also observed for the presence of full bridging or not, if complete bridging of the defect was achieved for any portion of the width of the bone samples were given a yes indication in regard to full bridging.

Study 6: Statistics.

One way analysis of variance (ANOVA) was used to determine differences between treatment groups, a p-value of less than 0.05 was be considered significant. If significant differences were detected by ANOVA, Tukey's post hoc test was used compare individual groups to one another. Non-parametric tests were used to determine whether or not the number of rats with fully bridged defects was different between groups.

Study 6: Results.

No significant differences in bone volume (Figure 4. 24) in the defect area between groups (n = 7 per group) were observed ($p > 0.07$). However, the 10 µg group tended to have more bone

volume in the defect area than the empty defect group (p = 0.150). The 30 µg group tended to have less bone in the defect area than the 10 µg group (p = 0.071).

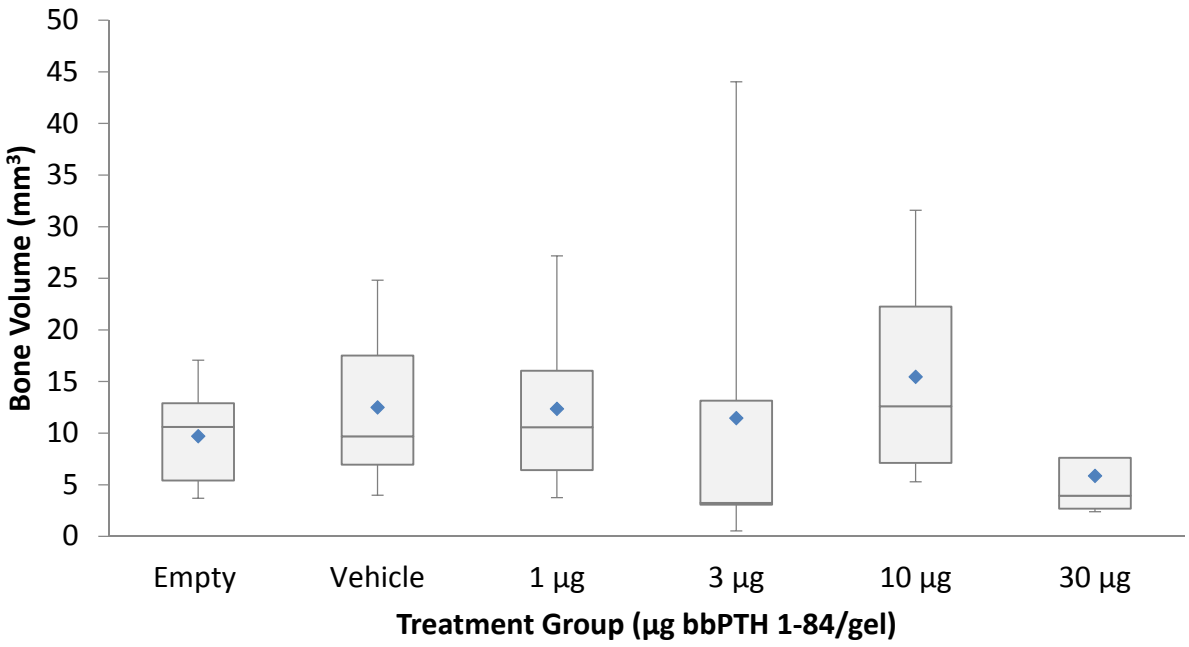

Figure 4. 24 : Bone Volume in the defect area of samples treated with PTH entrapped within the thiol-ene hydrogel matrix used in conjunction with a PPF scaffold.

No difference in % defect bridged measures (Figure 4. 25) or the mineral density of bone in the defect area was observed with the exception of the 10 µg group having a higher percent of the defect bridged than the 30 µg group (p = 0.035).

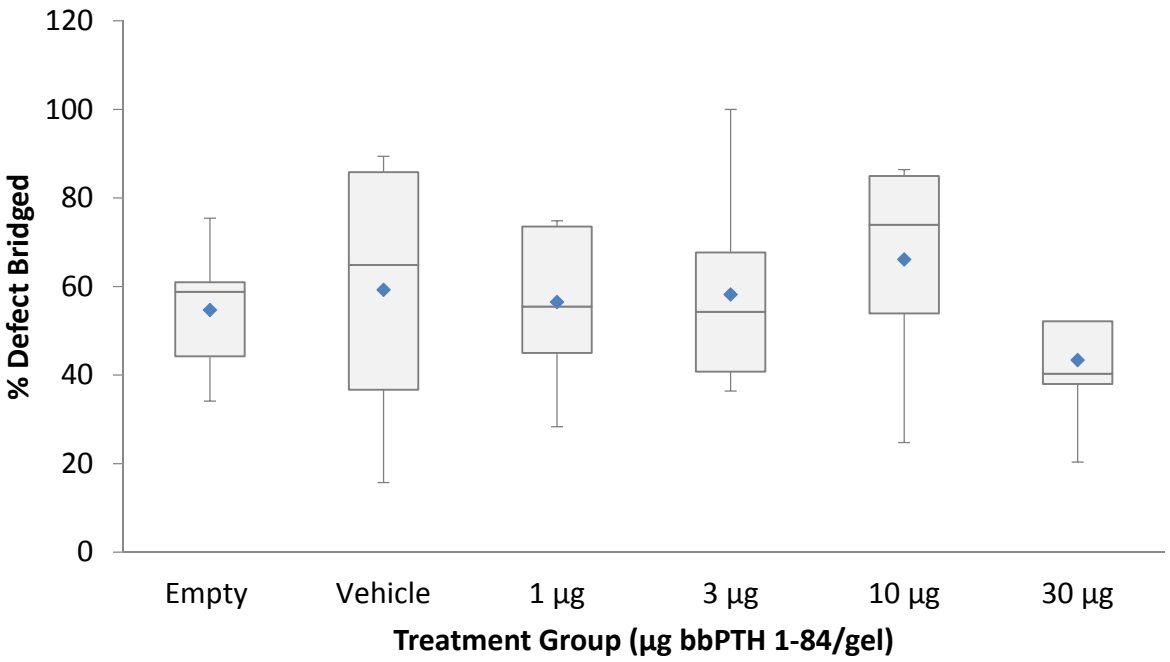

Figure 4. 25 : % defect bridged data for of samples treated with PTH entrapped within the thiol-ene hydrogel matrix used in conjunction with a PPF scaffold

Non-parametric testing showed no difference between the number of samples that had fully bridged in each group ($p = 0.273$)

Study 6: Discussion.

Based on the decrease in bone volume in the defect area in pilot study resulting in the 300 µg treatment group, the high dose 300 µg group was dropped for this study. Instead, lower dose groups were added in order to examine the lower range of treatment more closely. First and foremost, this study resulted in full bridging of some of the defects, which had not been observed in any pilot studies. Though there were no significant differences in bone volume, the 10 µg tended to have more new bone in the defect area than empty defects. Interestingly, the 30 µg group tended to have less bone in the defect area than did the 10 µg group and had. Similarly, treatment with 10 µg PTH in this study resulted in a significantly higher percent of the

defect bridged than treatment with 30 μg PTH. Results from this study do not indicate any enhanced healing as a result of local PTH delivery. Like the pilot study there does appear to be a point at which PTH delivered locally in this fashion may have a negative effect on bone formation in the defect area. However, the potential lack of effect on bone volume and bridging measures may be due to the way PTH is released from the scaffolds. In this study PTH is free to diffuse out of the hydrogel matrix relatively rapidly, tethering the PTH to the hydrogel matrix results in a mitigation of rapid diffusion. Longer retention of PTH in the defect area may result in observable differences in bone formation in the defect area between treatment groups.

Study 7: Thiol-ene hydrogel with PTH tethered to the matrix and PPF scaffold

Study 7: Thiolation of bb-PTH 1-84 for cross-linking to thiol-ene gels.

In samples where bbPTH 1-84 was cross-linked to the hydrogel matrix, PTH was modified by adding a sulfhydryl group to enable cross-linking capabilities. PTH was thiolated using trauts reagent. PTH was exposed to a 20 x molar excess of Trauts reagent (2-iminothiolene-HCL) and 3mM EDTA and incubated at room temperature for 2 hours. Excess trauts reagent was removed via a desalting column. Thiolaton of PTH was verified by HPLC, and thiolated PTH was stored at -80°C until use.

Study 7: Scaffold preparation.

Monomer solutions for the hydrogels were provided by Dr. Kristi Anseth's lab at CU Boulder as previously described (Fairbanks, Schwartz et al. 2009). The appropriate amount of thiolated PTH for the given treatment group was reconstituted in dPBS to be incorporated into the gel. Monomer solutions were combined and pipetted into the mold with the PPF scaffold.

Gels were polymerized around the scaffolds by placing the molds under a 2.5 mW/cm^2 UV lamp (365 nm) for 2.5 minutes.

Study 7: Surgery.

Male Sprague Dawley rats (240-300 g) underwent surgery to create a >5 mm segmental defect in the femur. Surgeon and animal aseptic preparation prior to the surgery was according to the Institutional Animal Care and Use Committee (IACUC) Guidelines for Rodent Survival Surgery. Rats were anesthetized by isoflurane inhalation (2-3%, to effect). After anesthesia the rat's fur was clipped to remove hair at the incision site. An incision was made over the lateral aspect of the femur. The diaphysis of the femur was approached, clearing away soft tissue with a combination of sharp and blunt dissection. A 4 pin internal fixation plate was attached to the femur with 0.45" threaded titanium k-wires and a >5 mm defect was created using gigli wire. After the defect was created one of 6 treatments (n = 7/group) was placed; the defect was left empty, a PPF + thiol-ene hydrogel (vehicle) containing no PTH was placed, a PPF + thiol-ene hydrogel + 1 μg bbPTH 1-84 was placed, a PPF + thiol-ene hydrogel + 3 μg bbPTH 1-84, a PPF + thiol-ene hydrogel + 10μg bbPTH 1-84 treatment was placed, or a PPF + thiol-ene hydrogel + 30 μg bbPTH 1-84 treatment was placed. The soft tissue was then sutured closed and wound clip staples were placed over the incision to help protect the incision. Animals received buprenorphine SR (0.6 - 0.8 mg/kg) subcutaneously 20-30 minutes prior to surgery. Animals also received cefazolin (20 mg/kg) at the end of surgery as a prophylactic antibiotic. Rats were allowed to recover and were observed daily for evidence of wound problems such as swelling or drainage. Healing was monitored via in vivo μCT scans at 4, and 8 weeks. At the end of the study (12 weeks)

animals were sacrificed, femurs were fixed in neutral buffered formalin for 72 hours then stored in 70% ethanol and healing was assessed via ex vivo μCT.

Study 7: In vivo μCT.

Healing was monitored by in vivo μCT (VivaCT 80, Scanco Medical) at weeks 4 and 8. Rats were anesthetized by isoflurane inhalation (2-3%, to effect). Once anesthetized rats were moved to a tube designed to hold them in position while in the μCT chamber. The femur was scanned 70 kVp, 114 μA, 8 W, FOV/diameter (mm) of 49.8. Rats were anesthetized for scans for 45min – 1 hour.

Study 7: Ex vivo μCT.

At 12 weeks bone volume and mineral density were assessed (ex vivo) by micro computed tomography (VivaCT 80, Scanco Medical). During scans samples were held in a 50 mL conical tube surrounded by 70% ethanol. The area between the two inner fixation pins was scanned at 70 kVp, 114 μA, 8 W, FOV/diameter (mm) of 31.5. As there was enough healing that native bone ends could not be easily discerned, the area of the scan evaluated was limited to the middle 3.5 mm of the defect area (Figure 4. 23). The region of interest was evaluated with a lower threshold of 220, gauss support = 1 and sigma = 0.8.

Study 7: Histology.

Three samples from each group were selected for histological analysis based on degree of healing for the respective group (as determined by μCT data). One sample representing a high amount of bone ingrowth, one representing average bone ingrowth, and low bone ingrowth for each treatment group. Samples were embedded in plastic at IUPUI, sectioned and stained with VonKossa MacNeil (3 thin sections per sample) and, hematoxylin and eosin (3 thin sections per

sample) to determine if any differences between groups were observable in the type of soft tissue bridging defects that did not exhibit complete bony bridging in order to gain insight on potential for full bridging or differences that may be evident at later timepoints than 12 weeks.. For example defects bridged by fibrous tissue are less likely to heal without intervention as compared to those bridged by a cartilaginous matrix if a later timepoint were selected. Slides were digitized and color thresholding was utilized to measure mineralized area, areas of cartilaginous matrix, and areas of fibrous tissue. The percent of the defect bridged by tissue types was also quantified.

Study 7: Statistics.

One way analysis of variance (ANOVA) was used to determine differences between treatment groups, a p-value of less than 0.05 was be considered significant. If significant differences were detected by ANOVA, Tukey's post hoc test was used compare individual groups to one another. Non-parametric tests were used to determine whether or not the number of rats with fully bridged defects was different between groups.

Study 7: Results.

In vivo μCT measures detected no difference in bone volume or % defect bridged at weeks 4 or 8 ($p > 0.122$). However, like the study with the thiol-ene gel, full bridging was achieved in some samples (Figure 4. 26).

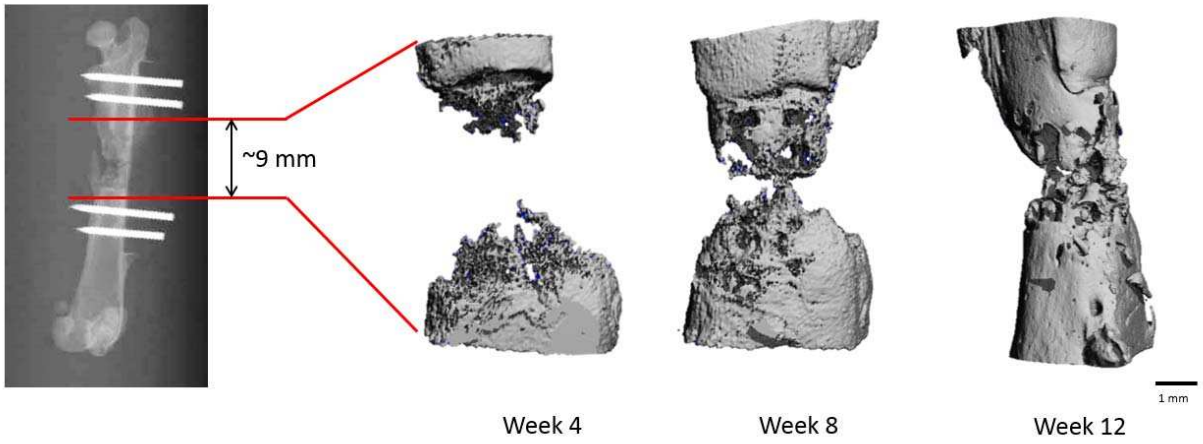

Figure 4. 26 : Healing progression over 12 weeks

At week 12 no significant differences were observed in bone volume in the defect area (Figure 4. 27), % defect bridged measures (Figure 4. 28) or mineral density measures of the bone in the defect area at week 4, 8 or 14 ($p > 0.157$).

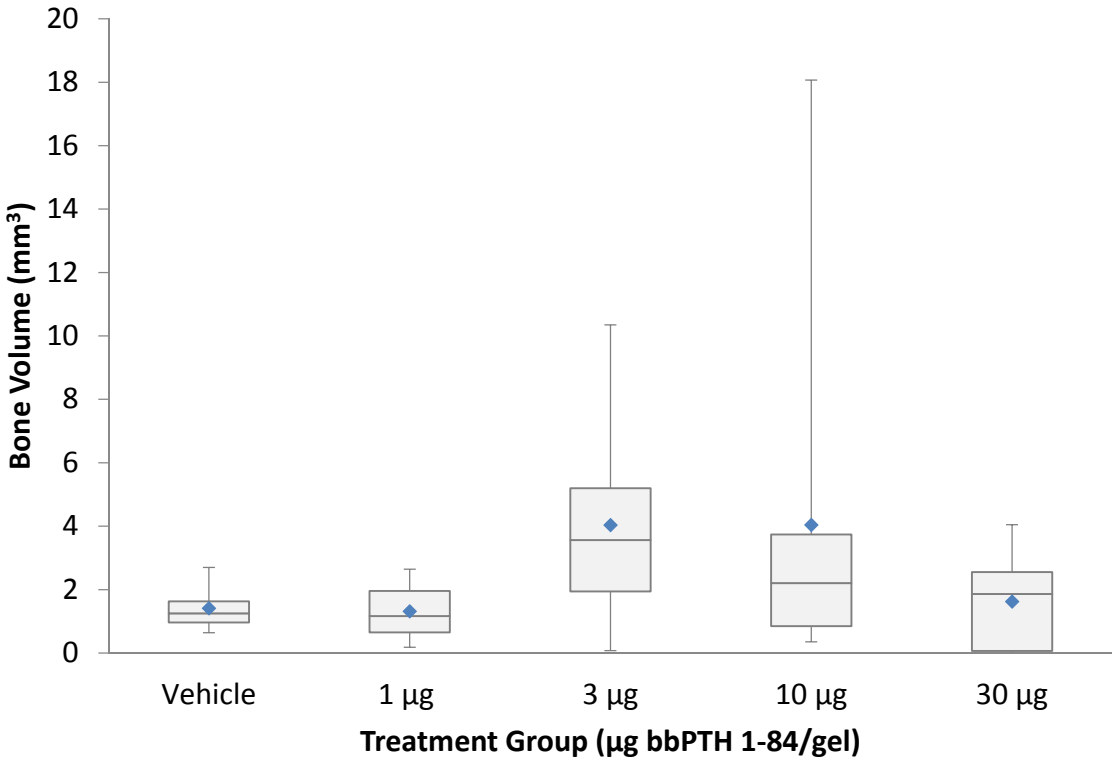

Figure 4. 27 : Bone volume at 12 weeks in samples treated with thiol-ene hydrogels with PTH tethered to the matrix, surrounding a PPF scaffold.

Though no significant differences were found between groups for % defect bridged, the 30 µg treatment tended to result in less bridging than 3 µg (p= 0.075). The 3 µg treatment group tended to result in more bridging than vehicle (p = 0.092).

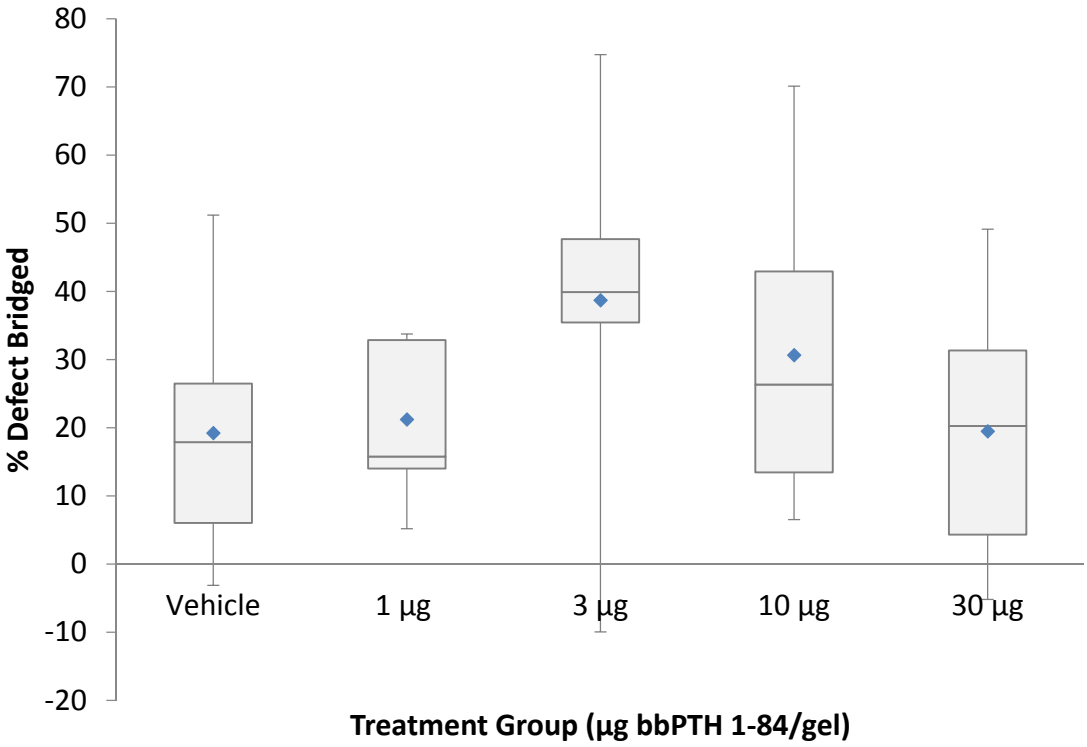

Figure 4. 28 : Thiol-ene hydrogel with PTH tethered to the matrix surrounding a PPF hydrogel % defect bridged data. Treatment with 3 µg PTH tended to result in a higher % of the defect bridged than vehicle samples.

Mineralized area, cartilaginous area and fibrous area were measured, however the presence of the PPF scaffold in the defect confounded 2-D data measurements, as there were varying amounts of scaffold in each section that did not always allow accurate representation of the tissue ingrowth in the defect area. When the percent of each defect bridged by a combination of mineralized and cartilaginous tissue was considered, data (as well as qualitative observations) indicated more bridging with treatment of 3 or 10 µg PTH per hydrogel. Figure 4. 29 shows longitudinal sections of two different samples. On the left, a sample that is bridged by a combination of cartilaginous and mineralized tissue. The section on the right shows a sample primarily bridged by loosely connected fibrous tissue.

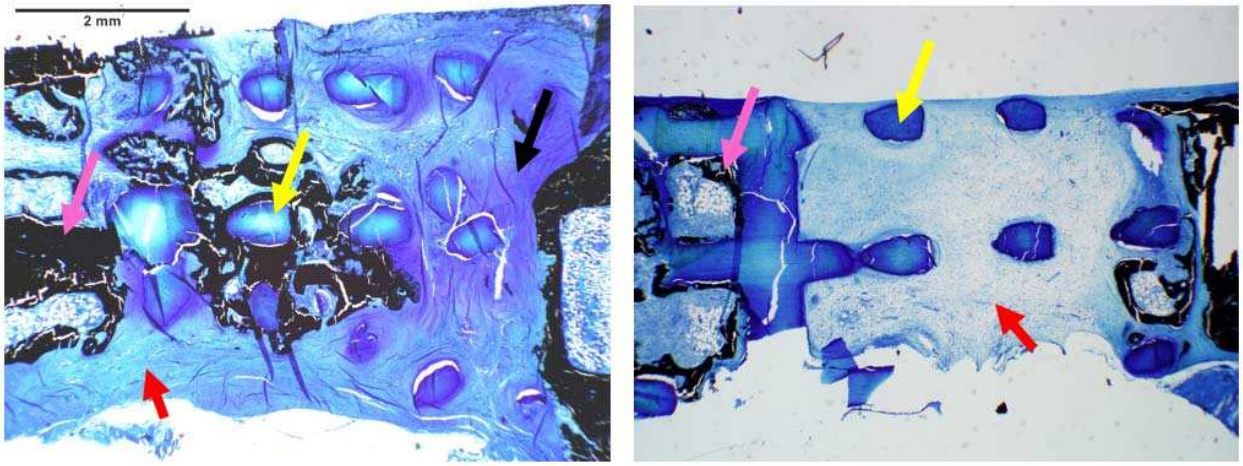

Figure 4. 29 : VonKossa MacNeil stained longitudinal sections of femur defect area. The PPF scaffold stains dark blue (indicated by yellow arrows), mineralized tissue stains black (indicated by pink arrow), cartilaginous material stains dark blue/purple (indicated by black arrow), and red arrows indicate areas of loosely connected fibrous tissue. The image on the left is a defect treated with 10 µg bbPTH 1-84 via thiol-ene hydrogel with a PPF scaffold at 12 weeks. Full bridging of the defect area by either mineralized or cartilaginous material is evident. The image on the right is a hydrogel/PPF control with no PTH treatment. The defect was bridged primarily by loosely organized fibrous tissue.

Treatment with 10 µg PTH resulted in defect areas that were bridged completely by some combination of mineralized and cartilaginous tissue in all three histologically prepared samples. Treatment with 3µg PTH resulted in defect areas bridged completely by some combination of mineralized and cartilaginous tissue in 2 of the 3 samples (Figure 4. 30). Full bridging by combination of mineralized and cartilaginous tissue was not observed in any other treatment group. In samples not bridged by a combination of mineralized and cartilaginous tissue loosely organized fibrous tissue was the predominate tissue type present in the defect area.

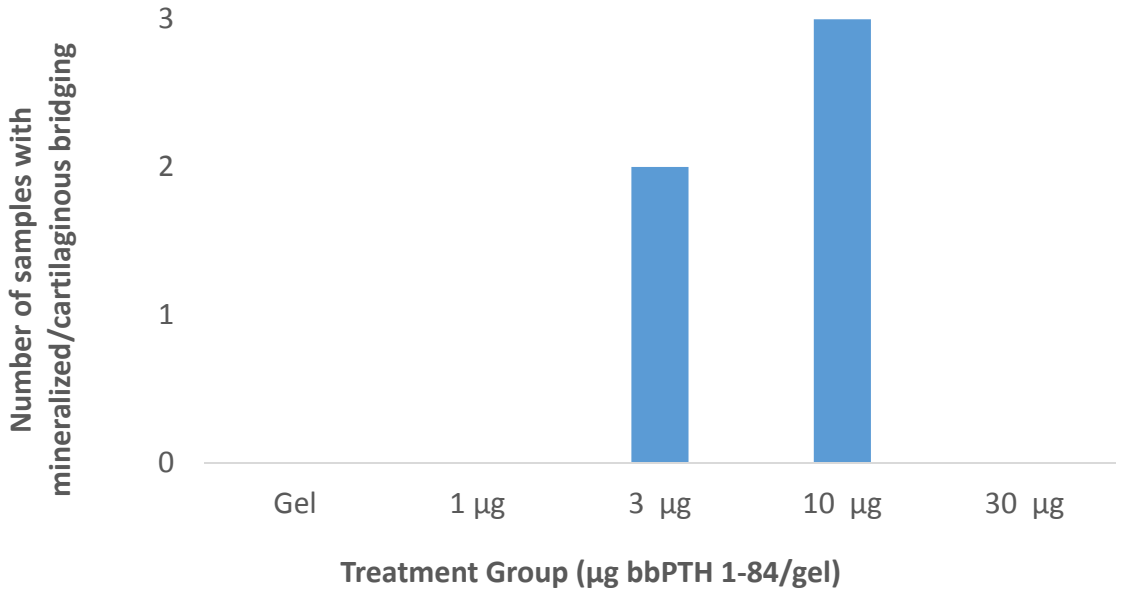

Figure 4. 30 : Number of samples bridged by a combination of mineralized and cartilaginous tissue.

Study 7: Discussion.

As it has been shown release profiles of bioactive molecules affect the impact they have on bone regeneration (Brown, Li et al. 2011), the same doses as the PPF scaffold + thiol-ene gel study were used for a study using the PPF scaffold + thiol-ene gel with PTH tethered to the matrix in order to assess whether any differences observed were due to modifications of the release profile. The modification in the release profile of PTH delivered via thiol-ene hydrogel seemed to have at least a small effect on the efficacy of locally delivered PTH for bone regeneration in this critical size defect model. Treatment with 3 µg PTH per hydrogel tended to result in more healing (as assessed by the percentage of the defect that had bridged) than vehicle. Likewise treatment with 3 or 10 µg PTH were the only treatments that resulted in complete bridging of the defect area with some combination of mineralized and cartilaginous tissue as opposed to bridging via

fibrous tissue. PTHrP and PTH are both required to achieve normal fetal skeletal morphogenesis (Miao, He et al. 2002). In endochondral ossification cartilage is gradually converted into bone (Ortega, Behonick et al. 2004, Mackie, Ahmed et al. 2008). The presence of cartilage in the defect area presents a foundation for bone to replace. In vitro, PTH and PTHrP inhibit mineralization of a cartilage like matrix and apoptosis and production of a mineralized bone like matrix. However, upon withdrawal of the hormonal stimulation, cells redirect toward their distinct microenvironment and terminal differentiation (Zerega, Cermelli et al. 1999). PTH has also been indicated as efficacious in cartilage repair studies (Kudo, Mizuta et al. 2011, Orth, Cucchiarini et al. 2013) as well as prevention of further cartilage damage and slowing of deterioration of subchondral bone in an osteoarthritis model (Yan, Tian et al. 2014). If samples had been collected at a later timepoint it seems likely much more distinct differences in bone volume and % bridging measures between treatment groups would be observed as samples bridged by a cartilaginous matrix are much more likely to heal than those bridged by loosely connected fibrous tissue. Interestingly, even at the 12 week timepoint, similar to findings in the study where PTH was not bound to the hydrogel, the 30 μg treatment tended to result in less bridging than 3 μg. The 3 studies performed utilizing the thiol-ene gel for PTH delivery all indicate a potential negative effect of the continuous local administration of PTH on critical size defect healing. Improved healing was only observed at lower doses when PTH is tethered to the hydrogel to provide a more constant low dose release from the hydrogel as opposed to a burst release followed by prolonged release.

References.

Andreassen, T. T. and V. Cacciafesta (2004). "Intermittent parathyroid hormone treatment enhances guided bone regeneration in rat calvarial bone defects." J Craniofac Surg **15**(3): 424-427; discussion 428-429.

Andreassen, T. T., C. Ejersted and H. Oxlund (1999). "Intermittent parathyroid hormone (1-34) treatment increases callus formation and mechanical strength of healing rat fractures." J Bone Miner Res **14**(6): 960-968.

Arrighi, I., S. Mark, M. Alvisi, B. von Rechenberg, J. A. Hubbell and J. C. Schense (2009). "Bone healing induced by local delivery of an engineered parathyroid hormone prodrug." Biomaterials **30**(9): 1763-1771.

Brown, K. V., B. Li, T. Guda, D. S. Perrien, S. A. Guelcher and J. C. Wenke (2011). "Improving bone formation in a rat femur segmental defect by controlling bone morphogenetic protein-2 release." Tissue Eng Part A **17**(13-14): 1735-1746.

Chen, H., E. P. Frankenburg, S. A. Goldstein and L. K. McCauley (2003). "Combination of local and systemic parathyroid hormone enhances bone regeneration." Clin Orthop Relat Res(416): 291-302.

Cunniffe, G. M., G. R. Dickson, S. Partap, K. T. Stanton and F. J. O'Brien (2010). "Development and characterisation of a collagen nano-hydroxyapatite composite scaffold for bone tissue engineering." J Mater Sci Mater Med **21**(8): 2293-2298.

Curtin, C. M., G. M. Cunniffe, F. G. Lyons, K. Bessho, G. R. Dickson, G. P. Duffy and F. J. O'Brien (2012). "Innovative collagen nano-hydroxyapatite scaffolds offer a highly efficient non-viral gene delivery platform for stem cell-mediated bone formation." Adv Mater **24**(6): 749-754.

Dadsetan, M., T. Guda, M. B. Runge, D. Mijares, R. Z. LeGeros, J. P. LeGeros, D. T. Silliman, L. Lu, J. C. Wenke, P. R. Brown Baer and M. J. Yaszemski (2015). "Effect of calcium phosphate coating and rhBMP-2 on bone regeneration in rabbit calvaria using poly(propylene fumarate) scaffolds." Acta Biomater **18**: 9-20.

Fairbanks, B. D., M. P. Schwartz, C. N. Bowman and K. S. Anseth (2009). "Photoinitiated polymerization of PEG-diacrylate with lithium phenyl-2,4,6-trimethylbenzoylphosphinate: polymerization rate and cytocompatibility." Biomaterials **30**(35): 6702-6707.

Fuerst, A., S. Derungs, B. von Rechenberg, J. A. Auer, J. Schense and J. Watson (2007). "Use of a parathyroid hormone peptide (PTH(1-34))-enriched fibrin hydrogel for the treatment of a subchondral cystic lesion in the proximal interphalangeal joint of a warmblood filly." J Vet Med A Physiol Pathol Clin Med **54**(2): 107-112.

Gleeson, J. P., N. A. Plunkett and F. J. O'Brien (2010). "Addition of hydroxyapatite improves stiffness, interconnectivity and osteogenic potential of a highly porous collagen-based scaffold for bone tissue regeneration." Eur Cell Mater **20**: 218-230.

Grim, J. C., I. A. Marozas and K. S. Anseth (2015). "Thiol-ene and photo-cleavage chemistry for controlled presentation of biomolecules in hydrogels." J Control Release **219**: 95-106.

Hamann, C., A. K. Picke, G. M. Campbell, M. Balyura, M. Rauner, R. Bernhardt, G. Huber, M. M. Morlock, K. P. Gunther, S. R. Bornstein, C. C. Gluer, B. Ludwig and L. C. Hofbauer (2014). "Effects of Parathyroid Hormone on Bone Mass, Bone Strength, and Bone Regeneration in Male Rats With Type 2 Diabetes Mellitus." Endocrinology **155**(4): 1197-1206.

Jung, R. E., D. L. Cochran, O. Domken, R. Seibl, A. A. Jones, D. Buser and C. H. Hammerle (2007). "The effect of matrix bound parathyroid hormone on bone regeneration." Clin Oral Implants Res **18**(3): 319-325.

Kempen, D. H., L. Lu, T. E. Hefferan, L. B. Creemers, A. Heijink, A. Maran, W. J. Dhert and M. J. Yaszemski (2010). "Enhanced bone morphogenetic protein-2-induced ectopic and orthotopic bone formation by intermittent parathyroid hormone (1-34) administration." Tissue Eng Part A **16**(12): 3769-3777.

Kempen, D. H., L. Lu, T. E. Hefferan, L. B. Creemers, A. Maran, K. L. Classic, W. J. Dhert and M. J. Yaszemski (2008). "Retention of in vitro and in vivo BMP-2 bioactivities in sustained delivery vehicles for bone tissue engineering." Biomaterials **29**(22): 3245-3252.

Kempen, D. H., L. Lu, C. Kim, X. Zhu, W. J. Dhert, B. L. Currier and M. J. Yaszemski (2006). "Controlled drug release from a novel injectable biodegradable microsphere/scaffold composite based on poly(propylene fumarate)." J Biomed Mater Res A **77**(1): 103-111.

Kempen, D. H., M. J. Yaszemski, A. Heijink, T. E. Hefferan, L. B. Creemers, J. Britson, A. Maran, K. L. Classic, W. J. Dhert and L. Lu (2009). "Non-invasive monitoring of BMP-2 retention and bone formation in composites for bone tissue engineering using SPECT/CT and scintillation probes." J Control Release **134**(3): 169-176.

Kim, H. W., H. H. Lee and J. C. Knowles (2006). "Electrospinning biomedical nanocomposite fibers of hydroxyapatite/poly(lactic acid) for bone regeneration." J Biomed Mater Res A **79**(3): 643-649.

Kim, J., T. E. Hefferan, M. J. Yaszemski and L. Lu (2009). "Potential of hydrogels based on poly(ethylene glycol) and sebacic acid as orthopedic tissue engineering scaffolds." Tissue Eng Part A **15**(8): 2299-2307.

Kudo, S., H. Mizuta, K. Takagi and Y. Hiraki (2011). "Cartilaginous repair of full-thickness articular cartilage defects is induced by the intermittent activation of PTH/PTHrP signaling." Osteoarthritis Cartilage **19**(7): 886-894.

Kumabe, Y., S. Y. Lee, T. Waki, T. Iwakura, S. Takahara, M. Arakura, Y. Kuroiwa, T. Fukui, T. Matsumoto, T. Matsushita, K. Nishida, R. Kuroda and T. Niikura (2017). "Triweekly administration of parathyroid hormone (1-34) accelerates bone healing in a rat refractory fracture model." BMC Musculoskelet Disord **18**(1): 545.

Lee, K. W., S. Wang, B. C. Fox, E. L. Ritman, M. J. Yaszemski and L. Lu (2007). "Poly(propylene fumarate) bone tissue engineering scaffold fabrication using stereolithography: effects of resin formulations and laser parameters." Biomacromolecules **8**(4): 1077-1084.

Lewandrowski, K. U., M. V. Cattaneo, J. D. Gresser, D. L. Wise, R. L. White, L. Bonassar and D. J. Trantolo (1999). "Effect of a poly(propylene fumarate) foaming cement on the healing of bone defects." Tissue Eng **5**(4): 305-316.

Livingston, T. L., S. Gordon, M. Archambault, S. Kadiyala, K. McIntosh, A. Smith and S. J. Peter (2003). "Mesenchymal stem cells combined with biphasic calcium phosphate ceramics promote bone regeneration." J Mater Sci Mater Med **14**(3): 211-218.

Luca, L., A. L. Rougemont, B. H. Walpoth, L. Boure, A. Tami, J. M. Anderson, O. Jordan and R. Gurny (2011). "Injectable rhBMP-2-loaded chitosan hydrogel composite: osteoinduction at ectopic site and in segmental long bone defect." J Biomed Mater Res A **96**(1): 66-74.

Mackie, E. J., Y. A. Ahmed, L. Tatarczuch, K. S. Chen and M. Mirams (2008). "Endochondral ossification: how cartilage is converted into bone in the developing skeleton." Int J Biochem Cell Biol **40**(1): 46-62.

Mariner, P. D., J. M. Wudel, D. E. Miller, E. E. Genova, S. O. Streubel and K. S. Anseth (2013). "Synthetic hydrogel scaffold is an effective vehicle for delivery of INFUSE (rhBMP2) to critical-sized calvaria bone defects in rats." J Orthop Res **31**(3): 401-406.

Martin, B. C., E. J. Minner, S. L. Wiseman, R. L. Klank and R. J. Gilbert (2008). "Agarose and methylcellulose hydrogel blends for nerve regeneration applications." J Neural Eng **5**(2): 221-231.

Martinez-Sanz, E., D. A. Ossipov, J. Hilborn, S. Larsson, K. B. Jonsson and O. P. Varghese (2011). "Bone reservoir: Injectable hyaluronic acid hydrogel for minimal invasive bone augmentation." J Control Release **152**(2): 232-240.

Miao, D., B. He, A. C. Karaplis and D. Goltzman (2002). "Parathyroid hormone is essential for normal fetal bone formation." J Clin Invest **109**(9): 1173-1182.

Milstrey, A., B. Wieskoetter, D. Hinze, N. Grueneweller, R. Stange, T. Pap, M. Raschke and P. Garcia (2017). "Dose-dependent effect of parathyroid hormone on fracture healing and bone formation in mice." J Surg Res **220**: 327-335.

Ngiam, M., S. Liao, A. J. Patil, Z. Cheng, C. K. Chan and S. Ramakrishna (2009). "The fabrication of nano-hydroxyapatite on PLGA and PLGA/collagen nanofibrous composite scaffolds and their effects in osteoblastic behavior for bone tissue engineering." Bone **45**(1): 4-16.

O'Loughlin, P. F., M. E. Cunningham, S. V. Bukata, E. Tomin, A. R. Poynton, S. B. Doty, A. A. Sama and J. M. Lane (2009). "Parathyroid hormone (1-34) augments spinal fusion, fusion mass volume, and fusion mass quality in a rabbit spinal fusion model." Spine (Phila Pa 1976) **34**(2): 121-130.

Oest, M. E., K. M. Dupont, H. J. Kong, D. J. Mooney and R. E. Guldberg (2007). "Quantitative assessment of scaffold and growth factor-mediated repair of critically sized bone defects." J Orthop Res **25**(7): 941-950.

Ortega, N., D. J. Behonick and Z. Werb (2004). "Matrix remodeling during endochondral ossification." Trends Cell Biol **14**(2): 86-93.

Orth, P., M. Cucchiarini, D. Zurakowski, M. D. Menger, D. M. Kohn and H. Madry (2013). "Parathyroid hormone [1-34] improves articular cartilage surface architecture and integration and subchondral bone reconstitution in osteochondral defects in vivo." Osteoarthritis Cartilage **21**(4): 614-624.

Paridis, D. and T. Karachalios (2011). "Atrophic femoral bone nonunion treated with 1-84 PTH." J Musculoskelet Neuronal Interact **11**(4): 320-322; quiz 323.

Reynolds, D. G., M. Takahata, A. L. Lerner, R. J. O'Keefe, E. M. Schwarz and H. A. Awad (2011). "Teriparatide therapy enhances devitalized femoral allograft osseointegration and biomechanics in a murine model." Bone **48**(3): 562-570.

Seebach, C., R. Skripitz, T. T. Andreassen and P. Aspenberg (2004). "Intermittent parathyroid hormone (1-34) enhances mechanical strength and density of new bone after distraction osteogenesis in rats." J Orthop Res **22**(3): 472-478.

Skripitz, R., T. T. Andreassen and P. Aspenberg (2000). "Strong effect of PTH (1-34) on regenerating bone: a time sequence study in rats." Acta Orthop Scand **71**(6): 619-624.

Tsunori, K., S. Sato, A. Hasuike, S. Manaka, H. Shino, N. Sato, T. Kubota, Y. Arai, K. Ito and M. Miyazaki (2015). "Effects of Intermittent Administration of Parathyroid Hormone on Bone Augmentation in Rat Calvarium." Implant Dentistry **24**(2): 142-148.

Vehof, J. W., J. P. Fisher, D. Dean, J. P. van der Waerden, P. H. Spauwen, A. G. Mikos and J. A. Jansen (2002). "Bone formation in transforming growth factor beta-1-coated porous poly(propylene fumarate) scaffolds." J Biomed Mater Res **60**(2): 241-251.

Yan, J. Y., F. M. Tian, W. Y. Wang, Y. Cheng, H. P. Song, Y. Z. Zhang and L. Zhang (2014). "Parathyroid hormone (1-34) prevents cartilage degradation and preserves subchondral bone micro-architecture in guinea pigs with spontaneous osteoarthritis." Osteoarthritis Cartilage **22**(11): 1869-1877.

Zerega, B., S. Cermelli, P. Bianco, R. Cancedda and F. D. Cancedda (1999). "Parathyroid hormone [PTH(1-34)] and parathyroid hormone-related protein [PTHrP(1-34)] promote reversion of hypertrophic chondrocytes to a prehypertrophic proliferating phenotype and prevent terminal differentiation of osteoblast-like cells." J Bone Miner Res **14**(8): 1281-1289.

Chapter 5: Conclusions and Future directions.

Approximately 2.2 million orthopaedic grafting procedures are done annually (Jahangir, Nunley et al. 2008). Autograft is the gold standard for treatment of bone defects complicated by segmental bone loss (Mahendra and Maclean 2007), but may not always be the most viable option as availability is limited and complications at the donor site may arise. Allograft, demineralized bone matrix (DBM) as well a variety of commercially available bone graft substitute materials like are presently alternatives when autograft is not the best option (Connolly 1995, Hak 2007). However, neither allograft nor bone graft substitutes provide the same quality of healing as autograft. Thus a number of biologics have been pursued as a way to improve bone graft substitute materials to further enhance healing potential for complex healing scenarios. In 2001 Bone morphogenetic proteins (BMPs) were FDA approved for use with a collagen sponge for spinal fusion and long bone non-union applications. Though BMP-2 and BMP -7 have been shown to perform as well as iliac crest bone grafts for spinal fusion and long bone applications (Kanakaris, Lasanianos et al. 2009, Zimmermann, Wagner et al. 2009), it is not without risk (Woo 2013). Alternative bioactive molecules may provide similar, if not better treatment options.

The evidence for the use of PTH for bone regenerations is abundant. PTH (as once daily injections) is presently FDA approved as an anabolic treatment for osteoporosis. As once daily injections PTH decreases the risk of fragility fractures, increases cortical thickness, and improves trabecular bone volume fraction and mineral density (Dempster, Cosman et al. 2001, Neer, Arnaud et al. 2001, Black, Greenspan et al. 2003, Jiang, Zhao et al. 2003). Daily injections of PTH have also been shown to improve bone regeneration in animal models (Tagil, McDonald et al. ,

Andreassen and Cacciafesta 2004, Kumabe, Lee et al. 2017). Though traditional methods indicate PTH be utilized as once daily injections to achieve an anabolic effect, there is also evidence that low dose continuous PTH levels may also be beneficial to the skeleton. Normal secretion from the parathyroid gland results in a combination of tonic (continuous) and pulsatile secretions. The tonic secretions account for approximately 70% of secretions from the parathyroid gland (Schmitt, Schaefer et al. 1996, Chiavistelli, Giustina et al. 2015). Though the classic presentation of primary hyperparathyroidism results in cortical bone loss, it is important to note sites of higher remodeling (i.e. trabecular bone) are preserved (Silverberg, Shane et al. 1989, Silverberg, Walker et al. 2013); and post-menopausal women with mild primary hyperparathyroidism have an apparent protective effect against post-menopausal osteoporosis (Dempster, Muller et al. 2007). Studies in bone regeneration indicated locally delivered PTH delivered in a sustained fashion improved healing (Jung, Cochran et al. 2007, Arrighi, Mark et al. 2009). Locally delivered low dose, continuous PTH may improve bone regeneration. This work examined the effects of locally delivered PTH on bone regeneration through examination of the direct effects of low dose continuous PTH treatment on osteoblasts, the effect of PTH on healing in a rat critical size femoral defect and characterization of the biomaterial carrier.

Local PTH delivery did not result in robustly improved bone ingrowth (as compared to control samples) in a critical size segmental femur defect model in these studies. However, outcome measures of percentage of the defect that had bridged indicated treatment with 3 or 10 μg PTH (delivered via tethering to a thiol-ene hydrogel) tended to increase defect bridging. Treatment with 30 μg of PTH (or higher) per hydrogel tended to result in less defect bridging as compared to the lower concentration treatment groups when PTH was entrapped within the

hydrogel matrix as well as when it was tethered to the matrix. These findings are consistent with observations from the in vitro work completed in Aim 1. Mineralization of MC3T3-E1 osteoblastic cells exposed to continuous treatment with PTH at the higher concentrations was less than vehicle control as well as low treatment concentrations. Future studies investigating the in vitro effects on osteoblastic cells in co culture with osteoclasts or cells isolated from a bone defect area after local delivery of PTH it utilized may build on these studies in helping to understand the threshold below which continuous local delivery of PTH may be optimized for an anabolic response. In vitro mineralization appears to be a useful and consistent marker of osteoblast activity in these studies as well as other published data on the effects of PTH on osteoblastic cells in culture (Milstrey, Wieskoetter et al. 2017). However, alkaline phosphatase activity (ALP) seemed to provide more variable results in this study as well as the recent work by Milstrey et al. It is possible the variable response is indeed characteristic of the expression pattern in longer term cultures and is perhaps not an ideal indicator of osteoblast differentiation. Future examination of other bone formation markers or signaling molecules that play a role in bone remodeling may provide further indication of the effect PTH has on bone regeneration.

When in vivo findings are considered in conjunction with in vitro release and in vivo degradation characteristics observed in Aim 2, the differences observed in percent bridging with 3 and 10 μg treatment groups between the studies indicate a potential effect of change in release profile. As gel degradation is not required for PTH to diffuse from the matrix when the PTH is entrapped within the hydrogel matrix (as opposed to tethered to it), the release profile is likely similar to the burst release observed in Aim 2 with approximately 80% of the PTH diffusing out by day 3. However, as the in vivo environment is less aqueous than a gel placed directly in PBS,

this burst may have been slightly less dramatic if fluid infiltration into the hydrogel is less. When PTH was tethered to the matrix it is likely PTH was released from the scaffold much more slowly even though MMPs would be present to break down the gel, hydrogels combined with PPF scaffolds remained present in subcutaneous pockets up to 8 weeks. Though in a defect model degradation would likely occur faster due to the increased damage and cellular response, it is unlikely degradation of the gel would be rapid enough to drastically change the PTH release profile. Future studies examining varying release profiles in a slightly different fashion may provide a more thorough insight as to the ideal release profile. Studies utilizing the same PPF/hydrogel scaffold system to bridge the defect area combined with PTH delivery via catheterized pump may provide a more controlled method by which to establish the ideal release profile for eliciting an anabolic response from locally delivered PTH. The scaffold system could then be tailored to match the optimal release profile.

Modification of the release profile of PTH from the hydrogels did not result in entirely different outcomes in the critical size defect model. In both studies, treatment with 30 μg PTH/gel resulted in less new bone in the defect area than other treatment groups. However, a tendency toward an increase in the percentage of the defect that had bridged with new bone with 3 and 10 μg treatment was observed when PTH was tethered to the hydrogel matrix. These observations may have resulted for a number of reasons. Firstly, perhaps neither release profile is the optimal release profile to obtain an anabolic response, resulting in observation of some anabolic potential, however, the response is not robust. Likewise, it is possible local delivery of PTH does not result in as robust an anabolic response as systemically administered PTH. Even though PTH is known to act on osteoblasts, perhaps the impacts PTH has on other organs plays a

pivotal role in its ability to affect the skeleton as effectively does. Lastly, histology data introduces the possibility that the 12 week timepoint was too early to observe large differences in outcome measures.

Treatment with 10 μg PTH resulted in defect areas being completely bridged by some combination of mineralized and cartilaginous tissue in all 3 samples examined. This was the case for two of the three samples in the 3 μg treatment group as well but not in any other treatment group. If samples had been collected at a later timepoint it seems likely much more distinct differences in bone volume and % bridging measures between treatment groups would be observed as samples bridged by a cartilaginous matrix are much more likely to heal than those bridged by loosely connected fibrous tissue because during endochondral ossification cartilage is gradually converted into bone (Ortega, Behonick et al. 2004, Mackie, Ahmed et al. 2008). The presence of cartilage in the defect area presents a foundation for replacement by bone. In vitro, PTH and PTHrP inhibit mineralization of a cartilage like matrix and apoptosis and production of a mineralized bone like matrix. However, upon withdrawal of the hormonal stimulation, cells redirect toward their distinct microenvironment and terminal differentiation (Zerega, Cermelli et al. 1999). PTH has also been indicated as efficacious in cartilage repair studies (Kudo, Mizuta et al. 2011, Orth, Cucchiarini et al. 2013) as well as prevention of further cartilage damage and slowing of deterioration of subchondral bone in an osteoarthritis model (Yan, Tian et al. 2014). Perhaps PTH treatment in these studies delays mineralization long enough to allow complete bridging of the defect area. Alternatively treatment may promote cartilage formation allowing bridging of the defect area. Regardless of mechanism, the likelihood for healing at a latertimepoint is improved with the presence of the cartilaginous matrix. In the event

mineralization did not progress as would be expected in this model, combination of this therapy with later release of VEGF to promote vascularization of the cartilaginous matrix and eventual remodeling to bone. These studies support further research examining the potential of PTH for regeneration of large segmental defects in bone.

References.

Andreassen, T. T. and V. Cacciafesta (2004). "Intermittent parathyroid hormone treatment enhances guided bone regeneration in rat calvarial bone defects." J Craniofac Surg **15**(3): 424-427; discussion 428-429.

Arrighi, I., S. Mark, M. Alvisi, B. von Rechenberg, J. A. Hubbell and J. C. Schense (2009). "Bone healing induced by local delivery of an engineered parathyroid hormone prodrug." Biomaterials **30**(9): 1763-1771.

Black, D. M., S. L. Greenspan, K. E. Ensrud, L. Palermo, J. A. McGowan, T. F. Lang, P. Garnero, M. L. Bouxsein, J. P. Bilezikian and C. J. Rosen (2003). "The effects of parathyroid hormone and alendronate alone or in combination in postmenopausal osteoporosis." N Engl J Med **349**(13): 1207-1215.

Chiavistelli, S., A. Giustina and G. Mazziotti (2015). "Parathyroid hormone pulsatility: physiological and clinical aspects." Bone Res **3**: 14049.

Connolly, J. F. (1995). "Injectable bone marrow preparations to stimulate osteogenic repair." Clin Orthop Relat Res(313): 8-18.

Dempster, D. W., F. Cosman, E. S. Kurland, H. Zhou, J. Nieves, L. Woelfert, E. Shane, K. Plavetic, R. Muller, J. Bilezikian and R. Lindsay (2001). "Effects of daily treatment with parathyroid hormone on bone microarchitecture and turnover in patients with osteoporosis: a paired biopsy study." J Bone Miner Res **16**(10): 1846-1853.

Dempster, D. W., R. Muller, H. Zhou, T. Kohler, E. Shane, M. Parisien, S. J. Silverberg and J. P. Bilezikian (2007). "Preserved three-dimensional cancellous bone structure in mild primary hyperparathyroidism." Bone **41**(1): 19-24.

Hak, D. J. (2007). "The use of osteoconductive bone graft substitutes in orthopaedic trauma." J Am Acad Orthop Surg **15**(9): 525-536.

Jahangir, A. A., R. M. Nunley, S. Mehta and A. Sharan (2008) "Bone-graft substitutes in orthopaedic surgery." AAOS Now.

Jiang, Y., J. J. Zhao, B. H. Mitlak, O. Wang, H. K. Genant and E. F. Eriksen (2003). "Recombinant human parathyroid hormone (1-34) [teriparatide] improves both cortical and cancellous bone structure." J Bone Miner Res **18**(11): 1932-1941.

Jung, R. E., D. L. Cochran, O. Domken, R. Seibl, A. A. Jones, D. Buser and C. H. Hammerle (2007). "The effect of matrix bound parathyroid hormone on bone regeneration." Clin Oral Implants Res **18**(3): 319-325.

Kanakaris, N. K., N. Lasanianos, G. M. Calori, R. Verdonk, T. J. Blokhuis, P. Cherubino, P. De Biase and P. V. Giannoudis (2009). "Application of bone morphogenetic proteins to femoral non-unions: a 4-year multicentre experience." Injury **40 Suppl 3**: S54-61.

Kudo, S., H. Mizuta, K. Takagi and Y. Hiraki (2011). "Cartilaginous repair of full-thickness articular cartilage defects is induced by the intermittent activation of PTH/PTHrP signaling." Osteoarthritis Cartilage **19**(7): 886-894.

Kumabe, Y., S. Y. Lee, T. Waki, T. Iwakura, S. Takahara, M. Arakura, Y. Kuroiwa, T. Fukui, T. Matsumoto, T. Matsushita, K. Nishida, R. Kuroda and T. Niikura (2017). "Triweekly administration of parathyroid hormone (1-34) accelerates bone healing in a rat refractory fracture model." BMC Musculoskelet Disord **18**(1): 545.

Mackie, E. J., Y. A. Ahmed, L. Tatarczuch, K. S. Chen and M. Mirams (2008). "Endochondral ossification: how cartilage is converted into bone in the developing skeleton." Int J Biochem Cell Biol **40**(1): 46-62.

Mahendra, A. and A. D. Maclean (2007). "Available biological treatments for complex non-unions." Injury **38 Suppl 4**: S7-12.

Milstrey, A., B. Wieskoetter, D. Hinze, N. Grueneweller, R. Stange, T. Pap, M. Raschke and P. Garcia (2017). "Dose-dependent effect of parathyroid hormone on fracture healing and bone formation in mice." J Surg Res **220**: 327-335.

Neer, R. M., C. D. Arnaud, J. R. Zanchetta, R. Prince, G. A. Gaich, J. Y. Reginster, A. B. Hodsman, E. F. Eriksen, S. Ish-Shalom, H. K. Genant, O. Wang and B. H. Mitlak (2001). "Effect of parathyroid hormone (1-34) on fractures and bone mineral density in postmenopausal women with osteoporosis." N Engl J Med **344**(19): 1434-1441.

Ortega, N., D. J. Behonick and Z. Werb (2004). "Matrix remodeling during endochondral ossification." Trends Cell Biol **14**(2): 86-93.

Orth, P., M. Cucchiarini, D. Zurakowski, M. D. Menger, D. M. Kohn and H. Madry (2013). "Parathyroid hormone [1-34] improves articular cartilage surface architecture and integration and subchondral bone reconstitution in osteochondral defects in vivo." Osteoarthritis Cartilage **21**(4): 614-624.

Schmitt, C. P., F. Schaefer, A. Bruch, J. D. Veldhuis, H. Schmidt-Gayk, G. Stein, E. Ritz and O. Mehls (1996). "Control of pulsatile and tonic parathyroid hormone secretion by ionized calcium." J Clin Endocrinol Metab **81**(12): 4236-4243.

Silverberg, S. J., E. Shane, L. de la Cruz, D. W. Dempster, F. Feldman, D. Seldin, T. P. Jacobs, E. S. Siris, M. Cafferty, M. V. Parisien and et al. (1989). "Skeletal disease in primary hyperparathyroidism." J Bone Miner Res **4**(3): 283-291.

Silverberg, S. J., M. D. Walker and J. P. Bilezikian (2013). "Asymptomatic primary hyperparathyroidism." J Clin Densitom **16**(1): 14-21.

Tagil, M., M. M. McDonald, A. Morse, L. Peacock, K. Mikulec, N. Amanat, C. Godfrey and D. G. Little "Intermittent PTH(1-34) does not increase union rates in open rat femoral fractures and exhibits attenuated anabolic effects compared to closed fractures." Bone **46**(3): 852-859.

Woo, E. J. (2013). "Adverse events after recombinant human BMP2 in nonspinal orthopaedic procedures." Clin Orthop Relat Res **471**(5): 1707-1711.

Yan, J. Y., F. M. Tian, W. Y. Wang, Y. Cheng, H. P. Song, Y. Z. Zhang and L. Zhang (2014). "Parathyroid hormone (1-34) prevents cartilage degradation and preserves subchondral bone micro-architecture in guinea pigs with spontaneous osteoarthritis." Osteoarthritis Cartilage **22**(11): 1869-1877.

Zerega, B., S. Cermelli, P. Bianco, R. Cancedda and F. D. Cancedda (1999). "Parathyroid hormone [PTH(1-34)] and parathyroid hormone-related protein [PTHrP(1-34)] promote reversion of hypertrophic chondrocytes to a prehypertrophic proliferating phenotype and prevent terminal differentiation of osteoblast-like cells." J Bone Miner Res **14**(8): 1281-1289.

Zimmermann, G., C. Wagner, K. Schmeckenbecher, A. Wentzensen and A. Moghaddam (2009). "Treatment of tibial shaft non-unions: bone morphogenetic proteins versus autologous bone graft." Injury **40 Suppl 3**: S50-53.

Appendix 1: Alkaline phosphatase activity of MC3T3 cells treated with Black Bear PTH 1-84

Protocol used by Claire Tucker, Sam Wojda

Time to complete: 6-8 weeks

Supplies Required	Supplier and Catalog Number	Storage Conditions	Location
Minimum Essential Media (Alpha Modification)	VWR SC45000-300	4°C	Fridge
0.25% Trypsin-EDTA	VWR 45000-664	4°C	Fridge
Penn-Strep	VWR 45000-652	4°C	Fridge
FBS (Characterized)	VWR 80058-556	4°C	Fridge
PBS	VWR 800858-556	Room Temp	On Chemical Shelf
L-Ascorbic Acid Cas# 50-81-7	Fisher Scientific A61-100	4°C	Fridge
β-Glycerophosphate	Cabiochem 35675	4°C	Fridge
Alkaline Phosphatase Assay Kit (Colorimetric)	Abcam ab83369	-20°C	ACC244 Freezer
BCA Protein Assay Kit	Pierce Thermo Scientific	Room Temp	Chemical cabinet
Black Bear PTH 1-84		-80°C	

Additional Supplies Required

- Pipet Aid (Hood)
- Refrigerated centrifuge (ACC240)
- Sonicator (ACC240)
- Incubator at 37°C +5% CO2
- Serological pipettes (5, 10, 25, 50 mL)
- Micropipettes
- Micropipette tips
- Sterile media bottles (100, 250, 1000 mL)

- Centrifuge tubes (15 and 50 mL)
- Culture dish (VWR: 82050-916)
- Culture flask (T-25, T-75)
- 6-well plates
- 96-well plate
- Eppendorf tubes (1.6 mL)
- Cell scrapers
- Invitrogen Countess Automated Cell Counter
- Countess Cell Counting Chamber Slides
- Colorimetric plate reader

General Notes:

Procedure

Grow Cells

1. Make MC3T3 growth media (500 mL) - (See bonelab MC3T3 SOP if needed)
    a. 89% α-MEM (445mL)
    b. 10% FBS (50 mL)
    c. 1% Penn-Strep (5 mL)
    d. Sterile filter all components
2. Add 14 mL warmed growth media to 75 cm^2 flask (T75)
3. Remove desired cell line from liquid nitrogen. Hold in heat bath until thawed. 1-2 min
4. Transfer cells to T75 flask and place in incubator (37°C + 5 % CO_2)
5. Change media within 24 hours.
6. Split cells when 70-80% confluent.
7. Change media every 2-3 days throughout cell growth process.
8. Cell count:
    a. Use Invitrogen Countess Cell Counter or Hemacytometer method.
    b. Need 103,500 cells/well (10,350,000 cells/mL)
        i. 15,000 cells/cm^2 (well: 6.9 cm^2)
        ii. 103,500 cells/well or 103,500 cells/□L
        iii. (# of cells grown) / ($10.35x10^6$ cells/mL) = _____mL to re-suspend pellet

Plate Preparation

1. Make MC3T3 differentiation media – (see bonelab MC3T3 differentiation SOP: 5-3 if needed)
    a. 89% α-MEM (445mL)
    b. 10% FBS (50 mL)

c. 1% Penn-Strep (5 mL)
d. 50 □g/mL L-Ascorbic Acid
e. 10 mM □-glycerphosphate
f. Sterile filter all components

2. Label 6-well plates with PTH concentrations (2 plates/time point; 10 plates/passage).
    a. t = 3, 7, 14, 21 and 28 days
    b. 10 different PTH concentrations
3. Add the following amounts of media to each labeled falcon tube. Add stock PTH to 100 nM. Vortex then remove and serial dilute (10-fold) rest of concentrations
    a. **STOCK**: 100 □M bbPTH
4. Add 2.5 mL of dilution to each well.

5 Time points (+ cushion)

Concentration	**Total Volume (2.5mL x 5.5)**	**Differentiation Media**	**PTH**
100 nM	13.750 mL	13.750 mL	13.75 □L of **STOCK PTH**
10 nM	13.750 mL	12.375 mL	1,375 µL of **100 nM** PTH
1 nM	13.750 mL	12.375 mL	1,375 µL of **10 nM** PTH
0.1 nM	13.750 mL	12.375 mL	1,375 µL of **1 nM** PTH
0.01 nM	13.750 mL	12.375 mL	1,375 µL of **0.1 nM** PTH
0.001 nM	13.750 mL	12.375 mL	1,375 µL of **0.01 nM** PTH
0.0001 nM	13.750 mL	12.375 mL	1,375 µL of **0.001 nM** PTH
0.00001 nM	13.750 ml	12.375 mL	1,375 µL of **0.0001 nM** PTH
0 nM	2.5 mL/well	2.5 mL	None
Intermittent	2.5 mL/well	2.5 mL	None (2.5µL of STOCK PTH for 2.5 hours/day (5days/week))

5. Cell seed:
    a. Plate cells at a density of 15,000 cells/cm^2.
    b. Lyse cells and combine into one falcon tube. Centrifuge at 1200 rpm for 5 min.
    c. Remove supernatant carefully with glass pipette.
    d. Add differentiation media to resuspend (counted cells) / (needed cells/mL) = mL for resuspension. Invert tube to mix.
    e. Using small micropipette, mix up and down several times. Place 10 µL into each well.

<u>Plate Maintenance</u>

1. Culture MC3T3 cells in differentiation media +/- PTH for 3, 7, 14, 21 or 28 days.

2. Apply 2.5 □□ stock PTH (100 □M) to intermittent wells for 2.5 hours, 5 days/week. Remove media and PTH after 2.5 hours and replace with fresh differentiation media.
3. Change media in each well every three days. Prepare media/PTH dilutions in 50 mL falcon tubes as described above. Use the following calculations dependent on how many time points remain.

4 Time points (+ cushion)

Concentration	**Total Volume (2.5mL x 4.5)**	**Differentiation Media**	**PTH**
100 nM	12.510 mL	12.510 mL	12.51 □L of **STOCK PTH**
10 nM	12.510 mL	11.259 mL	1,251 µL of **100 nM** PTH
1 nM	12.510 mL	11.259 mL	1,251 µL of **10 nM** PTH
0.1 nM	12.510 mL	11.259 mL	1,251 µL of **1 nM** PTH
0.01 nM	12.510 mL	11.259 mL	1,251 µL of **0.1 nM** PTH
0.001 nM	12.510 mL	11.259 mL	1,251 µL of **0.01 nM** PTH
0.0001 nM	12.510 mL	11.259 mL	1,251 µL of **0.001 nM** PTH
0.00001 nM	12.510 ml	11.259 mL	1,251 µL of **0.0001 nM** PTH
0 nM	2.5 mL/well	2.5 mL	None
Intermittent	2.5 mL/well	2.5 mL	None (2.5µL of STOCK PTH for 2.5 hours/day (5days/week))

3 time points (+ cushion)

Concentration	**Total Volume**	**Differentiation Media**	**PTH**
100 nM	9.73 mL	9.73 mL	9.73 µL of **100 □M stock** PTH
10 nM	9.73 mL	8.757 mL	973 µL of **100 nM**
1 nM	9.73 mL	8.757 mL	973 µL of **10 nM**
0.1 nM	9.73 mL	8.757 mL	973 µL of **1 nM**
0.01 nM	9.73 mL	8.757 mL	973 µL of **0.1 nM**
0.001 nM	9.73 mL	8.757 mL	973 µL of **0.01 nM**
0.0001 nM	9.73 mL	8.757 mL	973 µL of **0.001 nM**
0.00001 nM	9.73 mL	8.757 mL	973 µL of **0.0001 nM**
0 nM	2.5 mL/well	2.5 mL	**None**
Intermittent	2.5 mL/well	2.5 mL	None (2.5µL of STOCK PTH for 2.5 hours/day (5days/week))

2 time points (+ cushion)

Concentration	**Total Volume**	**Differentiation Media**	**PTH**
100 nM	6.95 mL	6.95 mL	6.95 µL of **100 □M stock** PTH
10 nM	6.95 mL	6.255 mL	695 µL of **100 nM**
1 nM	6.95 mL	6.255 mL	695 µL of **10 nM**
0.1 nM	6.95 mL	6.255 mL	695 µL of **1 nM**
0.01 nM	6.95 mL	6.255 mL	695 µL of **0.1 nM**
0.001 nM	6.95 mL	6.255 mL	695 µL of **0.01 nM**
0.0001 nM	6.95 mL	6.255 mL	695 µL of **0.001 nM**
0.00001 nM	6.95 mL	6.255 mL	695 µL of **0.0001 nM**
0 nM	2.5 mL/well	2.5 mL	**None**
Intermittent	2.5 mL/well	2.5 mL	None (2.5µL of STOCK PTH for 2.5 hours/day (5days/week))

1 time point (+ cushion)

Concentration	**Total Volume**	**Differentiation Media**	**PTH**
100 nM	3.475 mL	3.475 mL	3.475 µL of **100 □M stock** PTH
10 nM	3.475 mL	3.128 mL	347.5 µL of **100 nM**
1 nM	3.475 mL	3.128 mL	347.5 µL of **10 nM**
0.1 nM	3.475 mL	3.128 mL	347.5 µL of **1 nM**
0.01 nM	3.475 mL	3.128 mL	347.5 µL of **0.1 nM**
0.001 nM	3.475 mL	3.128 mL	347.5 µL of **0.01 nM**
0.0001 nM	3.475 mL	3.128 mL	347.5 µL of **0.001 nM**
0.00001 nM	3.475 mL	3.128 mL	347.5 µL of **0.0001 nM**
0 nM	2.5 mL/well	2.5 mL	**None**
Intermittent	2.5 mL/well	2.5 mL	None (2.5µL of STOCK PTH for 2.5 hours/day (5days/week))

<u>Sample Extraction at Each Time point</u>

1. Remove media from all 6 wells on one plate.
2. Wash with 2-3 mL PBS.
3. Add 200 µL ALP buffer (in Kit) to each well.
4. Scrape cells from each well using cell scraper. Use micropipette to remove lysate into labeled eppendorf (lysate from 1 well per eppendorf).
5. Repeat steps 1-4 with 2nd plate from the same time point.
6. Sonicate each lysate sample for 3 times: 2-3 seconds of sonication with 20 seconds between each cycle. Spray sonicator with ethanol and diH_2O between each sample.
    a. KEEP SAMPLES ON **ICE**

7. Centrifuge all samples at 13,000g for 3 min at 4°C
8. Remove supernatant from eppendorf using micropipette set to 200 µL and place in a clean labeled eppendorf. Be careful not to disturb pellet.
    a. KEEP SUPERNATANT
9. Place SUPERNATANT eppendorfs in -80°C freezer until ready to complete assays.
    a. If you don't do the BCA and ALP Assay on the same day, make a small aliquot for the protein assay so you don't freeze/thaw samples

<u>BCA Assay</u>

1. Follow instructions in assay kit – 96 well assay
    a. 10 µL sample
    b. Make Standards in ALP Buffer

<u>ALP Assay (see AbCam Protocol ab83369)</u>

1. Thaw samples on ice.
2. Dissolve 2 pNPP tablets in 5.4 ml assay buffer to make 5 mM work solution. Keep on ice.
3. Take 40 µl of the 5 mM work solution and add to 160 µl assay buffer to make 1 mM pNPP solution.
4. Standard curve preparation - Add 120, 118, 116, 112, 108, 104, 100 µL assay buffer in triplicate in 96-well plate. Add 0, 2, 4, 8, 10, 12, 16, 20 µL of 1 mM pNPP standard solution in triplicate to these wells to generate 0, 2, 4, 8, 16, 20 nmol/well pNPP standard. The final volume of each well should be 120 µL.
5. Sample wells - Take 40 µL of each lysate sample and 40 µL assay buffer (1:2 dilution) in duplicate to 96-well plate.
6. Add **50 µL 5 mM pNPP solution** to each **sample** well.
7. Add **10 µL of ALP enzyme** to each **standard** well.
8. Cover and incubate at RT for 1 hour.
9. Add **20 µL stop** solution to **each well**.
10. Run absorbance at **405 nm**.

<u>Data Analysis</u>

Plot pNPP Standard Curve. X axis in pNPP in µmol. Y axis is OD_{405nm} with correction for blank.

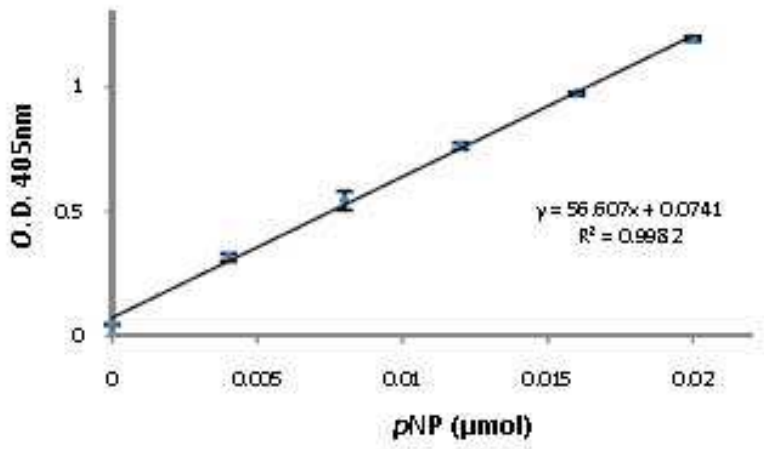

ALP activity (U/ml) = A/V/T

A = amount of pNPP generated by samples (in µmol)

V = volume of sample added in the assay well (in ml)

T = reaction time (in minutes)

Final Data Format:

ALP (U – ng)/Total Protein (ng)

References:

Abcam Protocol ab83369: Alkaline Phosphatase Assay Kit (Colorimetric). (2012).

Patntirapong S, Singhatanadgit W, Chanruangvanit C, Lavanrattanakul K, Satravaha Y (2012) Zoledronic acid suppresses mineralization through direct cytotoxicity and osteoblasts differentiation inhibition. *J Oral Pathol Med,* **41,** 713-20.

Wang YH, Liu Y, Buhl K, Rowe DW (2005) Comparison of the action of transient and continuous PTH on primary osteoblasts cultures expressing differentiation stage-specific GFP. *J Bone Miner Res,* **20,** 5-14.

Whyte MP (1994) Hypophosphatasia and the role of alkaline phosphatase in skeletal mineralization. *Endocr Rev,* **15,** 439-61.

Appendix 2: Alizarin Red staining of MC3T3 cells treated with Black Bear PTH 1-84

Protocol used by Sam Wojda

Time to complete: 6-8 weeks

Supplies Required	Supplier and Catalog Number	Storage Conditions	Location
Minimum Essential Media (Alpha Modification)	VWR SC45000-300	4°C	Fridge
0.25% Trypsin-EDTA	VWR 45000-664	4°C	Fridge
Penn-Strep	VWR 45000-652	4°C	Fridge
FBS (Characterized)	VWR 80058-556	4°C	Fridge
PBS	VWR 800858-556	Room Temp	On Chemical Shelf
L-Ascorbic Acid Cas# 50-81-7	Fisher Scientific A61-100	4°C	Fridge
β-Glycerophosphate	Cabiochem 35675	4°C	Fridge
Alizarin Red	Sigma	Room Temp	
10 % Neutral Buffered Formalin		Room Temp	
Black Bear PTH 1-84		-80°C	
EVOS cell imaging microscope		Room Temp	
Boquant Osteo		Room Temp	

Additional Supplies Required

- Pipet Aid (Hood)
- Incubator at 37°C +5% CO_2
- Serological pipettes (5, 10, 25, 50 mL)
- Micropipettes
- Micropipette tips
- Sterile media bottles (100, 250, 1000 mL)
- Centrifuge tubes (15 and 50 mL)

- Culture dish (VWR: 82050-916)
- Culture flask (T-25, T-75)
- 12-well plates
- Eppendorf tubes (1.6 mL)

General Notes: Alizarin red stains for mineralized tissue (does not account for phosphate –use VKM to assess both)

Procedure

Grow Cells

1. Make MC3T3 growth media (500 mL) - (see MC3T3 SOP: 5-14)
    a. 89% α-MEM (445 mL)
    b. 10% FBS (50 mL)
    c. 1% Penn-Strep (5 mL)
    d. Sterile filter all components
2. Add 14 mL warmed growth media to 75 cm^2 flask
3. Remove desired cell line from liquid nitrogen. Hold in heat bath until thawed. 1-2min
4. Transfer cells to T75 flask and place in incubator. 37°C + 5%CO_2
5. Change media within 24 hours.
6. Split cells when 70-80% confluent.
7. Change media every 2-3 days throughout cell growth process.
8. Cell count:
    a. Use Invitrogen Countess Cell Counter or Hemacytometer method.
    b. Need 57,000 cells/well
        i. 15,000 cells/cm^2 (well: 3.8 cm^2)
        ii. 57,000 cells/well
        iii. (# of cells grown) / (X cells/mL) = _____mL to re-suspend pellet

Plate Preparation

9. Make MC3T3 differentiation media – (see MC3T3 differentiation SOP: 5-3 if needed)
    f. 89% α-MEM (445 mL)
    g. 10% FBS (50 mL)
    h. 1% Penn-Strep (5 mL)
    i. 50 µg/mL L-Ascorbic Acid
    j. 10 mM β-glycerphosphate
    k. Sterile filter all components
10. Label 12-well plates with PTH concentrations (1 plates/time point; 5 plates/passage).
    l. t = 3, 7, 14, 21 and 28 days

m. 10 different PTH concentrations

11. Add the following amounts of media to each labeled falcon tube. Add stock PTH to 100 nM. Vortex then remove and serial dilute (10-fold) rest of concentrations
    n. **STOCK**: 100 µM bbPTH
12. Add 1 mL of dilution to each well.

    5 Time points (+ cushion)

Concentration	**Total Volume (1 mL x 5.5)**	**Differentiation Media**	**PTH**
100 nM	5.5 mL	5.5 mL	5.5 µL of **STOCK PTH**
10 nM	5.5 mL	4.95 mL	550 µL of **100 nM** PTH
1 nM	5.5 mL	4.95 mL	550 µL of **10 nM** PTH
0.1 nM	5.5 mL	4.95 mL	550 µL of **1 nM** PTH
0.01 nM	5.5 mL	4.95 mL	550 µL of **0.1 nM** PTH
0.001 nM	5.5 mL	4.95 mL	550 µL of **0.01 nM** PTH
0.0001 nM	5.5 mL	4.95 mL	550 µL of **0.001 nM** PTH
0.00001 nM	5.5 mL	4.95 mL	550 µL of **0.0001 nM** PTH
0 nM	1 mL/well	1 mL	None
Intermittent	1 mL/well	1 mL	None (1 µL of STOCK PTH for 2.5 hours/day (5 days/week))

13. Cell seed:
    o. Plate cells at a density of 15,000 cells/cm^2.
    p. Lyse cells and combine into one falcon tube. Centrifuge at 1200 rpm for 5 min.
    q. Remove supernatant carefully with glass pipette.
    r. Add differentiation media to re-suspend (counted cells) / (needed cells/mL) = ____mL for resuspension. Invert tube to mix.
    s. Using small micropipette, mix up and down several times. Place 10 µL into each well.

<u>Plate Maintenance</u>

14. Culture MC3T3 cells in differentiation media +/- PTH for 3, 7, 14, 21, or 28 days.
15. Apply 2.5 µL stock PTH (100 µM) to intermittent wells for 2.5 hours, 5 days/week. Remove media and PTH after 2.5 hours and replace with fresh differentiation media.
16. Change media in each well every three days. Prepare media/PTH dilutions in 50 mL falcon tubes as described above. Use the following calculations dependent on how many time points remain.

4 time points (+ cushion)

Concentration	**Total Volume (1 mL x 4.5)**	**Differentiation Media**	**PTH**
100 nM	4.5 mL	4.5 mL	4.5 µL of **STOCK PTH**
10 nM	4.5 mL	4.05 mL	450 µL of **100 nM** PTH
1 nM	4.5 mL	4.05 mL	450 µL of **10 nM** PTH
0.1 nM	4.5 mL	4.05 mL	450 µL of **1 nM** PTH
0.01 nM	4.5 mL	4.05 mL	450 µL of **0.1 nM** PTH
0.001 nM	4.5 mL	4.05 mL	450 µL of **0.01 nM** PTH
0.0001 nM	4.5 mL	4.05 mL	450 µL of **0.001 nM** PTH
0.00001 nM	4.5 mL	4.05 mL	450 µL of **0.0001 nM** PTH
0 nM	1 mL/well	1 mL	None
Intermittent	1 mL/well	1 mL	None (1 µL of STOCK PTH for 2.5 hours/day (5days/week))

3 time points (+ cushion)

Concentration	**Total Volume**	**Differentiation Media**	**PTH**
100 nM	3.5 mL	3.5 mL	3.5 µL of **100 µM stock** PTH
10 nM	3.5 mL	3.15 mL	350 µL of **100 nM**
1 nM	3.5 mL	3.15 mL	350 µL of **10 nM**
0.1 nM	3.5 mL	3.15 mL	350 µL of **1 nM**
0.01 nM	3.5 mL	3.15 mL	350 µL of **0.1 nM**
0.001 nM	3.5 mL	3.15 mL	350 µL of **0.01 nM**
0.0001 nM	3.5 mL	3.15 mL	350 µL of **0.001 nM**
0.00001 nM	3.5 mL	3.15 mL	350 µL of **0.0001 nM**
0 nM	2.5 mL/well	1 mL	**None**
Intermittent	2.5 mL/well	1 mL	None (1 µL of STOCK PTH for 2.5 hours/day (5days/week))

2 time points (+ cushion)

Concentration	**Total Volume**	**Differentiation Media**	**PTH**
100 nM	2.5 mL	2.5 mL	2.5 µL of **100 µM stock** PTH
10 nM	2.5 mL	2.25 mL	250 µL of **100 nM**
1 nM	2.5 mL	2.25 mL	250 µL of **10 nM**
0.1 nM	2.5 mL	2.25 mL	250 µL of **1 nM**
0.01 nM	2.5 mL	2.25 mL	250 µL of **0.1 nM**
0.001 nM	2.5 mL	2.25 mL	250 µL of **0.01 nM**
0.0001 nM	2.5 mL	2.25 mL	250 µL of **0.001 nM**
0.00001 nM	2.5 mL	2.25 mL	250 µL of **0.0001 nM**
0 nM	1 mL/well	1 mL	**None**
Intermittent	1 mL/well	1 mL	None (1 µL of STOCK PTH for 2.5 hours/day (5days/week))

1 time point (+ cushion)

Concentration	**Total Volume**	**Differentiation Media**	**PTH**
100 nM	1.5 mL	1.5 mL	1.5 µL of **100 µM stock** PTH
10 nM	1.5 mL	1.35 mL	150 µL of **100 nM**
1 nM	1.5 mL	1.35 mL	150 µL of **10 nM**
0.1 nM	1.5 mL	1.35 mL	150 µL of **1 nM**
0.01 nM	1.5 mL	1.35 mL	150 µL of **0.1 nM**
0.001 nM	1.5 mL	1.35 mL	150 µL of **0.01 nM**
0.0001 nM	1.5 mL	1.35 mL	150 µL of **0.001 nM**
0.00001 nM	1.5 mL	1.35 mL	150 µL of **0.0001 nM**
0 nM	1 mL/well	1 mL	**None**
Intermittent	1 mL/well	1 mL	None (1 µL of STOCK PTH for 2.5 hours/day (5days/week))

<u>Alizarin Red Stain Preparation</u>

1. 1g alizarin red S (Sigma: A5533) : 100 mL DI water
2. Adjust pH of solution between 4.1 and 4.3 using 0.1% ammonium hydroxide
3. Filter stain through sterile filter
4. Store tightly capped at RT protected from light (up to 3 months)
5. Aspirate formalin

Alizarin Red staining

1. Remove media from all 12 wells on one plate.
2. Wash with 2-3 mL PBS.
3. Add 2 mL 10% Neutral Buffered Formalin (NBF)
4. Incubate at RT for 1 hour
5. Aspirate NBF and discard
6. Rinse wells with 2 mL DI water and aspirate
7. Add 2 mL alizarin red to each well to be stained
8. Incubate at RT for 20 min then aspirate
9. Rinse with 2 mL DI water and aspirate
10. Repeat rinse step (step 14) 2 times, or until background is clear
11. Add a final 2 mL DI water to stained wells
12. Examine/image under microscope

Imaging/Digitization of stained wells:

1. The 4X objectives should work sufficiently to image plates. However, you may choose objective based on the amount of detail you can see and how comfortable you are making measurements at a given magnification.

2. To image wells: Using the stage controls on the EVOS cell imaging scope, orient the plate so you can see the well you want to image, locate the top and left sides.
    a. Image the entire well area by starting at a point that will allow you to move straight across the well taking images as seen below.

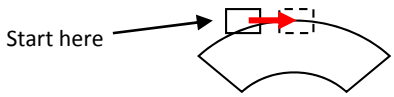

    b. Move down so the top of your image lines up with the bottom of your first row. Continue moving across and down the sample until you have imaged the entire defect area (figure below for pattern example (squares/pictures will “touch” from left to right and top to bottom.

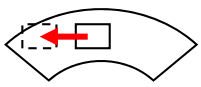

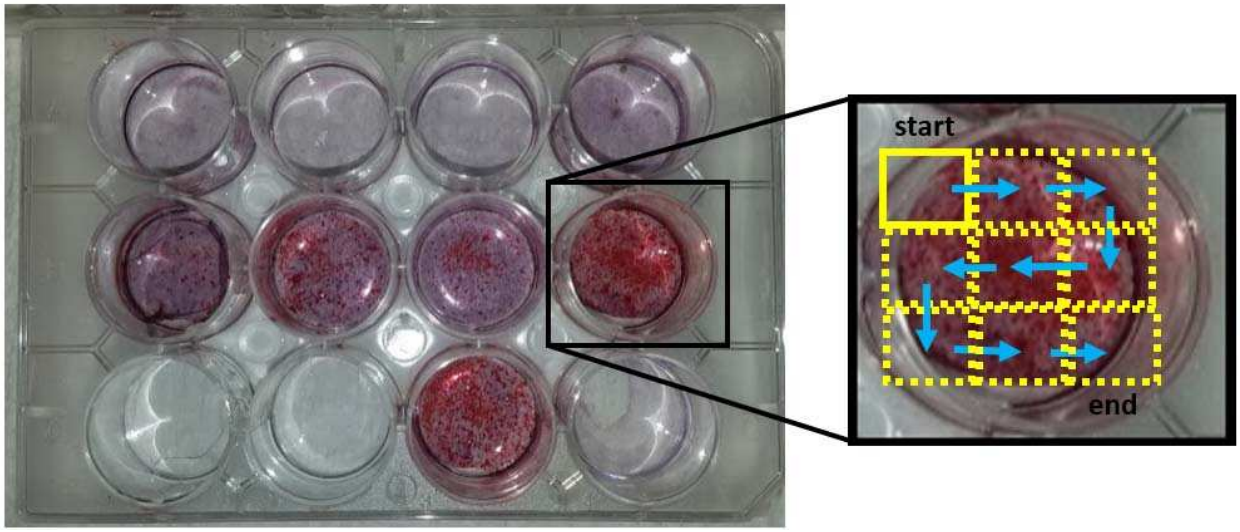

3. Repeat for all wells. Make sure you make clear file labels on the computer.
    a. Keep track of both sample number and magnification level of each image.
    b. If you have a method for imaging the entire section that is different but captures all required images, you may also use that.

<u>Mineralized Area Quantification</u>

1. To quantify mineralized area in each well open Bioquant Osteo on Donahue lab computer.

    (There is an online calendar signup to avoid scheduling conflicts. Please use it)

    a. Computer Username : DONAHUE-JPK11-2\bioquantinator
    Computer Password : bioquantinator

    b. Once bioquant is open, open the desired Data Volume

        1. File → Open Data Set… → Select whichever Data Volume and Data Set apply to your project → Open

        2. Prior to making measurements: Start by creating a new data set for your sample: File → Quick Data Set →Type in desired name (typically study name/sample number works well for organization). This copies data set settings but makes a new folder for data collection

    Note*: you don't need an individual data set for each image, it generally serves to help with organization, just make sure you create a new Data Set for each sample and a Data Volume for each project, do not overwrite someone else's work and don't delete data in an already made data set, just make a new one based on the data set.

c. Load calibration file. This is VERY IMPORTANT!!! Do not skip this step

    1. Measure → Calibration → File → Load → Select appropriate calibration file (Typically named by Scope_Camera_Date) → Open →Exit 'Optical Calibration' window

d. To start making measurements, load image (If you are accustomed to the full version of bioquant you may prefer to load sequential images to load all images for one sample. However, that functionality is not part of the present license, so analysis must be done one at a time.)

    1. File → Open Image → Select desired images from wherever on the computer you saved them. → Open

e. Once bioquant is open/calibration file is open/image is loaded you may measure until your heart's content.

f. To orient you:
    1. Mineralized Area = Red area (indicated by white arrow)
    2. Total Area = Entire area of image

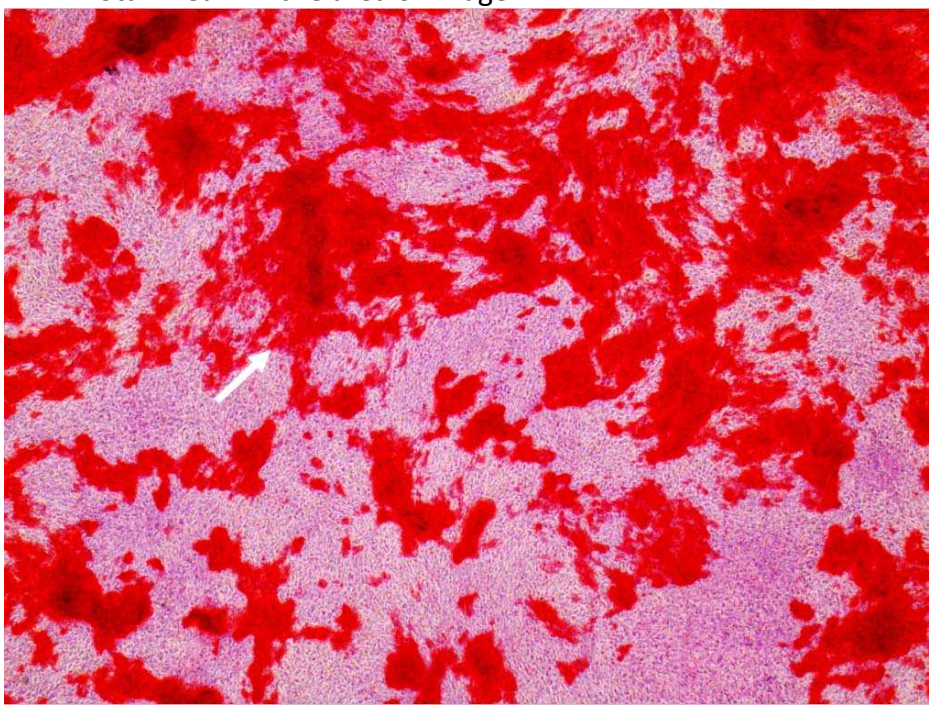

2. Start by defining the ROI and measuring Image Area (ie. use the A2 array for this function). To make arrays active double click on the arrays you want to use in the 'Available Arrays' toolbox. They will then show up in the Selected Arrays box. Click on A2 to select it for measurement. Glance at the 'Parameters' to double check/verify that the magnification level for the given array is accurate (these can get changed, a lot of people use these data

volumes, verify the magnification level listed matches that which you took your pictures at)

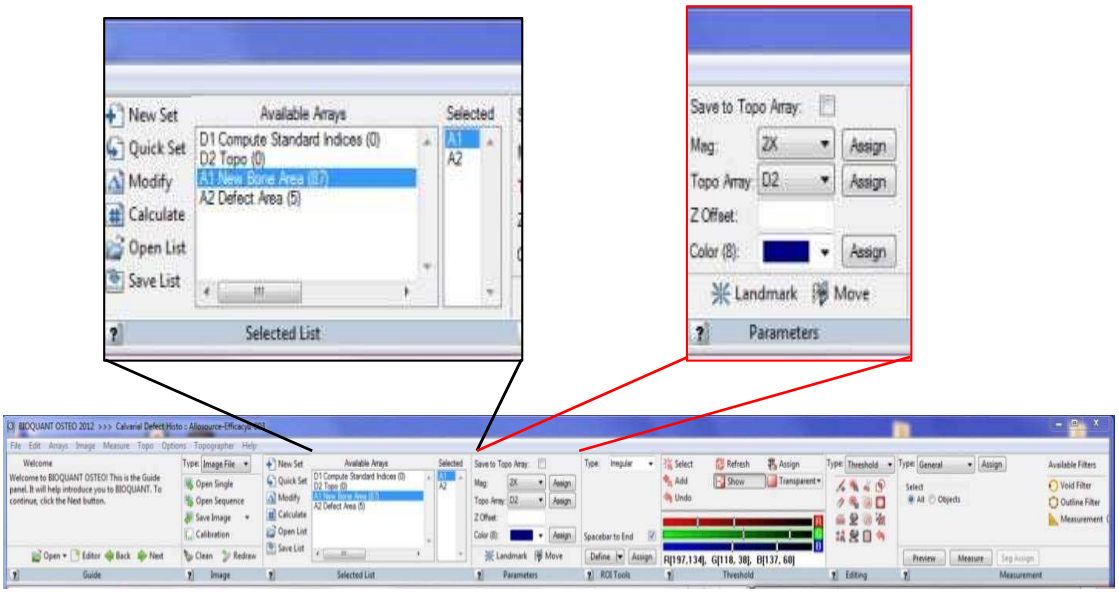

3. Make sure ROI type is 'Irregular' if you want anything other than the whole image or a square ROI.

    a. The "space bar to end" function is helpful if you aren't great at tracing with a mouse, to use this make sure the checkbox is checked.

        1. Otherwise you may trace by holding down the mouse the whole time.

        2. Click Define, your cursor will move to the image window, trace the desired ROI.

        3. In the measurement toolbox click preview and ensure you are happy with the selected ROI.

        4. If you are happy click "Measure'.

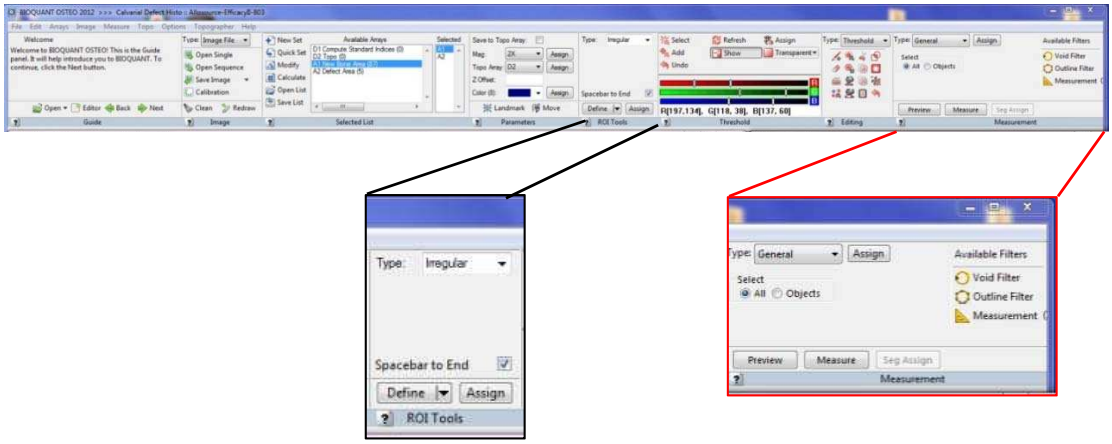

4. It will be recorded in the Raw Data toolbox.

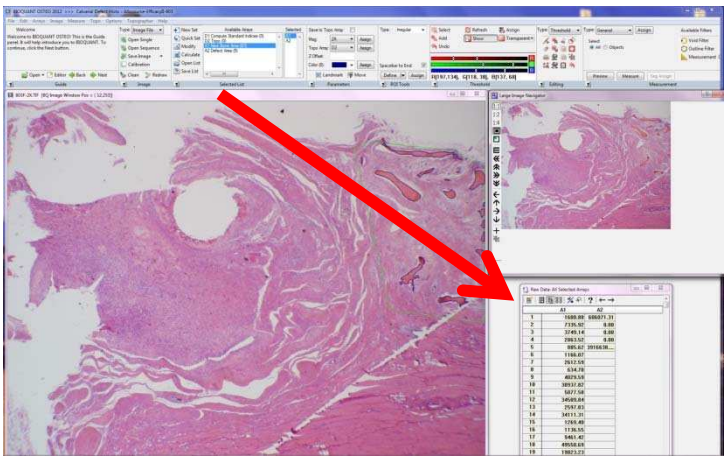

5. To measure mineralized area click the “A1” array to select it, this will measure the mineralized area using the thresholding tools. Due to differences in staining between wells and color differences it is likely in your best interest to set the thresholding for each sample manually.

    a. In the Threshold box click ‘select’ and click on red areas in the large image viewing window until much of the desired area is selected.

        1. You may further add or removed selected areas using the Editing tools.

        2. You may preview at any point to see If you like the selected area (when you click preview Bioquant will outline the areas it is going to measure).

        3. When you are happy with the preview click measure

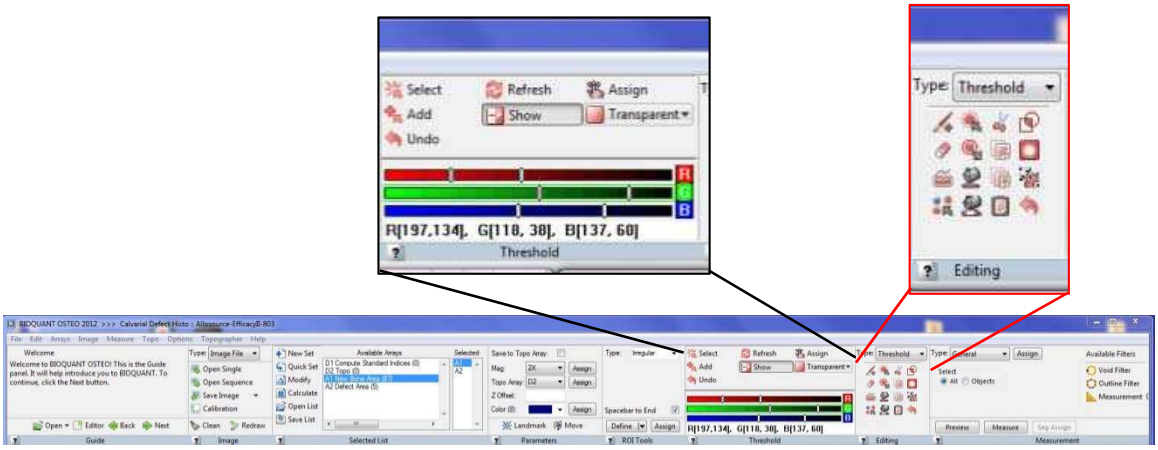

6. After the image is analyzed make a new line for data in the “Raw Data Toolbox” by Ctrl+Alt+i and click OK, move on to next picture or sample.

7. Rinse, Repeat.

Storage/Disposal Information

- Make sure to turn off microscope when you are finished.
- Cover all microscopes with proper covers when finished.
- If appropriate shut down computer when finished.
- Give yourself a hug.

Appendix 3: In vitro release of bbPTH 1-84 from hydrogels

Protocol used by Sam Wojda

Time to complete: 1-5 weeks

Supplies Required	Supplier and Catalog Number	Storage Conditions	Location
Hydrogel Monomer solutions	Kristi Anseth's lab	-20°C	Freezer
1mL syringes		Room Temp	
UV lamp		Room Temp	
PBS	VWR 800858-556	Room Temp	
BCA Protein Assay Kit	Pierce Thermo Scientific	Room Temp	Chemical cabinet
Black Bear PTH 1-84		-80°C	

General Notes

- Protocol used when PTH is entrapped within the matrix or tethered to the hydrogel matrix
- In some cases the immutopics canine PTH kit may be used to measure bbPTH 1-84 specifically. However, non-specific binding from some aspect of the hydrogel did not allow for its use in this case

Procedure

<u>Make Hydrogels</u>

1. Combine monomer solutions provided by Dr. Kristi Anseth's lab according to the excel sheet shown below
    a. bbPTH 1-84
        i. not modified if it is to be entrapped within the matrix
        ii. Thiolated (with Trauts reagent) if it is to be tethered to the matrix
    b. PEG –NB (6 wt %)
    c. Peptide cross-linker (MMP degradable)
    d. RGD peptides
    e. LAP (photo-initiator)

i. Modify concentrations as appropriate depending on stock solutions as well as number of binding sites for PTH or RGD to be tethered to the PEG-NB.
ii. Make gels in hood
iii. All monomer solutions sterile filtered

	A	B	C	D	E	F	G	H	I
1	MMP Degradeable Linkers (MMP1)							PEG-NB Characteristics	
2		Stock Conc.	Working Conc.	Volume (µL)	mole functionality	per ul gel		Number of arms	4
3	PEG-NB (wt%)	20	5.00	25.00	1.00E-06	0.25		MW (g/mol)	20000
4	MMP Degradable X-Linker (mM -SH)	160.4935379	7.50	4.67	7.50E-07	0.046730853			
5	RGD (mM)	57.25911173	1	1.75	1.00E-07	0.017464469			
6	PTH	100	0	0.00	0.00E+00	0			
7	LAP (mM)	68	0.75	1.10		0.011029413			
8	PBS	---------	---------	67.48		0.674775264			
9			total =	100.00		1		PEG (mM)	2.5
10	PTH(nM)	0						Pendant Nb (mole)	1.50E-07
11								Pendant Nb (mM)	1.5
12									
13		Concentration (mg/mL)	Purity	Peptide Content	Concentration (mm -SH)				
14	MMP xlink Thiol Concentration	124.3	0.956	0.881	160.4935379			Pendant Nb - PTH mol	
15	RGDSC concentration	39.5	0.947	0.822	57.25911173				-3.02638E-06
16									
17					7.41E+06				
18	5.5wt%, .8SH/Nb:	G' ~ 4 kPa							
19	5wt%, .8SH/Nb:	G' ~ 2.75 kPa							
20	4.5 wt%, .8SH/Nb:	G' ~ 1.65 kPa							
21									
22									
23									
24		30 ug/gel		0.444592468	uq/uL				
25	PTH concentration in PBS		4.70732E-05	mol/L					
26			3.17638E-06	mol					
27									
28									
29	Want norbornene moles > than total thiol moles from MMP and RGD								
30									

	A	B	C	D	E	F	G	H	I
1	MMP Degradeable Linkers (MMP1)							PEG-NB Characteristics	
2		Stock Conc.	Working Conc.	Volume (µL)	mole functionality	per ul gel		Number of arms	4
3	PEG-NB (wt%)	20	5	=C3*D9/B3	=(((D3/1000)*(B3/100))/($I$3)*$I$2)	=D3/$D$9		MW (g/mol)	20000
4	MMP Degradable X-Linker (mM -SH)	=E14	=E4/D9*10^9	=E4/B4*10^9	=0.75*E3	=D4/$D$9			
5	RGD (mM)	=E15	1	=C5*D$9/B5	=(C5*10^-3)*(D$9*10^-6)	=D5/$D$9			
6	PTH	100	0	=C6*D$9/B6	=D9*10^-6*B10*10^-9	=D6/$D$9			
7	LAP (mM)	68	=0.1*(C4+C5*10^-6)	=C7*D9/B7		=D7/$D$9			
8	PBS	---------	---------	=D9-SUM(D3:D7)		=D8/$D$9			
9			total =	100		=D9/$D$9		PEG (mM)	=(E3/4)/(D9/1000000)*1000
10	PTH(nM)	=(C6/26000)*10^6						Pendant Nb (mole)	=E3-SUM(E4:E5)
11								Pendant Nb (mM)	=I10/(D9*0.000000001)
12									
13		Concentration (mg/mL)	Purity	Peptide Content	Concentration (mm -SH)				
14	MMP xlink Thiol Concentration	124.3	0.956	0.881	=(2*B14*C14*D14*10^3)/(1304.6)			Pendant Nb - PTH mol	
15	RGDSC concentration	39.5	0.947	0.822	=B15*C15*D15*1000/537				=I10-C26
16									
17					=5000000*D9/D8				
18	5.5wt%, .8SH/Nb:	G' ~ 4 kPa							
19	5wt%, .8SH/Nb:	G' ~ 2.75 kPa							
20	4.5 wt%, .8SH/Nb:	G' ~ 1.65 kPa							
21									
22									
23									
24		30	ug/gel	=B24/D8	ug/uL				
25	PTH concentration in PBS		=((B24/D8)/9444.7)	mol/L					
26			=(C25*(D8/1000))	mol					
27									
28									
29	Want norbornene moles > than total								
30									
31									
32									
33									

2. Pipette solution into molds to be cross-linked in.
    a. For cylindrical gels for the femur defect model a 1 mL syringe with the taper removed works well.
    b. If a rigid PPF scaffold is to be used in conjunction with the hydrogel:
        i. Place the scaffold in the syringe
        ii. Pipette solution over/through/around the scaffold
3. Place gel in syringe under UV lamp to be cross-linked
    a. Lamp : ~2.5 mw/cm^2
    b. Stand lamp up at height : 4 7/8”
    c. Use aluminum foil as a “lampshade” when light is on

Release

1. Place gels in 1-2 mL PBS for subscribed amount of time for experiment
2. At appropriate timepoints collect PBS for assay
3. Store samples at -80°C until assay
4. Follow BCA or µBCA kit instructions (depending on amount of PTH expected)

Appendix 4: In vivo imaging of Alexa Fluor 680 labeled hydrogels

Protocol used by Sam Wojda

Time to complete: 1-8 weeks

Supplies Required	Supplier and Catalog Number	Storage Conditions	Location
Functionalized Alexa Fluor 680	Kristi Anseth's lab	-20°C	
Hydrogel Monomer solutions	Kristi Anseth's lab	-20°C	
Sprague Dawley rats			
Suture			
Scalpel			
IVIS spectrum imaging system			
Isoflurane			
Oxygen			

General Notes

- The imaging protocol may be used in future femur defect studies. However, it is important to modify the methods slightly. The PEEK plate used in this research fluoresces at the wavelengths used for Alexa Fluor 680 (as seen below), as well as those used for VivoTag800. Thus the plate or the fluorphore would need to be modified to avoid confounding results.
    - Similarly, some sutures fluoresce – be sure to check all components of the model prior to the start.

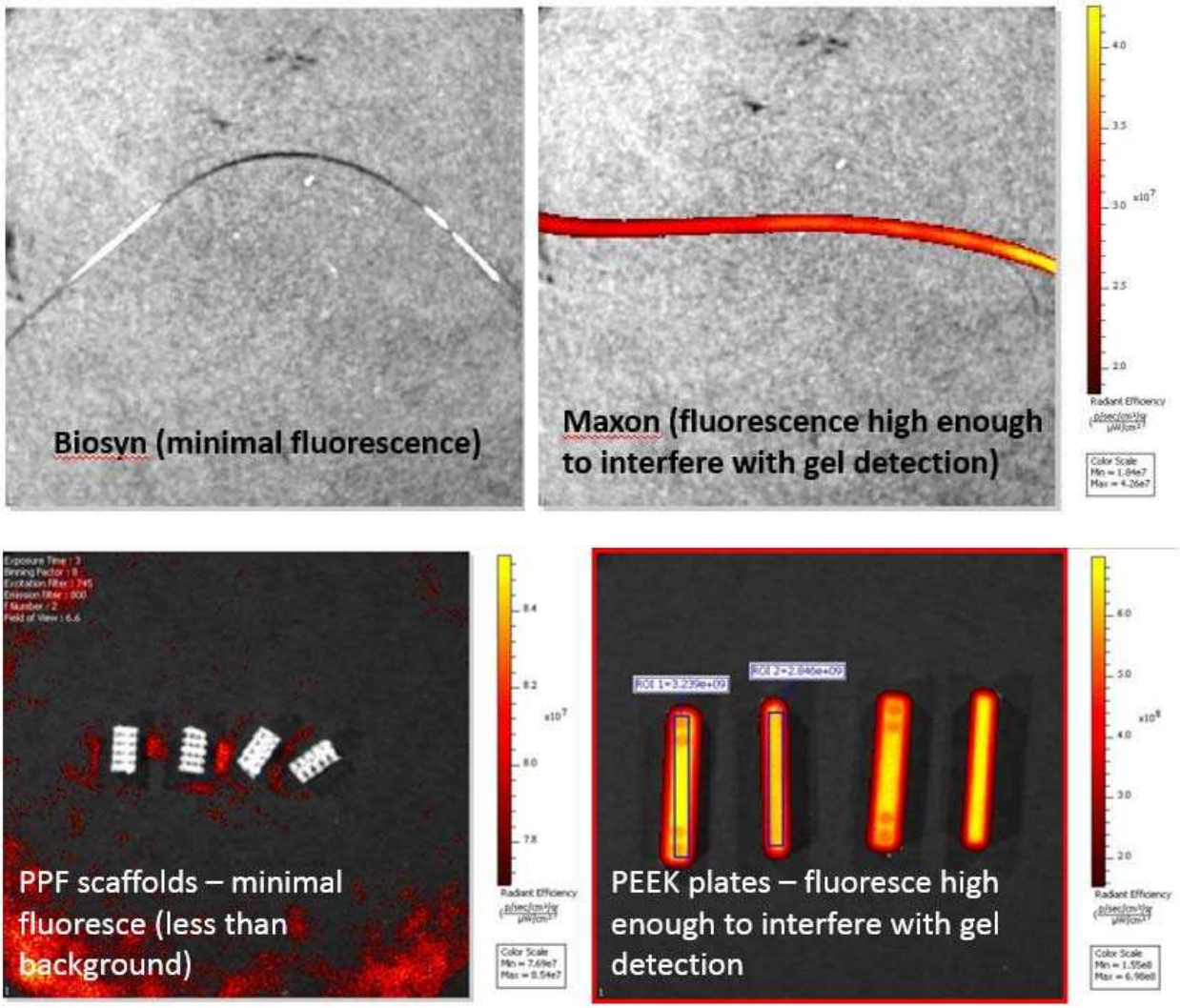

Procedure

Make Hydrogels

1. Make hydrogels according to SOP for hydrogel release

Subcutaneous Implantation of the materials

2. Prior to surgery make sure you are properly trained in aseptic surgical technique
3. Administer buprenorphine a minimum of 20 minutes prior to starting surgeries
    a. Example calculation for amount/dosing
    b. If using a 0.3 mg/mL solution of Buprenorphine and a dose of 0.5 mg/kg: calculation is Injection Volume = (rat weight * 0.05 mg/kg)/0.03 mg/mL
    c. **Err on the low side of the dosage range
    d. BE CAREFUL: remove ALL bedding AND enrichment devices for 72 hours if using buprenorphine SR. Sprague Dawley rats will eat until they suffocate themselves.

You can place paper towels in the cage to replace bedding. Make sure to change it daily as you monitor recovery of the rats.

4. Anesthetize rat with isoflurane 2-3% (to effect)
5. Shave surgical site with clippers (shave entire leg and up just past the hip)
6. "Wash" shaved leg with chlorhexidine 4%, then 70% Ethanol
7. Place anesthetized rat on heating pad (leg to be surgicated facing up) bottom leg and tail taped in place so nose cone does not slip.
8. Drape rat
9. Create an incision at the site you wish to implant the material
10. Use blunt dissection to make a subcutaneous pocket for the gel
11. Insert material into pocket
12. Suture to close
13. Staple (so rats don't chew the suture out)
    a. Staples will have to be removed for imaging and then replaced for the early timepoints (until they are removed permanently)

<u>IVIS Imaging</u>

1. Prior to imaging make sure you are properly trained and approved to use the IVIS imaging system and have read the user manual to ensure familiarity with the measurement system.
2. Anesthetize rat with isoflurane 2-3% (to effect)
    a. At later timepoints (once hair starts to grow back) you may need to re-shave the site to avoid fluorescence of the fur interfering with measures.
        i. Be careful not to damage the implant in the process
3. Place rat in imaging chamber (with nose in the nose cone to maintain anesthesia during imaging) as shown below

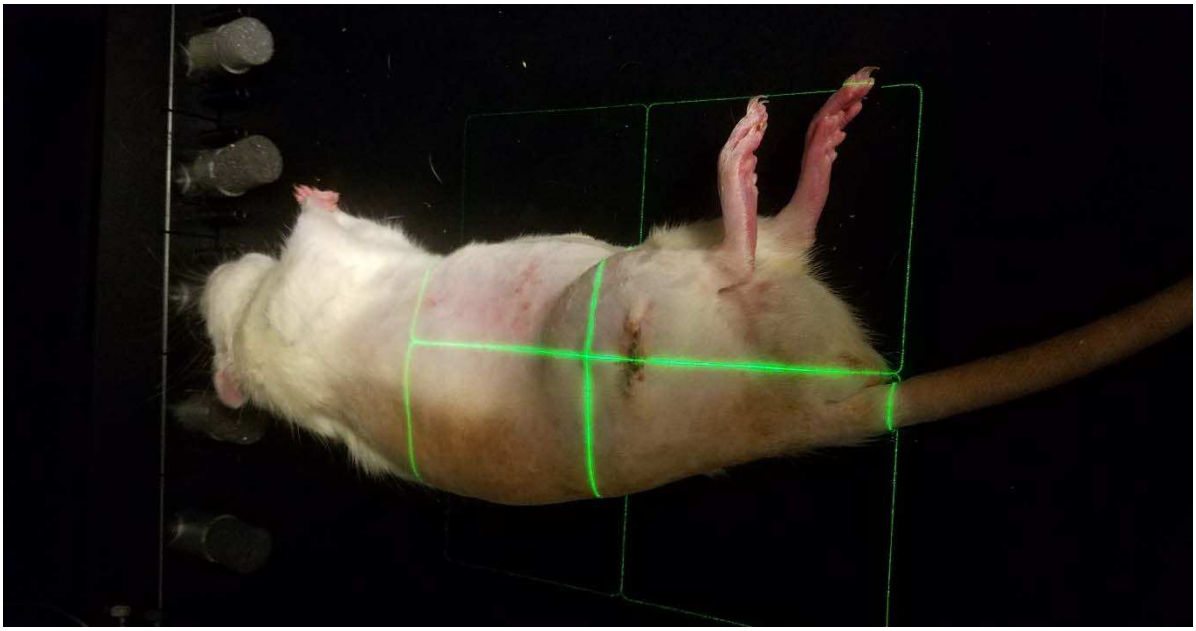

a. Center the crosshairs over the implant

    i. You will be able to see it as a raised bump through the skin (as indicated by black arrow in image below

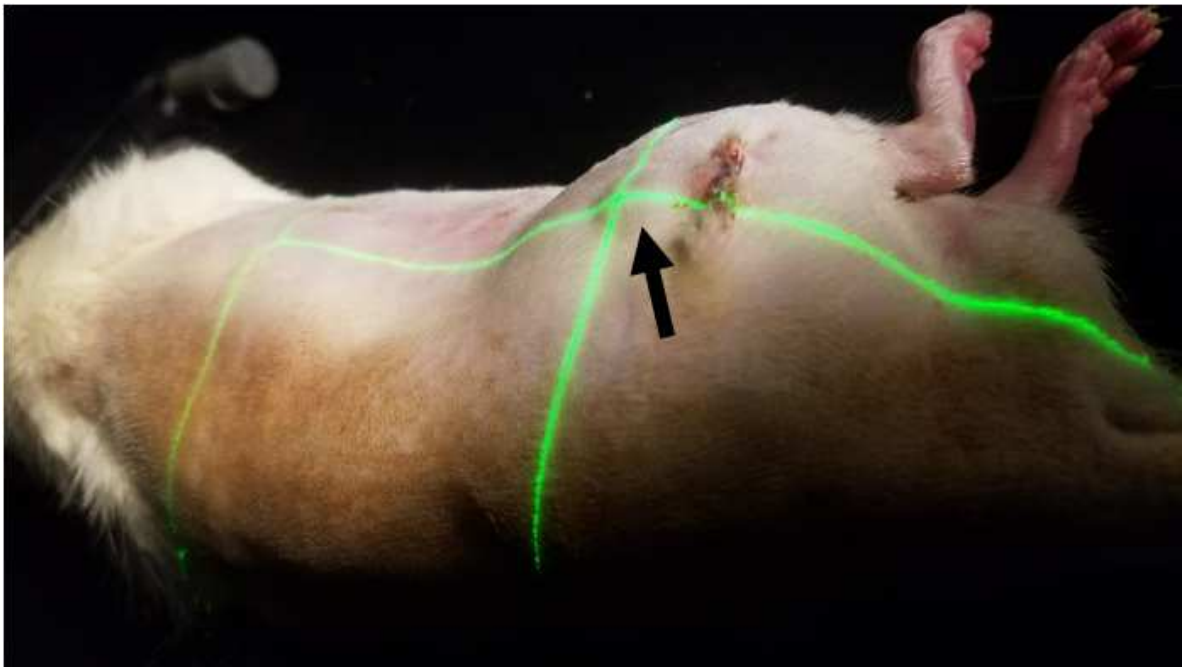

ii. In the event auto-fluorescence of the rat interferes with measures or makes distinction of the gel difficult, isolate the gel using black paper as shown below.

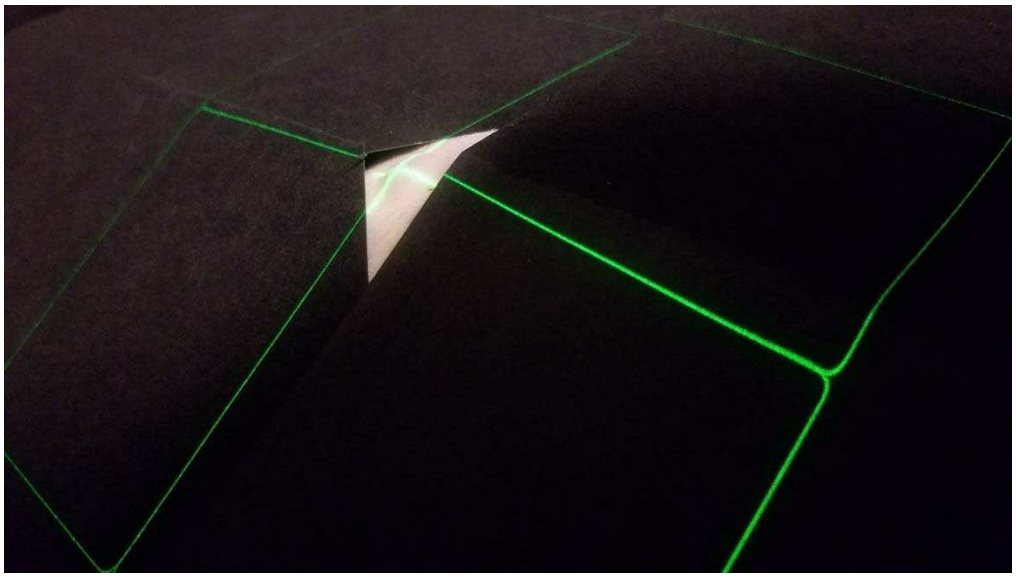

iii. Gels should be discernable as shown below

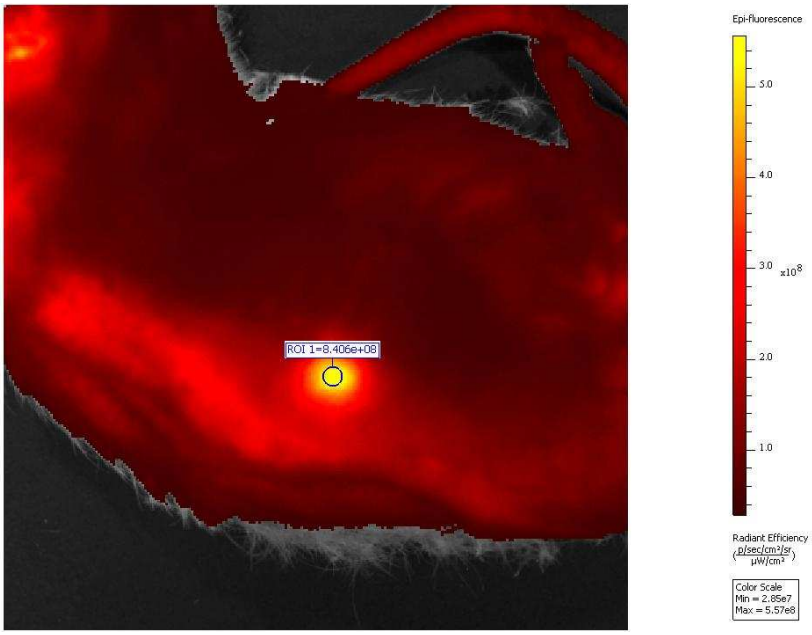

Appendix 5: MC3T3: cAMP Cell culture, stimulation and assay

Purpose: PTH-stimulated cAMP for hPTH and bbPTH in MC3T3-S4-E1 cells.

Protocol used by Sam Wojda

Time to complete: 1-2 weeks

Supplies Required	Supplier and Catalog Number	Storage Conditions	Location
Minimum Essential Media (Alpha Modification)	VWR SC45000-300	4°C	Fridge
0.25% Trypsin-EDTA	VWR 45000-664	4°C	Fridge
Penn-Strep	VWR 45000-652	4°C	Fridge
FBS (Characterized)	VWR 80058-556	4°C	Fridge
PBS	VWR 800858-556	Room Temp	On Chemical Shelf
L-Ascorbic Acid Cas# 50-81-7	Fisher Scientific A61-100	4°C	Fridge
β-Glycerophosphate	Cabiochem 35675	4°C	Fridge
Cyclic AMP kit	Cayman Chemical	-20°C	ACC244 Freezer
BCA Protein Assay Kit	Pierce Thermo Scientific	Room Temp	Chemical cabinet
Black Bear PTH 1-84		-80°C	
Forskolin	Sigma F6886	Room Temp	Chemical cabinet
IBMX	Sigma I5879	-20°C	ACC244 Freezer
DMSO	Sigma	Room Temp	Chemical cabinet

Additional Supplies Required

- Pipet Aid (Hood)
- Refrigerated centrifuge (ACC240)
- Sonicator (ACC240)
- Incubator at 37°C + 5% CO2
- Serological pipettes (5, 10, 25, 50 mL)

- Micropipettes
- Micropipette tips
- Sterile media bottles (100, 250, 1000 mL)
- Centrifuge tubes (15 and 50 mL)
- Culture dish (VWR: 82050-916)
- Culture flask (T-25, T-75)
- 6-well plates
- 96-well plate
- Eppendorf tubes (1.6 mL)
- Cell scrapers
- Invitrogen Countess Automated Cell Counter
- Countess Cell Counting Chamber Slides
- Colorimetric plate reader

General Notes:

Procedure

Example Timeline (once enough cells are cultured):
3/15/2012: Seeded 10^4 cells/cm^2 in 24 well plate. Seeded in MC3T3 growth medium (α-MEM + 10% FBS + 1% pen-strep).

3/16/2012 (approx. 24 hr later): Aspirate medium. Add MC3T3 mineralization medium (□-MEM + 10% FBS + 1% pen-strep + 50 µg/mL ascorbic acid + 10 mM β-glycerophosphate).

3/19/2012: Aspirate medium. Add fresh mineralization medium.

3/21/2012: cAMP stimulation

Preparation of Reagents

IBMX (Sigma I5879), MW 222.2

1. Make up IBMX in DMSO (According to product info sheet, IBMX is soluble in 100% DMSO at 1 M with gentle warming.)
2. For a 1 M solution, added 1.125 mL of DMSO to vial of IBMX (250 mg). Swirled and heated gently to get IBMX into solution. Aliquot and freeze at -20°C. Solution should be stable for several months.
3. With a 1 M solution, add 1 µL IBMX/mL of PBS (gives 1 mM IBMX, final DMSO concentration is: 0.1%).

Forskolin (Sigma F6886), MW 410.5

1. Make up forskolin in DMSO (DMSO recommended on product info sheet). Dissolve at 5 mg/mL and make subsequent dilutions in water. Forskolin solutions at 5 mg/mL in DMSO are stable for at least 6 months at room temp.
2. Purchased 10 mg forskolin, so dissolved in 2 mL of DMSO for 5 mg/mL. (This is a 12.18 mM solution). Aliquot.
3. For 10 µM forskolin, use 0.821µL/mL of PBS.

Grow Cells

9. Make MC3T3 growth media (500 mL) - (See bonelab MC3T3 SOP if needed)
    a. 89% α-MEM (445mL)
    b. 10% FBS (50 mL)
    c. 1% Penn-Strep (5 mL)
    d. Sterile filter all components
10. Add 14 mL warmed growth media to 75 cm^2 flask (T75)
11. Remove desired cell line from liquid nitrogen. Hold in heat bath until thawed. 1-2 min
12. Transfer cells to T75 flask and place in incubator (37°C + 5 % CO_2)
13. Change media within 24 hours.
14. Split cells when 70-80% confluent.
15. Change media every 2-3 days throughout cell growth process.
16. Cell count:
    a. Use Invitrogen Countess Cell Counter or Hemacytometer method.
    b. Need 103,500 cells/well (10,350,000 cells/mL)
        i. 10^4 cells/cm^2 in 6 well plate (well: 6.9 cm^2)
        ii. (# of cells grown) / (X cells/mL) = _____mL to re-suspend pellet

Plate Preparation

6. Seed 10^4 cells/cm^2 in 6 well plate. Seeded in MC3T3 growth medium (α-MEM + 10% FBS + 1% pen-strep).
    a. Cell seed:
        i. Plate cells at a density of 15,000 cells/cm^2.
        ii. Lyse cells and combine into one falcon tube. Centrifuge at 1200 rpm for 5 min.
        iii. Remove supernatant carefully with glass pipette.
        iv. Add growth media to resuspend (counted cells) / (needed cells/mL) = mL for resuspension. Mix well.
        v. Using small micropipette, mix up and down several times. Place 10 µL into each well.

7. Make MC3T3 differentiation media – (see bonelab MC3T3 differentiation SOP: 5-3 if needed)
    a. 89% α-MEM (445mL)
    b. 10% FBS (50 mL)
    c. 1% Penn-Strep (5 mL)
    d. 50 µg/mL L-Ascorbic Acid
    e. 10 mM β-glycerophosphate
    f. Sterile filter all components
8. 24 hours after seeding. Change media to differentiation media
9. Change media after 72 hours to fresh differentiation media
10. After 5 days of differentiation – stimulate for cAMP activity

<u>cAMP Stimulation</u>

1. Aspirate the media.
2. Wash each well one time with PBS (carefully).
3. Stimulate cells with vehicle, forskolin, or PTH in the presence of IBMX (1 mM).

    Stimulation occurs in PBS. Stimulate cells at 37^{o}C. Time point: 10 min

    Treatment groups:

    a. Vehicle (1 mM acetic acid) + 1 mM IBMX
    b. Hydrogel control (if experiment call for it)
    c. Forskolin (10 µM) + 1 mM IBMX (positive control)
    d. bbPTH 1-84 control
    e. bbPTH 1-84 released from hydrogels at appropriate timepoints/concentrations
        a. according to experiment details

4. At end of treatment period, aspirate PBS from plate.
5. Add 1 mL of 0.1 M HCl for every 35 cm^2 of surface area (use 275 µL/well for 6 well plate).
6. Incubate at room temp for 20 min.
7. Scrape cells off of the surface with a cell scraper.
8. Dissociate mixture by pipetting up and down until the suspension is homogeneous, and transfer to appropriately sized centrifuge tube.
9. Centrifuge at 1000xg for 10 min.
10. Decant the supernatant into a clean test tube. Remove 30 µL aliquot for protein assay.
11. These supernatants can be assayed directly, providing a dilution of at least 1:2 is used. A protein concentration of at least 1 mg/mL in the supernatant is recommended for reproducible results.

<u>BCA Assay</u>

2. Follow instructions in assay kit – 96 well assay
    a. 10 µL sample

b. Make Standards in ALP Buffer

cAMP assay (Cayman Chemical)

11. Follow kit instructions

Data Analysis

1. Cayman Chemical has a computer spreadsheed available for data anlaysis (www.caymanchem.com/analysis/elisa).

Appendix 6: Segmental Defect in Rat Femur

Protocol used by: Sam Wojda

Supplies Required	**Supplier and Catalog Number**	**Storage Conditions**	**Location**
Sprague Dawley Rats (~250-300 g minimum size)	NIH	Animal Care Facility	
PEEK fixation plates	Alpha Designs and plastics (technical drawing at end of SOP)	Room Temperature	
0.045" Threaded k-wires	Custom made	Room Temperature	
Gigli Wire			
Babcocks			
Scalpel			
Forceps (X2)			
ALF retractors			
Gauze/cotton swabs			
Dremel			
#66 Drill bits			
Chlorhexidine 4%			
70% Ethanol			
Buprenorphine or Buprenorphine SR			
Equipment for proper aseptic surgical technique			

General Notes:

- This SOP does not go over aseptic (sterile) surgical technique – make sure you are properly trained prior to performing surgeries on live animals.

- Sterilize all equipment prior to surgery

- In the past a dremel with oscillating saw has been used to cut the bone instead of Gilgli wire, this works, but results in more soft tissue trauma and is more difficult than using Gigli wire.

- Babcocks (this is the tool we used to hold the plate to the bone).

- Plates: flat or raised - Ve careful using raised plates, both labs here that use them are having issues with k-wire pull-out, and therefore fixation failure (radiographs below).
    - Recommendation: usescrews vs threaded k-wires if the raised plate design is to be pursued.

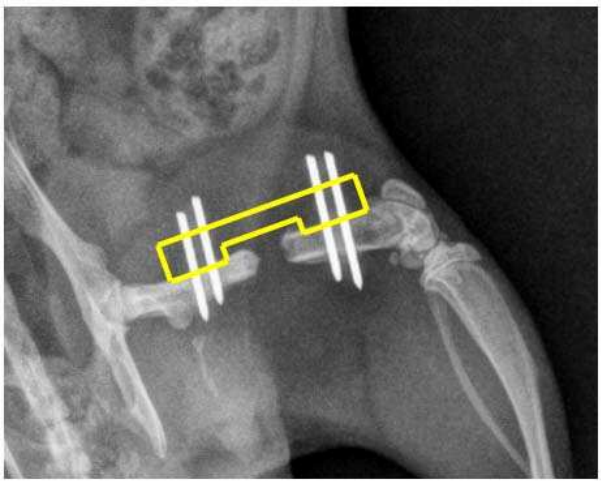

Day 21

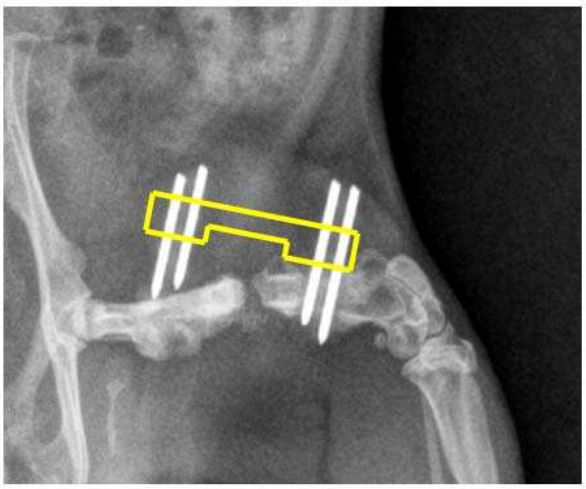

Day 42

Procedure

Rat Preparation prior to surgery:

1. Administer buprenorphine a minimum of 20 minutes prior to starting surgeries
    a. Example calculation for amount/dosing
    b. If using a 0.3 mg/mL solution of Buprenorphine and a dose of 0.05 mg/kg: calculation is Injection Volume = (rat weight * 0.05 mg/kg)/0.03 mg/mL
    c. **Err on the low side of the recommended dose
    d. BE CAREFUL: remove ALL bedding AND enrichment devices for 72 hours if using buprenorphine SR. Sprague Dawley rats will eat themselves to death. You can place paper towels in the cage to replace bedding. Make sure to change it daily as you monitor recovery of the rats.
2. Anesthetize rat with isoflurane 2-3% (to effect)
3. Shave surgical site with clippers (shave entire leg and up just past the hip)
4. “Wash” shaved leg with chlorhexidine 4%, then 70% Ethanol
5. Place anesthetized rat on heating pad (leg to be surgicated facing up) bottom leg and tail taped in place so nose cone does not slip.
6. Drape rat

Surgery:

1. Approaching anterolatterally- make an incision (through the skin) from the tip of the hip to the bottom of the knee.

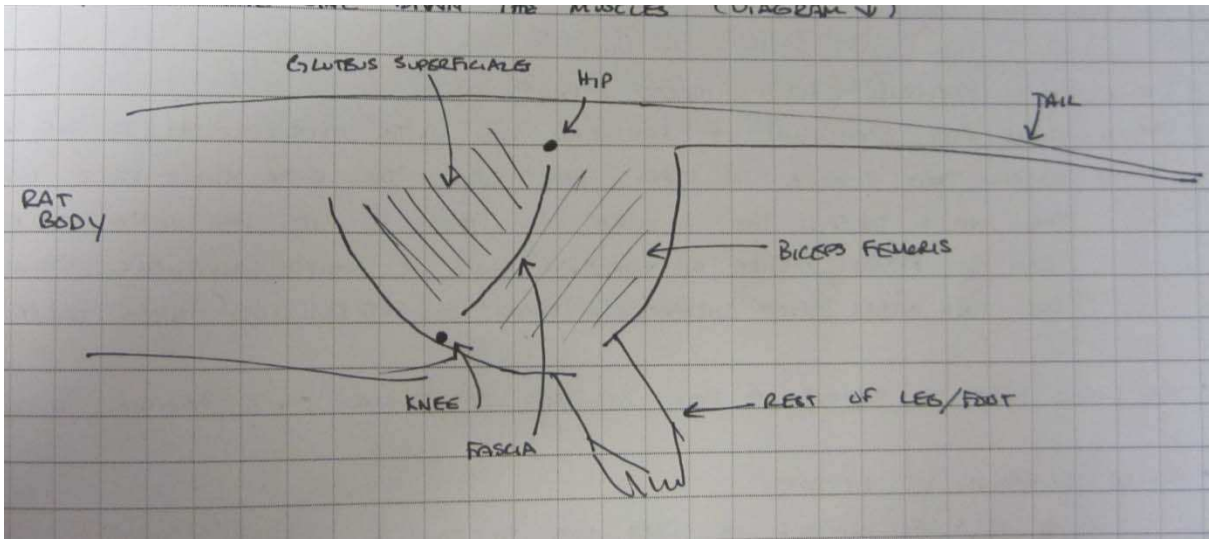

2. Once the muscle is exposed make an "incision" through the muscles to expose the femur
    a. Separate the muscles b cutting therough the fascia between the biceps femoris and gluteus superficiales – you do not need to actually cut any muscle and there won't be much bleeding.
    b. The fascia appears as a white line between the muscles
    c. There are a couple of other muscles between the biceps femoris and gluteus superficiales but it will be easy to separate along that line. Use blunt and sharp dissection to expose /clean femur to your confidence level.
    d. ***make sure not to cut too deep because the sciatic nerve and femoral artery could be damaged. Often when I use the retractors for the muscles I can see the sciatic nerve, if you can see it, that's ok, just make sure not to stretch it too much.
3. Use ALF retractors to hold the muscle away from the bone (not essential, but very helpful)
4. Place the fixation plate directly adjacent to the anterior side of the femur. Try to position the plate such that the defect can be cut approximately mid diaphysis.

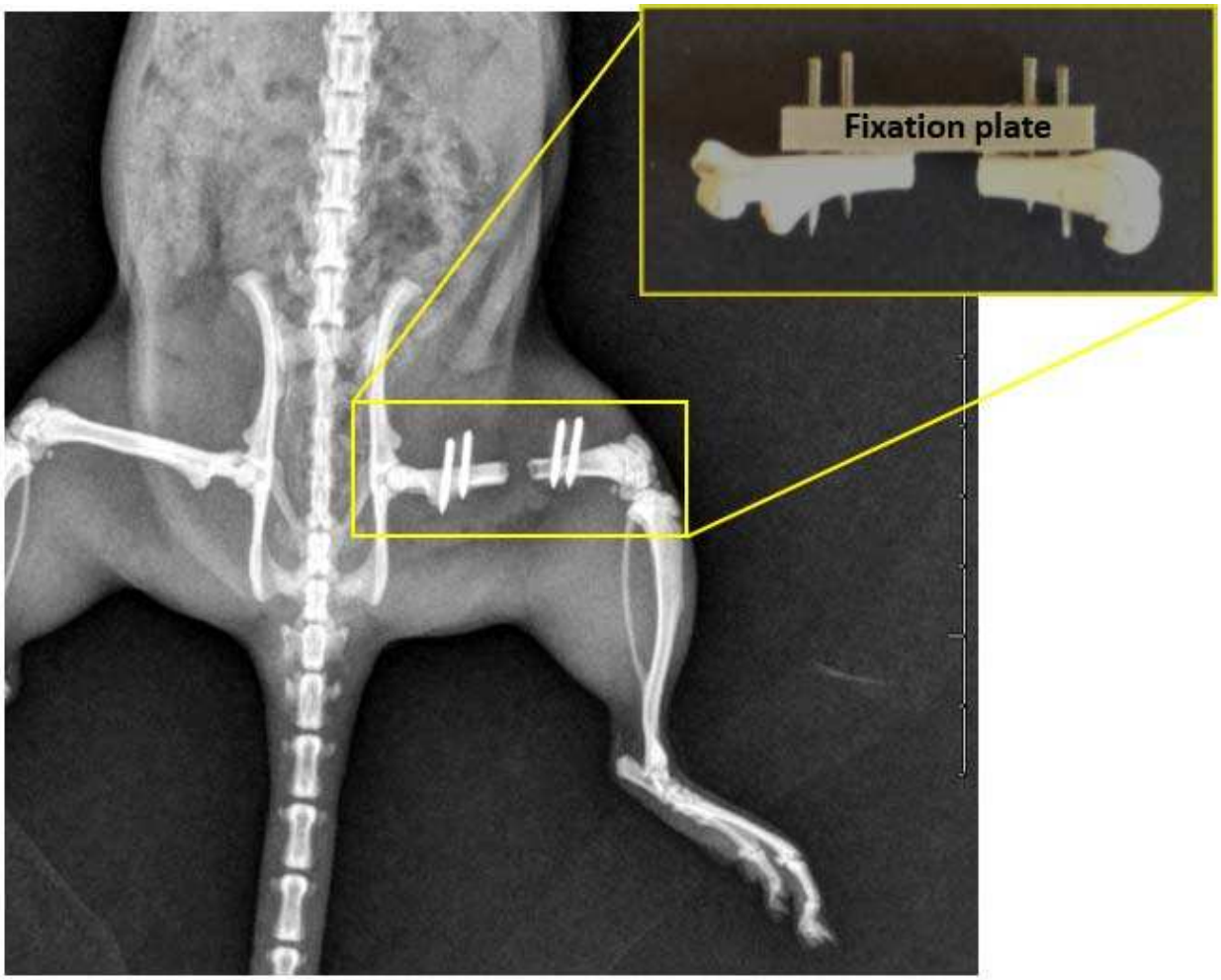

5. Using the babcocks grip the plate/bone (they should fit around the plate and bone, so you aren't clamping with the edges in contact with the bone or plate, rather the gap is "hugging' the bone/plate combo). IF you don't like the babcocks you can grip with forceps/hemostats/etc, you just need to hold in place to drill holes for the plate.
6. Once grip is established you can rotate the bone to allow easier access to the drill holes.
7. Predrill holes and thread k-wires in: (drill all at once then use nedles as place holdelrs
    a. Do this one hole at a time. Start with outside hole closest to the knee and thread that k-wire in first. Then drill the outer hole nearest the hip and thread that k-wire in. Then do the inner holes.
8. Use Gigli wire (or dremel) to removed 5 mm segment (or desired size large) once fixation is complete.
9. Place scaffold/treatment in defect

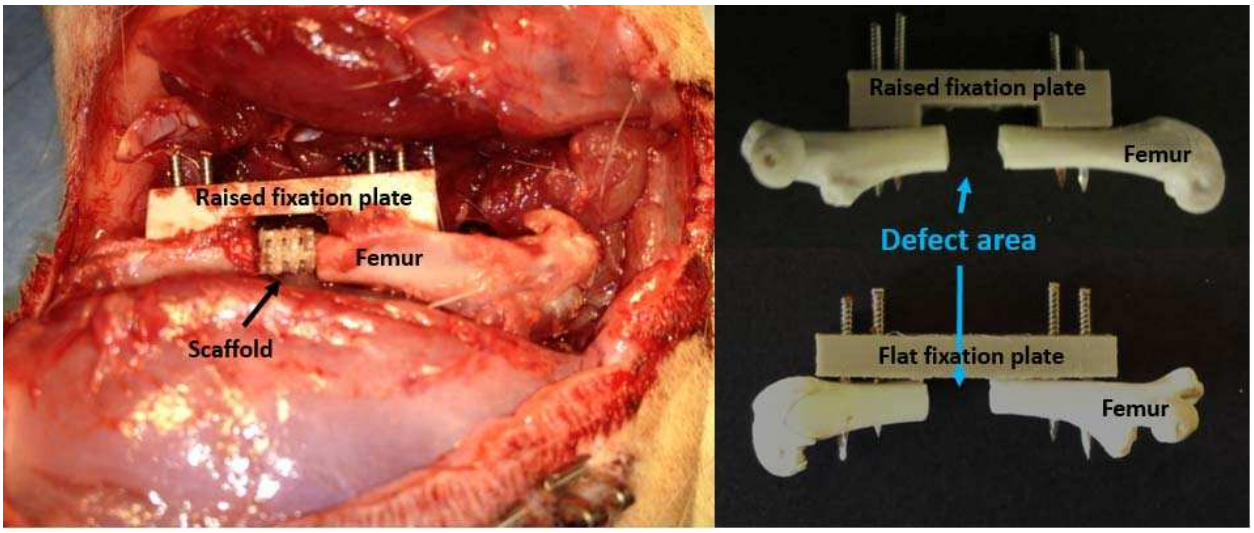

10. Pull the muscles back around the femur (as they were naturally) and suture (if your scaffold lacks mechanical integrity or you want to create a muscle pocket prior to placing the scaffold you can do that as well.
11. Suture skin
12. Place staples over suture line to ensure they don't chew stitches out.
13. Remove rat from ISO and let recover (not on heating pad unless you're using nude rats, then leave on heating pad while recovering.
    a. We've had issues with letting Sprague dawleys recover on heating pads, if you leave them too long or forget to turn the pad off once they start coming out they seem to die. We're not sure if they overheat or what. But this step depends on the strain of rat you use.) 350-400g rats is a good size for the raised plates. If you use flat plates 300-350g works ok.

Follow up notes:
If you want the scaffold to fit perfectly you can fix the plate to the distal side of the bone, cut out the bone segment place scaffold, reduce fracture (which means close the gap), then drill in the other side. We don't do this but they do it in people this way sometimes according to my committee member.

Closed fracture model: you can follow the same general technique and do one cut instead of a segmental defect. Or if you want to do the 3 point bend like you sometimes see in literature you could (but that might be hard to get IACUC approval).

We have also had fixation issues using the raised plate (see following figure): I

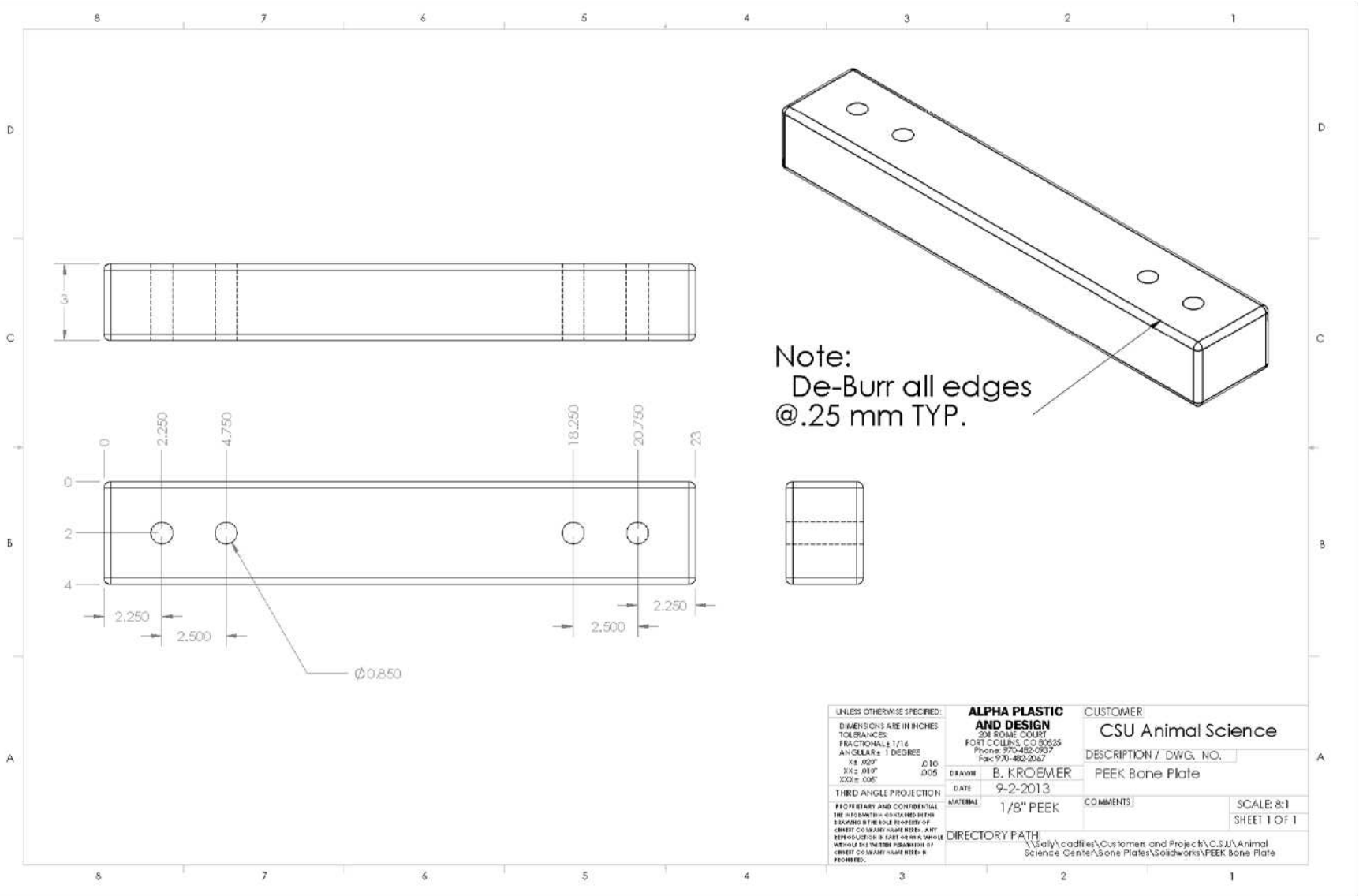
Note:
De-Burr all edges
@.25 mm TYP.
3
0
2.250
4.750
18.250
20.750
23
0
2
4
2.250
2.500
2.500
2.250
Ø0.850
UNLESS OTHERWISE SPECIFIED:
DIMENSIONS ARE IN INCHES
TOLERANCES:
FRACTIONALS 1/16
ANGULAR: ± 1 DEGREE
X ± .020" .010
XX ± .010" .005
XXX ± .005"
THIRD ANGLE PROJECTION
PROPRIETARY AND CONFIDENTIAL
ALPHA PLASTIC AND DESIGN
201 ROBIE COURT
FORT COLLINS, CO 80525
Phone: 970-482-0937
Fax: 970-482-2067
CUSTOMER
CSU Animal Science
DESCRIPTION / DWG. NO.
DRAWN B. KROEMER
PEEK Bone Plate
DATE 9-2-2013
MATERIAL 1/8" PEEK
COMMENTS
SCALE: 8:1
SHEET 1 OF 1
DIRECTORY PATH
\\Sally\cadfiles\Customers and Projects\C.S.U\Animal Science Center\Bone Plates\Solidworks\PEEK Bone Plate

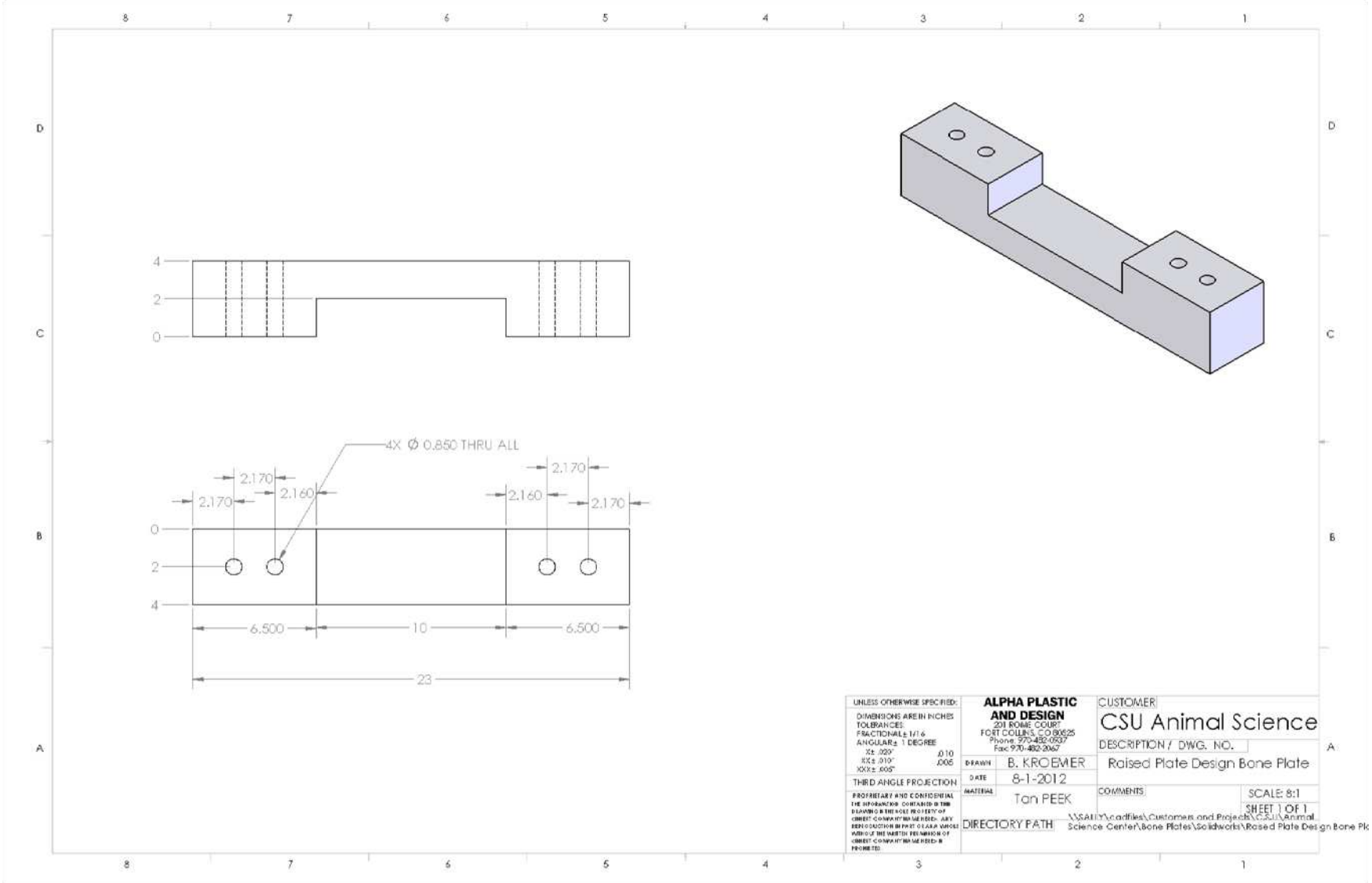
4X Ø 0.850 THRU ALL
2.170
2.160
2.170
2.170
2.160
2.170
6.500
10
6.500
23
ALPHA PLASTIC AND DESIGN
201 ROME COURT
FORT COLLINS, CO 80525
Phone: 970-482-0507
Fax 970-482-2067
CUSTOMER
CSU Animal Science
DESCRIPTION / DWG. NO.
Raised Plate Design Bone Plate
DRAWN
B. KROEMER
DATE
8-1-2012
MATERIAL
Tan PEEK
COMMENTS
SCALE: 8:1
SHEET 1 OF 1
DIRECTORY PATH
\\SALLY\cadfiles\Customers and Projects\CSU\Animal Science Center\Bone Plates\Solidworks\Raised Plate Design Bone Pl
UNLESS OTHERWISE SPECIFIED:
DIMENSIONS ARE IN INCHES
TOLERANCES
FRACTIONAL ± 1/16
ANGULAR ± 1 DEGREE
X ± .020" .010
XX ± .010" .005
XXX ± .005"
THIRD ANGLE PROJECTION
PROPRIETARY AND CONFIDENTIAL

Appendix 7: Microcomputed Tomography of Rat Femurs (µCT)

Protocol used by Sam Wojda

Time to complete: 1-8 weeks

Supplies Required	Supplier and Catalog Number	Storage Conditions	Location
Samples to be scanned			
10 % NBF			
70 % Ethanol			
50 mL Falcon Tubes			
Scanco vivaCT80			

General Notes

- Prior to performing any scans make sure you have attended all required trainings for use of the Scanco machine and make sure you have familiarized yourself with the user manual.
- MicroCT uses x-ray imaging (differences in x-ray attenuation properties of different materials) and computed tomography to provide high resolution 3-D images.
- Resolution is usually given as a characteristic size (µm) or a spatial frequency (line pairs/mm). VivaCT80 has the following possible resolution settings

Resolution:	Acquisition:	Reconstruction: *vivaCT 80*
Standard:	250 Projections	1024 x 1024
Medium:	500 Projections	1024 x 1024
High:	1000 Projections	2048 x 2048
Custom:	up to 1500 Projections	up to 4096 x 4096
Scan Mode	Number of Projections / 180°	Image Matrix

- Each MicroCT system will have its own unique Username and Password. These will be disclosed when you attend training sessions.
- Operating system is VMS
    - Scanco DOES NOT use a Windows computer system – DO NOT assume keyboard shortcuts will perform the same tasks. Some do, some do not- check the user manual
    - By default two windows will be displayed on the screen – *uCT toolbox* (left) and *Session manager* (right)

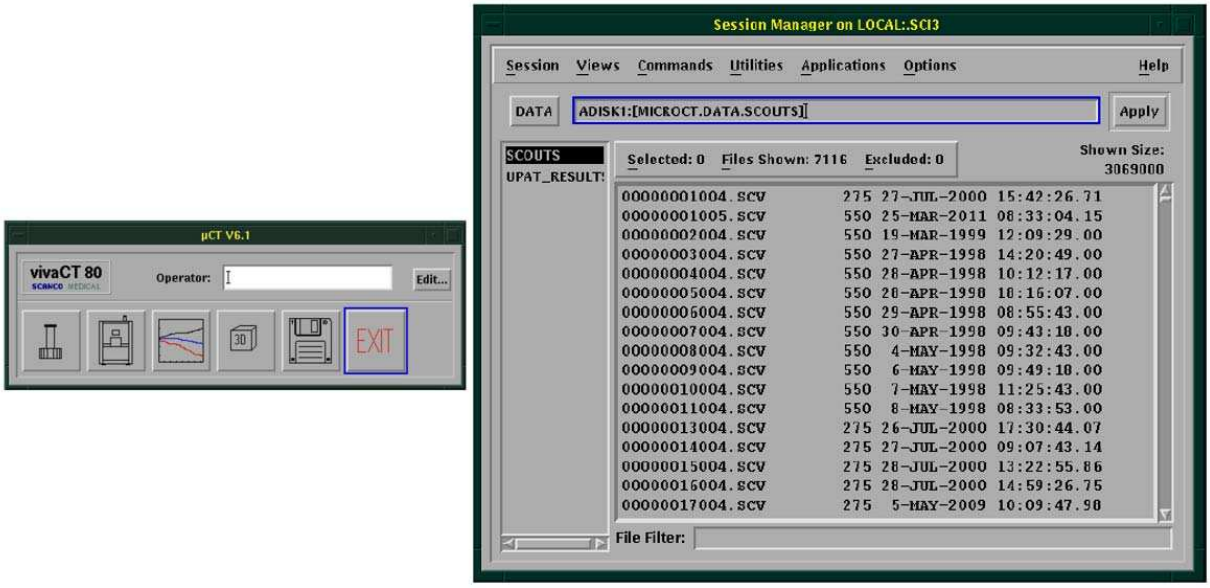

Procedure in vivo scans of femur defects

<u>Set up scan parameters</u>

1. Create Control file

Micro-CT Scanning Specifications:	
Scan Data:	5/24/2017
Project:	SJW: Femur Defect
Specimens:	Sprague Dawley Rat Femurs
Number of Scans:	1
Time to Scan:	~ 30-45 Minutes
Scanner Setup (General):	
Measurement Sample Name:	SethD_SJW-Femur Defect-Sample #
Holder Diameter:	Rat bed
Holder Type:	Generic, Any dia x L 145 mm
Evaluation:	Default
Control File Settings:	
Control File Name:	SJW Femur Defect
X-ray Settings:	Energy/Intensity: 70kVp, 114 uA, 8W
	Calibration: #3
Scoutview:	Position: 69.8 - 145
	Angle: 0
	Scan Region on Scout: 127.907
	Scoutview = True
CT – Scan:	Resolution: High
	FOV: 49.8 mm
	VOX: 24.2 µm
	#Slices: 285: 6.9 mm
	Rel. Pos. 1st Slice to Ref. Line: 0
	Integration: 250
	Averaging Data: 2
Analysis:	
Analysis : Bone Volume or Midshaft Analysis	
Scanned In Vivo	

To orient rats for in vivo scanning

4. Lay rat on its back in the holder
5. Orient femur perpendicular to the floor

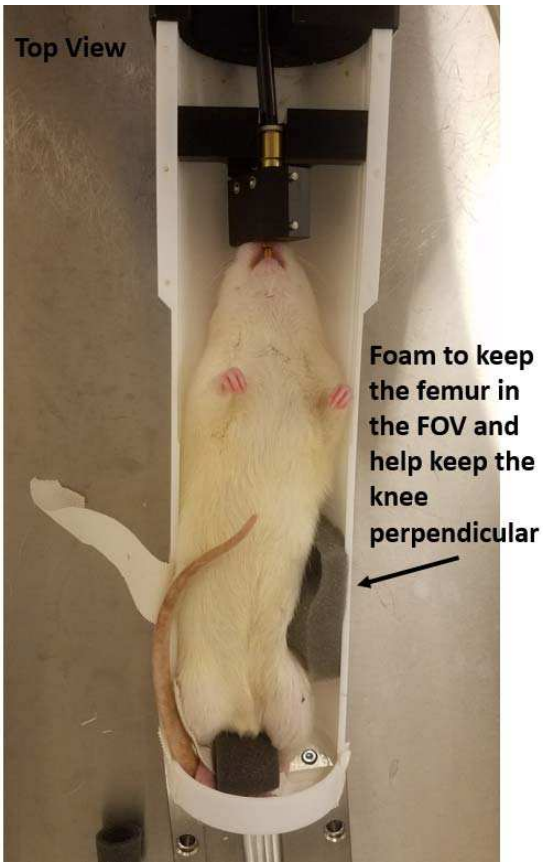

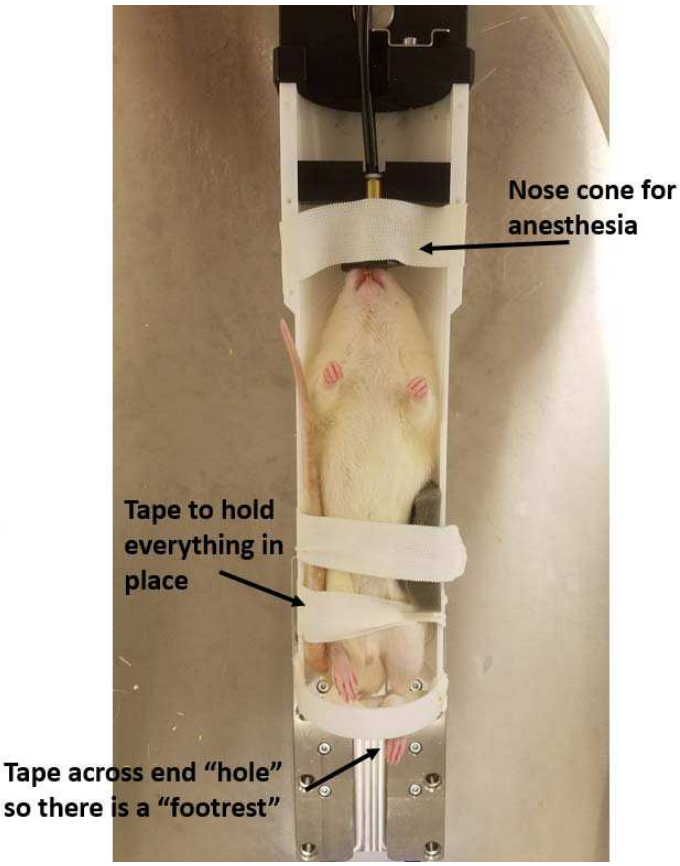

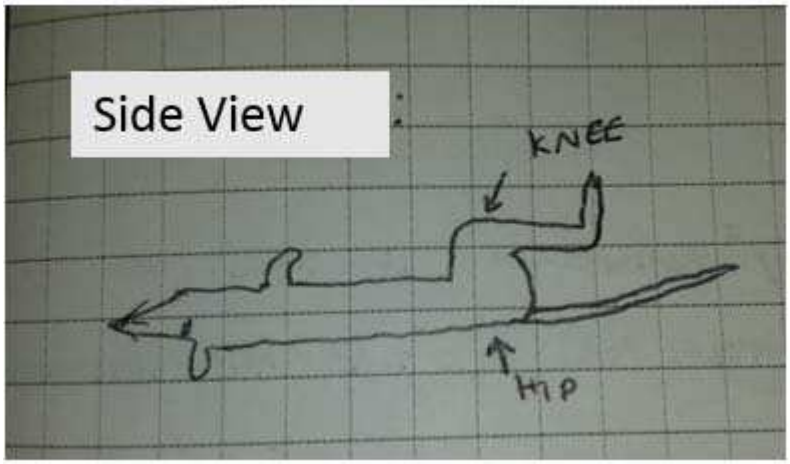

2. Place rat bed in scanner

3. Close scanner
4. Initiate scan and let it run to completion
    a. Example scout view for this orientation

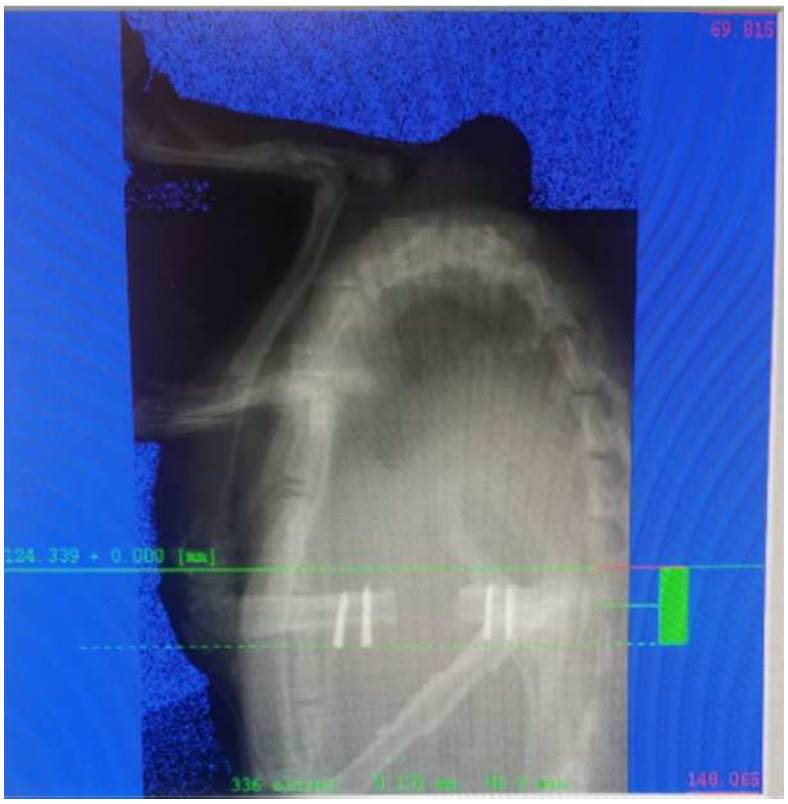

b. Intermittently monitor rats breathing rate through the observation glass.

c. Enter the Operator name in bottom left box and select the scanner icon; second from left in microCT operation box in the lower left corner of the screen

d. Sample name entry box will appear

    1. Unless warmup is required, then a warning for warmup will be displayed

e. Enter sample number (SethD_Project_Sample number)

    1. A pop up will appear with the name of the file to be saved, click ‘Save’ (bottom right) then go to the menu at the top and select ‘File’ → ‘ Exit’

f. Select Control file : For this project “SJW Femur Defect”

g. Select scout view box, then adjust start and stop point for scan, select “scout view” at right of scanning box

    1. If femur appears straight, select [reference line] and place the starting line as indicated by the green line in the example scout view in step a., hold down shift key to move bottom dashed line to the other side of the femur

2. If femur is not straight, select 'Cancel', select 'yes' to do you want to cancel without setting reference line prompt. Then select "Reset". When the scanner says "Open Access" the rat can be repositioned

h. When the scan has completed and "open access" is displayed on scanner, sample can be removed, positioning foam is removed and sample within the conical tube is placed back in secured storage cabinet.
i. To start new sample, select [New] below sample name; a pop-up box will appear, type in next sample name into Name field and click [save] at bottom right of the box. Go to top menu in box and select File: Exit.
j. Rinse - Repeat

5. Check scanned slices
    1. To check resulting scan, go to bottom left corner, select graph icon, 3rd from left, and select sample to view from list.
        b. Click on scan to view in right hand box to bring up images of the representative slices.
        c. An error box will appear if all slices are not yet reconstructed.
        d. Once they are reconstructed, go to first image and use the slide below main image window to scan through the slices and ensure all images are good quality ie not blurry or disrupted by artifact.
        e. If artifact is present or motion of the sample noted, re-scan the sample the following day (so the rats don't have to undergo multiple anesthetizations in one day).
        f. An example femur defect scan is shown below:

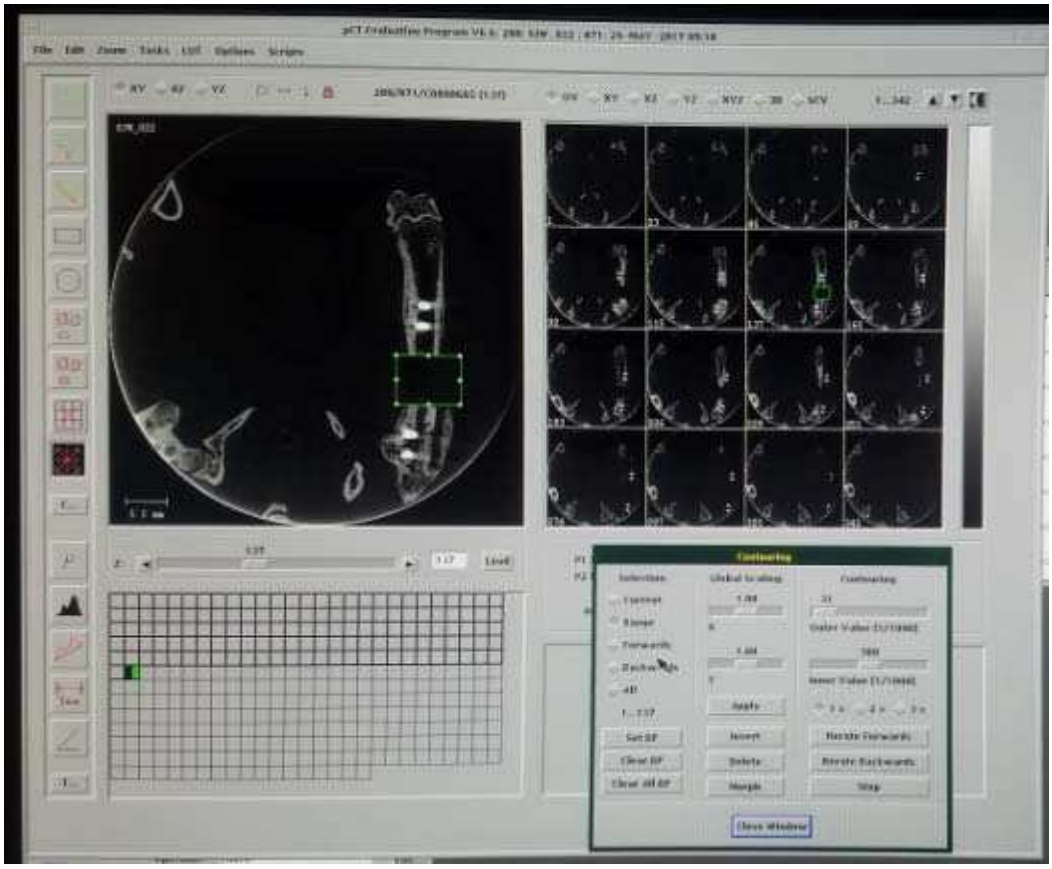

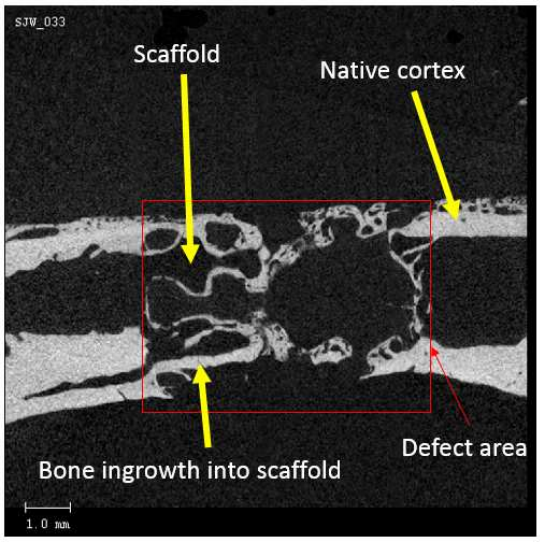

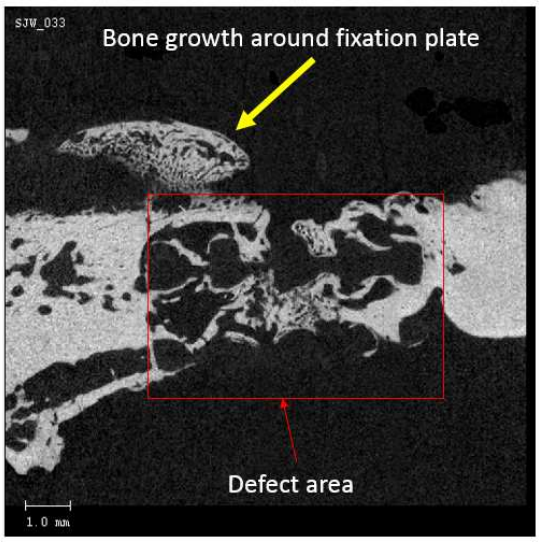

6. Due to the way the the beam rotates around the bed –if you orient the rat on i's side (an attempt to make the femur parallel to the floor) the effect of the titanium x-wires on the x-ray beam will result in a gap in the 3-D reconstruction.

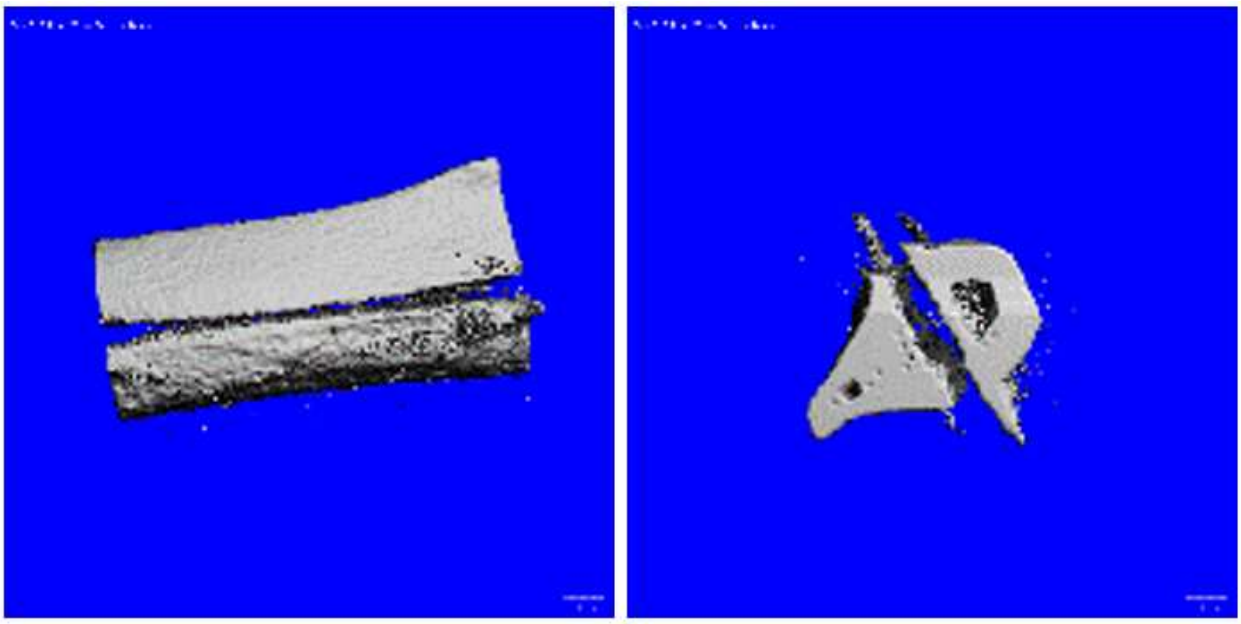

Reference Documents

- VivaCT 80 User's Guide: Revision 1.3; SCANCO Medical AG, CH-8306 Bruettisellen
- Scanco Medical Technical Document: µCTxx / vivaCTxx QC SOP; TD-289 Version 2.0
- Scanco Medical Technical Document: Consumer Training Guide µCT/vivaCT; TD-311, Version 1.2